Quantifying life history energetics of an oviparous elasmobranch subject to future warming water

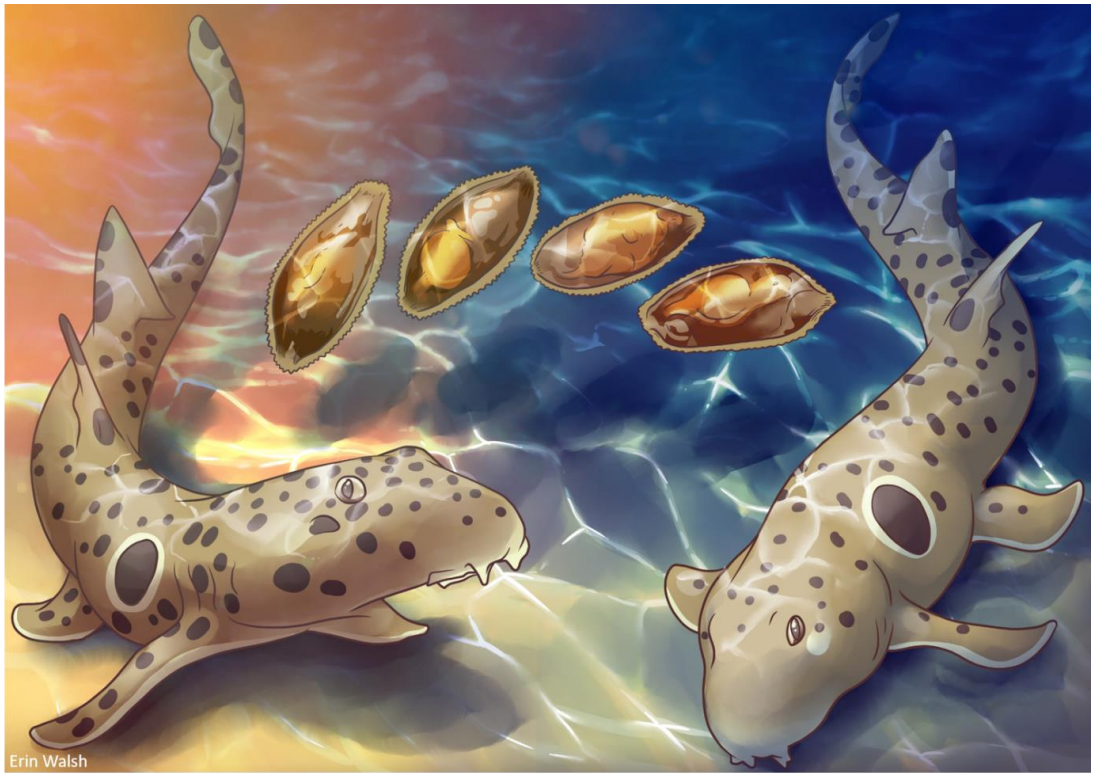

Thesis submitted by:

Carolyn Rose Wheeler

B.Sc., M.Sc.

For the degree of Doctor of Philosophy

Australian Research Council Centre of Excellence for Coral Reef Studies
James Cook University

and

The School for the Environment
The University of Massachusetts Boston

January 2023

Acknowledgments

First, I acknowledge the Traditional Owners and Custodians of the land and sea country on which this research was conducted, and recognize their continuing connection to land, waters, and culture. I pay my respect to their Elders past, present, and emerging.

I would like to thank my primary supervisors Drs. John Mandelman and Jodie Rummer for the past six years, for their encouragement and unwavering support. Both have taught me how to be a better scientist and entrusted me with some truly amazing projects. I would also like to thank my secondary supervisor Dr. Jan Strugnell and my committee member Dr. Helen Poynton for their support of this dissertation in recent years. A special thanks to Jeff Kneebone who helped me trouble shoot a variety of aspects of my dissertation and has become a trusted mentor of mine. I would like to thank Dr. Cynthia Awruch for welcoming me into her lab and providing invaluable technical support as well as becoming a valuable mentor to me in the past year. I thank my undergraduate advisor Dr. James Sulikowski, who provided me with a world of opportunities very early in my career, and without his long-term support I would not have completed this PhD. I would also like to thank a long list of previous teachers, mentors, and professors that have shaped me into the scientist I am today including Ms. Leanne Sweet, Robert Maiorano, Mr. Scott Klein, Dr. Walt Golet, Dr. Bianca Prohaska, and Dr. Ken Campbell. I'd also like to thank the two examiners of this thesis for their thorough and helpful comments and ideas to better this work. Finally, I'd like to thank Dr. Michelle Heupel, who's PhD thesis research is repeatedly referenced throughout this dissertation, and without her seminal work on the basic biology of epaulette sharks, this research would not have been possible.

I would like to thank the staff of the New England Aquarium including Emily Jones, Barbara Bailey, Hannah Cutting, Morgan Lindemayer, Rachel Moote, Caitlin Murphy, Lindsay Phenix, Monika Schmuck, and Sarah Tempesta. You all helped me selflessly during the two years I worked in Quincy and I'm grateful for all of the support you offered to the project. Furthermore, I would like to thank all of my lab mates from UMB and JCU for their support over the years including Connor

Capizzano, Ryan Knotek, Ian Bouyoucos, Adam Downie, Kelly Hannan, and Martina Lonati. I would like to thank the numerous volunteers that assisted in my various chapters including Shelby Vance, Chandler Schaeffer, Jamie Lockwood, Angelina Bacchar, Lauren Beattie, and Hailley Nieves. Finally, I would like to thank the NEAq, MARFU, and HIRS staff for all of their logistical support of my research, particularly the wonderful Ben Lawes and Simon Weaver.

Lastly, I would like to thank my friends and family from near and far for their unrelenting support for my PhD endeavour the last six years. Your physical, emotional, and financial support is the reason that I was able to complete this PhD. I would like to pay particular thanks to my parents Priscilla and Todd Wheeler, my sisters Grace Upadhyay, and Rebecca DeToma, and my brothers-in-law Saurav Upadhyay and Dan DeToma. Finally, I'd like to thank my partner Sam Findley for his endless understanding and support of my PhD the past two years. Thank you for enduring all the ups and downs this has brought us.

Statement of contribution of others

This thesis was funded by the Australian Research Council, the ARC Centre of Excellence for Coral Reef Studies, an anonymous donation to the Anderson Cabot Center for Ocean Life at the New England Aquarium (Chapters 2,4, and 6), the Save Our Seas Foundation (Chapters 3 and 5), the Australian Society for Fish Biology (Chapters 2, 3, and 4), the Australian Wildlife Society (Chapters 2, 3, and 4), and the American Australian Association provided one year of financial support to the author. This research was a collaborative effort of Prof Jodie Rummer, Prof Jan Strugnell, Dr. John Mandelman, and Dr. Jeff Kneebone who provided general scientific and financial support. In addition, chapter one of this thesis was contributed to by Dr. Rui Rosa, Dr. Connor Gervais, Martijn Johnson, and Shelby Vance. Chapter two was contributed to by Dr. Jeff Kneebone and Dr. Dennis Heinrich. Chapter 4 of this thesis was contributed to by Dr. Cynthia Awruch, chapter 5 was contributed to by Bethan Lang, and chapter 6 was contributed to by Barbara Bailey, Jamie Lockwood, and Shelby Vance. The thesis cover image is by Erin Walsh. Permission for use of these research works and images has been obtained by all parties.

Thesis Abstract

Marine ectotherms – organisms that do not regulate internal body temperature independent from the water temperature – are some of the most vulnerable organisms to oncoming global climate change. As anthropogenic greenhouse gas emissions continue, the oceans are acting as a large sink for atmospheric heat, where under current day emissions trends oceans will warm by 2-4°C by the end of the 21st century. Therefore, marine ectotherms stand to experience relatively rapid and alarming increases in environmental temperature, which for tropical species that already live near their thermal maxima, this warming could be of grave consequence to individuals, populations, and whole marine ecosystems.

Chondrichthyan fishes (*i.e.,* sharks, rays, and chimaeras) are cartilaginous fishes that tend to have slow growth, late age of maturity, long gestation/development times, and therefore overall have long generation times. Partially due to these factors, this taxon is globally threatened, mainly from fishing pressures, where Chondrichthyan life history is too slow to keep pace with fishing pressures. Furthermore, the majority of Chondrichthyan species are ectothermic, and therefore rely on environmental temperature to regulate their physiology and therefore ultimately their survival. Given the current global status of the group, and their potential susceptibility to ocean warming, climate change research in the taxon has recently become of interest. To date, only eleven small benthic species have been experimentally studied, and no singular species has been assessed across all life stages or in regard to potential direct impairment of adult reproduction. Therefore, the overall aim of this thesis was to study a small, tropical, and benthic shark species, the epaulette shark (*Hemiscyllium ocellatum*), to better understand basic life history physiological costs and to determine the interaction environmental temperature may have on these costs now and in the future under climate change-mediated ocean warming.

Epaulette sharks are a small coastal carpet shark found only along the Great Barrier Reef, Australia, where they inhabit shallow reef environments with large fluctuations in water temperatures from daily warming and cooling as well as tidal

influences. In **chapter 2** of this thesis, I aimed to assess how spring (25°C) and summer (28°C) water temperatures impact the routine metabolic costs of adult epaulette sharks, where I aimed to understand if constant and diel changes in temperature effected metabolic rate or if this basic measurement of physiological cost was maintained across 24-hours. Following various temperature treatment exposures for five weeks, and inclusion and removal of daily light cues during respirometry, I found that epaulette sharks maintained their routine metabolic rate regardless of seasonal and daily fluctuations in water temperature. Furthermore, all sharks demonstrated a distinct diel pattern of metabolic rate increasing by 1.7-times at night than during the day, indicating this species is crepuscular/nocturnal in nature. This diel rhythmicity of metabolic rate persisted regardless of water temperature, indicating epaulette sharks have a large circadian influence on their physiology, and perhaps perform some version of sleep or torpor during the day as an energy saving mechanism.

Beyond the costs of daily environmental fluctuations on physiology, life history costs such as growth, maturation, and oviparous (egg-laying) reproduction are also important aspects of the energetic budget of epaulette sharks. Therefore, in **chapters 3 and 4**, I studied how two energetic estimates can be used in epaulette sharks to understand long term physiological costs across life history stages. In **chapter 3**, I measured two estimates of body condition as potential proxies for whole body energetic changes and to potentially reflect changes in key energy stores and sinks (*e.g.,* the liver and gonads) from newly hatched neonates up to females in various stages of egg production. I assessed both a classic Fulton's condition factor and a girth condition analysis metric on both captive and wild sharks and determined that generally body condition decreases from neonates to juvenile stages, reflecting the usage of residual endogenous yolk from hatching and liver stores during early growth. Additionally, I found that mature females had higher body condition than males, and that with fine-scale measurements of mature female captive sharks, body condition changes across egg production are discernible. Finally, I found that incorporating girths into body condition analysis is valid for sharks and that it may improve our estimates by incorporating girths in key areas of energy stores not well represented by condition factor only incorporating length and mass measurements.

Body condition may be a good representation of whole-body energetic status; however, in physiological terms, metabolic rate is one of the most widely assessed measurements of aerobic energetic expenditures. Indeed, by measuring the oxygen uptake rates of an individual over time, we can estimate organismal oxygen demand as a proxy for all aerobic reactions occurring. However, to date, most metabolic physiology studies in Chondrichthyans focus on environmental influences and do not address the effect of reproductive effort on metabolism. In **chapter 4**, I assessed if female epaulette shark metabolic rate changed across the 19-day female egg production cycle to determine potential physiological changes, however I did not find any evidence that female reproduction influences routine metabolic rate. When energetic estimates from chapter 3 body condition was compared to metabolic estimates from chapter 4, there was no relationship between the two metrics. This indicates that although both approaches reflect organismal energetics, they are not comparable and that future studies should consider what the chosen metric is truly reflecting.

Now that I have established the life history energetic costs of epaulette sharks under current day conditions in the first half of my thesis, I now focus on incorporating climate change-mediated ocean warming effects. In **chapter 5**, I aimed to determine the upper thermal tolerance of wild epaulette sharks using a critical thermal maximum (CT_{max}) protocol. I hypothesized that life stages that were expending energy into growth or reproduction, such as juveniles and mature adults, would have lower tolerances than other groups such as non-reproducing subadults. A range of juveniles, subadults, and mature adults were temporarily collected from the Heron Island reef flat on the southern Great Barrier Reef, and I used a thermal ramping assay in combination with loss of righting reflex as an end point marker of upper tolerance. The results indicated that CT_{max} did not differ between sex or life stages, and that all groups had similar thermal tolerances. I was unable to find key vulnerable life stages on the reef flat such as newly hatched neonates or females that were actively encapsulating egg cases at the time of the trials. However, this research was conducted during the peak epaulette shark reproduction season, so other reproductive endocrinological activities (*e.g.,* folliculogenesis and spermatogenesis) were occurring in mature adults.

CT_{max} is a widely used physiological marker of thermal tolerance, however it involves an acute exposure, where a chronic exposure on the order of weeks to months may have detrimental effects not reflected in a thermal ramping assay. In **chapter 6**, I exposed 27 newly deposited epaulette shark egg cases to three temperature treatments of 27, 29, and 31°C across the three-to-five-month development period to determine if there were chronic thermal effects on critical early life stages. I found that sharks at the highest temperatures, which was representative of a 2100 ocean warming scenario, hatched more quickly, slightly underweight, undernourished, and with lower metabolic rates, indicating physiological impairment was beginning to occur at this temperature. Overall, I defined the *pejus* temperature (*i.e.,* when biological traits start to become impaired) of development for epaulette sharks between 29-31°C, which is predicted to occur on the southern Great Barrier Reef by 2100 under a current day emissions scenario. Furthermore, in **chapter 7**, I discuss supplemental data from this thesis that shows a preliminary indication that female reproduction shuts down at 28°C, the current summer average water temperature for the Great Barrier Reef.

Overall, in my thesis I have established the current day physiological costs of epaulette sharks in relation to water temperature and life history stages. I have assessed various methods of non-lethally assessing energetics in a taxon that is globally imperilled and generally requires non-lethal research methods. Finally, my thesis has investigated how future ocean warming will likely negatively impact two particularly vulnerable life stages of early development and female adult reproduction. These findings to my knowledge are the first fully inclusive assessment of ocean warming effects across life history stages of a Chondrichthyan species. For epaulette sharks and other benthic structure-dependent species that to our knowledge do not undertake large movements or migrations, my findings are concerning, as epaulette sharks are probably unlikely to move south to cooler areas as ocean warming ensues. Here, I propose these findings on epaulette sharks as a model for other coastal and tropical ectothermic Chondrichthyans that currently live near their thermal optima. More research on these questions in this threatened taxon in the future will continue to improve our understanding of basic biology and physiology of these ecologically, economically, and culturally important fishes in relation to climate change conservation, management, and policy efforts.

Table of Contents

Acknowledgements i

Statement of Contributions iii

Thesis Abstract iv

List of Tables 1

List of Figures 2

Chapter 1: General Introduction 4

1.1 Introduction 4

1.2 Climate change and elasmobranch life history 5

1.3 Epaulette sharks as an indicator elasmobranch 8

1.4 Thesis aims 9

Chapter 2: Diel rhythm and thermal independence of metabolic rate in a benthic shark 11

2.1 Summary 11

2.2 Introduction 12

2.3 Materials and methods 14

2.4 Results 20

2.5 Discussion 24

Chapter 3: Non-lethal assessment of ontogenetic shifts in energetics through body condition in large-bodied fishes 30

3.1 Summary 30

3.2 Introduction 31

3.3 Materials and methods 33

3.4 Results 38

3.5 Discussion 43

Chapter 4: The effects of epaulette shark (*Hemiscyllium ocellatum*) oviparity on metabolic physiology 50

4.1 Summary 50

4.2 Introduction 51

4.3 Materials and methods 53

4.4 Results 57

4.5 Discussion 61

Chapter 5: The upper thermal limit of epaulette sharks (*Hemiscyllium ocellatum*) across three life history stages, sex, and body size 66
5.1 Summary 66
5.2 Introduction 67
5.3 Materials and methods 69
5.4 Results 74
5.5 Discussion 78
Chapter 6: Future thermal regimes for epaulette sharks: growth and metabolic performance cease to be optimal 83
6.1 Summary 83
6.2 Introduction 84
6.3 Materials and methods 87
6.4 Results 91
6.5 Discussion 97
Chapter 7: General Discussion 104
7.1 Current-day thermal physiology 104
7.2 Non-lethal estimates of elasmobranch energetics across ontogeny 106
7.3 Thermal bottlenecks across elasmobranch life history stages 108
7.4 Conclusions and future directions 114
References 120
Appendices 141
Appendix A (Chapter 1 supplementary materials) 141
Appendix B (Chapter 2 supplementary materials) 145
Appendix C (Chapter 3 supplementary materials) 153
Appendix D (Chapter 4 supplementary materials) 168
Appendix E (Chapter 5 supplementary materials) 178
Appendix F (Chapter 6 supplementary materials) 183

List of Tables

Table 2.1. The treatment acclimation temperatures and photoperiods (NP= no photoperiod) used during respirometry across the study 18

Table 2.2 Ten generalized additive mixed models (GAMM) assessing change in metabolic rate estimates (as $\dot{M}O_2$) across a 24-hour trial 20

Table 3.1. Life history stage classification of epaulette shark based off age in days (neonates) or sex-specific total lengths at maturity reported in Heupel *et al.* (1999) 35

Table 3.2. Coefficients of the length-weight relationship of epaulette shark 38

Table 4.1. Individual female reproductive cycle data means of the cycle length, egg case encapsulation time, intra-cycle time, total length, and mass. 58

Table 5.1. Life history stage classification of epaulette sharks (*H. ocellatum)* from sex-specific total lengths and clasper lengths at maturity, as reported in Heupel *et al.* (1999) 72

Table 5.2. The mean critical thermal maximum (CT_{max}) for each life history stage and sex 74

Table 7.1. A summary table of the effects of ocean acidification (OA) and ocean warming (OW) studies and findings on epaulette sharks 119

List of Figures

Figure 1.1. The relationship between rearing temperature and incubation time (in days) of 28 oviparous chondrichthyan species 6

Figure 2.1. A representative $\dot{M}O_{2Rest}$ trace from a shark in a 24-hour respirometry trial 21

Figure 2.2. Resting metabolic rate estimates and GAMM (generalized additive mixed model) predicted fits over 24-hour trial periods and the respective temperature and photoperiod treatments. 22

Figure 2.3. Boxplots of mean, minimum, maximum, and diel scope of $\dot{M}O_{2Rest}$ across treatments 23

Figure 3.1. The epaulette shark growth curve between total length and mass 39

Figure 3.2. The body proportions of epaulette sharks across ontogeny 40

Figure 3.3. Four girths and girth condition analysis across life history and female reproductive stages of laboratory-maintained epaulette sharks 41

Figure 3.4. Relative condition factor and girth condition analysis across total length 42

Figure 3.5. The linear relationship between relative condition factor and girth condition analysis across life history stages 43

Figure 4.1. A schematic of the female epaulette shark egg production cycle 54

Figure 4.2. Metabolic rate across mass by female reproductive status 59

Figure 4.3. Metabolic rate means by female reproductive status 59

Figure 4.4. Mean reproductive hormone concentrations across female reproductive status 60

Figure 4.5. Mean haematological parameters of haematocrit, haemoglobin concentration, and mean corpuscular haemoglobin concentration across female reproductive status 61

Figure 5.1. Male epaulette shark total length verses average inner clasper length to assess maturity 72

Figure 5.2. Uncontrolled experimental conditions that could impact CT_{max} 75

Figure 5.3. Boxplots and linear regression of the mean CT_{max} across life history stages, sex, and body mass 76

Figure 5.4. The proportion of activity type (resting verses active) during CT_{max} trials across life history stages and between sexes 77

Figure 5.5. Ventilation rates (gill beats per minute) of epaulette sharks across CT_{max} assays between life history stages and between sexes 78

Figure 6.1. The growth rate, yolk-sac consumption rate, and embryonic oxygen uptake, over the *in ovo* incubation period at 27, 29, and 31 °C 92

Figure 6.2. Mean incubation time to hatching (days) and time of first exogenous feeding (post-hatch days) across three treatment temperatures of 27, 29, and 31°C 94

Figure 6.3. Mean mass, total length, and Fulton's condition factor at hatching across three temperature treatments of 27, 29, and 31°C 95

Figure 6.4. Boxplots of the $\dot{M}O_{2Rest}$, $\dot{M}O_{2Max}$, aerobic scope, and recovery time from $\dot{M}O_{2Max}$ for neonates across three rearing temperature treatments of 27, 29, and 31°C 97

Figure 7.1. The mean day time routine metabolic rate from the current thesis chapters 2,3, & 6, Routley *et al.* (2002), and Heinrich *et al.* (2014) across water temperature and life history stages 105

Figure 7.2. The linear relationship between body condition metrics girth condition analysis and relative Fulton's condition factor assessed in Chapters 3 & 5, and metabolic rates from Chapters 4 & 5 108

Figure 7.3. The daily mean water temperature from the southern and northern Great Barrier Reef 109

Figure 7.4. The cycle time from one clutch of egg cases to the next in days across time in captivity for three female epaulette sharks 112

Figure 7.5. The predicted shortening of the annual female reproductive thermal window and *in ovo* embryonic development time for epaulette sharks under ocean warming scenarios 113

Chapter 1: General introduction

Related publication

Wheeler, C. R., Gervais, C. R., Johnson, M. S., Vance, S., Rosa, R., Mandelman, J. W., & Rummer, J. L. (2020). Anthropogenic stressors influence reproduction and development in elasmobranch fishes. *Reviews in Fish Biology and Fisheries*, *30,* 373-386. https://doi.org/10.1007/s11160-020-09604-0

1.1 Introduction

Elasmobranchs (subclass elasmobranchii)—sharks, rays, and skates (Compagno *et al.,* 2005)—are important to aquatic ecosystems but are currently considered one of the most vulnerable classes of vertebrates (Baum and Worm 2009; Ferretti *et al.,* 2010; Ward-Paige *et al.,* 2012), with nearly a third of all species threatened by extinction (Dulvy *et al.,* 2021). Currently, the main threats to elasmobranch populations include overfishing, incidental fishing capture (*i.e.,* bycatch) (Mandelman *et al.,* 2013), and habitat destruction (Ellis *et al.,* 2005), with the latter being increasingly exacerbated by pollution and climate change (Ward-Paige *et al.,* 2012). Given that most elasmobranchs are apex or meso-predators, many are important to the health of their respective aquatic ecosystems (Hammerschlag *et al.,* 2019; White *et al.,* 2012), but also provide significant ecosystem services to countries, in the form of revenue and/or sustenance (e.g., eco-tourism and fisheries) (Gallagher and Hammerschlag 2011; Ward-Paige *et al.,* 2012).

Elasmobranchs, from a life history perspective, are K-strategists, meaning that species are typically long-lived, slow-growing, have a late age of sexual maturity, long reproductive cycles, and produce a low number of large, high-quality offspring (Conrath and Musick 2012). Elasmobranchs also display a diverse array of reproductive strategies, starting with internal fertilization, followed by a dozen reproductive modes including both oviparity (egg-laying) and viviparity (live-bearing) that vary in terms of maternal nutritional input and developmental location (i.e., internal vs. external) (Clark and Von Schmidt 1965; Dulvy and Reynolds 1997; Ebert et al., 2007). Each mode is associated with different costs and benefits embryonically and maternally, which, in turn, influences the potential

susceptibility of certain life history stages to anthropogenic impacts (Dahlke et al., 2020).

The wide range of elasmobranch reproductive modes likely contributes to species-specific differences in their vulnerability to anthropogenic stressors across all life stages. Thus, some elasmobranchs cannot reproduce quickly enough to counteract fishing pressure (Gallucci *et al.,* 2006) or potentially other detrimental human impacts like habitat degradation or climate change. Indeed, understanding life history traits is vital for evaluating and forecasting population changes and can result in more effective management and conservation strategies for imperilled species (Gallucci *et al.,* 2006). Particularly, understanding fecundity and early developmental influences as well as identifying essential habitats are all critical for estimating recovery rates (White *et al.,* 2012). This information allows management authorities to account for differences between species when conducting vulnerability assessments and managing ecosystems to protect declining populations (Field *et al.,* 2009; Hare *et al.,* 2016). However, there remains a paucity of research on reproduction, life history traits, and the physiological energetics (*i.e.,* how much does it cost an organism to exist within a particular life stage) underlying these life stages for elasmobranchs, particularly in the context of environmental change, which makes fundamental management difficult (Awruch *et al.,* 2009; Simpfendorfer *et al.,* 2011).

1.2 Climate change and elasmobranch life history

Increasing ocean temperatures from climate change are already having massive impacts on marine ecosystems worldwide (*e.g.,* Hughes *et al.,* 2017; Fox-Kemper *et al.,* 2021). Given that temperature affects the rate of nearly all physiological and biochemical reactions in ectothermic organisms, temperature will likely have profound effects on many elasmobranchs as climate change continues (Pereira Santos *et al.,* 2021). In the context of life history stage and reproductive vulnerabilities, oviparity may be particularly susceptible to changes in environmental temperatures, as embryos are confined to one location on the benthos throughout development and cannot move if water temperature becomes unfavourable (Chen and Liu 2006; Pretorius and Griffiths 2013). A clear relationship exists between water temperature and embryonic incubation time *in ovo* for

oviparous elasmobranchs, indicating that water temperature is an important factor in embryonic development (Table S1.2; Figure 1.1). Several studies have reported negative effects of elevated temperature on oviparous development, where both tropical and temperate species exhibit increased embryonic mortality at 4–5 °C above ambient (Di Santo 2015; Rosa *et al.,* 2014). On the contrary, in the temperate Port Jackson shark (*Heterodontus portusjacksoni*), +3°C above ambient conditions increased embryonic development rates but did not decrease survival (Pistevos *et al.,* 2015). With only a handful of studies, it is difficult to determine if there is a difference in tolerance to ocean warming scenarios between tropical and temperate embryonic elasmobranchs. Based on the climate variability hypothesis (Stevens 1989), temperate species should tolerate a wider range of temperature; yet more targeted studies that test wider thermal ranges are needed to elucidate whether this hypothesis holds true for embryonic elasmobranch development.

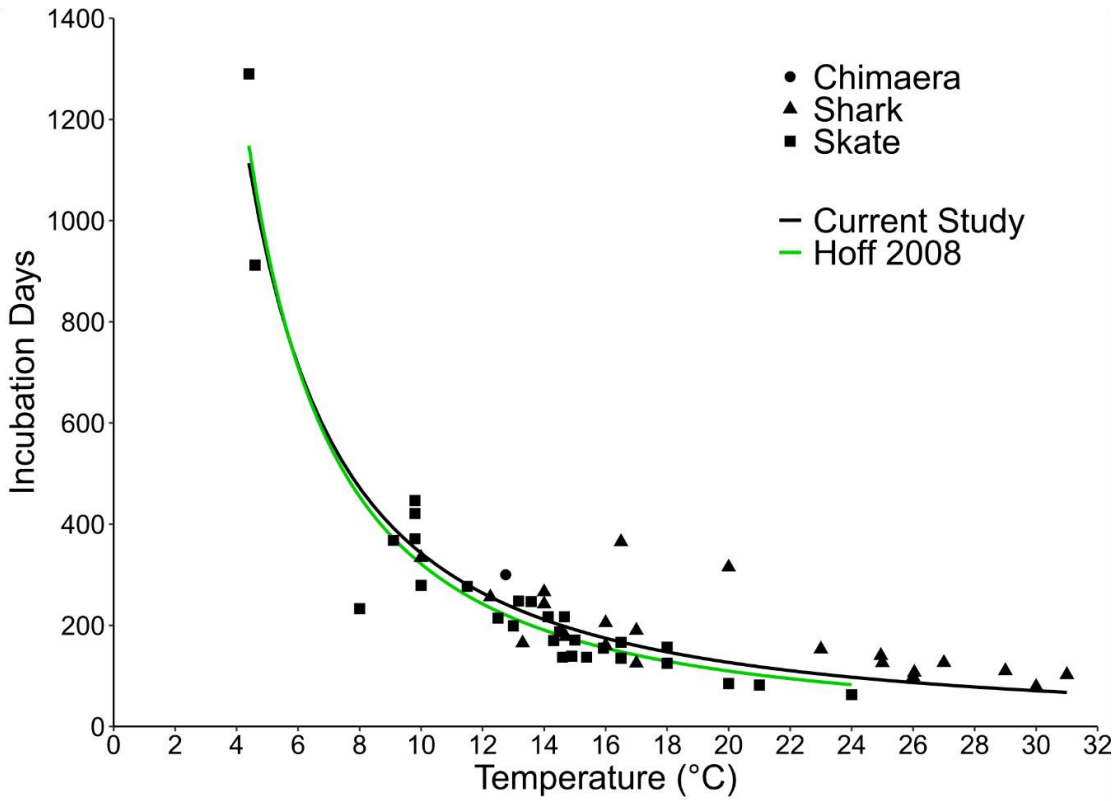

Figure 1.1. *The relationship between rearing temperature and incubation time (in days) of 28 oviparous chondrichthyan species. A nonlinear least squares (nls) regression was fit and compared to the exponential relationship reported in Hoff (2008) (see Table S1).*

After hatching, increased temperature decreases survival (Di Santo 2015; Rosa *et al.,* 2014) and growth rates in neonate and juvenile life stages (Gervais *et al.,* 2018). Of course, in juvenile life stages, unlike embryonic stages, individuals can thermoregulate by moving to cooler areas, which may prove to be physiologically advantageous (Gervais *et al.,* 2018). Furthermore, recent work has reported that, although Port Jackson shark embryonic survival was reduced by 41.7% with a 3°C increase in temperature above ambient, hatchlings from elevated temperatures were able to learn a task more quickly, which could aid in survival under non-ideal thermal conditions (Vila Pouca *et al.,* 2019). These findings indicate that there may be behavioral compensations in surviving offspring that account for the reduced survival from thermal effects within juvenile life stages, but more research is needed in tropical species to determine if these findings are a-pplicable.

Reproduction in adult elasmobranchs could also be affected by warming ocean temperatures, but the impacts may be hard to quantify. Elasmobranchs with annual reproductive cycles are suspected to use temperature as a cue during the reproductive season (*e.g.,* Elisio *et al.,* 2019; Heupel *et al.,* 1999; Tovar-Ávila *et al.,* 2007), and studies have also suggested adult elasmobranchs will use behavioral thermoregulation to reduce viviparous gestation times (Hight and Lowe 2007; Speed *et al.,* 2012; Sulikowski *et al.,* 2016; Wallman and Bennett 2006). For example, in a laboratory experiment, gravid Atlantic stingrays (*Hypanus sabina*) preferred temperatures that were 1°C higher than those of their non-gravid conspecifics; this slight increase in temperature was enough to reduce gestation times of gravid females by approximately 2 weeks (Wallman and Bennett 2006). Similarly, it has been hypothesized that the oviparous Pacific white skate (*Bathyraja spinosissima*) deposits their eggs near black smoker hydrothermal vents, presumably using the elevated temperatures to reduce embryo development times (Salinas-de-León *et al.,* 2018). To date, no studies have investigated the thermal limits of reproduction in elasmobranchs, which could be particularly important data for oviparous species that are typically benthic and are less likely to undertake large-scale range shifts due to ocean warming (Vilmar and Di Santo 2022).

1.3 Epaulette sharks as an indicator elasmobranch

The epaulette shark (*Hemiscyllium ocellatum*) is a small oviparous long-tailed carpet shark endemic to the Great Barrier Reef (GBR), Australia (Dudgeon *et al.,* 2019) that reaches a maximum total length of around one meter (Ebert *et al.,* 2021). This species is found on reef flats of coral cays, coastal intertidal zones, and intermediate depth reefs (up to 50 meters) along the GBR and is likely one of the most well-studied elasmobranchs, with over 40 publications to date. Indeed, we have a broad understanding of this shark's ecology (Heupel and Bennett 1996, 1998, 1999, 2007; Raoult *et al.,* 2018), reproduction (Heupel *et al.,* 1999), early growth and development (Johnson *et al.,* 2016; Payne and Rufo 2012), and physiology (*e.g.,* Chapman and Renshaw 2009; Chapman *et al.,* 2011; Gervais *et al.,* 2018; Heinrich *et al.,* 2014, 2015; Karsten and Turner 2003; Nay *et al.,* 2021; Schwieterman *et al.,* 2021).

The reef flats where epaulette sharks reside experience cyclical hypoxia in relation to the tidal cycle and photoperiod. For example, when a low tide occurs at night, the reef flat becomes completely isolated from the surrounding reef slope for several hours, where animal and coral respiration can lower oxygen levels to 30% of normal saturation (Kinsey and Kinsey 1967). To cope with these extreme environmental fluctuations, epaulette sharks can survive five hours in an anoxic environment (Renshaw *et al.,* 2009), and have a suite of physiological mechanisms to survive low oxygen with no apparent neurological damage (Chapman *et al.,* 2011; Mulvey and Renshaw 2009; Renshaw *et al.,* 2010; Routley *et al.,* 2002; Wise *et al.,* 1998). Indeed, epaulette sharks are thought to be a product of their environment, are in many ways a physiologically tolerant elasmobranch.

In the face of climate change epaulette sharks may act as a "canary in a coal mine" or indicator species, where we question that if this species struggles physiologically with aspects of climate change, how do other less-tolerant oviparous and/or benthic elasmobranchs then fare? Thus far, several studies on climate change effects have been conducted on epaulette sharks (Gervais *et al.,* 2016; Heinrich *et al.,* 2014, 2015; Johnson *et al.,* 2016), where singularly, ocean acidification scenarios (high pCO_2) did not have measurable impact on adult metabolic physiology (Heinrich *et al.,* 2014), foraging and sheltering behavior

(Heinrich *et al.,* 2015), or early growth and development *in ovo* (Johnson *et al.,* 2016). On the contrary, for epaulette shark embryos reared at current-day average summer water temperature (28°C), and a +4°C treatment (32°C), mortality was high (Gervais *et al.,* 2016, 2018). Furthermore, of the few hatchlings that survived, their coloration and pattern was irregular, indicating temperature negatively impacts early growth and development (Gervais *et al.,* 2016). Therefore, incorrect formation of these spots could be detrimental to survival. This research by Gervais *et al.* (2016) served as a starting point for this thesis, indicating there was more to be explored on the topic of thermal biology and physiology in epaulette sharks.

1.4 Thesis aims

In my thesis, I aim to assess ocean warming effects on epaulette shark energetics across ontogeny and reproduction to better understand the future for these and other tropical and coastal elasmobranchs. This overarching question is assessed through three main aims:

1. Understand energetics in this species under current-day upper thermal range (*i.e.,* spring and summer water temperatures) (Chapter 2)

2. Comparison of two non-lethal energetic markers across ontogeny to understand physiological costs under current day conditions (Chapters 3 & 4)

3. Assessment of ocean warming effects across life history stages on acute (Chapter 5) and chronic (Chapter 6) time scales.

In aim 1, I establish basic understanding of how metabolic physiology of the epaulette shark functions under current day conditions, with emphasis on the upper end of water temperatures experienced during the spring and summer months (Chapter 2). Next, considering the imperilled state of many elasmobranch species worldwide, I aimed to understand the energetics of epaulette sharks across life stages and reproduction via two commonly used metrics of energetic status. The first method of energetic assessment is through whole-animal body condition, which can be a proxy for energetic stores (*i.e.,* liver) and sinks (*i.e.,* gonads) (Chapter 3). Second, metabolic rate was assessed across ontogeny and female reproduction to assess real-time costs of maturation and egg production (Chapter 4). Next, future

effects of ocean warming was assessed across life history stages found on a reef flat using a common physiological metric of upper thermal tolerance (critical thermal maximum; CT_{max}) (Chapter 5). Additionally, effects of chronic elevated temperature were studied across *in ovo* growth and development (Chapter 6). Finally, I summarize the findings of these studies to form a full picture of the threats to epaulette sharks and other tropical, coastal, and oviparous elasmobranchs threatened by ocean warming.

Chapter 2: Diel rhythm and thermal independence of metabolic rate in a benthic shark

Associated publication

Wheeler, C. R., Kneebone, J., Heinrich, D., Strugnell, J. M., Mandelman, J. W., & Rummer, J. L. (2022). Diel Rhythm and Thermal Independence of Metabolic Rate in a Benthic Shark. *Journal of Biological Rhythms,* 37(5), 484–497. https://doi.org/10.1177/07487304221107843

Data availability

Data in this manuscript are available from the Research Data Repository at JCU: https://doi.org/10.25903/1n1k-7d65

2.1 Summary

Biological rhythms that are mediated by exogenous factors, such as light and temperature, drive the physiology of organisms and affect processes ranging from cellular to population levels. For elasmobranchs (*i.e.,* shark, rays, and skates), studies documenting diel activity and movement patterns indicate that many species are crepuscular or nocturnal in nature. However, few studies have investigated the rhythmicity of elasmobranch physiology to understand the mechanisms underpinning these distinct patterns. Here, we assess diel patterns of metabolic rates in a small meso-predator, the epaulette shark (*Hemiscyllium ocellatum*), across ecologically relevant temperatures and upon acutely removing photoperiod cues. This species possibly demonstrates behavioral sleep during daytime hours, which is supported herein by low metabolic rates during the day and a 1.7-fold increase in metabolic rates at night. From spring to summer seasons, where average temperatures for this species range 24.5 to 28.5°C, time of day, and not temperature, had the strongest influence on metabolic rate. These results indicate that this species, and perhaps other similar species from tropical and coastal environments, may have physiological mechanisms in place to maintain metabolic rate on a seasonal time scale regardless of temperature fluctuations that are relevant to their native habitats.

2.2 Introduction

The biological clock and its control and regulation of endogenous circadian rhythms is fundamental to physiological systems across eukaryotes (Brown 1972; Dunlap and Loros, 2016; Hastings and Sweeney 1957). It is well established that exogenous light plays a large role in regulating these rhythms, which affect all levels of biological organization from cellular processes to whole-organism and population behaviours (Brown 1972; Foulkes *et al.,* 2016; Reebs, 2002). However, the environment also provides other exogenous abiotic signals, which can also be cyclical. These 'zeitgebers' or time givers may also play a role in regulating endogenous rhythms (Foulkes *et al.,* 2016). For aquatic organisms such as fishes, cyclical patterns in water temperatures are often related to light, where water heats and cools across the day and night hours, respectively, offering another influence on endogenous rhythms (Brown 1972; López-Olmeda *et al.,* 2006; Sánchez-Vázquez *et al.,* 2019). Indeed, for various physiological traits such as metabolic rate (*i.e.,* the sum of all reactions occurring in the body), both light and water temperature are known to be influential (López-Olmeda *et al.,* 2006). For example, the metabolic rate of diurnal animals is typically higher during the day than at night, and the opposite is true for nocturnal animals (Kim *et al.,* 1997; Nixon and Gruber, 1998). Furthermore, there is a direct relationship between water temperature and physiological rate functions in nearly all aquatic ectotherms (Angilletta, 2009); however, our understanding of these two exogenous cues and their relative influence at the whole-organism physiological level is understudied for nocturnal-pattern fishes.

Of the aquatic ectotherms, the elasmobranchs (*i.e.,* sharks, rays, and skates) host an array of species that are crepuscular or nocturnal with diel periods of swimming activity (Byrnes *et al.,* 2021; Kadar *et al.,* 2019; Kelly *et al.,* 2020, 2021; Kneebone *et al.,* 2018; Metcalfe and Butler 1984). However, the ways in which cyclical biotic (*e.g.,* predator-prey interactions) and abiotic (*e.g.,* temperature, dissolved oxygen, salinity, light, tide stage) factors are reflected in their physiology are unclear and likely complex. For example, research on three species of rays (*Glaucostegus typus*, *Himantura australis*, and *Pateobatis fai*) indicated that these meso-predators remain in very shallow areas with sub-optimally warm

temperatures to reduce interactions with potential predators (Vaudo and Heithaus 2013). Lemon shark (*Negaprion acutidens*) diel activity patterns have been found more strongly influenced by light patterns than temperature or body size (Byrnes *et al.,* 2021). Indeed, temperature is the master factor governing most physiological pathways, and this may be via its influence on metabolism (Angilletta, 2009). But in an ecological context, it may be challenging to tease apart other factors that interact with temperature, such as time of day, availability of a heterogeneous environment to facilitate thermoregulatory behaviours (Nay *et al.,* 2021), and predation risk (Vaudo and Heithaus, 2013).

Within elasmobranchs, there are two main respiratory modes, ram-ventilating, where sharks must continuously swim to pass water over their gills, and buccal pumping, in which demersal sharks, skates, and rays use buccal movements to suction water into their mouths and across their gills for oxygenation (Butler and Metcalfe, 1988). The type of respiratory mode used is innately linked to activity patterns, where many ram-ventilating species change the magnitude of their activity in relation to the time of day but always maintain some level of activity for respiratory purposes (Papastamatiou *et al.,* 2018, Shipley *et al.,* 2018). In contrast, buccal pumping species can remain motionless and potentially use a form of sleep during the day and increase activity at night (Kadar *et al.,* 2019, Kelly *et al.,* 2020, 2021). Theoretically, if activity levels increase at night, then metabolic rate should also increase due to the increase in oxygen demand (Whitney *et al.,* 2007). However, only a few studies on elasmobranchs have reported oxygen uptake rates over a 24-hour period or between day and night (Hove and Moss, 1997; Nixon and Gruber, 1988; Whitney *et al.,* 2007) to clearly demonstrate a relationship between time of day and metabolic rate.

The first aim of this study was to characterize diel patterns in metabolism in a tropical benthic elasmobranch species. The second aim was to determine how temperature and photoperiod influence these diel patterns in metabolism. We used the well-studied epaulette shark (*Hemiscyllium ocellatum*), which is a species known for its physiological tolerance to challenging environmental conditions and one that is amenable to captivity (Heinrich *et al.,* 2014, 2016; Wise *et al.,* 1998). Moreover, this species can be found on tidally-isolated, shallow reef flats where a 3-

4°C temperature cycle – influenced by tides and time of day – regularly occurs over a 24-hour period (Nay *et al.,* 2021). We used intermittent-flow respirometry chambers to measure oxygen uptake rates as a proxy for metabolism for each shark. Furthermore, we implemented constant and diel temperature cycles like those experienced by this species during spring and summer. Finally, we acutely removed photoperiod to examine the master factor influencing changes in metabolic rates in this species.

2.3 Materials and Methods

Ethics

All experimental protocols in this study were assessed and approved by the James Cook University Animal Ethics Committee (protocol A2655). Collections were conducted under the appropriate Great Barrier Reef Marine Park Authority (GBRMPA #G19/43380.1) and Queensland Fisheries (#200891) permits.

Animal collection and husbandry

Nine adult epaulette sharks, including four females (69-83 cm total length (TL)) and five males (83-98 cm TL) were collected and used for experimentation. Maturity was assessed based on the 55 cm TL size at maturity for both sexes reported by Heupel *et al.* (1999). Three females were hand-collected with dip nets in shallow water from Magnetic Island (n=1, -19.129041 S, 146.877586 E) and Balgal Beach, QLD, Australia (n=2, -19.021387 S, 146.418124 E) in February and March 2020, respectively. Sharks were transported back to the Marine and Aquaculture Facility Unit at James Cook University (Douglas, QLD, Australia) within two hours of capture in 50l of clean, continuously aerated seawater. An additional five mature males and one female were sourced from Cairns Marine in September 2020 (Cairns, QLD, Australia).

Sharks were habituated to captivity for at least three months prior to experimentation. During habituation, sharks were maintained in same-sex pairs (with one group of three males) in five indoor 1000l round aquaria filled to ~850l, but connected to a shared 5,500l-reservoir with a heater, protein skimmer, bio-filtration, and UV-sterilization. Water quality parameters (pH, nitrites, nitrates, ammonia) were monitored daily for the first three months of introduction to the

system and were subsequently recorded biweekly, given that water quality was stable (Table S2.1). To ensure reservoir and aquaria temperatures were comparable, temperature was monitored within the external reservoir using a sensor that controlled the heater/chiller system and individual HOBO pendant loggers (Onset, USA) attached to the standpipe of each aquarium. Ambient day time lighting in the laboratory consisted of four ceiling mounted light-emitting diode (LED) (35 watt, 3600 lumens, 1210 x 115 x 75 mm LWH) panels evenly distributed across the room, and the light:dark (L:D) cycle was 12:12 hours during the three month habituation and subsequent experimentation. Each aquarium had one large air stone, a lid constructed of 30% light blocking shade cloth to prevent jumping, and a 30 cm diameter by 70 cm long PVC tube was provided as shelter for each shark. All sharks in the study were fed 2% of their body mass, *ad libitum*, three times weekly (6% body mass per week) with fresh frozen prawn, pilchard, and squid, as recommended for small benthic sharks (Janse *et al.,* 2004). Sharks were also supplemented with ElasmoTabs (The Aquarium Vet, Melbourne, AUS) to ensure no mineral or vitamin deficiencies occurred during captivity. Any food not consumed was removed, and the amount consumed by each shark was recorded.

Respirometry

To estimate the routine metabolic rate (RMR) of sharks, oxygen uptake rates ($\dot{M}O_2$) of each shark were measured using intermittent-flow, static respirometry over a 24-hour period. Each respirometry set-up was comprised of three opaque, PVC chambers with baffled ends to allow even water flow and a 15 cm by 8 cm viewing window allowing ambient light into the chamber. Two were small chambers (15 cm in diameter and 82 cm long, 15.5l total volume of the chamber, recirculating pump, and external loop; 10.1- 16.3 respirometry setup:organism volume), and one was a larger chamber (23.5 cm in diameter and 101.5 cm long, 44.6l total volume of the chamber, recirculating pump, and external loop; 22.2-27.9 respirometry setup:organism volume) to accommodate the range of body sizes. Preliminary trials indicated that the chamber size precluded significant movement of the animals, and no differences in metabolic rate estimates were detected due to chamber size. For each trial, the appropriate respirometry chamber was selected and submerged in 850l aquaria within the study system to ensure identical water

quality between holding conditions and trial conditions. Each chamber consisted of a flush pump (small chambers: 1200l hr^{-1}; large chamber: 2400l hr^{-1}) that pumped water from the water bath and one recirculating pump (small chambers: 1200l hr^{-1}; large chamber: 2400l hr^{-1}) that circulated water through an external loop for proper homogenous mixing within the chamber. Oxygen levels were measured every two seconds using an OXROB3 fibre optic probe inserted approximately 5 cm into the chamber proper via the overflow outlet (Bouyoucos *et al.,* 2020a) connected to a Firesting Optical Oxygen Meter (Pyroscience GmbH, Aachen, Germany).

Sharks were fasted 48 hours prior to and throughout trials to ensure metabolic rates were estimated while the sharks were in a post-absorptive state (Heinrich *et al.,* 2014). No other sharks in the system were fed during respirometry to eliminate cueing on food scents from other aquaria through shared circulating water. Upon commencing each trial, individual sharks were carefully introduced into the respirometry chamber prior to the lights turning on (*i.e.,* at 6:00 AM); the system was continuously flushed for the following six hours. Preliminary trials indicated that chamber O_2 levels decreasing immediately upon introducing the shark into the system but then slowly increased to 100% air saturation over the first four hours and remained constant thereafter. As in other benthic shark respirometry studies (*e.g.,* Heinrich *et al.,* 2014, Tunnah *et al.,* 2016), a six-hour habituation period was deemed sufficient.

After the six-hour habituation period, at 12:00 PM, a relay timer was used to intermittently turn off the flush pump (*i.e.,* for 5 minutes in the small chambers, 7.5 minutes in the larger chamber), which was deemed the measurement period. This time interval was long enough to ensure that the decline in O_2 could be detected but short enough such that O_2 levels within the chambers did not decrease below 80% air saturation (Svendsen *et al.,* 2016). Following each of the O_2 uptake measurement periods, the flush pump was turned on for ten minutes, thus returning O_2 levels in the chamber water back to 100% air saturation. These measurement and flush cycles were repeated for 24 hours until 12:00 PM on the following day, totalling 82 or 96 measurement periods (in the large and small chambers, respectively), which ensured a sufficient number of data points for each individual shark. Initially, during the first several respirometry trials, sharks were observed in the chamber every

hour over the 24-hour period to confirm they were at rest during the overnight hours when they are known to be more active (Heupel and Bennett, 1998).

At the end of each respirometry trial, each shark was removed from its chamber, weighed (to the nearest 5g), and then returned to their respective holding aquarium. Sharks consumed food within an hour after removal from the chamber. Empty respirometry chambers were also cycled for 30 minutes before and after each trial to account for microbial accumulation within each chamber, which was later subtracted from the total oxygen uptake rates. To reduce microbial build-up, each chamber was cleaned with a 10% bleach solution, thoroughly rinsed with freshwater, and allowed to air-dry after each trial.

Experimental treatments

Throughout their native distribution range, epaulette sharks experience annual temperatures that average daily between 20 and 28°C (Heupel *et al.,* 1999). To capture physiological changes in the upper end of this temperature range (*i.e.,* from spring to summer), we used treatments progressing from low to high temperatures between 24.5-28.5 and acutely removed photoperiod during the 24-hour trials, as detailed below, to determine how daily or seasonal cycles influence metabolic rates (Table 2.1). The experiments began with a constant 25°C treatment, followed by the introduction of diel cycles where water temperatures were the lowest at 6:00 AM and highest at 18:00 PM to reflect warming and cooling of a reef flat across the daytime hours (Table 2.1). For example, in the 25-28°C diel treatment, water temperature was set to 25°C at 6:00 AM, warming across the day to 28°C at 18:00 PM, and then cooling overnight back down to 25°C (Table 2.1). All water temperature changes between treatments occurred slowly at 0.5°C every other day and sharks were allowed to acclimate for at least five weeks before respirometry ensued (Johansen *et al.,* 2021).

Table 2.1. *The treatment acclimation temperatures and photoperiods (NP= no photoperiod) used during respirometry across the study from August 2020-June 2021.*

Treatment name	Temperature (°C)	Photoperiod (L:D (light:dark))
25°C	25	12:12
25°C X NP	25	0:24
25°C diel	24.5- 25.5	12:12
25-28°C diel	25-28	12:12
25-28°C diel X NP	25-28	0:24
28°C diel	27.5-28.5	12:12
28°C diel X NP	27.5-28.5	0:24

The previously described respirometry method was implemented during each experimental treatment, where trials were repeated at least twice for each temperature treatment, once under the ambient photoperiod (12:12 L:D), and once in complete darkness (*i.e.,* using 80% light-blocking shade cloth and an opaque black tarp) (Table 2.1). The dark photoperiod trials totaled 42 hours of dark exposure (12 hours the night prior to the trial, 6 hours of habituation in the chamber, followed by the 24-hour trial). Sharks were allowed at least one week of recovery time between trials. Sharks were maintained under a 12:12 hour (L:D) photoperiod when not in respirometry.

$\dot{M}O_2$ calculations and previous data

Oxygen uptake rates ($\dot{M}O_2$ in mg O_2 h^{-1}) were calculated as the absolute value of the slope of the linear decrease of oxygen during each measurement period using the *RespiroRS* package in R (Merciere and Norin, 2021; version 4.1.1, R Core Development Team, 2021). Background respiration was less than 5% of shark respiration and was modelled linearly across each trial and subtracted from $\dot{M}O_2$ estimates (Rummer *et al.,* 2016). Oxygen uptake slopes were linear (mean R^2= 0.96), and any uptake rates with $R^2 < 0.90$ were removed from the dataset. $\dot{M}O_2$ values were mass adjusted to a one kg animal to account for the range of masses between sharks (0.91–2.00 kg) using the equation described in Bouyoucos *et al.* (2020a) and a scaling exponent of 0.89 (Jerde *et al.,* 2019):

(1) $\dot{M}O_{2scaled} = \dot{M}O_2 (Mass \times Mass_{scaled}^{-1})^{(1-b)}$

where $\dot{M}O_{2scaled}$ is the mass adjusted RMR, and b is the scaling exponent. Therefore, because we standardized for mass, $\dot{M}O_2$ units are reported as mg O_2 h^{-1}.

Statistical analyses

Ten generalized additive mixed model (GAMM) structures (gamm, *mgcv* package; Wood, 2021; Table 2.2) were performed to assess patterns in RMR over the 24-hour respirometry trial between temperature and photoperiod treatments. Random effects, including sex, shark ID, and trial number for each shark were tested to account for conditioning effects to repeated respirometry (Table 2.2). The first order autocorrelation function (CorAR1) was included in all models to account for temporal autocorrelation from serial $\dot{M}O_2$ sampling. The model with the lowest Akaike information criterion (AIC) value was selected as the best fitting model. For each trial, diel scope (the change in $\dot{M}O_{2Rest}$ between day (minimum) and night (maximum); Figure 1) was calculated using the equation:

(2) Diel scope = $\dot{M}O_{2RestMax} - \dot{M}O_{2RestMin}$

Finally, linear mixed effects models (lme4 package, Bates *et al.,* 2015) with combinations of shark ID, trial number, and sex as random effects were assessed to compare the mean, minimum, maximum, and diel scope of $\dot{M}O_2$ across treatments. Like the GAMM models, the lmer model with the lowest AIC value was chosen for each $\dot{M}O_2$ type (Tables S2.2, S2.3, S2.4, S2.5). All statistical analyses were conducted in R, where results were considered significant at $\alpha < 0.05$.

Table 2.2. *Ten generalized additive mixed models (GAMM) assessing change in metabolic rate estimates (as $\dot{M}O_2$) across a 24-hour trial with a smoother (s(time)) and AR1 function for temporal autocorrelation applied. The fixed effects of the first model and the random effects of the third model were chosen, as it had the lowest AIC value.*

Determination of fixed effects:	**Model structure**	**Log(likelihood)**	**AIC**	**ΔAIC to null model**	**df**
0 (null model)	$\log(\dot{M}O_2) \sim 1$	-1226.5	2465.0	--------	6
1	$\log(\dot{M}O_2) \sim$ s(time)	-931.6	1877.3	587.7	7
2	$\log(\dot{M}O_2) \sim$ s(time) + treatment	-941.9	1999.1	465.9	13
Determination of random effects:				**ΔAIC to model 3**	
3	$\log(\dot{M}O_2) \sim$ s(time) Random= (ID, trial number, sex)	-931.6	1877.3	--------	7
4	$\log(\dot{M}O_2) \sim$ s(time) Random= (ID, trial number)	-934.0	1880.0	2.7	6
5	$\log(\dot{M}O_2) \sim$ s(time) Random= (ID, sex)	-960.4	1932.9	55.6	6
6	$\log(\dot{M}O_2) \sim$ s(time) Random= (trial number, sex)	-1007.6	2027.2	149.9	6
7	$\log(\dot{M}O_2) \sim$ s(time) Random= (sex)	-1011.5	2032.9	155.6	5
8	$\log(\dot{M}O_2) \sim$ s(time) Random= (ID)	-960.4	1930.9	53.6	5
9	$\log(\dot{M}O_2) \sim$ s(time) Random= (trial number)	-1023.9	2057.7	180.4	5

2.4 Results

Of the ten GAMM models (Table 2.2), model three without treatment as a fixed predictor and random effects of individual, trial number, and sex had the lowest AIC value and was therefore selected as the best fitting model (see Table 2.2). Overall, the diel pattern of increased $\dot{M}O_2$ at night and reduced $\dot{M}O_2$ during the day

was unchanged despite changes in temperature and photoperiod cues (Figure 2.2). Moreover, neither temperature nor photoperiod affected minimum, maximum, or diel $\dot{M}O_{2Rest}$ scope (Figure 2.3, see tables S2.2, S2.3, S2.4, S2.5). During the day, $\dot{M}O_{2RestMin}$ was low (59.3 ± 10.2 mg O_2 h^{-1}, mean ± S.E.M) and increased 1.7-fold at night (101.4 ± 12.4 mg O_2 h^{-1}) (Figures 2.3B). Acutely removing photoperiod during respirometry did not change the diel pattern of $\dot{M}O_2$ under any temperature treatment (Figure 2.1). All results in this study were consistently observed in each individual, regardless of sex or potential conditioning from repeated experimentation across time (Figure S2.1).

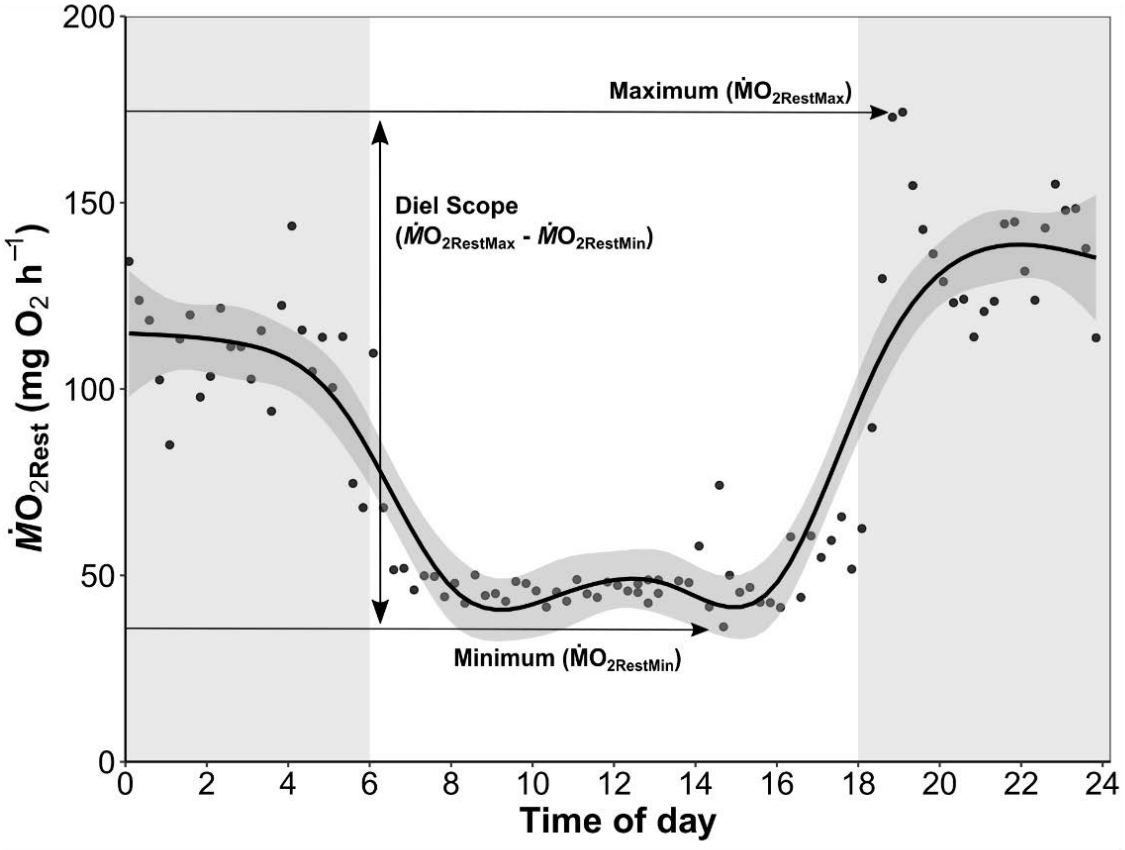

Figure 2.1. *A representative $\dot{M}O_{2Rest}$ trace from a shark in a 24-hour respirometry trial. White and grey areas represent photoperiod of light and dark respectively. Horizontal arrows indicate the minimum and maximum $\dot{M}O_{2Rest}$ GAMM (generalized additive mixed model) estimates from the trial, and the diel scope is the difference between these two extremes.*

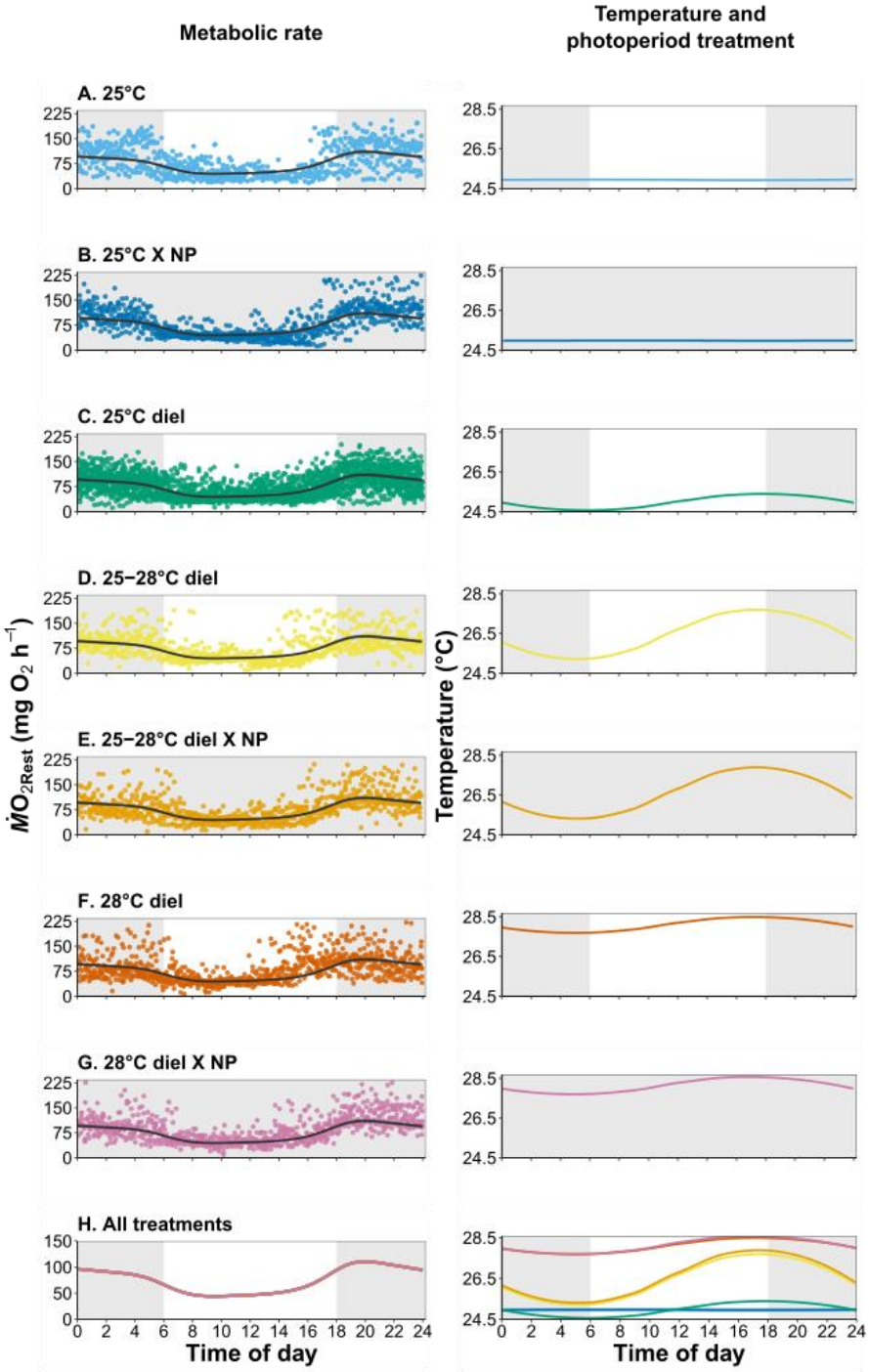

Figure 2.2. *Resting metabolic rate estimates (as $\dot{M}O_{2Rest}$) and GAMM (generalized additive mixed model 1) predicted fits over 24-hour trial periods (left column) and the respective temperature and photoperiod treatments (NP= no photoperiod; right column) where white represents light periods and grey represents dark periods. No significance was found at α= 0.05 in the GAMM model fit between any of the treatment groups.*

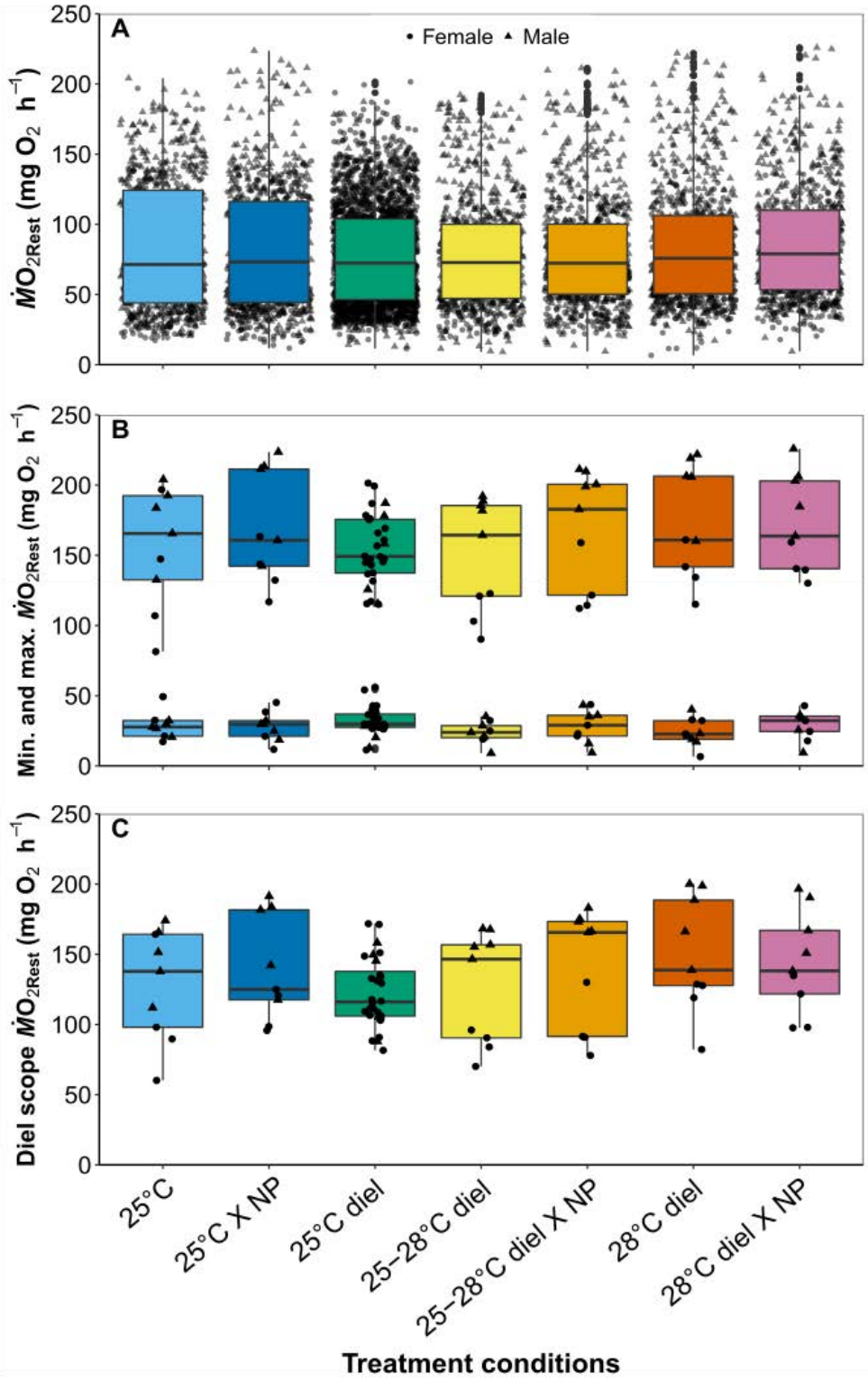

Figure 2.3. *Boxplots of mean (A), minimum (B), maximum (B), and diel scope (C) of $\dot{M}O_{2Rest}$ across treatments. Circular points represent females, and triangle points represent males. Colors correspond to treatment conditions in Figure 2. NP represents no photoperiod, and there was no significant difference between treatments at α= 0.05.*

2.5 Discussion

The 24-hour periodicity of resting metabolic rate (RMR) in epaulette sharks is biologically significant, where RMR nearly doubles at night when compared to daytime hours. Yet, this pattern was unaffected when sharks were acclimated to either of two ecologically relevant temperatures or upon acute photoperiod removal. There are a few examples in the literature documenting similar nocturnal metabolic patterns in sharks. For example, Nixon and Gruber (1988) reported diel metabolic patterns in lemon sharks (*Negaprion brevistostris*). However, this study used a large, static respirometry chamber, where sharks were able to increase their swimming speed/activity, which explained increased metabolic rates at night. Similarly, whitetip reef sharks (*Triaenodon obesus*) exhibit three-fold increases in activity and metabolic rates at night (Whitney *et al.,* 2007). In the little skate (*Leucoraja erinacea*), standard metabolic rate (SMR) follows a nocturnal rhythm as well, with night-time rates estimated to be 3-4 times higher than daytime rates (Hove and Moss, 1997). In the current study, despite the confines of the respirometry chambers and resulting inactivity, epaulette sharks still exhibited marked differences (*i.e.,* nearly double) in RMR between night and daytime hours. Although logistics precluded continuous monitoring of ventilation rates, it is likely that sharks increased ventilation/respiration rates at night despite inactivity, thereby accounting for the increased oxygen uptake rates. We suggest that the increase in RMR at night is related to when this species is actively foraging for food (Heupel and Bennett, 1998). Future studies where sharks are allowed to move freely, such as when using a whole-tank annular respirometry setup (*e.g.,* Lear *et al.,* 2017), would help strengthen the connections between activity type (*e.g.,* hiding, walking, burst swimming, etc.), diel metabolic scope, and abiotic factors.

The oxygen uptake rate ($\dot{M}O_2$) patterns of epaulette sharks over a 24-hour period are remarkably similar to distinct diel ventilation and activity patterns reported for other benthic sharks, including swell (*Cephaloscyllium ventriosum*), draughtboard (*Cephaloscyllium isabellum*), Port Jackson (*Heterodontus portusjacksoni*), and horn (*Heterodontus francisci*) sharks (Bass *et al.,* 2017; Kadar *et al.,* 2019; Kelly *et al.,* 2020, 2021; Nelson and Johnson 1970). Given the significantly lower metabolic rate estimates during the day, our findings also

strongly support the behavioral sleep hypothesis proposed by Kelly *et al.,* (2019, 2020, 2021). Indeed, we observed similarly sluggish behavior, as described by Kelly *et al.* (2019), where individuals were slow to react after being tipped out of shelters during the day, but typically came out of shelters on their own accord once the lights were turned off at night. Furthermore, we measured repeatedly low oxygen uptake rates, particularly between 8:00 and 15:00 hours (Figure 2.2), thus indicating a period of rest. Whether epaulette sharks in this study were, from a behavioral and physiological perspective, truly sleeping or in a state of torpor during the day is unknown. This topic will require further investigation in the future. The mean $\dot{M}O_{2RestMin}$ value across all treatments (58.9 ± 1.2 mg O_2 kg^{-1} h^{-1}, reported as *per kg* animal $\dot{M}O_2$ here for direct comparison to other studies) is remarkably similar to $\dot{M}O_2$ measured during the day in adult epaulette sharks by Routley *et al.* (2002) (63.7 ± 5.2 mg O_2 kg^{-1} h^{-1}; Table 2.3) and Heinrich *et al.,* (2014) (65.2 ± 2.1; Table S2.6). Furthermore, for other elasmobranchs that exhibit buccal pumping during standard metabolic rate (SMR) estimates, reported values range 15.9 to 378.0 mg O_2 kg^{-1} h^{-1} (Table S2.6). While partially dependent on temperature, values average 78.5 ± 17.6 mg O_2 kg^{-1} h^{-1} for temperate species and 112.2 ± 13.2 mg O_2 kg^{-1} h^{-1} for sub-tropical and tropical species (Table S2.6). Interestingly, Carcharhiniformes that buccal pump whilst confined in respirometry chambers, even though they naturally also ram ventilate, generally had higher SMR estimates, despite their inactivity during experiments (Table 2; Bouyoucos *et al.,* 2020b, 2022; Miklos *et al.,* 2003; Tunnah *et al.,* 2016; Whitney *et al.,* 2007). Given that $\dot{M}O_2$ values associated with daytime and/or inactivity are similar between tropical and temperate species, perhaps the metabolic savings of daytime behavioral sleep is similar across benthic buccal/spiracle pumping sharks and skates. More research is needed in this area.

It is unclear how long photoperiod cues need to be removed to interrupt the observed rhythmic pattern of metabolic rate in epaulette sharks, as many vertebrates will continue exogenous circadian rhythms under constant conditions (*i.e.,* no photoperiod) for days to weeks (de Almeida Moura *et al.,* 2017; Reebs 2002). Some of the earliest chronobiology studies in elasmobranchs noted that horn and swell sharks exhibit varying degrees of endogenous control of activity levels after 15 or 18 days of constant dark or light respectively (Finstad and Nelson, 1975; Nelson and Johnson, 1970). Diel activity patterns can be interrupted by changes in

photoperiod in Port Jackson sharks, but not as easily in draughtboard sharks (Kelly *et al.,* 2020). Constant light photoperiod or anesthetization by tricaine methanesulfonate (MS-222) results in diminished diel SMR patterns in the little skate (Hove and Moss, 1997). In the current study, a 42-hour dark exposure during respirometry trials did not affect mean RMR or diel scope. However, the purpose of dark photoperiod trials during this study was to assess whether light cues themselves were causing the diel pattern of metabolic rate, which we found was not the case (Figure 2.2). To tease apart how to remove or shift diel patterns seen here with light cues, the photoperiod should be removed for a longer period, at least on the order of several days to weeks (Nelson and Johnson, 1970; Reed, 2002). More research in this area coupled with exploration of clock genes/cells may help further elucidate the role of the biological clock and circadian rhythms in elasmobranch physiology, which is essentially an unstudied field for this taxon.

Our findings also contribute to best practice respirometry methods for elasmobranchs. In other vertebrates, it is common practice to measure and select $\dot{M}O_2$ data from only the inactive portion of the circadian rhythm as standard metabolic rate (e.g., Angilletta and Sears 2000; Nilsson and Råberg 2001; Van Dyke and Beaupre 2011); however, this is not as common in fishes. Therefore, the strong diel $\dot{M}O_2$ pattern seen in our data is an important factor to consider when assessing metabolic rate as part of a study. Indeed, a mean value alone will not reflect this interesting trend, and this 24-hour pattern is likely often overlooked. Moreover, resting or standard metabolic rate estimates are not necessarily reflected by a single mean value, but rather a pattern of oxygen uptake rates over a 24-hour period (*e.g.,* see Speers-Roesch *et al.,* 2018). Assessment over a full 24-hour cycle allows for diel scope to be calculated, and the shifts in $\dot{M}O_2$ peaks and troughs can indicate if a species is crepuscular or nocturnal or perhaps show treatment effects (*e.g.,* hypoxia, pCO_2, temperature) that may otherwise be masked in using a mean $\dot{M}O_2$. Furthermore, if $\dot{M}O_2$ for a buccal pumping elasmobranch does not exhibit a diel pattern, it may be that optimal unstressed conditions that are needed to estimate SMR may not be met. This means that behavioral sleep may not occur due to the stress of the experiment. In this case, an alternative respirometry chamber design and/or a longer habituation period should be considered. It may be more difficult to achieve such repeatable results – particularly for $\dot{M}O_{2\mathrm{RestMin}}$ – with recently

caught, large, or mobile species. Finally, while it is likely that the minimum $\dot{M}O_{2Rest}$ values reported here represent the true standard metabolic rate (SMR) for epaulette sharks, we conservatively identify all metabolic rates in this study as variations (*i.e.,* minimum, maximum, and diel scope) of RMR, on the basis that sharks were sexually mature and reproducing (Chabot *et al.,* 2016). Our findings add to the growing body of literature that is helping to fine tune methods and techniques that are critical in the fields of conservation and ecological physiology.

Life stage may also play an important role in the trends we observe in metabolic rates. Past studies have already indicated that epaulette shark embryos, neonates, and juveniles are negatively impacted by elevated temperatures (*e.g.,* 27-32°C; Gervais *et al.,* 2016, 2018; Wheeler *et al.* 2021), those that represent current-day summer averages and ocean warming scenarios. For neonates, resting $\dot{M}O_2$ increased in sharks reared at 29°C when compared to sharks reared at 27°C but then decreased in sharks reared at 31°C (Wheeler *et al.* 2021). The thermal effects observed by Wheeler *et al.* (2021) on embryos and neonates contrast the lack of thermal effects in the current study, which could be due to several factors. First, Wheeler *et al.* (2021) included warmer treatments than were used in the current study. Second, early life history stages (e.g., embryos and neonates) are known to have narrower thermal windows for an array of physiological traits, making them more vulnerable than later life stages (Angilletta 2009). Third, studies on the effects of elevated temperatures on early life stages of epaulette sharks were conducted in the laboratory, where embryos did not experience diel fluctuations in abiotic conditions, thus perhaps not providing pre-conditioning, which may be important and is worthy of future investigations.

In contrast to early life stage epaulette sharks reared under controlled laboratory conditions, the adults investigated in this study presumably spent at least 2-6 years exposed to natural fluctuations in abiotic conditions in the wild before captivity (*i.e.,* based on approximate age of maturation in captivity, Wheeler personal observation). This begs the question: how important are fluctuations in abiotic conditions in shaping physiological tolerance? Experiments that exposed epaulette sharks to repeated hypoxia (hypoxic-preconditioning) reported metabolic depression (Routley *et al.,* 2002). Perhaps this species uses similar

strategies for thermal compensation as well. Indeed, other sub-tropical and tropical elasmobranch species have been noted to have low metabolic temperature sensitivities as well, including blacktip reef sharks (*Carcharhinus melanopterus*), sicklefin lemon sharks (*Negaprion acutidens*), bull sharks (*Carcharhinus leucas*), and largetooth sawfish (*Pristis pristis*) (Bouyoucos *et al.,* 2020a, 2022; Lear *et al.,* 2020). This poses interesting questions revolving around mainly coastal, warm water species that experience large diel fluctuations in temperature and how this shapes their physiological responses. Future studies that assess other physiological mechanisms that may be more temperature sensitive, such as muscle dynamics or swimming speed, may help elucidate thermal effects not observed herein on metabolic rate (*e.g.,* von Herbing 2002, Lauder and Di Santo 2016).

On Heron Island, the largest studied population of epaulette sharks (Heupel and Bennett, 2007), year-round average temperatures range 20 to 28°C, with extremes of 16 and 34°C (Nay *et al.,* 2021). Water temperatures across a single day can be homogenous across the partially isolated reef flat, and epaulette sharks do not behaviorally thermoregulate by moving to a preferred temperature (Nay *et al.,* 2021). It is possible that, by not using behavioral thermoregulation, epaulette sharks must use other physiological mechanisms for thermal compensation. In the current study, sharks were given five weeks to acclimate to experimental temperatures, where shorter exposure times may have elicited greater changes in metabolic rates (Johansen *et al.,* 2021). Studies where metabolic rate is assessed across a full annual temperature range while quantifying potential thermal compensation pathways (*e.g.,* tissue citrate synthase and lactate dehydrogenase enzyme activities) may help discern why, in this study, temperature had no measurable impact on metabolic rate.

For epaulette sharks, time of day may have a stronger influence on metabolism than temperature. This may be reflective of their role in their natural environment where they dwell in the shallow reef flats that are subject to dramatic fluctuations in abiotic conditions. Within the context of predator-prey interactions, compensating for sub-optimal temperatures may represent a tradeoff to ensure survival (Vaudo and Heithaus, 2013), as this small, benthic, meso-predator hides during the day to avoid predators, even when water temperatures increase to

potentially sub-optimal conditions. Our findings strongly support the notion that diel patterns in metabolic rate exist and are profound in this taxon, particularly for benthic buccal pumping elasmobranchs. This finding should be considered in future studies assessing metabolic rate in the laboratory. Finally, our findings contribute to the growing literature on this extremely tolerant shark species, where we continue to unveil different aspects of the epaulette shark's ecological physiology to understand adaptations that may be key to how they survive and thrive under challenging conditions.

Chapter 3: Non-lethal assessment of ontogenetic shifts in energetics through body condition in large-bodied fishes

Associated publication

In review.

Data availability

Data associated with this chapter are available upon request and will be made publicly available upon publication.

3.1 Summary

Body condition is an important proxy for overall health and energetic status of fishes. The classically-used Fulton's condition factor requires length and mass measurements, but mass can be difficult to obtain in large species. Span measurements can replace mass for wild pelagic sharks. However, span-calculated condition has not been validated against Fulton's condition factor intra-specifically, across ontogeny or reproduction, or in a controlled setting. We used the epaulette shark (*Hemiscyllium ocellatum*) to track fine-scale body condition changes across life stages, oviparous reproduction, and between methods. We measured four girths, total length, and mass of fifteen epaulette sharks over eighteen months and tracked female reproduction daily. We also collected length and mass data from an additional 72 wild-caught sharks and 155 sharks from five previous studies and two public aquaria to build a growth curve for this species. Even though data were derived from a variety of sources, a predictable growth curve (R^2= 0.990) was achievable, indicating that combining data from a variety of sources could help overcome knowledge gaps regarding basic life history characteristics. We also found that condition factor decreased during early life stages, then increased again into adulthood, with predictable changes across the female reproductive cycle. Finally, we determined that both Fulton's and girth condition analyses were comparable. Outcomes from this study uniquely provide body condition changes across of the complete life history, including fine-scale female reproductive stages and validate the use of girths or spans as a non-lethal whole-organism energetic assessment for large-bodied fishes.

3.2 Introduction

Body condition is a common metric used to assess the overall energetic status of fishes, where changes can indicate energetic or health shifts across ontogeny in relation to growth, development, reproduction, and illness (Cone 1989; Lambert & Dutil 1997, Murphy *et al.,* 1991; Stevenson & Woods, 2006). Long-term energetic patterns can help discern population-level reproductive cycles as well as indicate large-scale environmental patterns that impact body condition (*e.g.,* Abujanra *et al.,* 2009; Brosset *et al.,* 2017; Lyons *et al.,* 2020). Indeed, habitat loss or climate change effects that cause ecosystem imbalances can reduce food sources and therefore shift energetics of individuals (Stevenson & Woods 2006). Broadly, improving our understanding of individual and population level fish conditions ultimately provides an indication of overall ecosystem health.

Given the generally imperilled state of many fish species globally, non-lethal research methodologies have become increasingly popular (Hammerschlag & Sulikowski 2011). These methodologies are even more pertinent for many large-bodied fish taxa (*i.e.,* fishes with body masses on the order of kilograms in adulthood), such as elasmobranchs (sharks, rays, and skates) and Acipenseriformes (paddlefishes and sturgeons). Indeed, non-lethal methods for estimating condition for these fishes may improve our understanding of the energetics of current-day populations and allow for better non-lethal monitoring of these fishes under anthropogenic stressors now and in the future (Hammerschlag & Sulikowski 2011).

Amongst the fishes, body condition is classically assessed using whole animal length and mass and the simplest form of Fulton's seminal equation ($K = (mass/length^3) \times 100$), in which the cubed exponent is a scaling estimate (Fulton 1904). Intra-specifically, if length and mass data are available across a wide range of life history stages and both sexes, sex-specific log-log linear regression coefficients can be estimated, where the y-intercept (*b*) replaces the cube exponent when determining body condition (*i.e.,* relative condition factor, $K_n = ((mass/length^n) \times 100)$; Froese 2006; Le Cren 1951). However, even when body condition can be estimated by length and mass, there can be large inter-specific variations due to differences in body plan (*i.e.,* fusiform versus depressiform) as well as intra-specific variability between life stages, seasons, and populations (Froese

2006, Le Cren 1951). However, despite this, K has endured in fish research for more than a century, partially because of its simplicity and familiarity (Stevenson & Woods 2006). In other organisms, a variety of methods (*i.e.*, using mainly length and mass) to calculate body condition have been assessed, but these ideas are not yet common in fish research (Hayes and Shonkwiler 2001; Krebs and Singleton 1993; Labocha et al., 2014; Peig and Green 2009; Viblanc et al. 2012).

Two other measurements, gonadosomatic and hepatosomatic indices (GSI and HSI respectively), in which the proportion between reproductive tissues or liver mass are assessed as proportion of somatic mass (Rizzo & Bazzoli 2019), have also been used to assess fish energetic status. The gonads are a known energy sink, given that gamete production is an energetically costly process (*e.g.,* Hayward & Gillooly 2011; Martin *et al.,* 2017). Fishes are known to store substantial energy in the liver, which can be used during juvenile growth (*e.g.,* Stallings *et al.,* 2010) or can be mobilized through processes like vitellogenesis to ultimately create yolk in the ovaries during female reproduction (Awruch 2015; Lambert & Dutil 1997). Therefore, both GSI and HSI are good indicators of short-term and seasonal changes in condition related to energy stores, reproduction, and even the influence of environmental factors such as temperature or environmental contaminants (Hoffmayer *et al.,* 2006: Hussey *et al.,* 2009; Lyons *et al.,* 2017; Rizzo & Bazzoli 2019; Weideli *et al.,* 2019). However, sampling to obtain GSI or HSI is lethal, and therefore not feasible for many species (Hammerschlag & Sulikowski 2011), and in many large-bodied fishes such as pelagic sharks, obtaining body mass can be logistically challenging, if possible, at all (Irschick & Hammerschlag 2014). Alternatively, a body condition metric using the sum of spans and length has been developed (Irschick & Hammerschlag 2014). This method aims to reflect changes in body condition without weighing the animal and has been implemented on various large-bodied shark species such as bull (*Carcharhinus leucas*), blacktip (*C. limbatus*), blacktip reef (*C. melanopterus)*, nurse (*Ginglymostoma cirratum*), tiger (*Galeocerdo cuvier*), and white sharks (*Carcharodon carcharias*) (Gallagher *et al.,* 2014; Irschick & Hammerschlag 2014; Merly *et al.,* 2019; Moorhead *et al.,* 2020; Weideli *et al.,* 2019). However, to date, no comparison between this metric and length-mass calculated condition factor has been conducted for a species across all life history stages.

The epaulette shark (*Hemiscyllium ocellatum*) is an oviparous long-tailed carpet shark that is docile, capable of reproduction in captivity, and an ideal candidate for tracking body condition changes across life history stages. We examined newly hatched neonates up to reproducing adults, and we also used fine-scale semi-weekly tracking to quantify body condition changes across the female reproductive cycle. Additionally, we compared K_n and girth condition analysis (GCA, A_{gc}; adapted from Irschick & Hammerschlag 2014) by compiling data on total length, mass, and environmental variables from five other studies and two public aquaria to improve our assessment of the epaulette shark length-mass relationship. Overall, we aim to use epaulette sharks to validate an alternative body condition metric and for this species to serve as a proxy for non-lethal energetic assessment for elasmobranchs and other large-bodied taxa of fishes.

3.3 Materials and Methods

Ethics

All experimental protocols in this study were assessed and approved by the James Cook University Animal Ethics Committee (protocols A2655 and A2739). Collections and sampling were conducted under the appropriate Great Barrier Reef Marine Park Authority (GBRMPA G19/43380.1 and G21/44922.1) and Queensland Fisheries (#200891 and #255136) permits.

Animal collection and husbandry

Six female epaulette sharks that were at least 61 cm total length (TL) to ensure maturity (Heupel *et al.* (1999) reports female maturity above 55 cm TL) were hand collected with dip nets in shallow water from Magnetic Island (n=1, -19.129041, 146.877586) and Balgal Beach, QLD, Australia (n=4, -19.021387, 146.418124) in February and March 2020 respectively. Sharks were transported back to the Marine and Aquaculture Research Facility Unit at James Cook University (Douglas, QLD, AUS) within two hours of capture in 50 liters of fresh seawater with aeration packs to provide oxygen. Furthermore, six mature adults (1F, 5M), and five juveniles (3F, 2M) were obtained from Cairns Marine in September 2020 and June 2021 respectively (Cairns, QLD, Australia).

Sharks were maintained in five 1000l oblong tanks connected to a 5,500l reservoir fitted with a heater, protein skimmer, bio-filtration, and UV sterilization. Adult males and females were segregated into separate tanks, and the five juveniles were maintained in one tank together. The system was maintained at 25°C with a 0.5°C diel temperature change (24.5- 25.5°C over a 24-hour period), to mimic diel changes in water temperature. This water temperature was chosen to promote year-round reproduction, where this species typically follows a seasonal cycle in the wild (Heupel *et al.,* 1999), but will reproduce year-round when maintained at water temperatures experienced during the wild reproductive season (Wheeler, personal observation). Temperature was monitored within the external reservoir by a sensor that controlled the heaters and chillers as well as individual HOBO pendant loggers (Onset, USA) attached to the standpipe inside each tank. Water quality parameters (pH, nitrites, nitrates, and ammonia) were monitored daily for the first month of introduction that sharks were introduced to the system and subsequently checked weekly (Table S0). Additionally, each tank had one large air stone, a lid constructed of 30% light blocking shade cloth, and two PVC pipes provided as shelter. All sharks in the study were fed 2% of their body mass three times weekly (6% body mass per week) of prawn, squid, and pilchard as recommended for small benthic sharks (Janse *et al.,* 2004). Any pieces not consumed were removed and the amount consumed was recorded. Sharks were supplemented with ElasmoTabs (The Aquarium Vet, Melbourne, AUS) to ensure no deficiencies occurred during captivity. Wet mass and total length were measured for each shark every 2-4 weeks throughout the study after 72-hours of fasting.

Captive female reproductive monitoring

Female reproductive monitoring occurred from March 2020 to March 2021, where egg deposition and quality (i.e., wind versus viable yolk sac) was monitored daily. Adult female sharks were measured 2-3 times per week for four girths: (1) posterior of the pectoral fins, (2) anterior of the pelvic fins, (3), anterior of the first-dorsal fin, and (4) anterior of the second-dorsal fin (see the schematic in Figure 3.3). The first two girths were chosen to represent potential changes in liver and reproductive tissue volumes (and thereby energy stores), and the two tail girths were chosen to represent changes in non-hepatic skeletal muscle tissue energy

stores. Sharks were freely resting in the aquaria during these measurements to ensure minimal stress, and girth measurements were accurate to 0.1 cm. Sharks were measured just prior to a feeding event so that all measurements were post-absorptive and standardized to 48 hours after the previous feeding. Next, female sharks were palpated between the pectoral and pelvic fins to determine if egg cases were within the oviducts/uteri. The reproductive cycle was divided into four distinct phases by combining egg deposition timing and palpation information, where a female was classified as resting (*i.e.,* had been reproductively inactive for at least one month), follicular, encapsulating an egg case(s), or within 48-hours post-oviposition following Heupel *et al.* (1999) and Koob and Callard (1999) (see Table 3.1 for details).

Table 3.1*. Life history stage classification of epaulette shark based off age in days (neonates) or sex-specific total lengths at maturity reported in Heupel et al. (1999). Female reproductive stages were sub-divided based off elasmobranch oviparous reproduction reported in Koob and Callard (1999).*

Life stage	Reproductive stage	Determination criteria	Age or total length (TL)
Neonates			Up to 30 days post-hatch
Juveniles			30 days post-hatch to sub-adult lengths
Sub-adult			Males: 53-61 cm TL Females: 55-61 cm TL
Mature female	Resting	Above total length of maturity (Heupel *et al.,* 1999) but not producing egg cases for at least one month.	> 61 cm TL
	Egg case encapsulation and retention	Egg case present in one or both oviduct/uteri, confirmed with post-absorptive palpation.	
	Post-oviposition	Within 48-hours of depositing the last egg case of the cycle.	
	Follicular	The period after the post-oviposition stage and prior to detection of any forming egg cases.	
Mature male			> 61 cm TL

Field sampling

In addition to the captive epaulette sharks, data were also collected from wild sharks during catch and release sampling. Epaulette sharks were sampled at Balgal Beach, QLD (n=12; -19.021387, 146.418124) from May to June in 2021 and 2022 and on the Heron Island reef flat, QLD (n=60; -23.444622, 151.914889) from October to November 2021. Sharks were caught and measured in the same manner as described above. Sharks were photographed for spot ID, and a passive integrated transponder (PIT) tag (Hallprint, AU) was implanted into the dorsal musculature to ensure they could be identified if recaptured. Sharks were all released in excellent condition at the location of capture.

Literature data compilation

To further inform the length-mass relationship and body condition across life history stages, individual total length and mass data were sourced from six epaulette shark studies (Gervais *et al.,* 2018; Heinrich *et al.,* 2014; Nay *et al.,* 2020; Payne and Rufo 2012; Schwieterman *et al.,* 2021; and Wheeler *et al.,* 2021), the New England Aquarium, and the New York Aquarium, where sex, location (captivity vs. wild), and maturity (*i.e.,* if females were producing egg cases, or if males had calcified claspers) were obtained when available. Sharks were categorized into life history stages based off days post-hatch for neonates or otherwise total length from sex-specific total length at maturity data reported in Heupel *et al.* (1999) (Table 3.1).

Isometry assessment

Top-down images of epaulette shark neonates reared in Wheeler *et al.* (2021) and in the current study that were all at James Cook University were used to assess whether body proportions changes across life history stages. From each photo, we measured head (from the tip of the rostrum to fifth gill slit), abdomen (from fifth gill slit to the most anterior part of the pelvic fin), and tail (from anterior pelvic fin to end of caudal fin; Figure 3.2) lengths down the midline using a scale bar in the photo and ImageJ (Schneider *et al.,* 2012). Each body measurement was then standardized as a proportion of TL.

Statistical Analyses

Compiled length and mass data from this study, previous research, and public aquaria contributions were log transformed and fit with four linear mixed effects models (*lme4*, Bates *et al.,* 2015) to allow combinations of fixed effects of sex and location (captivity vs. wild) at the time of the measurements as well as the individual shark as a random effect to account for repeated measurements of captive individuals over time to all be tested (see Table S3.1A for model structures). Rufo and Payne (2012) data were not included in this model, as no sex-specific data were reported. Ultimately, the model with the lowest Akaike information criterion (AIC) value was selected, which was the model including only the random effect of individual shark (model 4, Table S3.1A). We did not perform sex-specific growth curves due to sparse data for animals larger than 70 cm TL, where growth differences are most likely to occur (*e.g.,* Sen *et al.,* 2018). The slope of this linear model was derived (Table 3.2), and the y-intercept (*b* value) was used to calculate a slope-adjusted species-specific relative condition factor (K_n; Froese 2006) where:

$$(1)\ K_n = \text{mass}/\ \text{total length}^{\mathbf{2.782}}$$

Given that *b* for the log-log length-mass relationship was less than 3, this may indicate that epaulette sharks elongate with growth (*i.e.,* they grow longer without significant increases in mass) (Froese 2006). Therefore, we analysed for differences in body proportions across life history stages to assess potential allometric shifts using a log-ratio linear regression (Table S3.2).

Next, the four girth morphometrics were standardized for total length (girth/total length *100) given that all males in the captive portion of the study had longer total lengths and therefore proportionally larger girths. Next, a modified version of span condition analysis, first reported in Irschick and Hammerschlag (2014), was calculated. Given epaulette sharks are a small-bodied docile species, we used standardized girths instead of span measurements in the following modified function to conduct girth condition analysis (GCA):

$$(2)\ A_{gc} = (\text{PPG} + \text{APG} + \text{AFG} + \text{ASG}) \times \text{total length}^{-1}$$

where PPG is posterior pectoral girth, APG is anterior pelvic girth, FDG is anterior first dorsal girth, and SDG is anterior second dorsal girth (see Figure 3.3 for girth

schematic). The four standardized girths (girth x TL^{-1}) were assessed across reproductive and life history stages using mixed linear effects models (*lme4*, Bates *et al.,* 2015), accounting for repeated sampling of captive sharks with each individual shark treated as a random effect (Table S3.3ABCD). Finally, the linear relationship between K_n and A_{gc} was assessed using a linear mixed effects model with an interaction between K_n and life history stage and the individual sharks as a random effect (Table S3.4).

For all linear mixed effects models, pairwise *post-hoc* comparisons were conducted between estimated marginal means (EMMs) of the life history stages using the *emmeans* package (Lenth, 2022). All data met the assumptions of normality, non-multi-collinearity, and homoscedasticity, noting that the mixed-effects models used here are fairly robust for minor violations of these assumptions (Schielzeth *et al.,* 2020). All statistical analyses were conducted in R (version 4.1.1, R Core Development Team, 2021), where results were considered significant at $\alpha = 0.05$.

3.4 Results

Length-mass relationship and scaling

There was an exponential relationship between length and mass, which was highly linear after log transformations of both variables (Figure 3.1, Table 3.2 & S3.1, conditional $R^2 = 0.99$). Overall, the body proportions assessed were fairly constant across life history; there was a slight elongation of the tail after the neonate stage (Figure 3.2, Table S3.2). Furthermore, the *b* coefficient of the length-mass linear model was less than 3 (*b*= 2.78, Table 3.2), also indicating a small elongation and/or decreasing body condition with increasing length (Froese 2006).

Table 3.2 *Slope (a) and y-intercept (b) coefficients of the length-weight relationship of epaulette shark. The form factor $a_{3.0}$ was estimated from Froese (2000) assuming an elongated body shape.*

log10(*a*) ± 95% CI	***a***	***b* ± 95% CI**	**$a_{3.0}$ (form factor)**	**R^2**	**n**
-2.216 ± 0.165	0.109	2.782 ± 0.097	0.00513	0.990	318

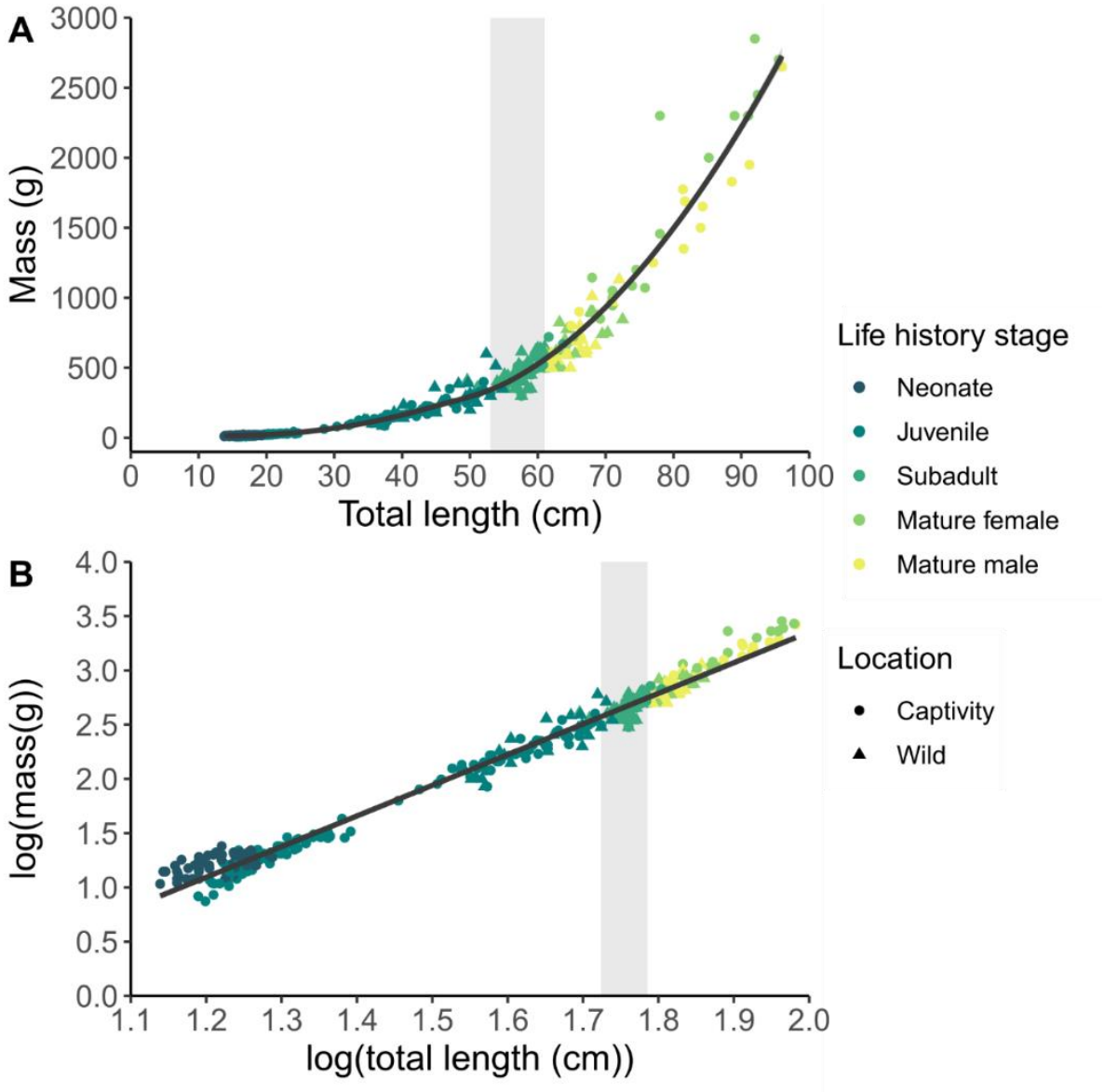

Figure 3.1 *(A) The epaulette shark growth curve between total length (cm) and mass (g) observations from 245 individual sharks, 318 data points, and eight sources (current study, five previous studies, and two public aquaria). (B) The log-log relationship between total length and mass (R^2= 0.990). The grey vertical regions represent the range of length at maturity from Heupel et al. (1999), data point colours represent the life history stage, and the point shape represents the location of the shark at the time of the measurements.*

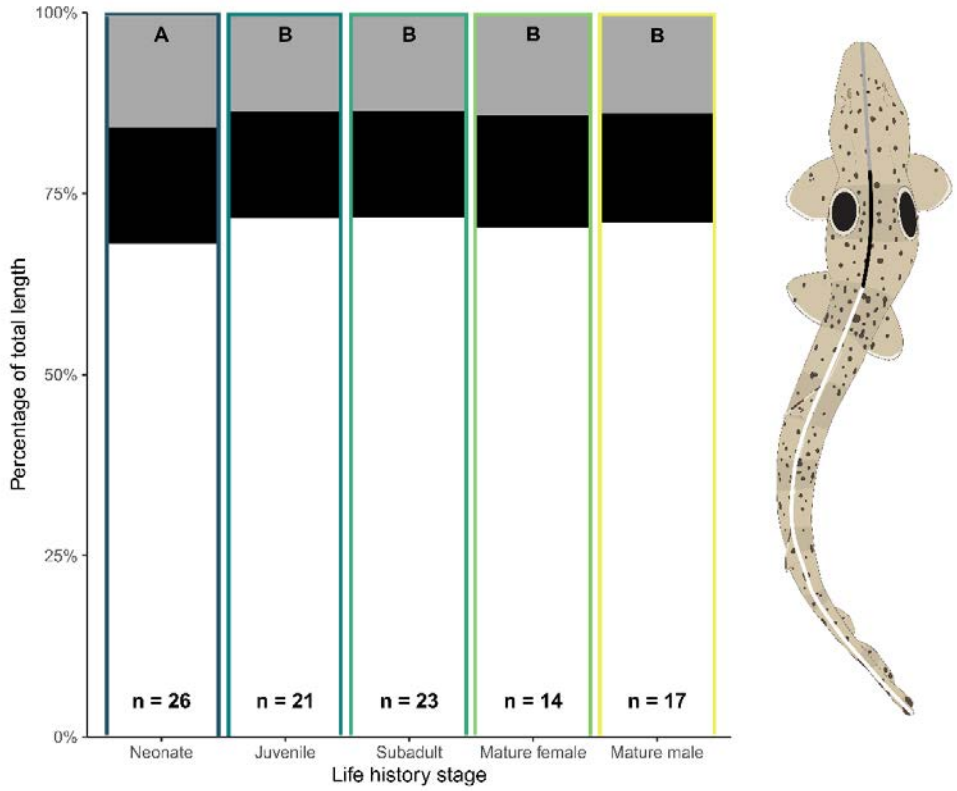

Figure 3.2 *The head (grey), abdomen (black), and tail (white) proportion of total length across epaulette shark life history stages. Outlining colours correspond to life history stages. Differing letters in each category represent statistically significant differences in proportions between life stages at α = 0.05.*

Life history stages and girth changes

For pectoral and pelvic standardized girths (PPG and APG), neonates and reproducing females had the highest values (Figure 3.3AB). Indeed, these girths were high after hatching, decreasing into the juvenile life stage, and increasing into adulthood. Resting female pectoral and pelvic girths increased through folliculogenesis, peaking during egg encapsulation, then decreased after both egg cases were deposited (Figure 3.3AB, Table S3.3AB). Mean male pectoral and pelvic girths were comparable to juveniles and resting female girths (Table S3.3AB, Figure 3.3AB). Both tail girths (AFG and ASG) were high in neonates, then decreased into the juvenile stage, and then for the first dorsal fin girth, increased into adulthood

(Figure 3.3CD, Table S3.3CD). Overall, from summing these girths and calculating A_{gc}, this condition metric was highest in neonates and reproducing females, highlighting that small body condition changes occur across the egg production cycle (Figure 3.3E, Table S3.3E). Male A_{gc} did not differ from neonates, juveniles, or any phase of female reproduction (Figure 3.3E, Table S3.3E).

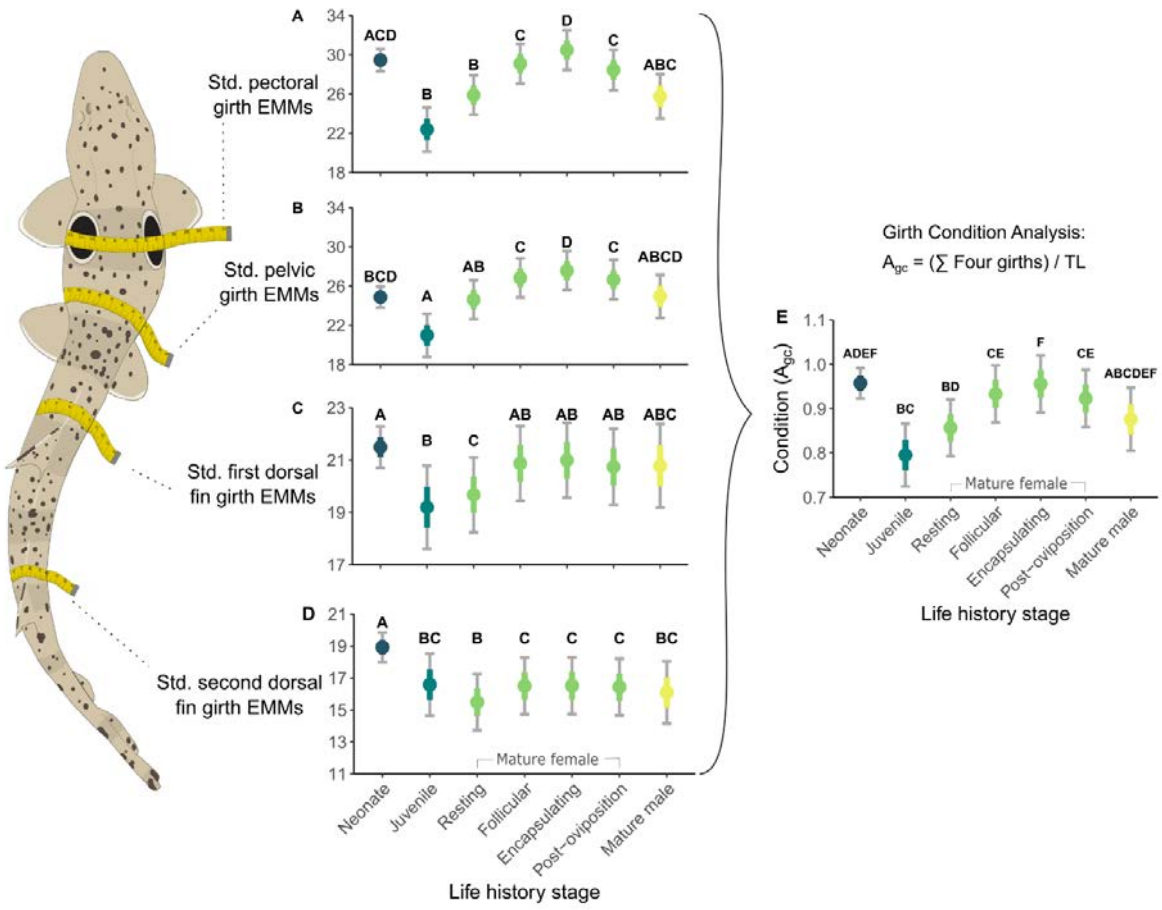

Figure 3.3 *The changes in the estimated marginal means (EMMs) of four girths (panels A, B, C, and D) and condition (A_{gc}, panel E) across life history and female reproductive stages of 15 laboratory-maintained epaulette sharks. The coloured points and bars represent the EMMs and standard error, and the grey error bars represent the 95% confidence intervals. Differing letters represent significant differences at α = 0.05, and NS represents no significance between any groupings.*

Condition factor indices K_n and A_{gc}

Both K_n and A_{gc} were high in neonates, decreased into the juvenile stage, and then increased after subadult ranges into adulthood (Figure 3.4AB). This trend was more prominent in K_n, as the dataset was more robust for this metric, but a similar pattern was still evident in A_{gc} (Figure 3.4). Finally, there was a moderately positive linear relationship between K_n and A_{gc} (conditional R^2= 0.68), where the slope of the relationship only differed between juveniles and adult males (Figure 3.5, Table S3.4, Figure S3.1).

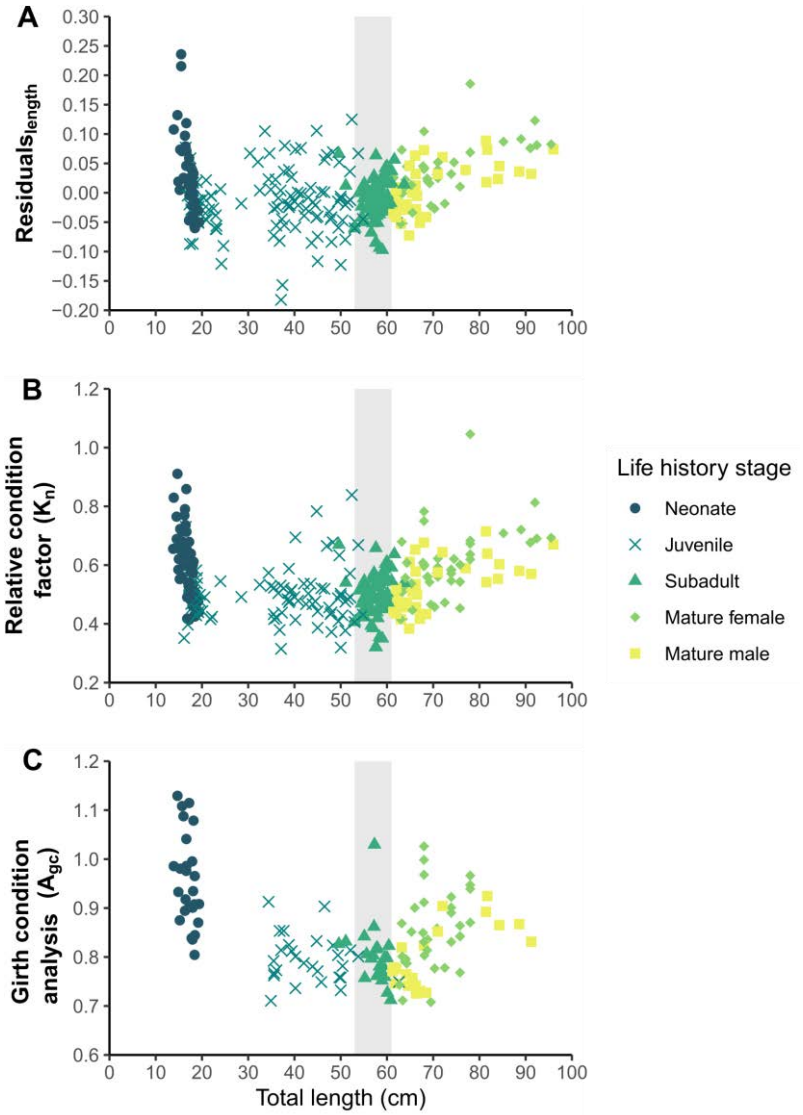

Figure 3.4 *(A)The residuals from the log-log linear mixed model regression of length and mass, (B) the relative condition factor (K_n) (C) and girth condition analysis (A_{gc}) across total length (cm). The grey vertical regions represent the range of length at maturity reported in Heupel et al. (1999), and the data point colours and shapes represent the life history stage.*

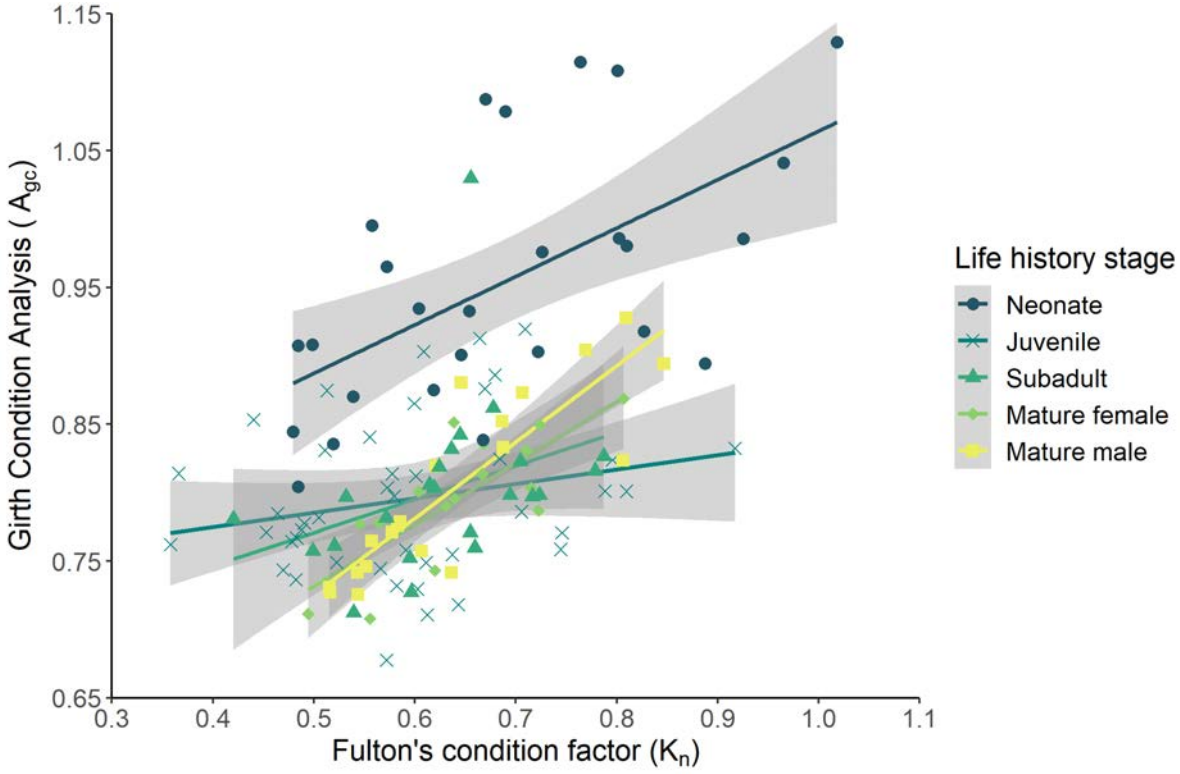

Figure 3.5 *The linear relationship (and 95% confidence interval) between relative condition factor (K_n) and girth condition analysis (A_{gc}) across life history stages. Data point colours and shapes represent the life history stages. The slopes of the fits only differed between juveniles and adult males (see Table S3.4, Figure S3.1)*

3.5 Discussion

Body condition is a common and important metric for assessing energetics and overall health in fishes and relates to energy content and stores of an individual (Lambert & Dutil 1997). Here we established a growth curve for a model oviparous shark, and then assessed two body condition metrics across a complete range of life history stages and reproductive stages. Data compiled from the current study, five previously conducted studies on epaulette sharks, and animals from two public aquaria produced a well-correlated exponential growth curve from 245 individuals (Figure 3.1). The log-log length-mass model fit coefficients reported herein indicate that epaulette sharks have slight negative allometry across ontogeny (Table 3.2: b= 2.78 ± 0.097; where b= 2.5 - 3.5 indicates isometry; Froese 2006), and that this species has an "elongated" body plan (Table 3.2, $a_{3.0}$ = 0.00513; Froese 2006). The epaulette shark b coefficient here is similar to estimated values for other

hemiscylliid sharks, such as the Arabian carpet shark (*Chiloscyllium arabium, b*= 2.372-2.588; Alhajji *et al.,* 2022), the grey bamboo shark (*C. griseum, b*= 2.56-2.83; Kishore Kumar *et al.,* 2021), the whitespotted bamboo shark (*C. plagiosum*, *b*= 2.51-2.93; Kishore Kumar *et al.,* 2021), and the brownbanded bamboo shark (C. punctatum, *b*= 2.81-3.21; Pattarapongpan *et al.,* 2021). Our estimates of epaulette shark body proportions were different in neonates compared to every other life history grouping, where neonates had disproportionally larger heads and abdomens, indicating some elongation occurs during the transition to the juvenile stage (Figure 3.2). Additionally, we also noted a decrease in body condition from neonates to juveniles (Figure 3.3 & 3.4), which could also be a factor influencing estimates of *b* than were less than three (Froese 2006). Whole body isometry is likely the rule and allometry the exception in elasmobranchs, where most length-mass relationships for elasmobranchs report *b* values between 2.5-3.5 (Irschick *et al.,* 2017; Kishore Kumar *et al.,* 2021; Motta *et al.,* 2014). However, morphological features such as fin proportions do show allometric growth in some species (*e.g.,* Ahnelt *et al.,* 2019; Fu *et al.,* 2016; Irschick and Hammerschlag *et al.,* 2015). These ontogenetic shifts are potentially linked to changes in swimming kinematics and/or feeding behaviour (Ahnelt *et al.,* 2019), but more research in this area is required.

Of the four girths assessed, the pectoral and pelvic girths should exhibit the largest changes across ontogeny. The high pectoral and pelvic girths in neonates reported herein therefore reflect post-hatch endogenous yolk reserves and the large liver size (Figure 3.3AB, Lechenault *et al.,* 1993). These girths then decreased as sharks expended energy growing into juveniles (Figure 3.3AB). Both tail girths also decreased between neonate and juvenile stages, indicating that growth is a costly process during which time energy stores from both the liver and skeletal muscle may be mobilized as fuel (Figure 3.3CD). The smaller changes observed within the two tail girths could reflect changes in skeletal muscle energy stores (*e.g.,* glycogen) and the subsequently affected water content (Spargo *et al.,* 1979). Another explanation for changes in tail girths during the early stages could be the transition from very limited body movement in the final stages of development *in ovo* and furthermore reduced activity after hatching when endogenous yolk stores may inhibit foraging and thereby activity. Then, as late-stage neonates/juveniles begin foraging, activity increases, thus decreasing tail girths via exercise. Overall, during

neonatal and juvenile stages, length increased disproportionally to mass (Figure 3.1A), which is reflected in decreasing body condition (Figure 3.3E). In other fishes, HSI also decreases when neonates transition to juveniles (Corsso *et al.,* 2018; Hussey *et al.,* 2009, 2010; Lyons *et al.,* 2020). In the Brazilian sharpnose shark (*Rhizoprionodon lalandii*), but not the dusky shark, condition factor decreased as HSI decreased during this early life stage transition (Corsso *et al.,* 2018, Hussey *et al.,* 2009). Perhaps the differences in body plans between Carcharhinid sharks and the epaulette shark explains why the condition factors assessed here are likely good tools for detecting early life stage HSI shifts when this was not the case in dusky sharks (Hussey *et al.,* 2009).

Within female reproduction, both pectoral and pelvic abdominal girths increased when females transitioned from resting to reproducing stages (Figure 3.3AB), reflecting an increase in abdomen volume caused by changes in the reproductive tract (*i.e.,* increase in ovarian and oviducal gland volumes). Indeed, the increase in pectoral girth during the two to three week-long reproductive cycle is well explained by the presence of large ova in the ovaries and the 2-4-fold increase in oviducal gland volume reported in Heupel *et al.* (1999), both located in the same region as these girth measurements. In adult elasmobranchs, females generally have larger livers and consequently HSI, which is due to vitellogenesis, which is the process whereby the liver creates lipoproteins that are used for oocyte formation within the ovaries (Awruch *et al.,* 2008; Capapé *et al.,* 2014; Chen and Lui 2006; Craik 1978; Estalles *et al.,* 2009; Kousteni and Megalofonou 2020; Rossouw 1987). Prior to the reproductive season, HSI increases, then decreases when reproduction ensues, as stored hepatic energy is mobilized, mainly vitellogenesis (Awruch *et al.,* 2008; Craik 1978; Estalles *et al.,* 2009; Koob and Callard 1999). It is likely that for the reproducing females in this study, the increase in abdominal girths and overall body condition reflects an increase in GSI, masking expected decreases in HSI (Awruch *et al.,* 2008). In several other oviparous shark species, immature females had high HSI values that then decreased upon maturing into reproducing females (Awruch *et al.,* 2008; Craik 1978). For example, in both the oviparous whitespotted bamboo shark (*C. plagiosum*) and the Arabian carpet shark (*C. arabicum*), close relatives of the epaulette shark, female GSI increases during the reproductive season while HSI concurrently decreases, showing a clear reproductive energetic

shift (Chen and Liu 2006, Alhajji *et al.,* 2022). Indeed, it is difficult to discern from our data whether HSI is changing, as the reproductive tract is generally increasing body condition. So, although body condition is increasing, the energetic status in these individuals in relation to hepatic stores may be reduced, as energy is allocated to reproduction.

Both tail girths increased as females transitioned from resting to active reproduction stages (Figure 3.3CD). However, within the reproductive cycle, the tail girths were consistent, indicating that non-hepatic energy use from tail skeletal muscle tissue may be consistent across the cycle or that energy may be stored and unused (Figure 3.3CD). More research assessing the seasonality of various girths in this species or in an elasmobranch with prolonged viviparous gestation may indicate how hepatic versus non-hepatic stores contribute to reproductive costs. Furthermore, research where energetic stores (*e.g.,* amino acids, fatty acids, glycogen) are directly measured across ontogeny may help further elucidate these findings (Speers-Roesch and Treberg 2010).

In oviparous sharks, mature males generally have lower HSI values compared to mature females (Awruch *et al.,* 2008; Chen and Liu 2006; Craik 1978). In epaulette sharks, we found that mature male girths and body condition did not differ from most other life history or female reproductive stages. Indeed, only the male pectoral girth differed from females that were actively encapsulating egg cases (Figure 3.3A). Seasonally, male sharks do show small changes in GSI and HSI (Hoffmayer *et al.,* 2006), although usually less so than females (Awruch *et al.,* 2008; Chen and Liu 2006; Craik 1978). However, because sharks in this study were maintained at water temperatures that promote year-round reproduction, male condition was consistent. Furthermore, a seasonal analysis of condition in wild sharks was not possible here, as we were only able to sample during three months of the year. In the future, more research assessing wild shark condition across a full range of months would better inform cyclical changes in condition related to both male and female reproductive seasonality in this species.

Traditionally, when compared to body condition, GSI and HSI have been the best metrics to reflect short and long-term energetic shifts; however, incorporating targeted girths/spans in key areas (*i.e.,* the body cavity and the tail) may provide an

alternative, non-lethal option with excellent short-term resolution. We were unable to compare our condition data directly to GSI or HSI given the non-lethal nature of the study. Yet, we saw similarities in our condition data with HSI reported over ontogeny and reproduction for dusky sharks in Hussey *et al.,* (2009), which is promising. We hypothesize that the decrease in body condition that occurs when neonates transition to juveniles is due to decreasing HSI; whereas the increase in body condition that occurs when juveniles transition into adulthood reflects increasing GSI related to reproduction (Figure 3.4). It is highly likely that HSI decreases during reproduction in the epaulette shark but was potentially masked in body condition metrics by increasing GSI. More research using non-lethal energetic markers (*i.e.,* fatty acids) and reproductive hormones involved in energy transfer (*i.e.,* vitellogenin and estradiol) in a controlled laboratory setting may help further elucidate the relationship between HSI and GSI during reproduction for this species.

Overall, both K_n and A_{gc} showed similar patterns across ontogeny in comparison to the residuals of the log-log relationship (Figure 3.4A) and each other (Figure 3.4BC), and whilst K_n seemed to better reflect condition changes, this is likely due to having more data than for A_{gc} (Figure 3.4A). In neonatal blacktip reef sharks (*Carcarhinus melanopterus*), the relationship between Fulton's condition factor and a girth condition factor, like the one used in this study also produced a weak linear correlation (Weideli *et al.,* 2019; supplemental materials). We found these two metrics had a moderate linear correlation (Figure 3.5), showing promise that either metric can be used depending on the study design and feasibility. The incorporation of other measurements beyond length and mass into whole-animal condition scoring is not common in fishes. However, in milkfish (*Chanos chanos*), a body condition metric incorporating mass, length, and body height performed better than K_n (Ritcher *et al.,* 2000), indicating that in elasmobranchs and other large-bodied fishes, improving condition calculations with additional measurements that reflect body shape may be useful.

Length-mass relationships and body condition in fishes can vary between populations and under different environmental factors (*e.g.,* water temperature, food availability; Hussey *et al.,* 2009, Lear *et al.,* 2021). Herein, despite sourcing data from a variety of captive and wild epaulette sharks with differing thermal histories

and feeding regimes, mass and length were well correlated, and body condition changes across ontogeny were similar across data sources (Supplement figure S3.2). So, in the case of rare or critically endangered species where data are lacking, compilation from various sources can still provide useful growth curve information pertinent to conservation of imperilled species. Furthermore, defining length-mass relationships provides more accurate species-specific scaling coefficients for condition factor analyses (Froese 2006).

For tracking short and long-term changes in growth, reproduction, and overall health in small-bodied sharks, we recommend A_{gc}. This metric is also a useful tool for identifying the reproductive status of subadult and adult females that are not confirmed to be actively producing egg cases, as the body condition of non-reproducing juveniles and resting female adults is significantly reduced in comparison (Figure 3.3E). In application, it is important to note that we observed significant abdominal swelling post-feeding, therefore it is imperative that measurements are post-absorptive for repeatability and accuracy. This factor, of course, causes issues with wild sharks where feeding status is unknown at the time of capture. For larger sharks that are not as easily measured for girth or spans (*e.g.,* species that are monitored through aerial surveys or without capture), we recommend investigating extensions of laser photogrammetry techniques (*e.g.,* Leurs *et al.,* 2015; Rohner *et al.,* 2015) to estimate spans for condition analysis, but validation would be needed against specimens. In public aquaria settings, long-term tracking of length, mass, and body condition can help quantify growth rates that are difficult to determine from wild sharks, as well as identify potential health issues or insufficient food rationing. Furthermore, batoids are typically assessed with disc width and total length, but given their flat body plan, are not conducive to girths. Therefore, other methods like a combination of disk spans and abdominal thickness should be investigated for this superorder of Chondrichthyans.

The techniques described herein are not only applicable within Chondrichthyan fishes, but large-bodied Teleostei (*e.g.,* groupers), Acipenseriformes (sturgeon and paddlefishes), and Holostei (gar and bowfin fishes). For example, in sturgeon, an order of fishes where most species are threatened in the wild, and where species are not externally sexually dimorphic

(Billard and Lecointre 2001), assessing body condition with girths could aid in non-lethal and non-invasive sex determination and therefore improve detection of spawning timings and locations. Indeed, in lake sturgeon (*Acipenser fulvescens*) there may be slightly higher condition factors and pectoral girths in females, but the difference was not significant (Craig *et al.,* 2009). Perhaps testing and validating the inclusion of multiple girths in condition could be conducted in a sturgeon aquaculture setting where individual sex is known.

Validation of girth/span condition analysis to HSI may help clarify how hepatic and non-hepatic energy stores are used throughout reproduction, where GSI changes here likely masked HSI differences in adults. However, from this research, we provide strong evidence that the A_{gc} condition metric can reflect changes across life history and between sexes; however, large sampling efforts may be required for desired resolution. Overall, the incorporation of standardized and repeatable (*i.e.,* easily and quickly measured in an exact body location in a field setting) span, girth, width, and/or height measurements in condition factor may improve non-lethal estimates of whole-fish energetics. General improvement in estimations and better detectability of small differences of body condition can aid scientists in understanding the life history and reproductive timing of fishes, a key understanding for conservation and management strategies.

Chapter 4: The effects of epaulette shark (*Hemiscyllium ocellatum*) oviparity on metabolic physiology

Associated publication

Unpublished.

Data availability

Data associated with this chapter are available upon request and will be made publicly available upon publication.

4.1 Summary

For chondrichthyan fishes (i.e., sharks, rays, and chimaeras), a group with slow generation times, reproduction is a long-term and an energetically costly process. Reproductive efforts have not been well quantified for this taxon, where a few limited studies have used lethal methods to assess energy stores. To begin to fill this knowledge gap for chondrichthyans, we used the oviparous epaulette shark (*Hemiscyllium ocellatum*) to quantify reproduction effort from a metabolic perspective. To do so, we used fine-scale tracking of the three-week reproductive cycle and measured whole-organism metabolic rate before, during, and after egg case encapsulation and oviposition. Furthermore, we tracked changes in reproductive hormones (testosterone, 17β-estradiol, and progesterone) and blood oxygen-transport capacity haematological parameters (*i.e.,* haematocrit, [haemoglobin]) to further discern the physiological regulation of oviparity in epaulette sharks. Overall, as expected, metabolic rate scaled with increasing female mass, but there was no change in metabolic rate across the average nineteen-day egg production cycle. Furthermore, there was little change in reproductive hormones, where we only found T decreasing at the beginning of the cycle. There was also no change in haematological parameters across the cycle. Given the lack of sizable change of any measured physiological or endocrinological parameters here, it is likely that epaulette sharks are continuously exerting a constant reproductive effort during the egg production cycle. Future research that uses water temperature changes that mimic the species' natural annual pattern and thereby eliciting a

resting period would further illustrate reproductive effort costs. Overall, to my knowledge, this is the first study to directly measure the metabolic effects of Chondrichthyan oviparity, bring forth new questions about reproduction efforts from an energetics perspective in this taxon.

4.2 Introduction

Reproduction is a fundamental biological process that presents a large energetic effort by the individual but is imperative for maintaining populations (Bell 1980; Reznick 1985). Direct parental reproductive energetic efforts include hepatic and gonadal processes such as vitellogenesis leading to folliculogenesis and oogenesis for females, and spermatogenesis for males. Furthermore, indirect reproductive efforts, particularly maternally, include changes in locomotion related to shifts in body morphometrics, pregnancy maintenance, brooding behaviours, and parental care (Buddle et al., 2020; Foucart *et al.,* 2014; Gillooly and Baylis 1999; Olsson *et al.,* 2000; Reardon and Chapman 2010; Smith and Wootton 1995; Van Dyke and Beaupre 2011; Vézina *et al.,* 2006). The degree of reproductive effort may also be inherently linked to the reproductive strategy, where viviparity (live-bearing) surpasses oviparity (egg-laying) in effort, especially when considered temporally, given the extended time and maintenance requirements of the former (Foucart *et al.,* 2014). In other vertebrates (*i.e.,* reptiles and passerine birds), reproductive costs are reflected in female metabolism for both viviparity and oviparity (Angilletta and Sears 2000; DeMarco 1993; Foucart et al., 2014; Munns 2013; Nilsson and Råberg 2001; Vézina *et al.,* 2003, 2006; Vezina & Williams 2002). However, energetic content of reproductive organs and metabolic costs are not always comparable (Vezina and Williams 2002). Furthermore, studies assessing changes in metabolism during fish reproduction for both viviparity and oviparity are generally lacking and need to be addressed (Arnold *et al.,* 2021).

In this study, we aimed to better quantify fine-scale changes in metabolic rate of reproduction in chondrichthyan fishes (sharks, rays, and chimaeras). This taxon was chosen given it includes ~400 oviparous species characterized by their late age of sexual maturity, long reproductive times, and low fecundity (Cailliet *et al.,* 2005), making reproduction a comparatively energetically taxing process. However, despite the wide range of strategies in this taxon, there is very limited research on

the various costs of these modes (Lawson *et al.,* 2019, 2022). Our primary knowledge stems from bomb calorimetry of embryos and reproductive tissues (*e.g.,* Lawson *et al.,* 2022), assessing the relationship between hepatosomatic and gonadal somatic indices (HSI and GSI, respectively) that reflect energy storage and usage in relation to reproduction (*e.g.,* Awruch *et al.,* 2008; Hoffmayer *et al.,* 2006), and measurements of circulating energetic blood markers in reproducing individuals (*e.g.,* Hammerschlag *et al.,* 2018; Rangel *et al.,* 2021ab). However, these costs likely do not easily highlight temporal changes in reproductive energetic effort, which needs to be measured in the whole organism over time (Van Dyke and Beaupre 2011).

Here, we use used the epaulette shark (*Hemiscyllium ocellatum*), a water-breathing, oviparous, long-tailed carpet shark species. The reproductive biology of this species is well understood through a previous assessment of wild sharks at Heron Island on the Great Barrier Reef (Heupel *et al.,* 1999), as well as via anecdotal reports from captivity (Payne & Rufo 2012). Epaulette sharks are a single oviparity species, meaning they produce only one egg case per uterus at any given time, with typically two egg cases formed per cycle. After the egg case is formed and sclerotized (hardened), it is deposited onto the benthos soon after, with the entire process requiring only a few days (Nakaya *et al.,* 2020). In the wild, epaulette shark reproduction is seasonal, where peak egg-laying season is from September to December, likely ending when summer water temperatures ensue (Heupel *et al.,* 1999). However, epaulette sharks will produce eggs year-round in captivity when maintained at a constant water temperature that mimics the laying season (Heupel *et al.,* 1999). Given the established knowledge of epaulette shark reproduction and their amenability to captive breeding, we used this model shark to quantify the potential metabolic costs of reproducing females. We used a combination of methods including metabolic rate estimates via respirometry, blood oxygen transport markers (*i.e.,* haematocrit; Hct, haemoglobin concentration; [Hb], and mean corpuscular haemoglobin concentration; MCHC), and reproductive hormones (*i.e.*, testosterone; T, 17β-estradiol; E_2, and progesterone; P_4) to better understand the fine-scale regulation and reproductive efforts in epaulette sharks.

4.3 Materials and Methods

Ethics

All experimental protocols in this study were assessed and approved by the James Cook University Animal Ethics Committee (protocol #A2655) and furthermore, conducted in accordance with all relevant guidelines and regulations. Collections were conducted under the appropriate Great Barrier Reef Marine Park Authority (GBRMPA #G19/43380.1) and Queensland Fisheries (#200891) permits.

Animal collection and husbandry

Four mature female epaulette sharks over 61 cm total length (TL) (Heupel *et al.* (1999) reports 50% maturity at 55 cm TL) were hand-collected with dip nets in shallow water from Magnetic Island (n=1, -19.129041, 146.877586) and Balgal Beach, QLD, Australia (n=3, -19.021387, 146.418124) in February and March 2020. Sharks were transported back to the Marine and Aquaculture Research Facility Unit at James Cook University (Douglas, QLD, AUS) within two hours of capture in 50 litres of clean, well-aerated seawater. Additionally, one mature female was sourced from Cairns Marine in September 2020.

Sharks were maintained in four 1000l round tanks connected to a 5,500l reservoir fitted with a heater, protein skimmer, bio-filtration, and UV sterilization. The system was maintained at 25°C with a half a degree Celsius diel temperature change (*i.e.*, 24.5- 25.5°C over a 24-h period) and a 12:12 (light:dark) light cycle to mimic the reproductive seasonality of this species in the wild (Heupel *et al.,* 1999). Water quality parameters (pH, nitrites, nitrates, ammonia) were monitored daily for the first month of introduction to the system and subsequently checked weekly (Table S4.1). Temperature was monitored within the external reservoir by a sensor that controlled the heater/chiller system as well as individual HOBO pendant loggers (Onset, USA) attached to the standpipe of each tank. Additionally, each tank had one large air stone, a lid constructed of 30% light blocking shade cloth, and a 30cm x 80 cm PVC pipe that was provided as shelter for each shark. All sharks in the study were fed rations at 2% of their body weight *ad libitum* three times weekly (6% body weight per week) comprised of fresh frozen prawn and pilchard, as

recommended for small benthic sharks (Janse *et al.,* 2004). Any pieces not consumed were removed and the amount consumed was recorded.

Female reproductive monitoring

Female reproductive monitoring occurred from March 2020 to January 2022. Epaulette sharks deposit typically 2 egg cases per reproductive cycle every 2-4 weeks, one per uterus (Wheeler, unpublished necropsy data). Here, we divided the reproductive cycle into three distinct phases: pre-encapsulation, encapsulation of an egg case(s), and post-oviposition (see Figure 4.1). First, in the first 48 hours following the deposition (laying) of a clutch, we deemed sharks in a post-oviposition phase. Next, for several weeks the sharks were considered pre-encapsulating, where no egg cases were detected via daily palpations. Finally, once egg cases of the next clutch were felt during palpations, the sharks were in the encapsulating phase. When both sharks in a shared aquaria were encapsulating egg cases at the same time, a divider was temporarily placed in the tank to ensure egg cases were attributed to the correct female.

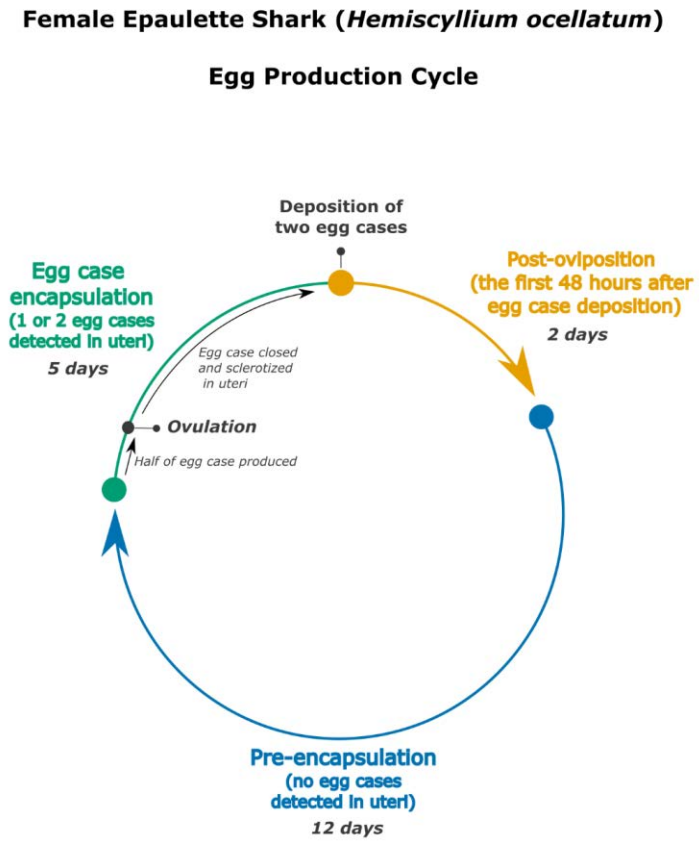

Figure 4.1 *A schematic of the categorization of the reproductive cycle of epaulette sharks use in this study. Colours of each phase correspond to all subsequent figures.*

Respirometry: oxygen uptake measurements

To quantify the resting metabolic rate (RMR) of sharks across reproductive stages, oxygen uptake rates ($\dot{M}O_2$) of each shark were measured using intermittent-flow, static respirometry. The respirometry setup was comprised of opaque PVC chambers with small viewing windows and with baffled ends to allow even water flow and were 15.5l in volume (15 cm diameter x 82 cm length, 1,200l hr^{-1} flush recirculating pumps). These chamber sizes proved to be sufficient size to obtain linear oxygen uptake slopes while still limiting movement. Oxygen levels within the chambers were measured every two seconds using an OXROB3 fibre optic probe inserted approximately 5 cm into the chamber proper via the overflow outlet connected to a Firesting Optical Oxygen Meter (Pyroscience GmbH, Aachen, Germany).

Sharks were fed three days before respirometry trials, and then allowed to fast for the next two days to ensure the sharks were in a post-absorptive state (Heinrich *et al.,* 2014; Wheeler *et al.,* 2022). Sharks were carefully introduced into the respirometry chamber at 6:00 AM and were constantly supplied with filtered, well-aerated seawater for the first six hours via the flush pump; this time period, as determined from preliminary trials, allowed sharks to sufficiently habituate to the chambers following the transfer. At 12:00 PM, a relay timer was used to intermittently turn off the flush pump for five minutes. These time intervals were long enough to ensure that the decline in O_2 was linear (average R^2= 0.96) but short enough such that O_2 levels within chambers did not decrease below 80% saturation at any point of the trials. Following each of the O_2 uptake measurement periods, the flush pump was turned on once again, thus returning O_2 levels in the chamber water back to 100% air saturation; flush duration was ten minutes. These measurement and flush cycles were repeated for 24 hours until 12:00 PM of the following day to ensure sufficient data points for each individual. Immediately after the shark was removed from the respirometry chamber, it was weighed (*i.e.,* wet mass in grams).

Respirometry chambers were also cycled empty for 30 minutes before and after each trial to account for microbial accumulation within each chamber; although, calculations demonstrated microbial respiration to be negligible (less

than 5% of shark respiration). Oxygen uptake rates ($\dot{M}O_2$ in O_2 h^{-1}) were calculated using the *RespiroRS* package in R (Merciere & Norin, 2021).

Blood collection and analysis

Directly after each respirometry trial ended at 12:00 PM, a small blood sample (1.5-2 ml, not exceeding 0.2% of the shark's body mass) was collected via caudal puncture using a 23 G x 1" needle and syringe coated with sodium heparin in a phosphate buffered saline. Sharks were then returned to their respective holding conditions and typically ate within three hours of these experiments, with all sharks feeding within 24 hours. We ensured that all phlebotomy sessions occurred at least two weeks apart.

All blood samples collected in the study were stored on ice for no more than 15 minutes and three haematological metrics that reflect blood-oxygen transport capacity were assessed. Haematocrit (Hct, in %), was measured as the ratio of packed red blood cells to total blood volume via capillary centrifuging at 11,500 rpm (13,000 *g*) for 5 min. Haemoglobin ([Hb] in g dl^{-1}) was measured using a HemoCue (Brae, CA) that has been previously validated for epaulette sharks, and a correction factor was applied ([Hb]*0.91 – 0.53; Schwieterman *et al.,* 2019). Mean corpuscular haemoglobin concentration (MCHC, g l^{-1}) was calculated by dividing [Hb] by Hct then multiplying by 100. Subsequently, whole blood samples were centrifuged at 1240*g* for five minutes, and the plasma was removed and stored at -80°C for later steroid hormone analysis.

The reproductive steroid hormones T, E_2, and P_4 were measured by radioiummunoassay (RIA) following protocols described in Awruch *et al.* (2008). First, each plasma sample was extracted twice from 300 µl of plasma using 1500 µl of ethyl acetate (1:5) with 30 seconds of vortexing and subsequent freezing at -20°C before the aqueous phase was separated. After the second extraction, duplicate 100 µl aliquots were evaporated into assay tubes before reconstitution with a 0.05 *M* phosphate buffer (0.1% gelatin, 0.01% Thimerosal). To account for procedural loss, five replicates of pooled sample were spiked with 3000 counts min^{-1} of H^3-labelled steroids (Perkin-Elmer, Australia), and extracted twice in the same manner as the samples. The extraction efficiencies were determined to be 91, 84, and 83% for T,

E_2, and P_4, respectively. The antisera for the assays were obtained from Novus Biologicals (Australia), and assays were validated by parallelism to serially diluted standard curves. All radioactivity was detected with a Hidex 300 SL liquid scintillation counter. The lower detection limits of the assay were 68.2, 65.6, and 30.7 pg ml^{-1} for T, E_2, and P_4, respectively. The intra-assay variances were 8, 10, and 9%, and the inter-assay variances were 9, 11, and 12% for T, E_2, and P_4, respectively.

Statistical Analyses

All dependent variables (*i.e.,* $\dot{M}O_2$, hormone concentrations, haematological parameters,) were log transformed to achieve normality and assessed across the three discrete female reproductive stages (Figure 4.1). For $\dot{M}O_2$, an analysis of covariance (ANCOVA) with mass and individual as covariates was applied and for all hormone and haematological parameters ANCOVA with individual as a covariate was used. The *emmeans* package (Lenth, 2022) was used for *post hoc* comparisons between reproductive status categories when applicable. Furthermore, all data met the assumptions of normality (after log transformation) and homoscedasticity, All statistical analyses were conducted in R (version 1.4.1106, R Core Development Team 2021), where results were considered significant at α= 0.05.

4.4 Results

Female reproductive cycle

From the five reproducing individuals in this study, we observed 196 egg cases deposited over 98 cycles from March 2020 to January 2022. The female reproductive cycle length averaged 19 (± 5.7 s.d.) days long at 25°C, where intra-individual variability was low (Table 4.1). Each cycle at 25°C produced a median value of two egg cases, where a few cycles at the beginning of the reproductive season only produced one wind egg case (i.e., an empty egg case with no yolk sac) or three egg cases (two containing yolk-sacs and one wind). Egg case encapsulation, on average, required 5.3 (± 3.2 s.d.) days, ranging from 2-10 days (Table 4.1). For the majority of cycles assessed, the two egg cases of the clutch were laid between 0-2 nights apart (Table 4.1). When egg cases were not deposited on the same night, the egg case from the right uterus was deposited first in all cases. Female sharks consumed their full feeding rations throughout the reproductive cycle, except when

within two days of egg deposition. During this window, in 35% of feedings, sharks did not consume any food, but resumed normal feeding after oviposition occurred.

Table 4.1 *Individual female reproductive cycle data means (± s.d.) of the cycle length (from one set of egg cases to the next), egg case encapsulation time (time the egg cases were present in the oviduct), intra-cycle time (time from oviposition of the first egg case to the second within one cycle), total length (TL), and mass.*

Individual	Cycle length (days)	Egg case encapsulation time (days)	Intra-cycle time between egg cases (days)	TL (cm)	Mass (kg)
Female 1	16.3 ± 3.8	7.5 ± 1.4	0.5 ± 0.9	81.0	1.46 ± 0.095
Female 2	19.5 ± 5.2	6.2 ± 3.1	0.8 ± 0.8	68.0	1.14 ± 0.123
Female 3	17.6 ± 5.1	3.1 ± 1.2	1.5 ± 1.2	73.9	1.09 ± 0.076
Female 4	20.0 ± 3.5	5.0 ± 2.6	2.1 ± 1.4	75.8	1.07 ± 0.123
Female 5	30.4 ± 6.4	8.1 ± 3.2	4.8 ± 2.1	70.8	0.96 ± 0.080
Mean	19.0 ± 5.7	5.3 ± 3.2	1.7 ± 1.7	73.9 ± 5.0	1.16 ± 0.202

Resting metabolic rate ($\dot{M}O_2$)

Respirometry was performed 96 times throughout this study, and there was no evidence of a conditioning effect from the repeated trials in any of the sharks (see Figure S4.1). Furthermore, the small diel temperature cycle in this study (24.5-25.5°C) did not affect $\dot{M}O_2$ (assessed in Chapter 2; Wheeler *et al.,* 2022). There was no effect of female reproductive status on $\dot{M}O_2$, but both mass and individual did effect $\dot{M}O_2$ (Figure 4.2, 4.3, Table S4.2).

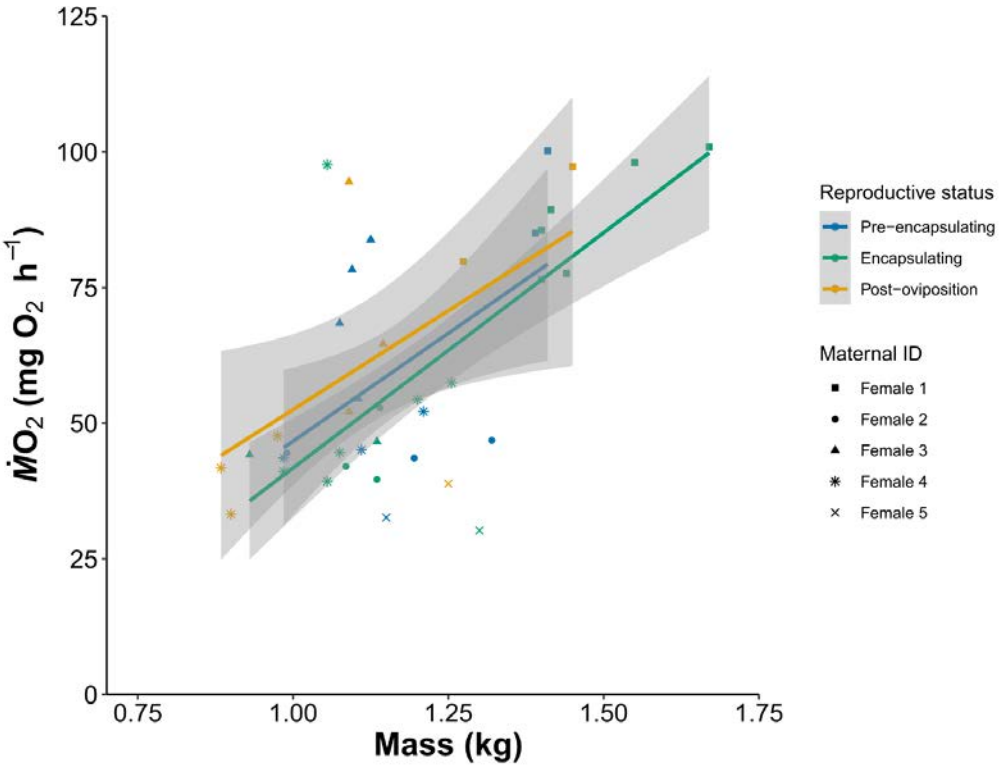

Figure 4.2 *The metabolic rate (as RMR (mg O_2 h^{-1})) over mass of five female epaulette sharks across three stages of the reproductive cycle. The linear fits of each reproductive status with individual as a co-variate did not differ between any groupings at α= 0.05.*

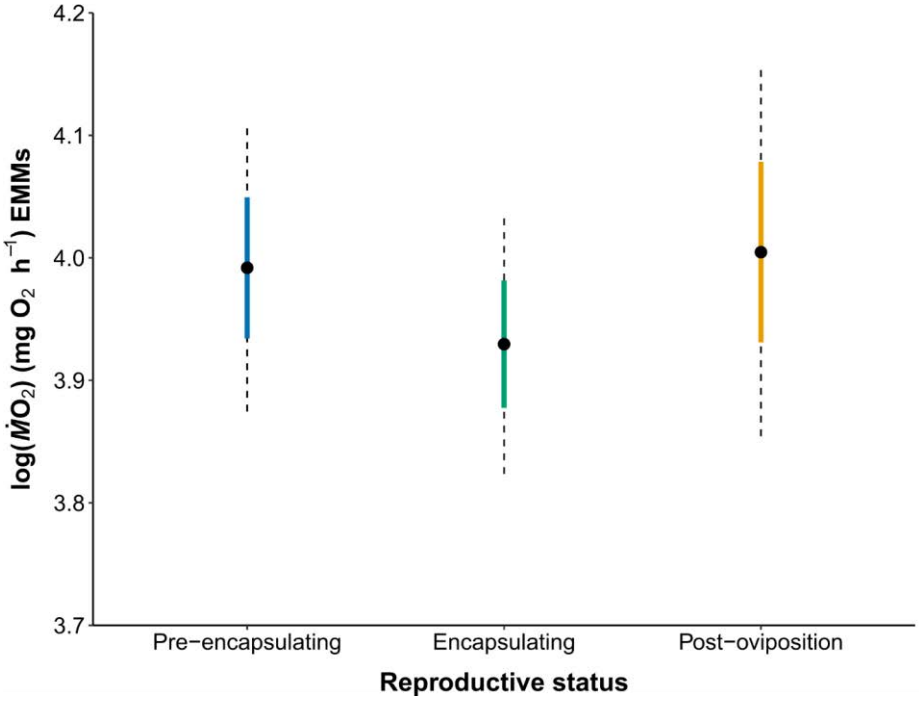

Figure 4.3 *Estimated marginal means (EMMs) of log(metabolic rate) ($\dot{M}O_2$) across female epaulette shark oviparity. Coloured bars represent the EMMs standard error, and the dotted black bars represent the 95% confidence intervals. There were no statistically significance differences between statuses at α = 0.05.*

Haematological parameters

Across female reproduction, T peaked during the pre-encapsulating stage, and both E_2 and P_4 were consistent across the cycle (Figure 4.4, Table S4.3, S4.4, & S4.5). Across all haematological parameters assessed (Hct, [Hb], and MCHC), there were no significant changes (Figure 4.5, Tables S4.6, S4.7, & S4.8).

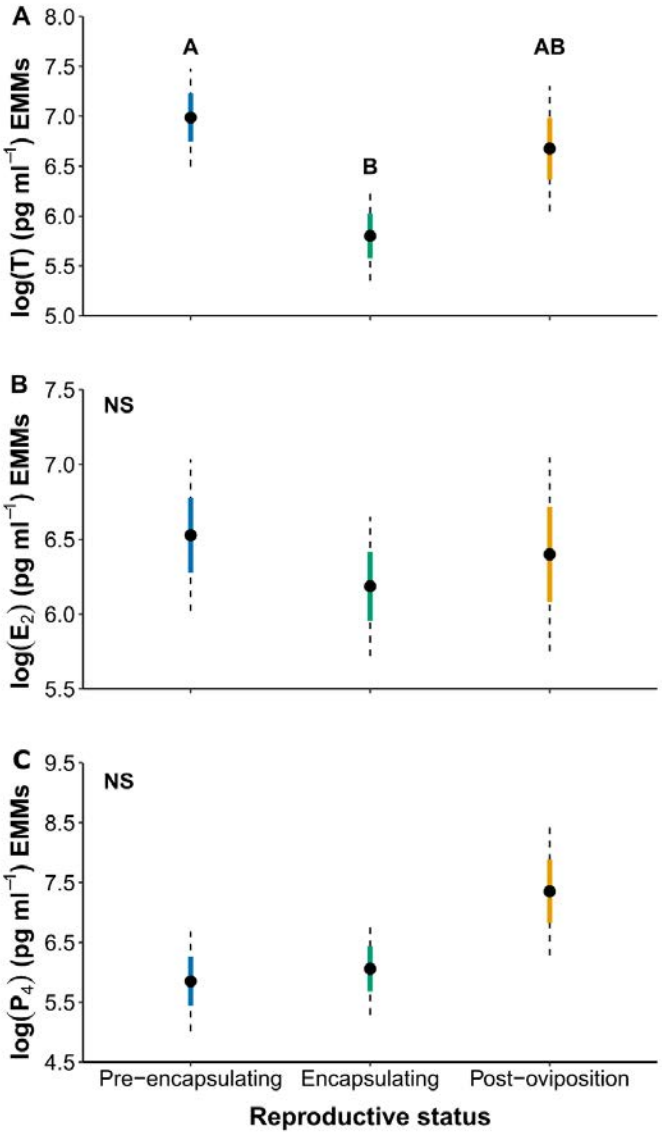

Figure 4.4 *Estimated marginal means (EMMs) of circulating reproductive steroid hormone concentrations of (A) testosterone (T, in pg ml^{-1})), (B) estradiol (E_2, in pg ml^{-1}), and (C) progesterone (P4, in pg ml^{-1})) across life history stages. Colored bars represent the EMMs standard error, and the dotted black bars represent the 95% confidence intervals. NS denotes non-significance, and differing letters denoted significant differences at α= 0.5.*

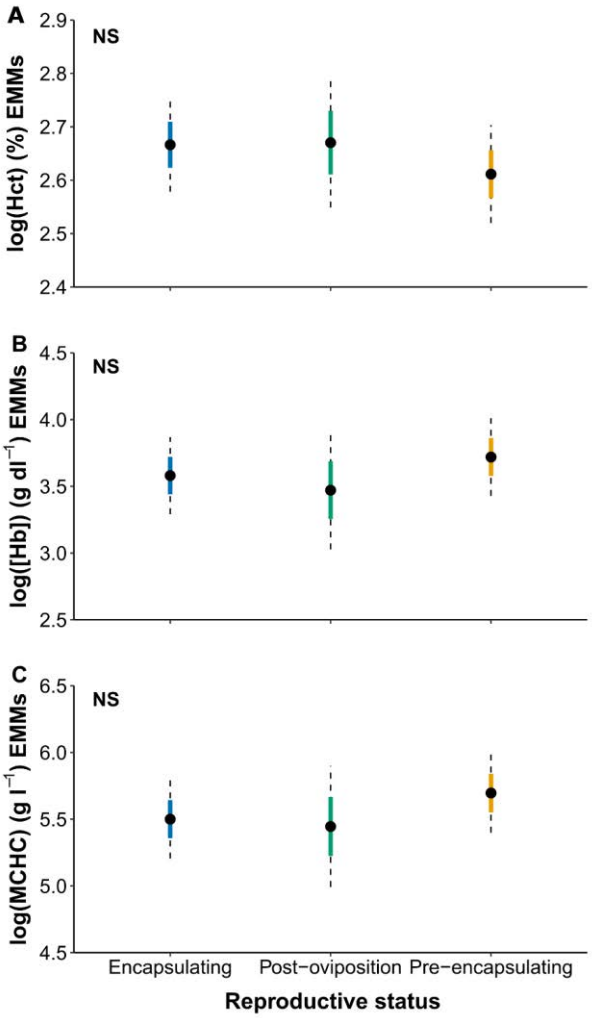

Figure 4.5 *Estimated marginal means (EMMs) of the hematological parameters of (A) hematocrit (hct, in %), (B) hemoglobin concentration ([Hb], in g dl^{-1}), and (C) mean corpuscular hemoglobin concentration (MCHC, in g l^{-1}).. Colored bars represent the EMMs standard error, and the dotted black bars represent the 95% confidence intervals. NS denotes non-significance at α= 0.5.*

4.5 Discussion

In this study we aimed to use fine scale daily tracking of female epaulette shark oviparity to assess effects of this biological process on metabolic demands. We expected that female RMR would increase during egg case encapsulation and then decrease after oviposition, but our findings did not reflect these changes

(Figure 4.2 & 4.3). A likely explanation of these findings may be related to the lack of seasonal timing and it's effect on breeding strategy of the sharks in this study. When epaulette sharks are reproducing seasonally in the wild, they likely employ a capital breeding strategy, where energy is stored in the liver during the resting period from January to July. Then, during the reproductive season from August to December, these hepatic energy stores are mobilized via vitellogenesis to create ovarian follicles for reproduction (McBride *et al.,* 2015). However, because epaulette sharks in this study were stimulated via water temperature to reproduce year-round, females may have transitioned to an income breeding strategy to continuously acquire energy via food intake for continuous egg production (McBride *et al.,* 2015). Indeed, unpublished data suggests that, when offered food to satiation, mature females consumed higher percentages of their body weight per feeding than mature males (B. Lewis, unpublished data). Furthermore, given the continuous nature of egg production here and that E_2 and P_4 hormones did not change across the egg production cycle, vitellogenesis and subsequent folliculogenesis were likely occurring continuously in the background (Koob and Callard 1999). Upon necropsy of female epaulette sharks, pairs of similarly sized follicles increasing in size have been noted, where follicles for any given cycle have been forming over the course of several months (Wheeler, unpublished data). Therefore, the continuous nature of vitellogenesis and folliculogenesis within an income breeding strategy may keep the general size and therefore oxygen demand of the ovary consistent across time and therefore no changes in RMR were detected.

Within the egg production cycle, many of the main reproductive changes occur within the oviducal gland, where this gland is responsible for secretion and formation of the egg case capsule and is thought to have a considerable metabolic requirement (Callard *et al.,* 2005). The oviducal gland begins formation of the egg case prior to ovulation of the follicle, so the gland must be controlled by endocrine factors, presumably from the ovary (Callard *et al.*, 2005). Oviducal gland growth coincides with increased circulating E_2 in other oviparous elasmobranchs (Koob *et al.,* 1986; Heupel *et al.,* 1999), so in this study where E_2 was consistent across the egg production cycle, the oviducal gland may have remained consistent in size across constant reproduction, thereby maintaining RMR. These glands are small in mass compared to the whole shark mass, and therefore any increased oxygen

demand of these glands during egg case encapsulation may be minimal in comparison to the oxygen demand of the whole organism. In other words, despite the fact that the oviducal gland during encapsulation may have a high metabolic demand, the glands are small, and therefore the increased demand is not well reflected in whole organism oxygen uptake rates. In the future, research that assesses oviparous reproduction using seasonal changes in water temperature to mimic wild conditions that up and down regulate the reproductive tract will be key to capturing the overall energetic effort of reproduction beyond the egg production cycle. Furthermore, altering feeding amount and/or food items whilst tracking egg case production characteristics (*i.e.,* the amount and category – *e.g.,* number of wind cases produced) may indicate if continuously reproducing epaulette sharks are using an income breeding strategy that can be shifted by caloric restriction.

Overall, reproductive hormone changes across the reproductive cycle were minimal (Figure 4.4). Female T was elevated in the pre-encapsulating phase (Figure 4.4A), where this increase could be inducing egg case secretion from the oviducal glands halfway through the cycle, but the complete picture of endocrine control on the oviducal gland in elasmobranchs is still understudied (Koob and Callard *et al.*, 1999; Callard et al., 2005). We expected that P_4 would peak during the peri-ovulatory and encapsulation period, as P_4 is thought to regulate ovulation, egg-retention, and oviposition in other oviparous chondrichthyans (Koob and Callard 1985; Koob *et al.,* 1986; Rasmussen *et al.,* 1999; Awruch *et al.,* 2008; Falahiehzadeh and Salamat 2020; Inoue *et al.,* 2022). Heupel *et al.* (1999) serially sampled one captive epaulette shark daily and reported that P_4 peaked in the post-oviposition phase. Here, on average, P_4 did not change throughout the egg product cycle, however there were three samples (circled in Figure S4.2) during the encapsulating and post-oviposition periods where P_4 was 11 to 14 times higher than average (Figure S4.2). These could be isolated cases where we captured the short 24–48-hour peak in P_4 that is easily missed given the brief periodicity. Not including these peaks, our P_4 values were similar concentrations to wild reproductively active female epaulette sharks in Heupel *et al.* (1999). It is still unclear in oviparous chondrichthyans whether the purpose of this mid to late-cycle P_4 peak is related to egg-retention and/or oviposition, to stimulate steroidogenesis of T and E_2 for the next cycle, and/or to inhibit hepatic synthesis of vitellogenin (Koob and Callard

1999). Continued experimental work with fine-scale monitoring and hormonal manipulation may help elucidate the undoubtably important role of P_4 in chondrichthyan oviparity.

From a haematological standpoint, Hct, [Hb], and MCHC did not differ between life stages or reproductive stages. Similarly, in the oviparous cloudy catshark, Hct also did not vary across oviparity (Inoue *et al.,* 2022). To our knowledge, there are no studies that assessed [Hb] and MCHC across chondrichthyan oviparity, precluding a comparison. Epaulette sharks have been demonstrated to maintain red blood cell (RBC) size (*i.e.,* no swelling occurs) after air exposure or exhaustive exercise (Schwieterman *et al.,* 2019) but exhibit RBC swelling during anoxia exposure (Chapman and Renshaw 2009). However, there may also be an effect of captivity on these haematological properties (Wise *et al.,* 1998; Chapman and Renshaw 2009), and so more research is needed to fully understand how this species uses haematological adjustments to cope with various forms of stress and how reproduction may play a role.

There are several applications and future directions from this work regarding fisheries management of chondrichthyan fishes, where fisheries interactions are the largest threat to this taxon globally (Dulvy *et al.,* 2021). Viviparous species are more susceptible than oviparous species to pre-mature parturition or abortion caused by capture stress (Adams *et al.,* 2018; Wosnick *et al.,* 2018). To our knowledge, there are no examples of an oviparous shark or skate demonstrating pre-mature oviposition from stress (Adams *et al.,* 2018). Indeed, herein, we handled and collected blood samples from females actively encapsulating egg cases and did not see any pre-mature oviposition. We hypothesize that the lack of metabolic elevation during female egg production reported here could explain why oviparous species seem less susceptible to pre-mature parturition/oviposition; although, a directed study is needed to test this hypothesis.

Overall, this study is the first to my knowledge that directly assess the effects of oviparity on metabolism in chondrichthyans and has indicated that the reproductive budget is complex and may not be directly reflected via oxygen uptake rates. However, more research that incorporates seasonal variation and a control in

the form of a non-reproducing treatment group is needed to further elucidate reproductive effort in the context of an organismal energy budget for oviparous Chondrichthyans.

Chapter 5: The upper thermal limit of epaulette sharks (*Hemiscyllium ocellatum*) across three life history stages, sex, and body size

Associated publication

Wheeler, C.R., Lang, B.J., Mandelman, J.W., Rummer, J.L. (2022). The upper thermal limit of a tropical elasmobranch is conserved across three life history stages, sex and body sizes. *Conservation Physiology*, 10(1): coac074. https:// doi.org/ 10.1093/conphys/coac074

Data availability

The data underlying this article are available from Research Data JCU at James Cook University at https://doi.org/10.25903/ zqvp-6h47.

5.1 Summary

Owing to climate change, most notably the increasing frequency of marine heatwaves and long-term ocean warming, better elucidating the upper thermal limits of marine fishes is important for predicting the future of species and populations. The critical thermal maximum (CT_{max}), or the highest temperature a species can tolerate, is a physiological metric that is used to establish upper thermal limits. Among marine organisms, this metric is commonly assessed in bony fishes but less so in other taxonomic groups, such as elasmobranchs (subclass of sharks, rays, and skates), where only thermal acclimation effects on CT_{max} have been assessed. Herein, we tested whether three life history stages, sex, and body size affected CT_{max} in a tropical elasmobranch, the epaulette shark (*Hemiscyllium ocellatum*), collected from the reef flats surrounding Heron Island, Australia. Overall, we found no difference in CT_{max} between life history stages, sexes, or across a range of body sizes. Findings from this research suggest that the energetically costly processes (*i.e.,* growth, maturation, and reproduction) associated with the life history stages occupying these tropical reef flats do not change overall acute thermal tolerance. However, it is important to note that neither embryos developing *in ovo,* neonates, nor females actively encapsulating egg cases were observed in or collected from the reef flats. Overall, our findings provide the first evidence in an elasmobranch that upper thermal tolerance is not impacted by life history stage or size. This information will help to improve our understanding of how anthropogenic

climate change may (or may not) disproportionally affect particular life stages and, as such, where additional conservation and management actions may be required.

5.2 Introduction

Ectothermic fishes are dependent on environmental water temperature to regulate all aspects of their biology, where organisms have optimal temperature ranges for their growth, reproduction, and ultimately their survival (Angilletta, 2009). When temperatures shift outside of optimal ranges, negative consequences arise for individuals that can cascade to population level issues and overall ecosystem health (*e.g.,* Angilletta, 2009; Pörtner and Peck, 2010). With the increasing occurrence of marine heatwaves and sustained ocean warming due to anthropogenic climate change (Fox-Kemper *et al.,* 2021), the biological thermal constraints of marine ectothermic fishes are of growing concern (Pörtner and Peck 2010). Therefore, it is imperative that we assess thermal ranges and end points (minima and maxima) to understand current thermal constraints and aid our understanding of the role that thermal plasticity may play in a warming ocean (Angilletta 2009, Gunderson and Stillman 2015, Seebacher *et al.,* 2015). To do so, one physiological metric, critical thermal maximum (CT_{max}), which marks an organism's highest acute temperature tolerance, is commonly established by incrementally increasing water temperatures until the individuals lose motor function or the onset of muscle spasms occurs (Lutterschmidt and Hutchison, 1997; Kingsolver and Umbanhowar 2018). Although the high temperatures reached during these tests for most species do not reflect non-captive ecological scenarios, they provide a measure of the upper thermal capability of a species that can be repeated and compared intra- and inter-specifically (Morgan *et al.,* 2018).

For elasmobranch fishes (sharks, rays, and skates), aside from being one of the most globally threatened taxa due to fisheries interactions (Dulvy *et al.,* 2021), ocean warming has also become of concern (Pereira Santos *et al.*, 2021). This subclass of mostly ectothermic fishes exhibits slow generation times on the order of years to decades (Conrath and Musick, 2012), thus reducing their potential for thermal transgenerational adaptation (Pereira Santos *et al.*, 2021). Furthermore, many elasmobranch species are demersal and exhibit a degree of site fidelity (*e.g.*, Awruch *et al.*, 2012; Kneebone *et al.*, 2020), potentially limiting their ability to

undertake large-scale migrations to relocate to cooler, more suitable thermal conditions that also provide adequate benthic habitat (Vilmar and Di Santo, 2022). So, despite mounting global concerns for elasmobranch populations, and that their life history strategies may preclude their ability to quickly adapt to changing environments, the thermal biology of most elasmobranch species remains under-investigated (Pereira Santos *et al.*, 2021). For example, CT_{max} estimates from elasmobranchs are limited to only four species and have only been assessed in relation to thermal history (Fangue and Bennett, 2003; Dabruzzi *et al.*, 2013; Gervais *et al.*, 2018; Bouyoucos *et al.*, 2020).

Different life history stages, because of their associated energetic demands, may be differentially impacted by warming and temperature stress (Pörtner and Farrell, 2008; Przeslawski *et al.,* 2015; Dalhke *et al.*, 2020). During life stages where growth, development, and gamete production result in high energetic costs, organisms are hypothesized to exhibit reduced upper thermal tolerance (Dahlke *et al.*, 2020). There may also be inherent thermal tolerance differences between sexes and across increasing mass over life stages, as large-bodied fishes heat internally more slowly, producing higher CT_{max} values (Stevens & Fry, 1974; Zhang and Kieffer, 2014; Messmer *et al.*, 2017). However, these hypotheses have never been tested in an elasmobranch species, where the time scale of development and reproduction can span months to years (Conrath and Musick, 2004), representing large energetic costs. Moreover, species from this taxon generally have larger body mass ranges compared to teleost species investigated in most CT_{max} studies (*e.g.,* Ospina and Mora, 2004; Messmer *et al.*, 2017; Morgan *et al.*, 2018, 2019; Firth *et al.*, 2021; Penney *et al.*, 2021).

To understand the influence that life history stage, sex, and body size have on the thermal tolerance of elasmobranchs, we studied the epaulette shark (*Hemiscyllium ocellatum*), which is a small demersal shark found throughout the Great Barrier Reef (GBR), Australia (Dudgeon *et al.*, 2019). This tropical species inhabits shallow, coastal environments that vary daily but reside within a narrow thermal niche, where they may experience (on average) only 6-7°C of water temperature change annually (Heupel *et al.*, 1999; Nay *et al.*, 2021). Furthermore, epaulette sharks are abundant in multiple life stages (juveniles to adults) on reef

flats throughout the GBR, and the relationship between body size and maturity has been previously established (Heupel *et al.*, 1999). Epaulette sharks are oviparous (egg-laying), reproducing continuously from July to December each year (Heupel *et al.*, 1999). Therefore, this species allows us to assess thermal limits within a singular season to mitigate seasonal acclimatization effects (Gervais *et al.*, 2018) while still using a range of life history stages, including reproducing adults.

We hypothesized that reproducing adults may have a reduced thermal tolerance when compared to other life stages, as high energetic investments toward gamete production likely reduce the amount of energy available for thermal stress responses (*e.g.,* Freitas *et al.*, 2010; Komoroske *et al.*, 2014; Clark *et al.*, 2017; Dahlke *et al.*, 2020). Furthermore, we hypothesize that the upper thermal tolerance of juveniles and subadults would be similar regardless of sex, but mature adult females would have a lower thermal tolerance than mature adult males, given that female reproduction appears to be more costly than male reproduction (Hayward and Gillooly 2011). Finally, we hypothesized that larger body mass individuals would have a higher upper thermal tolerance when compared to smaller conspecifics. Overall, outcomes from this study will inform whether certain life history stages in the epaulette shark – and potentially other similar species – are more vulnerable to warming, which is important information for current and future frameworks of elasmobranch conservation under the threat of ocean warming (Pereira Santos *et al.*, 2021).

5.3 Materials and Methods

The experimental protocols in this study were approved by the James Cook University Animal Ethics Committee (protocol A2739). The temporary collections were conducted under the appropriate Queensland Fisheries (#255136) and Great Barrier Reef Marine Park Authority (GBRMPA G21/44922.1) permits.

Collections and temporary holding

Thirty epaulette sharks were collected from the Heron Island reef flat (23.4423°S, 151.9148°E) during low tides in October and November 2021 during the peak reproductive season (Heupel *et al.*, 1999). Sharks were hand-caught with dip nets, sexed, and photographed for their unique spot pattern for identification

purposes and transported back to the Heron Island Research Station. The individuals were temporarily maintained for two to seven days in a 364 cm by 364 cm aquarium (flow-through system) supplied with 4,770 liters of seawater from the reef flat. The aquarium was located outside with natural photoperiod and diel changes in water temperature that mirrored the reef flat where the sharks were collected. Sharks were not fed during their time in captivity so that experimentation could commence with animals that had been fasted for at least 48 hours. No more than fifteen sharks were in captivity at any given time, and sharks were provided with shelters, given their propensity to hide in their natural habitat.

Critical thermal maximum assays

To determine CT_{max}, a 156 cm diameter by 56 cm high cylindrical aquarium was filled with 363l of clean seawater at the same temperature as the holding aquarium, and a weighted basket made of plastic mesh measuring 60 cm by 42 cm by 42 cm was placed inside to restrict movement of the sharks. Thermal ramping rate, or how quickly the water is warmed during a CT_{max} assay, can impact the final endpoint, where slower thermal ramping rates produce lower CT_{max} values and vice versa (Illing *et al.*, 2020; Kingsolver and Umbanhowar, 2018; Messmer *et al.*, 2017). Therefore, it is important to choose a rate that allow the internal body temperatures to increase in parallel, which is especially important for larger fish species, given the body mass differential, but fast enough such that it precludes acclimation (Illing *et al.*, 2020; Kingsolver and Umbanhowar, 2018; Messmer *et al.*, 2017). We used a 2000-watt titanium heater to heat the water at a rate of 0.1°C min^{-1}, which is slower than previous CT_{max} elasmobranch studies (*i.e.,* 0.3°C min^{-1}: Fangue and Bennett, 2003; 0.25°C min^{-1}: Dabruzzi *et al.*, 2013; 0.26°C min^{-1}: Gervais *et al.*, 2018; 0.28°C min^{-1}: Bouyoucos *et al.*, 2020), but likely an improved rate for this generally large-bodied taxon. Both water temperature and oxygen concentrations were logged every five seconds throughout the assays with an OXROB3 fibre optic probe connected to a Firesting Optical Oxygen Meter (Pyroscience GmbH, Aachen, Germany). An air stone and two 1000l hr^{-1} pumps were used to ensure homogeneous mixing of water throughout the experimental aquarium during assays, and oxygen concentrations did not drop below 80% air saturation. Starting water temperature of the assays ranged from 22.8 to 26.7°C, but could not be

controlled for, as inflowing water came directly from the reef flat, which warms throughout the day. As a result, morning assays started at lower temperatures than afternoon assays.

Sharks were allowed to habituate to the experimental aquarium for one hour prior to thermal ramping (Gervais *et al.*, 2018), and we ensured the sharks were at rest for at least 10 minutes prior to the start of the assay. Ventilation rates (gill beats per min; bpm) were measured every 15 minutes for the first part of the assays, while rates were increasing; then, after ventilation rates peaked and began to remain constant or decrease, measurement frequency increased to every two minutes (Gervais *et al.*, 2018). At each ventilation count, it was noted whether the shark was active or resting. After each of the two-minute interval ventilation measurements, the sharks were flipped ventrally 180 degrees along the longitudinal axis to test for the loss of righting reflex (LRR; Lutterschmidt and Hutchison, 1997; Gervais *et al.*, 2018). Sharks were considered to have lost their righting reflex when they were unable to right themselves within ten seconds (Zhang and Kieffer, 2014). After LRR was reached, sharks were immediately removed to a water bath at the initial starting temperature of the assay, and the end point temperature of LRR was recorded. Sharks were allowed to recover for 24-hours after the assays were conducted.

Life history staging

After recovery, sharks were measured for total length (TL; cm), mass (kg), and, for males, inner clasper length. Female sharks were palpated to detect the presence or absence of egg cases. Sharks were classified into three life history stages of juvenile, subadult, or mature adult, based on total lengths reported in Heupel *et al.* (1999; Table 5.1). Similar to findings from Heupel *et al.* (1999), males in the 49-61 cm TL range had claspers that ranged in length and calcification status (Figure 5.1), and so we prioritized clasper length and calcification over TL when categorizing male life history stages. For example, males are considered juveniles when TL is less than 53 cm, but two of the small males in this study (49.6 and 51.1 cm TL) also had partially elongated and calcified claspers that were 3.8 and 5 cm, respectively (asterisk marked data points, Figure 5.1). Therefore, we classified these sharks as subadults and not juveniles, as maturation had clearly begun.

Table 5.1. *Life history stage classification of epaulette sharks (H. ocellatum) from sex-specific total lengths and clasper lengths at maturity, as reported in Heupel et al. (1999).*

Life history stage	Total length (cm)
Juvenile	M: < 53 cm F: < 55 cm
Subadult	M: 53-61 cm TL **OR** inner clasper length ≥ 3.0 cm F: 55-61 cm
Mature adult	> 61 cm

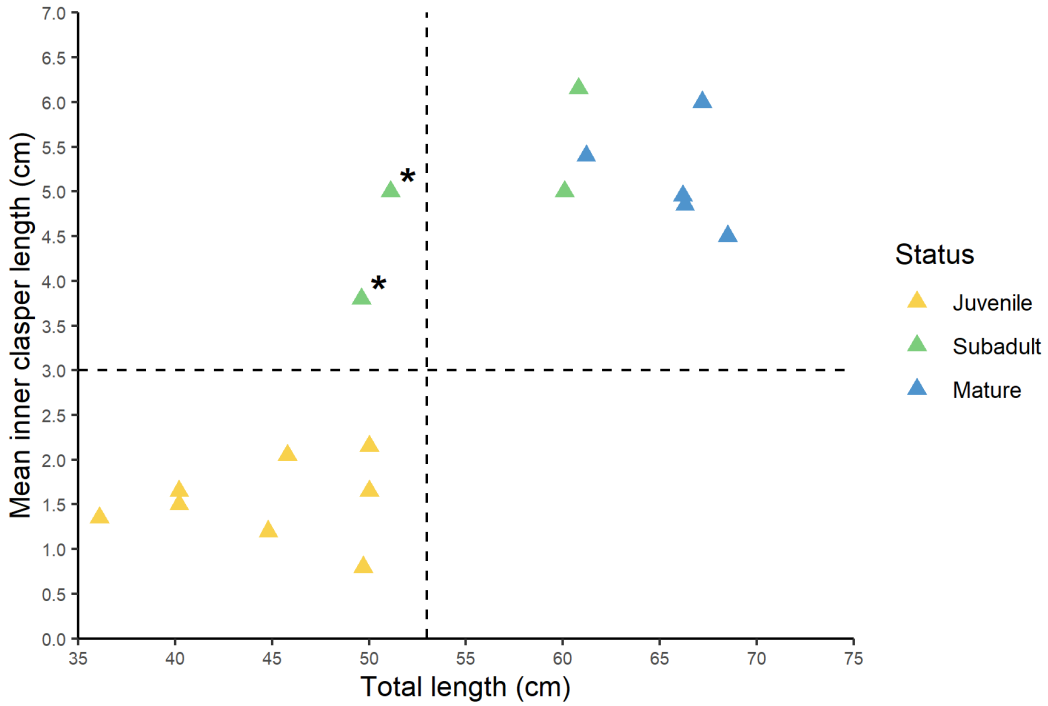

Figure 5.1 *Male epaulette shark total length (cm) verses average inner clasper length (cm) assessed in this study. The horizontal and vertical dashed lines respectively represent the cut-off between juvenile and subadult clasper length and total length. Two sharks (denoted with *) had total lengths indicative of juvenile status but also had elongated and partially calcified claspers and were therefore deemed subadults.*

Finally, each shark was implanted with a passive integrated transponder (PIT) tag into the dorsal musculature to the left of the first dorsal fin to ensure no shark was re-captured and repeated in our experiments. All sharks were released

onto the reef flat at the location of capture in good health (*e.g.*, exhibiting normal ventilation rates and behavior, and no change in overall coloration or redness on the ventral side, as per Gendron and Menzies, 2004). Of the 30 sharks assessed for CT_{max}, nine were juveniles (8 M; 1 F), eight were subadults (4 M; 4 F), and 13 were mature adults (5 M; 8 F; Table 2). No females were encapsulating egg cases at the time of capture or at the time of CT_{max} assays.

Statistical analyses

First, one outlier was identified by a Dixon's Q test and was removed from the dataset (Q= 0.50595, p= 0.001172) (Supplement S5.0) (Komsta 2022). To test for the effects of non-controlled trial conditions, a linear regression was performed incorporating the number of days each shark was in holding at the field station prior to the CT_{max} trials. Additionally, the time of day of the start of the trial and the starting water temperature were included in an interaction term to account for changes in water temperature across the course of the day (Supplemental Table S5.1). Next, a linear model was fit to assess the effect of life history stage, sex, and mass on CT_{max}, where all factors were included in an interaction term to account for inherent relationships between these factors (*e.g.,* mature sharks have higher mass) (Supplemental Table S5.2).

To assess how activity level during CT_{max} trials differed between life history stages and sex, we performed a binomial (*i.e.,* active vs resting) generalized linear mixed-effects model (GLMM) with individual as a random effect (Supplemental Table S5.3) (*lme4*; Bates *et al.,* 2015). Next, to assess ventilation rates across CT_{max} trials, we considered activity level findings from the previously described GLMM model. Although not significant, some subadults were more active during trials, which artificially inflated the subadult overall ventilation rate model fits when data from both activity levels were included. Additionally, we were not able to quantify the duration or magnitude of swimming activity across the trial or at each observation, where fast or sustained swimming would increase ventilation rates more quickly over time. Therefore, we have only included ventilation rates from resting sharks herein, so data are directly comparable between groupings. We performed a generalized additive (GAM) model of ventilation rate over a smoother of the experiment time with an interaction term for life history stage and sex (*mgcv*;

Wood 2011) (Supplemental Table S5.4). We also included the first order auto-correlation function to account for the fact that ventilation rates are inherently dependent on the previously measured rate (*nlme*; Pinheiro *et al.,* 2021) (Supplemental Table S5.4). Finally, the estimated marginal means within each sex were compared between life history stages (*emmeans*; Lenth 2022) (Supplemental Table S5.4). All models were visually checked for normality and homoscedasticity using qqplots and residual plots, and all analyses were conducted in R (version 4.1.1., R Core Team, 2021).

5.4 Results

Despite the assay starting water temperature ranging from 22.8 to 26.7°C, this factor did not affect the CT_{max} end point ($F_{1,24}$ = 0.50, P = 0.48; Figure 5.2B). Furthermore, the number of holding days before the assay ($F_{1,24}$ = 0.33, P = 0.57; Figure 5.2A), the time of day of the assay ($F_{1,24}$ = 0.18, P = 0.68; Figure 5.2C), nor the interaction term ($F_{1,24}$ = 1.42, P= 0.25) had any effect on CT_{max}; these factors were therefore excluded from the subsequent CT_{max} models. CT_{max} did not change across the distinct life history stages of juveniles, subadults, or mature adults ($F_{2,18}$= 0.60, P = 0.56; Table 5.2, Figure 5.3A). Furthermore, CT_{max} did not differ between sexes ($F_{1,18}$= 2.80, P = 0.11; Table 5.2, Figure 5.3B) or over body mass ($F_{1,18}$= 1.33, P = 0.26; Table 5.2, Figure 5.3C). This model did include significant interactions between life history stage and mass ($F_{2,18}$= 4.56, P = 0.02) as well as sex and mass ($F_{1,18}$= 6.03, P = 0.02) (Supplemental Table S5.2).

Table 5.2 *The mean CT_{max} and standard deviation (s.d.) for each life history stage and sex with one outlier removed (see Table S0).*

Life history stage	Mean mass (kg) (±s.d.) [range]	Mean total length (cm) (±s.d.) [range]	Mean CT_{max} (°C) (±s.d.)	n
Juvenile	0.26±0.10 [0.11-0.39]	44.6±5.0 [36.1-50.0]	36.14±0.26	9
Subadult	0.47±0.10 [0.35-0.62]	56.3±4.1 [49.6-60.8]	36.17±0.35	8
Mature adult	0.67±0.07 [0.54-0.64]	65.6±2.8 [61.2-66.3]	36.20±0.27	12
All females	0.58±0.18 [0.18-0.78]	61.0±6.8 [45.0-70.3]	36.24±0.23	12
All males	0.42±0.19 [0.11-0.74]	53.4±10.4 [36.1-68.5]	36.13±0.30	17

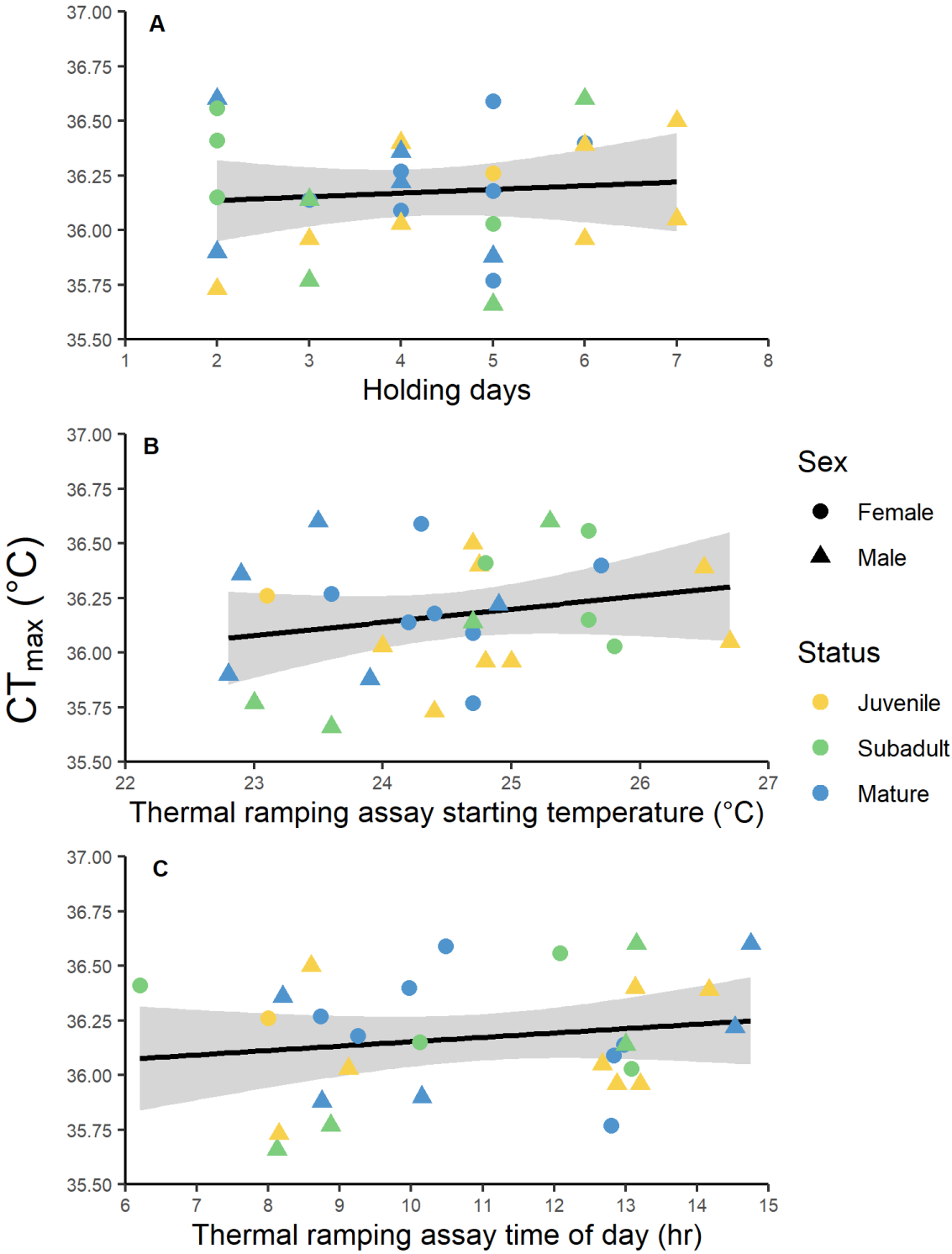

Figure 5.2 *Uncontrolled experimental conditions that could impact CT_{max}. There was no effect of (A) number of days in captivity prior to assays (P = 0.57), (B) starting water temperature of the assays (P = 0.48), or (C) time of day when assay commenced (P = 0.68) on CT_{max}. Shaded areas represent the 95% confidence intervals of the linear models.*

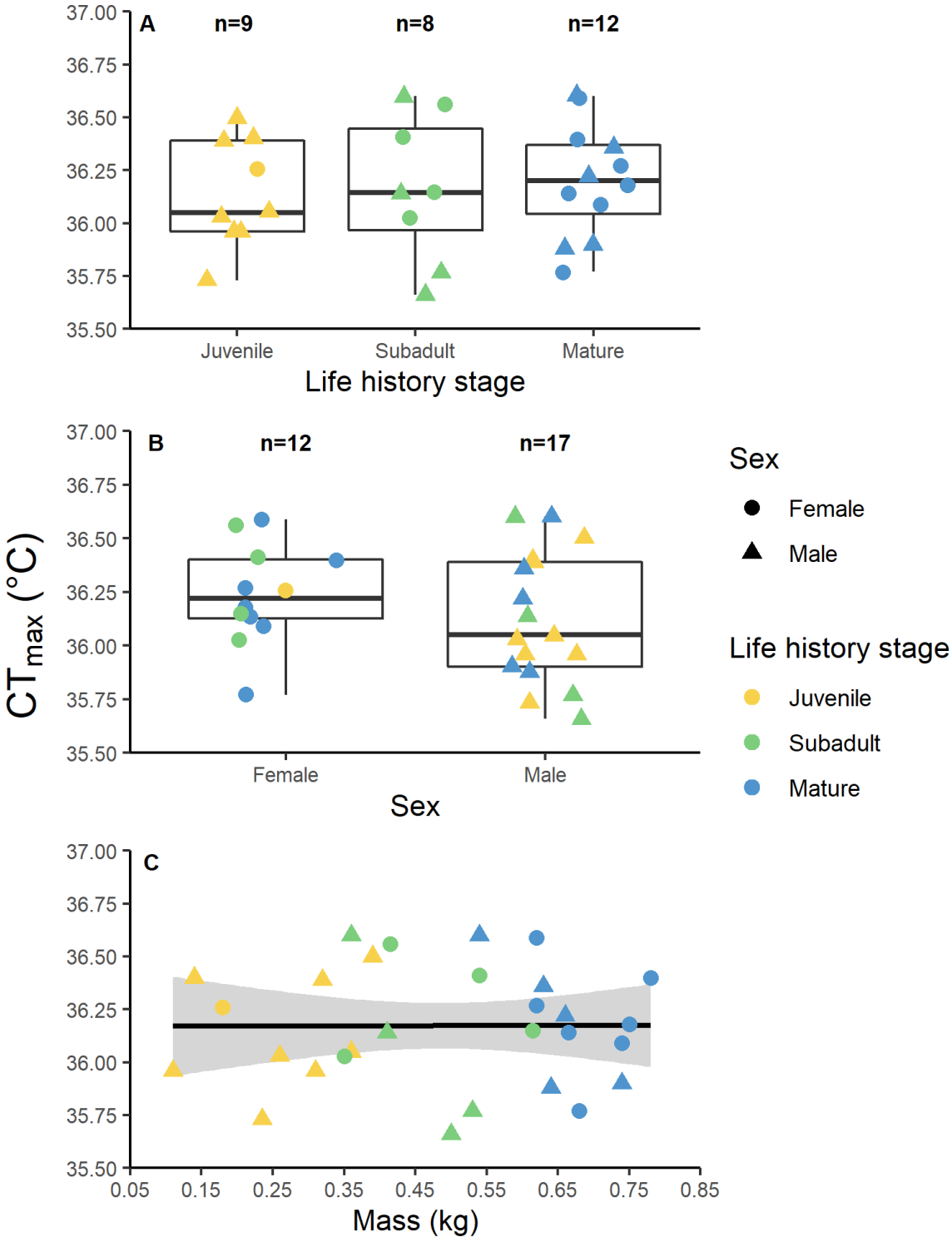

Figure 5.3 *Boxplots and linear regression of the mean CT_{max} across (A) life history stages (P = 0.56), (B) sex (P = 0.11), and (C) body mass (P = 0.26). The shaded area represents the 95% confidence intervals of the linear fit.*

During CT_{max} trials, there was no difference in the proportion of time spent resting versus active between life history stages (χ^2 = 3.14, *P* = 0.21; Figure 5.4A) or sexes (χ^2 = 0.58, *P* = 0.45; Figure 5.4B) (Supplemental Table S5.3). The resting ventilation rates of sharks did not differ between sexes (F= 3.87, *P* = 0.05, Figure 5.5) (Supplemental Table S5.4). Within females, subadults had higher ventilation rates than juveniles (t-ratio= -3.44, *P* = 0.00) and adults (t-ratio= 2.42, *P* = 0.04), and within males, both juveniles (t-ratio= 3.81, *P* =0.00) and subadults (t-ratio= *P* =0.01) differed from mature adults (Figure 5.5, Supplemental Table S5.4).

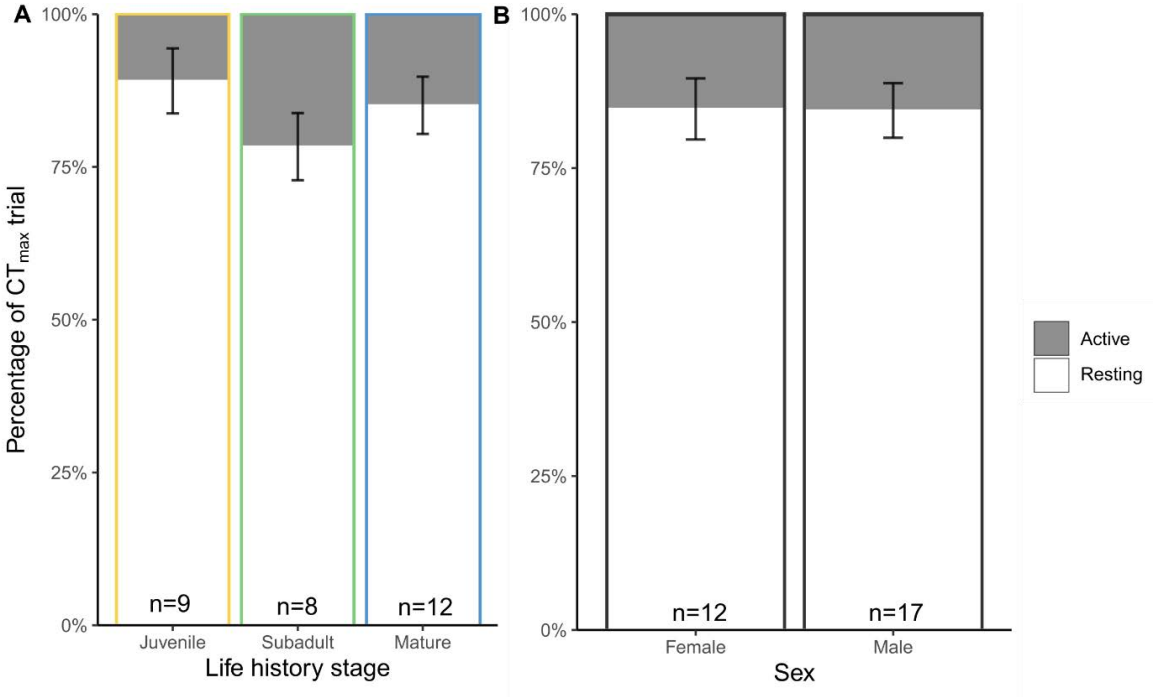

Figure 5.4 *The proportion of activity type (resting verses active) during CT_{max} trials across (A) life history stages and (B) between sexes. Error bars represent standard error of the mean and there was no significant difference between any groupings (life history stage: P= 0.21; sex: P= 0.45).*

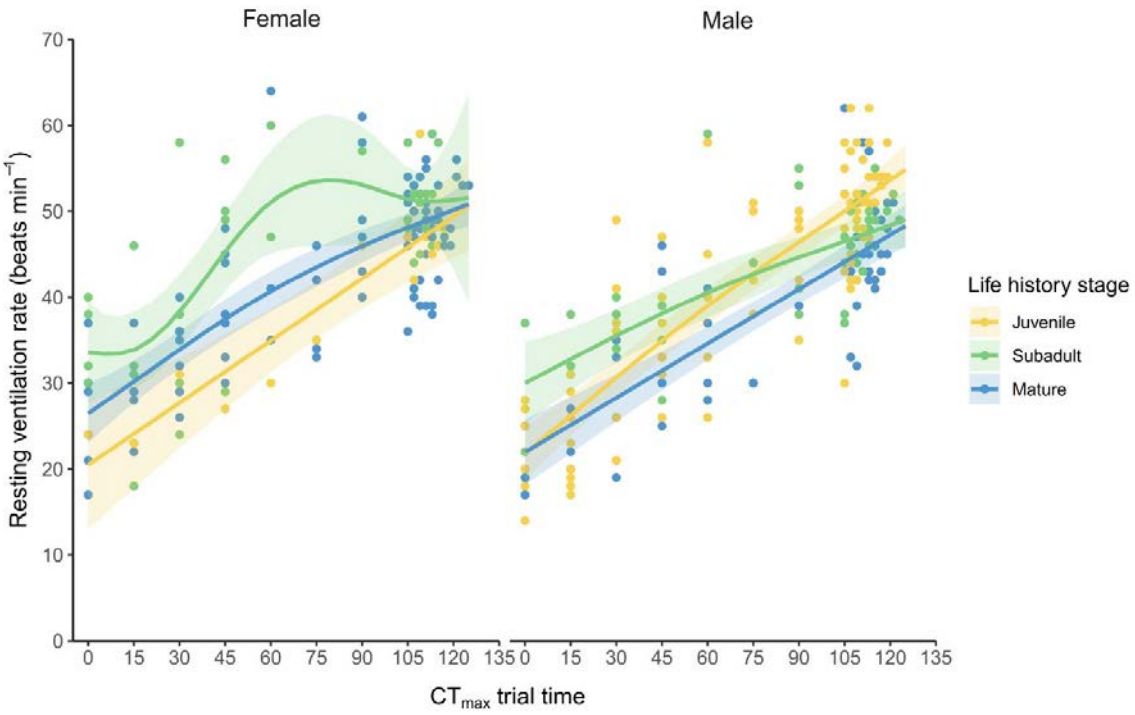

Figure 5.5 *Ventilation rates (gill beats per minute) of epaulette sharks across CT_{max} assays between (A) life history stages and (B) between sexes. Ventilation rates were measured every 15 minutes for the first 105 minutes, and then every two minutes until the loss of righting reflex occurred. Shaded areas represent the 95% confidence intervals of the linear mixed effects model fits.*

5.5 Discussion

With the aim to determine whether three life history stages, sex, and body size affected the upper thermal tolerance limits of a tropical elasmobranch species, this study did not find any effects of these factors on CT_{max} (Table 5.2, Figure 5.3). Although CT_{max} trials were not identical in terms of animal holding time (*i.e.*, time from temporary collection to the CT_{max} trial), starting water temperature, or time of day, we found no effect of these experimental design variables on CT_{max} (Figure 5.2). Finally, we did find small differences in the resting ventilation rates during CT_{max} trials, particularly within males (Figure 5.5B). Our findings fuel the question: how are various life history stages and each sex impacted by thermal stress if it is not reflected in their upper thermal tolerance? Moreover, what are the most useful physiological markers to inform this question in future research? Answering these questions will provide a more uniform approach amongst researchers working to understand thermal limits in the context of climate change.

Life history stage and sex effects on CT_{max}

Having synthesized thermal limits across teleost fishes, Dahlke *et al.* (2020) proposed that thermal tolerance differs across life history stages. During embryonic stages of development, individuals do not have a fully developed cardiorespiratory system, and embryos would have a reduced capacity to circulate oxygen to tissues (Pörtner and Peck, 2010). Furthermore, in spawning adults, energy is diverted to gamete development, thus reducing the amount of oxygen available for a thermal response (Pörtner and Peck, 2010; Dahlke *et al.*, 2020). These hypotheses are well reflected in the synthesized data; however, Pottier *et al.* (2022) has contested these findings, indicating that the thermal threshold data were compared between different methodologies (*e.g.,* CT_{max} versus field temperatures), where some datasets were likely underestimating upper thermal tolerance in embryos and adults. Indeed, many studies including multiple life stages have not found differences in CT_{max} (*e.g.,* Ospina and Mora 2004; Recsetar *et al.*, 2012; Andreassen *et al.,* 2022); however, including a full range of life stages within a singular study is challenging, as most studies are lacking the very earliest life stages or validated reproducing adults (Johnson 1976; Ospina and Mora 2004; Recsetar *et al.*, 2012; Andreassen *et al.,* 2022).

In the context of the current study, we were not able to include embryonic and neonate life stages, as egg cases and newly hatched neonate sharks have not been documented on the Heron Island reef flat (Heupel *et al.*, 1999 and this study). Including these earlier life stages could help elucidate if a bottleneck in CT_{max} exists in this species. However, embryonic CT_{max} would likely require a different endpoint metric than LRR used here and across many other studies, given that elasmobranch embryos are attached to a large yolk and do not necessarily maintain a specific orientation and would therefore not right themselves. Perhaps cessation of other motor functions such as tail movements during early developmental stages and the onset of muscle spasms during later developmental stages would suffice. However, these endpoints are likely not directly comparable to LRR, as muscle spasms, for example, occurs well after LRR, which is why studies using that endpoint tend to produce higher CT_{max} estimates (Lutterschmidt and Hutchison, 1997).

In this study, we were also unable to assess CT_{max} in females that were actively encapsulating egg cases. The egg encapsulation process for this species is only 2-5 days long (Wheeler, unpublished data), which is difficult to capture when collecting wild sharks. However, adult sharks in this study were presumably undergoing other reproductive processes beyond egg encapsulation during our experiments, such as spermatogenesis for males and vitellogenesis and folliculogenesis for females. Indeed, we conducted this study during the reproductive season (Heupel *et al.,* 1999), and ejaculate was found on several calcified claspers of adult males during physical exams. Although nothing is known of reproductive effects on CT_{max} in elasmobranchs, there are some findings in viviparous teleosts, although limited and conflicting. Auer *et al.* (2021) reported that CT_{max} was similar from pre-gestation to early gestational stages but decreased by nearly 0.5°C in late stages prior to parturition. Contrarily, Johnson *et al.* (1976) found no difference in CT_{max} between gravid and non-gravid female counterparts, but that females overall had higher CT_{max} estimates than males. More research comparing reproductive effects on CT_{max} through stages of both oviparity and viviparity as well as the effects of maternally experienced thermal stress on the health of offspring would be pertinent future research.

As water temperatures increase, ectotherms increase aerobic oxygen uptake rates to a point before switching to unsustainable anaerobic pathways (Pörtner and Peck, 2010). So, it follows that we observed increases in ventilation rates with increasing temperatures during experimentation (Angilletta, 2009). Given that all life stages in this study had fully developed cardiorespiratory systems (*i.e.*, we did not examine embryos in this study), the reason for the slight increases in juvenile and subadult ventilation rates compared to adults, particularly in males, is unclear (Figure 5.4). Given that there was only one juvenile female in the study, it is difficult to determine if there is physiological significance to these results. During these ventilation counts, we did observe that sharks were typically at rest for the first hour of the trials until ~30°C was reached. In many cases, from 30°C to the CT_{max} endpoint, sharks became more agitated and active, which is consistent with previous teleost work (Lutterschmidt and Hutchison, 1997; Wells *et al.*, 2016; Firth *et al.*, 2021). Overall, because we did not detect any differences in CT_{max} across life

stages or between sexes, our data suggests that when a singular metric of upper thermal tolerance is used, upper thermal tolerance is conserved.

Body size and CT_{max}

Beyond specific life history stages and the associated energetic investments, body size itself also plays a role in upper thermal tolerance. Core body temperatures of large-bodied fishes heat more slowly than in smaller fishes due to lower surface area to volume ratios (Stevens & Fry, 1974; Zhang and Kieffer, 2014; Messmer *et al.*, 2017). Many studies have found small changes in CT_{max} with increasing body size, including both positive (Ziegeweid *et al.*, 2008; Zhang and Kieffer, 2014, Clark *et al.,* 2017) and negative relationships (*e.g.,* Komoroske *et al.,* 2014; Clark *et al.,* 2017; Messmer *et al.,* 2017; Leiva *et al.,* 2019), and it is possible that differences in thermal ramping rates partially explain these differences. To fully clarify why the relationship between upper thermal tolerance, life history stage, and body size is conflicting across the literature, future studies should include a full range of life stages, an appropriate thermal ramping rate, the same end point across stages, and validate the reproductive status of adults.

Implications and future directions

Attention to experimental design and implementation of CT_{max} estimates will be key to furthering our understanding of elasmobranch upper thermal tolerance. For example, in Gervais *et al.* (2018), Heron Island reef flat epaulette sharks demonstrated seasonal plasticity in CT_{max}, where values were 2.93°C higher in the summer compared to the winter. Instead, our CT_{max} estimates averaged at 36.22°C (± 0.36°C s.d.), which was 1.17°C degrees lower than expected for the spring season based on Gervais *et al.* (2018). However, in our study, we chose a slower thermal ramping rate for assays of 0.1°C min^{-1}, whereas Gervais *et al.* (2018) used 0.26°C min^{-1}. This methodological difference is likely why we found lower CT_{max} values than expected, because slower ramping rates typically produce lower CT_{max} end points (Illing *et al.*, 2020; Kingsolver and Umbanhowar, 2018; Messmer *et al.*, 2017). Therefore, selecting appropriate and consistent thermal ramping rates that allow the internal body temperature to mirror the thermal ramping assay is an important

consideration moving forward with both inter- and intra-specific comparisons of CT_{max} among large-bodied fishes.

Considering which physiological metric to use when assessing upper thermal tolerance also warrants more investigation. For example, median lethal temperature (LT50) is also an excellent estimate of upper thermal tolerance in fishes (Pottier *et al.,* 2022), and would be easier to implement than CT_{max} in embryonic stages. However, given the lethal nature of this method, it may not be appropriate for studies on wild-caught elasmobranchs. Thermal effects on metabolic rate may also be a useful, non-lethal method to assess changes in organismal energetic costs. Adult epaulette shark metabolic costs do not differ between current day spring and summer mean water temperatures (25 versus 28°C) (Wheeler *et al.,* 2022), but prolonged, chronic exposure to future ocean warming temperatures of 31°C does reduce physiological performance of embryos and neonates (Wheeler *et al.,* 2021). Indeed, chronic exposure to elevated temperatures that are well below CT_{max} may provide a better picture of sublethal effects of ocean warming across ontogeny.

Epaulette sharks are thought to reach maturity in 2-4 years (Vanderwright *et al.,* 2021), which for an elasmobranch, is a relatively short generation time. This may provide some scope for intergenerational adaptation in parallel to ocean warming within this species; however, most other elasmobranchs have longer generation times and may not keep pace, which could render species in this group particularly vulnerable as warming continues. Moving forward from this study, researchers can now refine experimental designs to better elucidate the thermal tolerance limits and overall physiological performance of this and other elasmobranch species in the context of continued ocean warming.

Chapter 6: Future thermal regimes for epaulette sharks: growth and metabolic performance cease to be optimal

Associated publication

Wheeler, C. R., Rummer, J. L., Bailey, B., Lockwood, J., Vance, S., & Mandelman, J. W. (2021). Future thermal regimes for epaulette sharks (*Hemiscyllium ocellatum*): growth and metabolic performance cease to be optimal. Scientific Reports, 0123456789, 1–12. https://doi.org/10.1038/s41598-020-79953-0

Data availability

Data in this manuscript are available from the Research Data Repository at JCU: https :// doi.org/10.25903 /YTXC-N035.

6.1 Summary

Climate change is affecting thermal regimes globally, and organisms relying on their environment to regulate biological processes face unknown consequences. In ectotherms, temperature affects development rates, body condition, and performance. Embryonic stages may be the most vulnerable life history stages, especially for oviparous species already living at the warm edge of their distribution, as embryos cannot relocate during this developmental window. We reared 27 epaulette shark (*Hemiscyllium ocellatum*) embryos under average summer conditions (27 °C), or temperatures predicted for the middle and end of the twenty-first century with climate change (*i.e.,* 29 and 31°C) and tracked growth, development, and metabolic costs both *in ovo* and upon hatch. Rearing sharks at 31°C impacted embryonic growth, yolk consumption, and metabolic rates. Upon hatch, 31°C-reared sharks weighed significantly less than their 27°C-reared counterparts and exhibited reduced metabolic

performance. Many important growth and development traits in this species may peak after 27°C and start to become negatively impacted nearing 31°C. We hypothesize that 31°C approximates the *pejus* temperature (i.e., temperatures at which performance of a trait begin to decline) for this species, which is alarming, given that this temperature range is well within ocean warming scenarios predicted for this species' distribution over the next century.

6.2 Introduction

Ocean warming, resulting from global climate change, is already causing unprecedented changes to aquatic ecosystems worldwide (Fox-Kemper *et al.,* 2021). The oceans absorb the Earth's excess trapped heat that comes from anthropogenic emissions, and as such, sea surface temperatures are predicted to increase by as much as 4.0 °C under continued high emission scenarios1. These shifts are thought to have the most impact on tropical ecosystems where many species are adapted to narrow temperature ranges and because seasonal temperature changes are small in comparison to those experienced in temperate zones (Angilletta 2009; Payne *et al.,* 2016). Therefore, an organism's ability to adapt to a change, whether by phenotypic or transgenerational plasticity, will become increasingly more important to surviving the changing conditions over the next century (Fox-Kemper *et al.,* 2021). As most aquatic organisms are ectotherms, water temperatures regulate the biological and physiological processes that are crucial for survival (Gillooly and Dodson 2000). Consequently, performance traits that reflect fitness (*e.g.,* growth rates) exhibit thermal dependence, and this relationship can typically be depicted as a thermal performance curve (Angilletta 2009; Kellermann *et al.,* 2019). In the context of ocean warming, establishing thermal performance curves for traits and species can help determine the suitability of future thermal habitats and help to predict both acute and chronic effects of warming on populations and ecosystems (Huey *et al.,* 2012; Sinclair *et al.,* 2016).

The embryonic life stage in ectotherms represents a thermal bottleneck when it comes to climate change vulnerability (Dahlke *et al.,* 2020; Pörtner and Farrell 2008). Across ectotherms, embryos are generally less thermally tolerant than juveniles and non-reproducing adults. For example, embryos exhibit a narrower thermal performance curve—the difference between their maximum and

minimum critical temperatures—and a lower thermal safety margin, which is the difference between their optimal temperature and their mean habitat temperature (Dahlke *et al.,* 2020; Pörtner and Peck 2010). However, embryos, particularly of oviparous species, must also possess mechanisms to tolerate temperature changes throughout development because they cannot freely move and/or choose temperatures that are more favorable while *in ovo* (Wheeler *et al.,* 2020). Consequently, the mismatch between an increase in thermal vulnerability and the inability to behaviorally thermoregulate during the embryonic stages will likely have negative consequences for many aquatic ectotherm species in the face of ocean warming.

Chondrichthyan fishes (*i.e.,* the class including sharks, rays, skates, and chimaera of which are mostly ectothermic) present a challenge in relation to ocean warming vulnerability, as many species are globally threatened (*i.e.,* mainly from fisheries) (Dulvy *et al.,* 2014), poorly characterized in terms of basic life history (Cortés 2000), have slow generation times and low reproductive output, and are logistically challenging for controlled laboratory experiments. However, these fishes have ecological, economical, and cultural significance worldwide, and require proper assessment and management, particularly with the rapidly changing marine environment (Ward-Paige *et al.,* 2012). Given that there are more than 1200 species of Chondrichthyans (Dulvy *et al.,* 2021), it is impractical to assume that comprehensive research investigating the effects of climate change can be conducted broadly. Therefore, we argue for a strategic focus on studies that investigate physiological tolerance limits and thresholds and to identify bioindicator species. Indeed, the indicator species concept is common in fields that include ecological and environmental monitoring to track the health of an ecosystem or to monitor the effectiveness of management (Lindenmayer and Likens 2011; Siddig *et al.,* 2014). However, it is less common to study an indicator species' physiology—particularly via a thermal performance lens—for extrapolation within a taxonomic group, but that is the aim.

Because oviparous (egg-laying) chondrichthyans tend to be smaller in comparison to viviparous (live-bearing) species within this taxonomic group and are well suited to captivity, climate change impacts on in *ovo* growth and

development have been studied in several species (Di Santo 2015; Johnson *et al.,* 2016; Pistevos *et al.,* 2015; Rosa *et al.,* 2014). In fact, in *ovo* incubation time negatively correlates with increasing water temperatures in 28 species of sharks, skates, and chimaera that have been investigated to date (Wheeler *et al.,* 2020). Indeed, the maximum thermal limits for growth and development are imperative to understanding species and population level vulnerabilities. Therefore, given the similarities with regard to growth and development patterns, at least within oviparous species, an oviparous chondrichthyan may be ideal as an indicator species, especially for investigating physiological thermal tolerance with respect to climate change. The epaulette shark (*Hemiscyllium ocellatum*), one such small oviparous shark endemic only to the Great Barrier Reef (GBR), Australia (Dudgeon *et al.,* 2019), has been the focus of many climate change related laboratory studies (Gervais *et al.,* 2016, 2018; Heinrich *et al.,* 2014, 2015; Johnson *et al.,* 2016), because this species thrives in captivity and is considered of least concern in the wild by the International Union for Conservation of Nature (IUCN) Red List Criteria (Bennett *et al.,* 2015). Additionally, epaulette sharks possess unique morphological and physiological traits that allow them to hunt in isolated tidal pools and survive extreme and repeated hypoxia conditions (Routley *et al.,* 2002; Wise *et al.,* 1998). Therefore, this shark species may be resilient to challenging abiotic conditions, and as such, we propose that the epaulette shark could serve as a conservative indicator species for chondrichthyans that are physiologically sensitive or logistically difficult to study. In other words, if epaulette sharks cannot cope with, in this case, thermal stress, how will other, less tolerant species fare?

Throughout the southern portion of their range on the GBR, epaulette sharks inhabit the reef flats where water temperatures seasonally vary, on average, from 21.7 to 27.9°C (Heupel *et al.,* 1999). While adult epaulette sharks do not use movement to behaviorally thermoregulate30, their maximum critical thermal limit (CT_{max})—the highest temperature at which acute survival is possible—is between 36 and 39 °C, which although seasonally-dependent, is well beyond temperatures that are predicted for their native range during the twenty-first century due to ocean warming (Gervais *et al.,* 2018). Yet, this CT_{max} value only applies to adult survival and over short exposure periods (hours). Moreover, this value does not likely reflect the critical temperatures for other performance traits, such as growth

and development, which would span longer periods (months to years). This value also does not necessarily apply to the more vulnerable life stages, such as embryos and neonates. Indeed, processes like growth and development that are most associated with early life stages are energetically more costly than acute survival alone; therefore, such growth and development traits may exhibit a narrower thermal range and more conservative thermal limits (multiple performances-multiple optima hypothesis (Clark *et al.,* 2013; Dahlke *et al.,* 2020) than other traits and in other life stages. Given that rearing embryos and neonates at 32 °C has already resulted in significant mortality in this species (Gervais *et al.,* 2016), we hypothesize that the *pejus* temperature range (temperatures at which performance traits begin to decline (Farrell 2016)) is just below 31 °C. To determine this, we investigated the effects of rearing temperatures including 27, 29, and 31 °C on growth, development, and physiological performance traits in epaulette sharks both *in ovo* and until 60 days post-hatch.

6.3 Materials and methods

Ethics

All experimental protocols in this study were assessed and approved by the New England Aquarium Animal Care and Use Committee ethical code (protocol #: 2017-05), and furthermore conducted in accordance with all relevant guidelines and regulations.

Embryonic growth and development

This work commenced in June 2017 and was completed in June 2019 at the New England Aquarium's Animal Care Center (Quincy, MA, USA). Here, 27 epaulette shark egg cases were reared under three ecologically-relevant temperature treatments (27 °C: n = 14; 29 °C: n = 7, and 31 °C: n = 6) from 10 to 14 days post-deposition (dpd) until 60 days post-hatch. These eggs were collected from a singular breeding pair that had been maintained long term at the New England Aquarium (Boston, MA, USA). Then, all eggs were incubated in one of two 320l aquarium systems, each fitted with a 250l reservoir, UV sterilization, protein skimmer, two titanium heaters, and a 9:15 (d:n) hour photoperiod. Each egg case was suspended mid-water column with the proper polarity to ensure maximal success of

development. All experiments were run either between June 2017 and May 2018, with a control 27 °C and experimental 29 °C temperature treatment, or between June 2018 and June 2019, where a replicated 27 °C and an experimental treatment of 31 °C were used. Temperature, salinity, ammonia, and pH were monitored daily, and nitrates and nitrites were measured weekly (Table 1).

The outer most fibrous layer of the egg capsule was carefully removed using a razor blade to allow for better viewing within the capsule without any negative effects on the embryos (Harahush *et al.,* 2007; Johnson *et al.,* 2016). Eggs were candled 2–3 times per week in a 10l aquarium after allowing five minutes of habituation following transfer. This was important, as embryos of oviparous sharks are known to cease movement when there is a perceived external threat (Kempster *et al.,* 2013). Images and videos of each embryo were captured using a GoPro on narrow viewing setting so that growth rates (cm day^{-1}) and yolk-sac consumption rates (cm^2 day^{-1}) could be tracked over time. Content was corrected for fisheye bending around the edges, and ImageJ (Schneider *et al.,* 2012) was used to measure embryo length as well as yolk length, width, and area to the nearest 0.1 cm.

Embryonic oxygen uptake measurements

To quantify the metabolic cost of development in relation to temperature, oxygen uptake rates ($\dot{M}O_2$) of each embryo were measured *in ovo* using intermittent-flow respirometry. This was done every two weeks following the first 30 days of development because until ~ 30 days post deposition, the O_2 of the embryos was too small to detect while maintaining a chamber size large enough to accommodate the egg case. The whole respirometry setup comprised four glass chambers that were each 6 cm in diameter and 12 cm long (~ 339ml volume) with baffled ends to allow even water flow. All four chambers were submerged in an 80l water bath that received water directly from the animals' respective aquaria to ensure identical water quality between holding conditions and test conditions. This water bath was also fitted with a standpipe so that the volume of water bath completely replenished ten times per hour. Each chamber consisted of a flush pump (293.5l h^{-1}), which pumped water from the water bath, and a recirculating pump (302l h^{-1}) that circulated water throughout the chamber and through a glass

segment consisting of an OXSP5 oxygen sensor spot connected to a fiber optic cable and a Firesting O_2 system (Pyroscience, Aachen, Germany).

Embryos were carefully introduced into each respirometry chamber so that the egg case was never exposed to air. Upon transfer, chambers were covered with a small viewing window and were constantly supplied with filtered, oxygenated seawater for 2 h via the flush pump; this time period allowed embryos to habituate to the chambers following the transfer and found to be a sufficient period of time following preliminary trials31. After this 2-h habituation period, a relay timer was used to intermittently turn off the flush pump for 5, 10, or 15 min, depending on the stage of development; shorter measurement periods were used as the embryo developed. These time intervals were long enough to ensure that the decline in O_2 could be detected but short enough such that O_2 levels within chambers did not decrease below 80% saturation (Svendsen *et al.,* 2016). Following each this O_2 uptake measurement period, the flush pump was turned on once again, thus returning O_2 levels in the chamber water back to 100% air saturation; flush duration was always five minutes, regardless of embryo development stage. These measurement and flush cycles were repeated for 4 h (12–24 cycles depending on the measurement period) to ensure sufficient data points for each individual. After each respirometry trial, each embryo was returned to their respective holding conditions. Respirometry chambers were also cycled empty for 30 min before and after each animal trial to account for microbial accumulation within each chamber; although, calculations demonstrated microbial respiration to be negligible (less than 2% of embryonic respiration).

Respirometry chambers were also cycled with empty egg cases that had been maintained under the same conditions as the respective hatched neonates to account for the microbial respiration of each egg case; this too was also negligible (less than 3% of embryonic respiration). Oxygen uptake rates ($\dot{M}O_2$ in mg O2 embryo^{-1} h^{-1}) were calculated as $\dot{M}O_2 = SV$ where S represents the rate of change of O_2 within the chamber, and V is the volume of the chamber (Svendsen *et al.,* 2016). Metabolic rates typically include a correction factor to account for body mass; however, because the embryos were maintained within the egg cases to determine incubation time to hatching, data were calculated as per whole embryo rates, similar

to the protocols of Rosa *et al.* (2014). We did not correct for changes in mass using growth or yolk consumption rates, given that the former exhibited a linear and the latter a non-linear relationship (Fig. 1AB); therefore, we could not interpolate changes in embryonic mass over development to use in $\dot{M}O_2$ calculations.

Neonate survivorship, condition, and oxygen uptake measurements

Within 12 h of hatching, length (cm) and mass (g) of each neonate were measured, and the Fulton's condition factor (K = mass/length^3 (Froese *et al.,* 2006)) was calculated. Neonates were offered a mix of minced shrimp and clam, daily, after hatching to determine the time of first feeding (*i.e.,* dph). Neonates were also provided pieces of PVC pipes for shelter. Neonate resting oxygen uptake rates ($\dot{M}O_{2Rest}$) were measured at 30 days post-hatch, as this allowed enough time post-hatch to ensure that feeding had switched from residual internal yolk stores to exogenously offered food. Prior to respirometry trials, however, neonates were fasted for 48 h to ensure they were in a post-absorptive state (Heinrich *et al.,* 2014). Neonates were weighed and introduced directly to their respective respirometry chambers, using the same intermittent-flow respirometry setup described for embryos, and then neonates where allowed to habituate to the chambers for 2 h. Then, the $\dot{M}O_{2Rest}$ for each individual was measured using a cycle consisting of five min of measurement and five min of flushing the chambers with clean, well-aerated seawater for a period of 4 h. Trials were always executed during daytime hours. Similar to embryos, this period was determined to be the shortest trial duration to ensure the individual was in a resting non-stressed state (Clark *et al.,* 2013). Finally, maximum oxygen uptake rates ($\dot{M}O_{2Max}$) were measured in neonates at 45 days post-hatch using a standardized 3-min chase protocol with a 1-min air exposure (Rummer *et al.,* 2016). This specific protocol and time were chosen because epaulette sharks are not continuous but rather burst swimmers; after 3 min of being chased, the neonate's response changed from avoidance to a rolling behavior. Neonates were then immediately placed in the same intermittent flow respirometry setup that was used for embryos. The initial slope of oxygen uptake was used to calculate $\dot{M}O_{2Max}$, and then neonates remained in the chamber until oxygen uptake rates returned to $\dot{M}O_{2Rest}$ levels measured for the individuals during their respective previous trial at 30 days post-hatch. A scaling exponent of 0.89 was used to correct

the mass of each individual for the allometric relationship of mass and metabolic rate (Bouyoucos *et al.,* 2020; Jerde *et al.,* 2019). Finally, aerobic scope (AS) was calculated as $\dot{M}O_{2Max} - \dot{M}O_{2Rest}$ (Clark *et al.,* 2013).

Statistical analysis

Mixed linear effects (embryo length) and generalized additive mixed models (GAMM; yolk consumption and RMR) using round (which encompasses the two rounds and systems) as a random fixed effect were applied to the data to determine if the rate of growth, yolk consumption, and oxygen uptake rates changed over time *in ovo* (see S6.1). All neonate data met all criteria of normality, non-multi-collinearity, and homoscedasticity from initial qq and residual plots and were analyzed using a series of mixed linear models and one way analysis of variance (ANOVA) (see S6.2–S6.4). All statistical analyses were performed in R (version 1.4.1106, R Core Development Team 2021) where results were considered significant at $\alpha = 0.05$.

6.4 Results

Embryonic growth and development

Embryonic growth rates (cm day^{-1}) were faster for embryos reared at both 29 and 31 °C when compared to embryos reared at 27 °C, but there were no differences in growth rates for embryos reared at 29 or 31 °C (Fig. 6.1A, adjusted $R^2 = 0.85$, $F_{3,570} = 1091$, $P = 0.022$, see S6.1A). Correspondingly, yolk consumption (cm^2 day^{-1}) was also significantly faster in embryos reared at both 29 and 31°C when compared to embryos reared at 27°C (Fig. 6.1B, adjusted $R^2 = 0.721$, $F_{3,609} = 176.10$, $P < 0.0001$, see S6.1B). Embryonic RMR estimates were significantly different between embryos from all temperature treatment groups; specifically, RMR was higher in embryos reared at 29 °C when compared to those reared at 27 °C but then decreased in embryos reared at 31 °C (Fig. 6.1C, adjusted $R^2 = 0.756$, $F_{3,193} = 88.23$, $P < 0.0001$, see S6.1C).

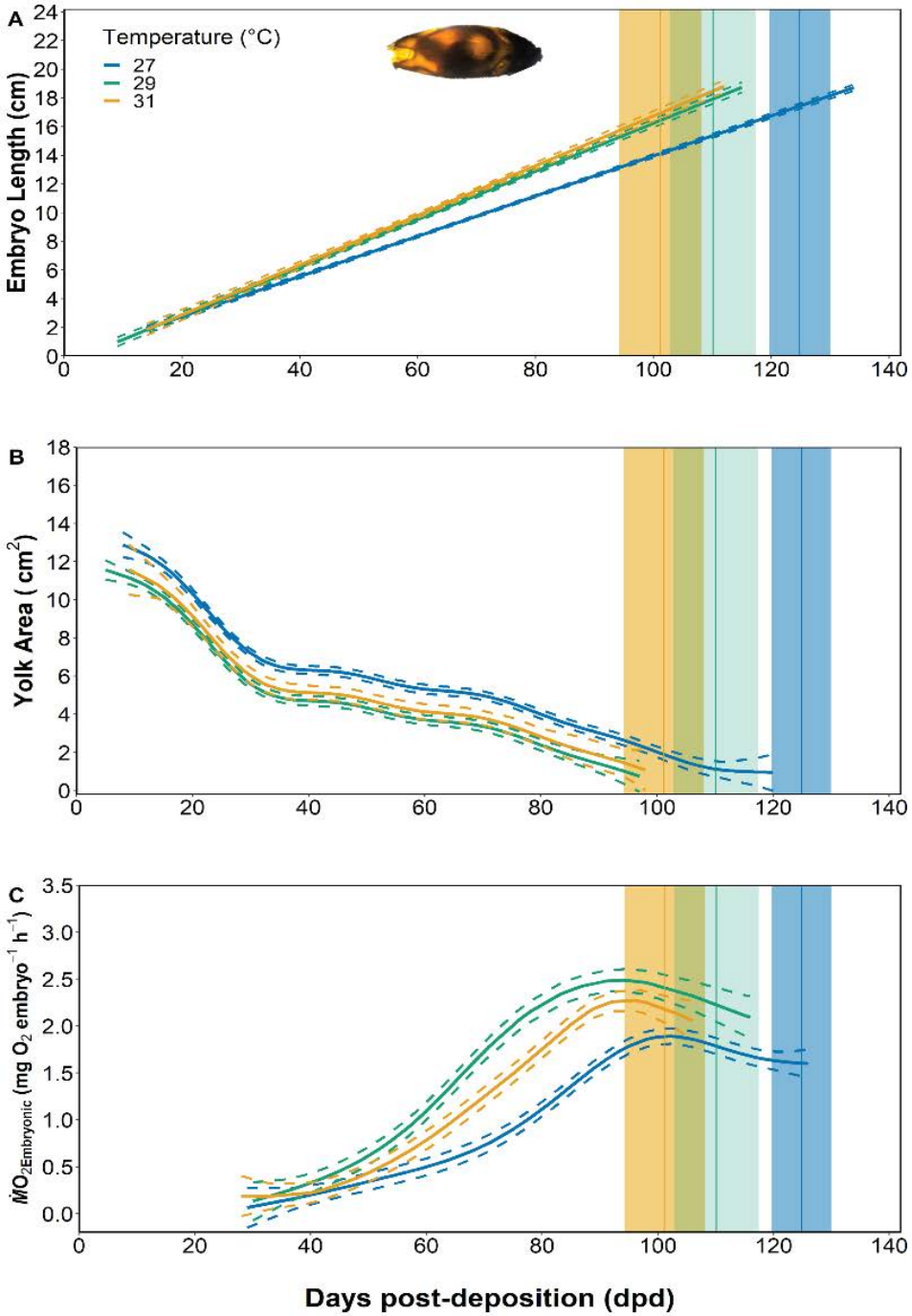

Figure 6.1 *The growth rate (cm day^{-1}) (A), yolk-sac consumption rate (cm^2 day^{-1}) (B), and embryonic oxygen uptake (mg O_2 embryo h^{-1}) (C), over the in ovo incubation period at 27, 29, and 31 °C. The embryonic length data were fit using a mixed linear model (S6.1A), and yolk-sac consumption and RMR were fit with a generalized additive mixed model (GAMM) (S6.1BC). Model fits are represented by solid lines, and 95% confidence intervals are represented by dashed lines. Model fits were considered significant at α = 0.05. The vertical lines represent the mean incubation time at each temperature treatment, and the shaded boxes represent the standard error around the mean.*

Neonate survivorship and condition

Embryonic and neonatal survival was 100% throughout the study, irrespective of rearing temperatures. All except for two sharks—one reared at 27°C and one reared at 29°C—hatched during the dark photoperiod hours. Hatching time was significantly impacted by temperature as well; incubation time decreased from 125±5 dpd to 110±7 dpd and 101±7 dpd in 27, 29, and 31°C reared embryos, respectively (Fig. 6.2A, ANOVA; temperature, $F_{2,24} = 38.04$, $P < 0.0001$; see S6.2A). The fastest incubation (*i.e.,* 95 dpd) occurred in 31°C reared embryos. Neonates were significantly lighter in mass (*i.e.,* by 2.6 ± 0.4 g) if the embryos had been reared at 31°C, but no differences could be detected in neonate mass when embryos were reared at 27 or 29°C (Fig. 6.3A, ANOVA; temperature, $F_{2,24} = 5.561$, $P = 0.01037$; see S6.3A). However, rearing temperatures did not affect neonate length or body condition (*i.e.,* Fulton's condition factor) (Fig. 6.3B, length ANOVA; temperature, $F_{2,24} = 1.284$, $P = 0.2954$, see S6.3B; Fig. 6.3C, Fulton's condition factor ANOVA; temperature, $F_{2,24} = 2.002$, $P = 0.1570$, see S6.3C). Finally, the time it took for neonates to feed exogenously for the first time was 6±1 days earlier for neonates reared at 31°C when compared to neonates reared under the other temperature treatments (Fig. 6.2B, ANOVA; temperature; $F_{2,24} = 55.28$, $P = < 0.0001$; see S6.2B).

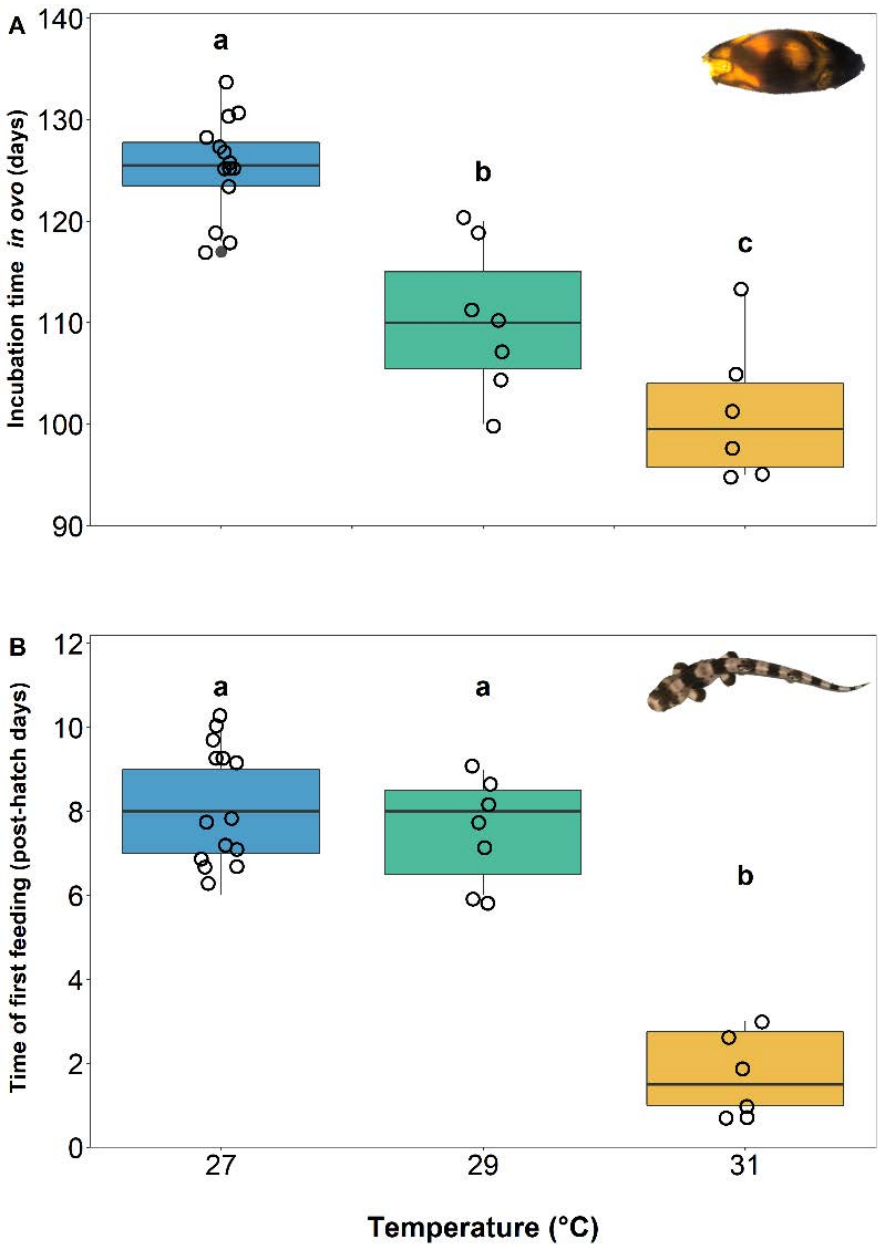

Figure 6.2 *Mean incubation time to hatching (days) (A) and time of first exogenous feeding (post-hatch days) (B) across three treatment temperatures of 27, 29, and 31 °C. Boxes and whiskers represent the median, 25th, and 75th quartiles and 10 and 90th percentiles, respectively. The filled circles represent outliers, and open circles represent observations. Differing lowercase letters denote statistically significant differences at α = 0.05 (see S6.2).*

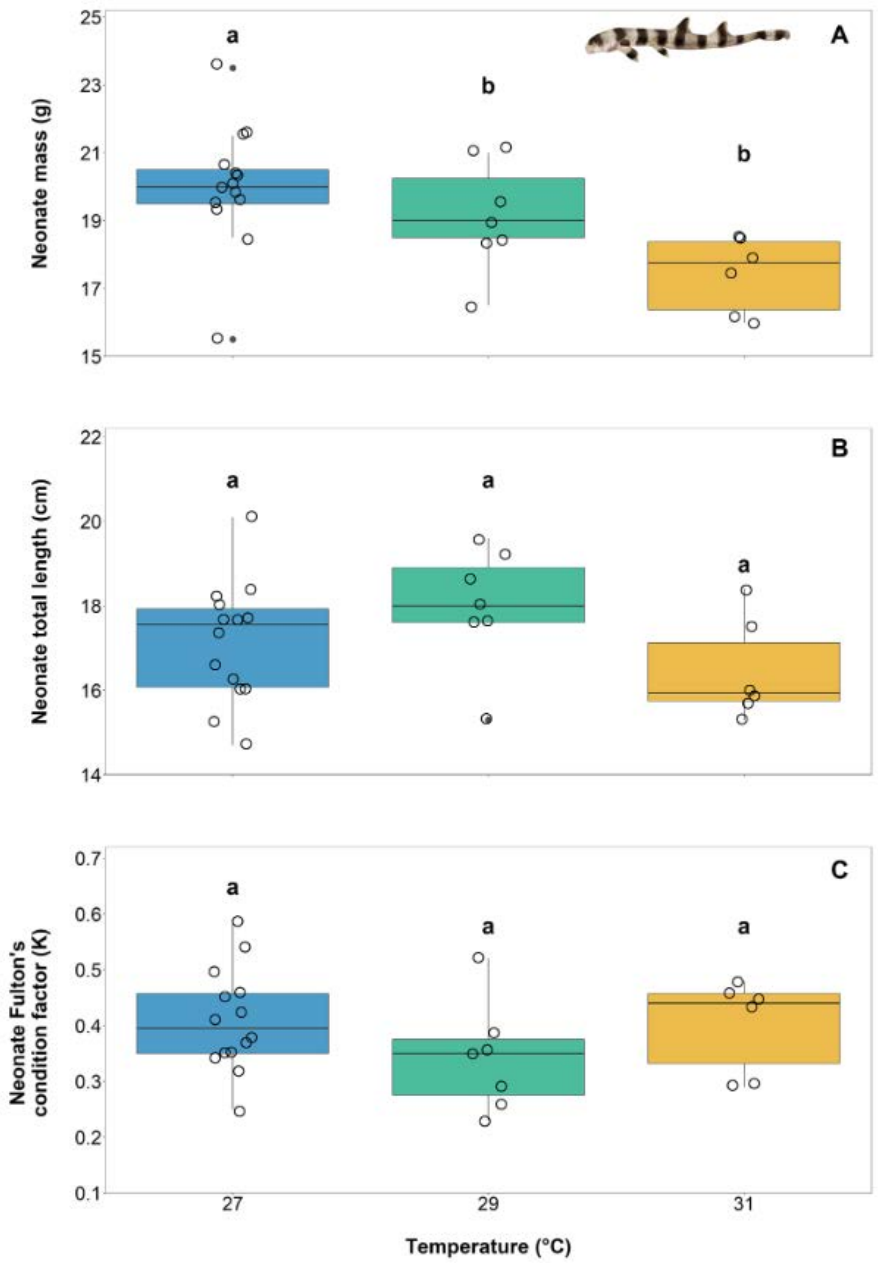

Figure 6.3 *Mean (± SE) mass (g) (A), total length (cm) (B), and Fulton's condition factor (K) (C) at hatching across three temperature treatments of 27, 29, and 31 °C. Boxes and whiskers represent the median, 25th, and 75th quartiles and 10 and 90th percentiles, respectively. The filled circles represent outliers, and open circles represent observations. Differing lowercase letters denote statistically significant differences at α = 0.05 (see S6.3).*

Neonate metabolic rates

In neonates reared at 29°C, $\dot{M}O_{2Rest}$ was significantly higher than in neonates reared at 27°C, but values for neonates reared at 31 °C were not significantly different than those from the other temperature treatments (Fig. 6.4A; ANOVA; temperature; $F_{2,24}$ = 6.25; P = 0.006531; see S6.4A). A similar pattern was evident with $\dot{M}O_{2Max\,x}$; however, in neonates reared at 31°C, MO_{2Max} decreased below values observed in neonates reared under the other temperature treatments (Fig. 6.4B; ANOVA; temperature; $F_{2,24}$ = 12.82; P = 0.0001635; see S6.4B). Aerobic scope (AS = $\dot{M}O_{2Max\,x} - \dot{M}O_{2Rest}$) was similar in neonates reared at under 27 and 29°C treatments but decreased in neonates reared at 31°C (Fig. 6.4C; ANOVA; temperature; $F_{2,24}$ = 4.53; P = 0.02142; see S6.4C). Finally, there was a significant relationship between temperature and the time to recover following exercise (i.e., time from $\dot{M}O_{2Max}$ to $\dot{M}O_{2Rest}$); as rearing temperatures increased, recovery time increased (Fig. 6.4D, MO_{2Max} recovery ANOVA; temperature, $F_{2,19}$ = 16.727, P < 0.0001; see S6.4D). Neonates reared at 27°C required an average of 71±5 min to recover from exercise; whereas neonates reared at 29°C and 31°C required, on average, 107±7 and 138±6 min, respectively (Fig. 6.4D). There was nearly a doubling in recovery time with a 4 °C increase in rearing temperature.

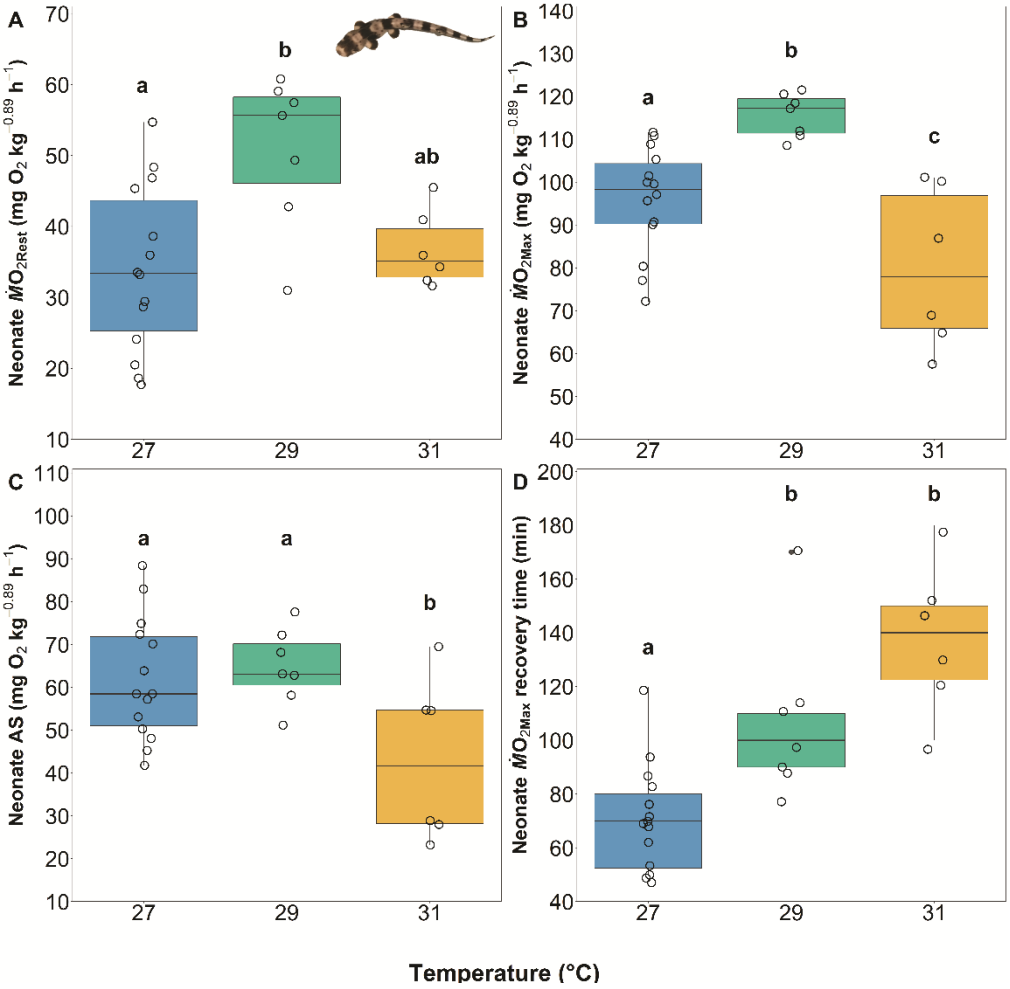

Figure 6.4 *Boxplots of the* $\dot{M}O_{2Rest}$ *(mg* O_2 $kg^{-0.89}$ h^{-1}*) (A),* $\dot{M}O_{2Max}$ *(mg* O_2 $kg^{-0.89}$ h^{-1}*) (B), aerobic scope (AS) (*$\dot{M}O_{2Max}$ *—* $\dot{M}O_{2Rest}$*; mg* O_2 $kg^{-0.89}$ h^{-1}*) (C), and recovery time (min) from* $\dot{M}O_{2Max}$ *(D) for neonates across three rearing temperature treatments of 27, 29, and 31 °C. Boxes and whiskers represent the median, 25th, and 75th quartiles and 10 and 90th percentiles, respectively. The filled circles represent outliers, and open circles represent observations. Differing lowercase letters denote statistically significant differences at* $\alpha = 0.05$ *(see S6.4).*

6.5 Discussion

Here, we investigated how growth, development, and metabolic performance traits of embryonic and neonate epaulette sharks, a tropical, shallow-water, oviparous shark species, were affected by increased temperatures relevant to mid and end-of-century ocean warming scenarios. We hypothesized that the *pejus* temperature for these traits was between 29 and 31°C, which stems from

previous research reporting high mortality of epaulette shark offspring at 32°C (Gervais *et al.,* 2016, 2018). Our findings support this hypothesis. While survival was unaffected, embryos that were reared under elevated temperatures (*i.e.,* 31 °C) grew more quickly, exhibited reductions in metabolic performance, and hatched at a lighter mass than their current temperature counterparts. Furthermore, upon hatch, 31 °C-reared neonates exhibited a reduction in aerobic scope, indicating thermal impairment during this vulnerable life stage. Without phenotypic or transgenerational plasticity in these key traits, our findings could foreshadow biogeographic redistribution or changes in breeding season timing with future ocean warming scenarios, which could not only apply to epaulette shark populations on the GBR but also other similar species worldwide. This information is timely—especially given the rapid succession of mass coral bleaching events and other global heatwaves since the early twenty-first century—for inclusion in vulnerability assessments for the Great Barrier Reef as well as coral reef ecosystems worldwide.

While epaulette sharks have been investigated within the context of environmental stress since the start of the twenty-first century (*e.g.,* Wise *et al.,* 1998), it was only recently determined that prolonged exposure to elevated temperatures could be the most detrimental to this species, especially during early life stages. Indeed, previous research on this species demonstrated that simulated ocean acidification conditions (elevated pCO_2) have little impact on early growth, development, and survivorship of embryos and neonates (Johnson *et al.,* 2016) and do not affect foraging behavior or metabolic performance of adults (Heinrich *et al.,* 2014, 2015). Moreover, this species is noted as the most hypoxia and anoxia tolerant shark species studied to date (Routley *et al.,* 2002; Wise *et al.,* 1998). In contrast, preliminary work to this study found that, when epaulette sharks were reared at 32 °C, survival to hatching was extremely low (37.5%), neonates exhibited irregular coloration and lacked their distinct black epaulette markings, and only one 32°C-reared neonate from the study survived beyond three days post-hatch (Gervais *et al.,* 2016). Furthermore, after the remaining neonate was transitioned back to 28°C, proper patterns and coloration still did not develop (Gervais *et al.,* 2016). Juvenile epaulette sharks—at least until 171 days post-hatch—were also negatively affected when acclimated to 32 versus 28°C. Notably, survival and growth rates were

reduced, despite maintained food consumption (Gervais *et al.,* 2018). Based on these findings, we focused only on the effects of elevated temperatures and chose 31°C as the highest temperature treatment in an effort to observe only sub-lethal, if any, effects throughout our study.

Here, embryonic growth rates were tightly coupled with faster yolk consumption rates, presumably fuelling the accelerated growth rates that were also observed (Figs. 6.1AB). Interestingly, growth rates were similar in animals reared at 29 and 31°C, perhaps indicating that the *pejus* temperature for this trait is between these temperatures, but nearing 31°C. Johnson *et al.* (2016) reported slower growth rates during the early stages of embryonic development that increased after embryos had progressed to one third of their total incu+bation time. However, our data exhibited a linear relationship that did not reflect this temporal difference in growth rates.

The 31°C-reared neonates in this study either hatched with more internal yolk reserves or consumed internal yolk stores more quickly during their final days *in ovo* when compared to their lower temperature reared counterparts. For oviparous chondrichthyan embryos, in general, the yolk transfers from the external yolk sac, through a yolk stalk, and then into an internal yolk sac that feeds into the spiral intestine where it is digested to provide energy for growth and development (Ballard *et al.,* 1993). When the external yolk is depleted, there remains an internal reserve that feeds the late-stage embryo for a short period of time (*i.e.,* 5–7 days in epaulette sharks) and neonates for weeks to months after hatching (Conrath and Musick 2012). The shift from endogenous energy sources (*i.e.,* yolk) to exogenous feeding in neonates could therefore indirectly indicate the time at which the internal yolk has been consumed, thus allowing yolk consumption rates to be calculated. External yolk-sac consumption rates for 29 and 31°C reared embryos were similar (Fig. 6.1B); the last visible signs of external yolk for embryos from both treatments was around 97 ± 2 dpd but closer to 118 ± 4 dpd for 27°C-reared embryos. As such, hatching occurred significantly earlier (101 ± 7 dpd) in 31°C-reared animals than in 29°C-reared animals (110 ± 7 dpd) (Fig. 6.1B). From these findings, we hypothesize that there is a distinct relationship between internal yolk depletion and time of hatching, which is further supported by the time of first feeding. The 31°C-reared

neonates commenced exogenous feeding significantly sooner (Fig. 6.2B) than their lower temperature reared counterparts. One 31°C-reared individual consumed food only 24 hours after hatching. This overall finding regarding the fast rate of energy depletion *in ovo* and the early timing of exogenous feeding in 31°C-reared epaulette sharks could have clear fitness implications relative to energy use, growth, and survival over the longer term.

Our findings regarding changes in embryonic $\dot{M}O_2$ ($\dot{M}O_{2\text{Embryonic}}$) represent, to our knowledge, the most fine-scale (6–12 data points per embryo) data set to date for a chondrichthyan species and especially over a climate change relevant temperature range. Estimates of RMR increased as temperature increased from 27 to 29°C, demonstrating the regulatory role temperature plays on metabolic rate for ectotherms. However, $\dot{M}O_{2\text{Embryonic}}$ then declined in 31°C-reared embryos when compared to those reared at either 29 or 27°C. This could indicate a reduction in metabolic performance and/or a decrease in embryonic activity (tail-beating or ventilation) as an energy-saving strategy (Fig. 1C). Across treatments, $\dot{M}O_{2\text{Embryonic}}$ increased to a peak at 10–20 days prior to hatching and slightly decreased thereafter. The shape of this $\dot{M}O_{2\text{Embryonic}}$ curve has only been documented in one other oviparous chondrichthyan species (Rodda 2000); all other studies report a continuous increase in RMR over development (Rosa *et al.,* 2014). This decrease in O_2 uptake rates during the final stages of development when the embryo has completely absorbed the external yolk sac (stage 34 from Ballard *et al.,* 1993; stage 7 from Musa *et al.,* 2018) could indicate crowding and mild hypoxia caused by the limited surface area for oxygen exchange across the egg case apertures and could underpin the mechanism signalling hatching.

The embryonic and neonate survival rates (*i.e.,* 100%) throughout the present study imply that any negative effects of the rearing temperatures were only sub-lethal, at least during these early life stages. Incubation time was significantly impacted by temperature (Fig. 2A), which is a phenomenon that has been well-documented in development studies on ectothermic oviparous invertebrate and vertebrate species from both aquatic and terrestrial habitats (Gillooly and Dodson 2000; Wheeler *et al.,* 2020; Zuo *et al.,* 2012). Here, neonates had significantly lower mass if they were reared at 31°C when compared to those reared at 27°C, which

supports the general hypothesis that warmer temperatures produce smaller offspring, a trend also observed across ectothermic invertebrate and vertebrate species alike (Atkinson 1994). Furthermore, the reduction in mass in 31°C-reared animals further supports our hypothesis that expedited use of the internal yolk store may have, in part, signalled hatching. The reduction in body mass could be partially due to faster yolk consumption rates, which could compromise metabolic performance upon hatch.

At 30 days post-hatch, $\dot{M}O_{2Rest}$, which represents an estimate of SMR, increased in 29°C-reared animals when compared to 27°C-reared animals, and although not significant, decreased slightly in 31°C-reared animals (Fig. 6.4A). A similar trend occurred for $\dot{M}O_{2Max}$, an estimate of MMR, which increased in 29°C-reared animals when compared to 27°C-reared animals but was followed by a significant decrease in 31°C-reared animals (Fig. 6.4B). As such, AS decreased in 31°C-reared animals when compared to animals from the lower rearing temperatures. The increase in $\dot{M}O_{2Rest}$ between 27 and 29°C-reared animals and decrease of $\dot{M}O_{2Max}$ between 29 and 31°C animals indicates an overall reduction in metabolic performance, and that the *pejus* temperature likely falls between 29 and 31°C (Figs. 6.4AB). The time required for 31°C-reared animals to recover from the exercise protocol that was used to induce $\dot{M}O_{2Max}$ was twice the amount of time required for 27°C-reared animals to recover (Fig. 6.4D). Collectively, these data indicate a decrease in the capacity for aerobic performance with elevate temperatures in neonates, which could translate to reduced survival beyond the 60 days post-hatch time period examined in this study.

Overall, we found that all metrics assessed, except length, Fulton's condition factor, and $\dot{M}O_{2Rest}$, were negatively impacted in 31°C-reared animals. Embryos in this treatment group hatched more quickly (Fig. 6.2A), were lighter in mass (Fig. 6.3A), exhibited reductions in metabolic performance (decreased $\dot{M}O_{2Max}$ and AS; Fig. 6.4BC), and required twice as long to recover from exhaustive exercise (Fig. 6.4D) than their lower temperature reared counterparts. Therefore, we conclude that thermal performance curves for the assessed traits for this species peak after 27 but before 31°C, and would decrease thereafter, as supported by Gervais *et al.* (2016). While we recognize the genetic variation limitations that come with using

only a single breeding pair, as was done in this study, we also note that the effects detected are, therefore, more likely solely due to temperature than genetic variability. To this end, more studies are needed, both within controlled laboratory conditions and amongst wild populations across latitudes.

Within an ecological context, epaulette sharks are distributed throughout the Great Barrier Reef in Australia and particularly occupy shallow reef flats where environmental conditions, such as dissolved oxygen and temperature, fluctuate quickly and often (Heupel *et al.,* 1999). Heron Island in the southern Great Barrier Reef, has vast a reef flat where epaulette sharks are common. Given that peak egg deposition period at Heron Island is between August and December (Heupel *et al.,* 1999), eggs deposited at the end of this time frame would develop on the benthos between December and March, when daily average temperatures peak at 28°C. With mid- and end-of-century climate change predictions, it is likely that summer average temperatures could increase to upwards of 32°C at this location. Gervais *et al.* (2018) found that juvenile epaulette sharks acclimated to 32°C exhibited reduced growth rates despite maintaining constant food consumption rates. Moreover, these sharks behaviourally sought out warmer temperatures despite the fact that the thermal stress eventually resulted in 100% mortality. Overall, findings from Gervais *et al.* (2016; 2018) and the present study suggest that, under future ocean warming scenarios, epaulette shark habitats could become too warm to support proper growth and development of embryos, neonates, and juveniles. The native range of epaulette sharks (*i.e.,* the GBR) has already experienced heatwaves that have resulted in three widespread coral bleaching events (2016, 2017, and 2020 (Hughes *et al.,* 2017; Skirving 2020)). These events, although acute, could sustain throughout the developmental window of this species, thereby greatly affecting reproductive success and therefore reducing the size of that particular year class of sharks. Indeed, both acute (*e.g.,* a heatwave, a coral bleaching event) and chronic (*i.e.,* ocean warming) thermal stress could be detrimental to individual year classes and population stability over the long term.

Overall, we concluded that, for epaulette sharks, a species otherwise resilient to severe changes in abiotic conditions, at least those investigated in isolation (*e.g.,* acute exposure to temperature changes, ocean acidification scenarios, and extreme

hypoxia and anoxia), the *pejus* temperature for development is between 29 and 31°C. Because most oviparous sharks and skates are heavily dependent on the benthos, they are unlikely or unable to undertake large movements to more ideal temperatures (Nay *et al.,* 2021; Wheeler *et al.,* 2020). Therefore, we expect these species to contract their geographical range to areas where thermal conditions remain optimal, but given the importance of meso-predators, this could come at the expense of ecosystem health. Indeed, species like the epaulette shark will be the ones to observe. Ultimately, our findings suggest that, under ocean warming scenarios for the middle and end of the twenty-first century, tropical oviparous chondrichthyan species will likely be exposed to their upper thermal limits for critical activities such as growth and development, which causes concern for the future health of the ecosystems they help to support.

Chapter 7: General Discussion

7.1 Current-day thermal physiology

In this thesis I have expanded our understanding of the thermal physiology of epaulette sharks across ontogeny and under current day conditions. During spring and summer months, when water temperatures range from 24.5-28.5°C, epaulette sharks maintain metabolic rates; time of day more profoundly influences diel rhythm than temperature (Chapter 2, Wheeler *et al.,* 2022). Given that epaulette sharks typically experience seasonal water temperatures ranging 20 to 30°C, more research is needed to better elucidate their thermal physiology under the cooler temperatures of this range. However, my research supports that thermal sensitivity is low. In other words, the traditional Q_{10} relationship – the thermal quotient for ectothermic species representing a doubling of metabolic rate for every 10°C temperature change – does not apply to epaulette sharks within their native temperature range. When metabolic rates measured in epaulette sharks by different researchers, methods, and on different individuals are compared (*e.g.,* Routley *et al.* 2002; Heinrich *et al.* 2014), rates are consistent, repeatable, and similar across temperatures (Figure 7.1). The main difference between studies is life history stage, where with body size as a covariate, neonates had lower metabolic rates than juveniles and adults across this and all other studies (Figure 7.1).

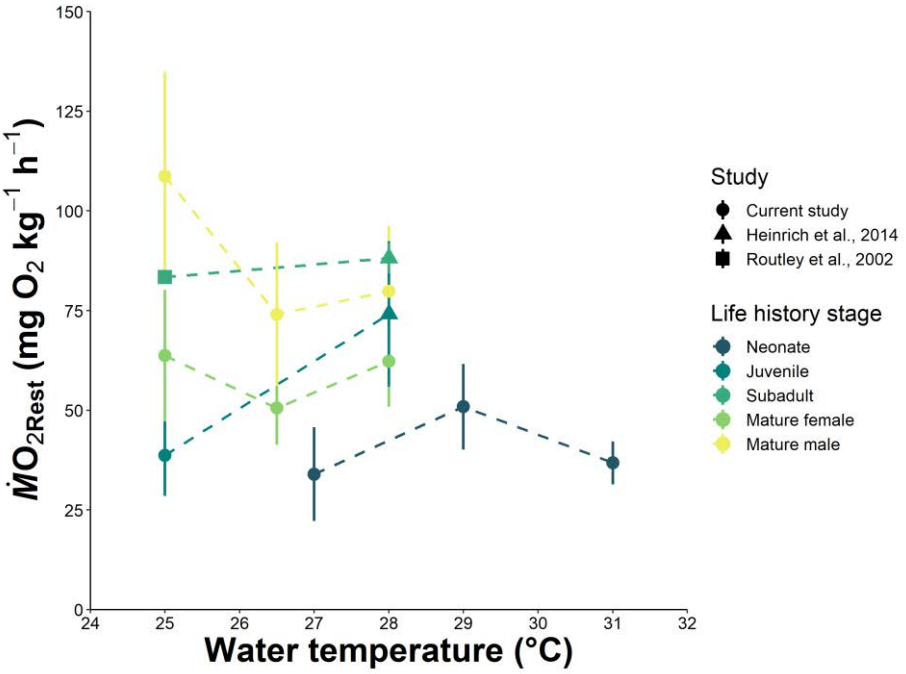

Figure 7.1 *The mean day time RMR (as MO_{2Rest} ± s.d.) from the current thesis chapters 2,3, & 6, Routley et al. (2002), and Heinrich et al. (2014) across water temperature and life history stages.*

This thesis and other studies (*i.e.,* Bouyoucos *et al.,* 2020a, 2022; Tullis and Baillie 2005; Lear *et al.,* 2020) suggest that benthic and/or tropical, coastal elasmobranchs are not thermally sensitive to the temperatures that occur most often in their rapidly fluctuating environments, and that they only become sensitive at extreme temperatures that occur less often during only a few weeks in the winter and summer. For example, the whitespotted bamboo shark (*C. plagiosum*), which is a close relative of the epaulette shark, exhibits a thermally sensitive metabolic rate at the ends of their thermal range (*i.e.,* 15 and 30°C), but relatively relative insensitivity in the middle of their range (20 and 25°C; Tullis and Baillie 2005). Therefore, it is important that future studies include the extremes of the thermal range to fully understand when thermal sensitivity and insensitivity occurs over seasonal timescales. Additionally, to understand why and how thermal insensitivity occurs, more research that assesses other energetic markers, such as activity levels and swimming speed coupled with aerobic and anaerobic enzymes and metabolites (*e.g.,* citrate synthase, lactate dehydrogenase, ketone bodies) and markers for protein degradation and cell stress (*e.g.,* ubiquitin, heat shock proteins) may better

explain the physiological mechanism(s) underpinning thermal compensation and thermal insensitivity.

Nay *et al.* (2021) reported that epaulette sharks do not behaviourally thermoregulate on the Heron Island reef flat, meaning that when short periods of warm water occur, the sharks do not seek cooler water but instead endure to the next tidal influx. However, epaulette sharks are also found on intermediate depth reefs not adjacent to islands with reef flats, and so more research is needed to determine whether there are population-level behaviours or physiological tolerances depending on location and corresponding environmental conditions. For example, epaulette sharks not associated with reef flats may not have the same tolerances as reef flat conspecifics because they are not exposed to large tidally influenced water temperatures and oxygen levels. More research on this species beyond reef flats and spanning the latitudinal gradient of the GBR is needed to gain a full picture of this species' unique tolerances under current day conditions, as some populations of epaulette sharks may be more vulnerable to future climate change than others.

7.2 Non-lethal estimates of elasmobranch energetics across ontogeny

In the 21st century, non-lethal chondrichthyan research has become increasingly more important as, worldwide, one third of these species are threatened by overfishing (Dulvy *et al.,* 2021; Sulikowski and Hammerschlag 2011). However, due to the large size of most species and the challenging logistics of field work, it is not uncommon to have only one sample and little to no validation from laboratory experiments to understand how different energetic measurements correlate. Additionally, in field studies, the digestion and assimilation status of the individual is unknown; therefore, determining whether changes in energetic metrics, such as body condition or plasma markers (*i.e.,* glucose, fatty acids), are related to either a recent feeding event or reproduction is extremely difficult. As relevant to this study, more research is needed in a controlled setting to validate various energetic markers across ontogeny and reproduction.

In this thesis, I used an established breeding colony of epaulette sharks to validate various forms of body condition measurements (Chapter 3) against

another, indirect proxy of energetic status, metabolic rate (Chapter 4). For the 15 epaulette sharks assessed over time for body condition (*i.e.,* via relative condition factor, K_n, and girth condition analysis, A_{gc}; Chapter 3) and metabolic rate (*i.e.,* via respirometry; Chapter 4), there was no correlation between the energetic markers (Figure 7.2AB). So, beyond body size scaling of metabolic rate, there may not be a direct relationship between body condition estimates and whole-organism metabolism. Moving forward, my findings highlight the importance of choosing the proper metabolic trait to reflect the research question and to be cautious in the assumptions we make around what a particular metric indicates. Indeed, individuals can have the same body condition score but differing fitness (Wilder *et al.,* 2016). However, in the case of large aquatic, threatened species like Chondrichthyans, there are limited alternatives. The dominant corticosterone in Chondrichthyans, 1α-hydroxycorticosterone, could potentially be a good proxy for energetic status, but this hormone is unique to this taxon and therefore not viable for most research groups to measure at this time (Anderson 2012). Other options like total body composition from imaging such as X-ray absorptiometry and magnetic resonance imaging would be informative, but would be logistically difficult to perform, although possible on anaesthetized individuals (Stetter 2004). Perhaps the best direction forward is to assess changes in circulating energetic and nutritional markers (*i.e.,* lipids, amino acids) across life stages and reproduction via controlled laboratory studies. This type of research would allow us to better understand how these markers fluctuate in relation to life history whilst controlling diet and feeding effects, which is not necessarily feasible in field studies (Rangel *et al.,* 2021, 2022). Building a better understanding of how to measure individual energetics in a quick, accurate, and non-lethal way will improve our overall understanding of these fishes in relation to a host of anthropogenic challenges including changing ocean conditions.

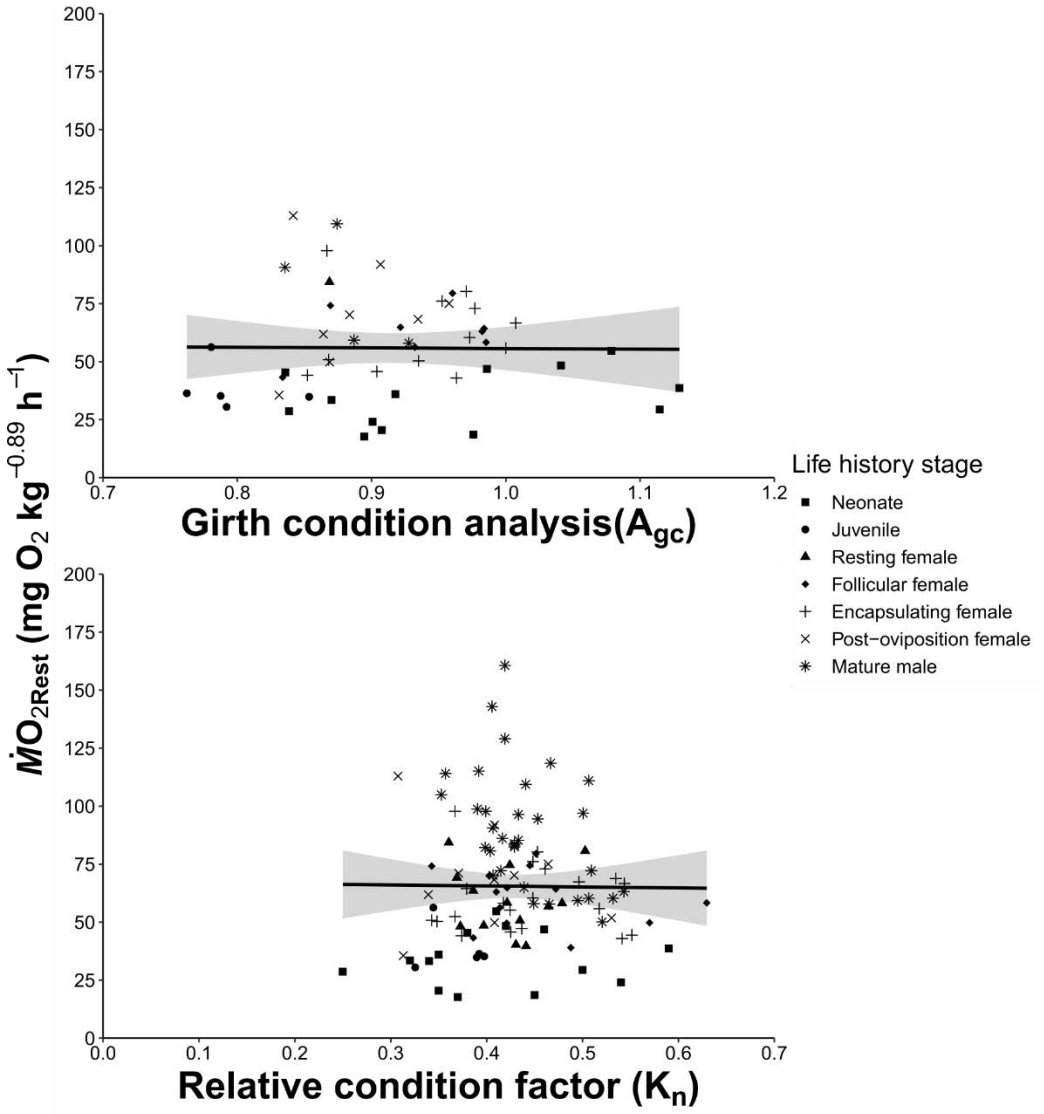

Figure 7.2 *The linear relationship between body condition metrics including girth condition analysis (A_{gc}) and relative Fulton's condition factor (K_n) assessed in Chapters 3 & 5 and metabolic rates (RMR as MO_{2Rest}) from Chapters 4 & 5.*

7.3 Thermal bottlenecks across elasmobranch life history stages

Amongst all extant vertebrates, reproduction is a crucial yet potentially costly aspect of their biology, and in chondrichthyans, some degree of seasonality of reproduction is nearly ubiquitous across all species (Conrath and Musick 2012). Consequently, water temperature, as a function of season, is an important factor mediating reproductive physiology and endocrinology (Elisio *et al.,* 2019). At Heron Island on the southern GBR, the annual trough and subsequent peak of water temperatures from August to January is thought to be the factor controlling epaulette shark annual reproduction (Figure 7.3; Heupel *et al.* 1999). Indeed, my

thesis findings support this hypothesis. Throughout my studies, when female epaulette sharks were maintained at a constant 25°C, year-round, the temperature chosen to mimic peak-egg laying in the wild, they consistently produced eggs.

Given the ~2,300-kilometre length of the GBR, spanning approximately 13° in latitude and associated temperatures differences (Figure 7.3), it is possible that a latitudinal gradient of epaulette shark reproductive seasonality exists. For example, at Lizard Island, in the northern GBR, winter water temperatures are 2-3°C warmer than at Heron Island, in the southern GBR (Figure 7.3). Therefore, if water temperature is the main regulator of reproductive timing, northern populations may exhibit a shifted reproductive season when compared to southern populations. This hypothesis is supported here by one wild female epaulette shark sampled at Balgal Beach (a mid-GBR location) in June 2021; this individual was encapsulating egg cases at the time of capture. Compared to the known Heron Island epaulette shark reproductive season, this individual was producing egg cases approximately two months earlier than southern GBR epaulette sharks. More research is needed to determine whether this phenomenon may indicate which populations of epaulette sharks on the GBR are more susceptible to warming than others, especially given that lower latitudes are potentially likely to experience temperatures outside of the thermal reproductive window earlier in the coming years than southern populations.

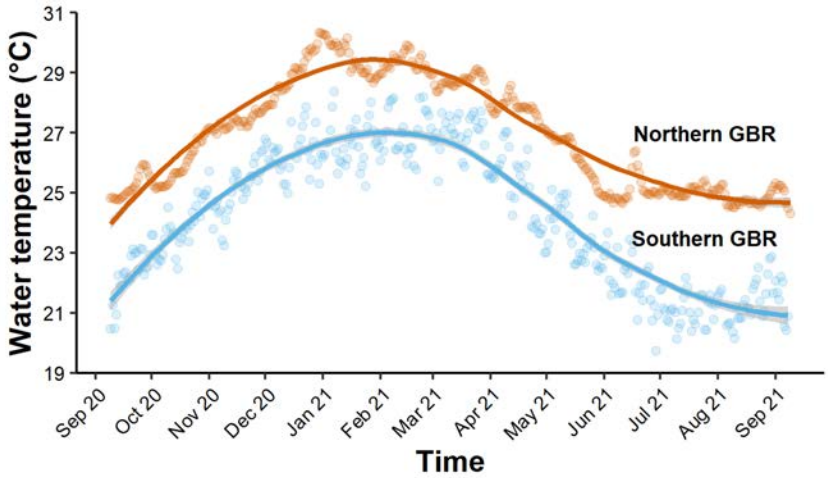

Figure 7.3 *The daily mean water temperature from the southern (Heron Island reef flat; blue) and northern (Lizard Island reef flat; red) Great Barrier Reef (GBR) (data sourced from AIMS, 2022).*

During my thesis research, I also found preliminary evidence that both mature males and females may be suspectable to ocean warming. During the temperature changes described in Chapter 2 (*i.e.,* Wheeler *et al.,* 2022), where sharks were exposed to 25-28°C and 28°C diel temperature treatments, egg laying patterns and egg quality were negatively affected by elevated temperatures (Figure 7.4). Oviposition rate not only decreased and became sporadic (Figure 7.4), but 66% of the egg cases produced during this period were wind (empty) and only contained albumen (*i.e.,* no yolk sac was present). Although there were only three females laying during this time, these results provide – to my knowledge – some of the first direct evidence that temperature regulates oviparity in sharks. This finding warrants further research. Despite this preliminary evidence that increased water temperature reduces or shuts down reproduction, we are unsure if water temperature is the only factor because day length could also influence reproductive seasonality. However, day light hours do not change considerably on the GBR across the year, given the proximity to the equator. So, photoperiod may be a co-factor but directly triggering reproduction; yet, further investigation is needed. Herein, mature males have the highest routine metabolic costs (Chapter 4), and slightly reduced thermal maximum limit (Chapter 5). The vulnerably of mature males to increased temperatures could be further investigated by assessing sperm quality across seasonal and predicted future water temperatures. More research that assesses sex-specific metabolic traits and thermal tolerance may improve our understanding as to sex-specific vulnerabilities with respect to climate change.

In chapter 6 of this thesis, I found evidence that epaulette shark development is negatively impacted at temperatures just beyond current-day summer averages. Under these scenarios, epaulette shark neonates hatched slightly underweight, undernourished, and showed early signs of physiological impairment. Indeed, at even one degree Celsius warmer (32°C) than the Chapter 6 treatments, mortality can be high for embryos, neonates, and juvenile epaulette sharks (Gervais *et al.,* 2016, 2018). Like adult reproduction, it is also possible that in the northern GBR, embryonic and neonate epaulette sharks have better thermal tolerance given the warmer summer averages they experience at lower latitudes. More research assessing potential differences in the latitudinal gradient of development and the physical location of egg case deposition and subsequent development (*i.e.,* reef flats

verse cooler, deeper reefs), would help better elucidate the physiological findings in Chapter 6.

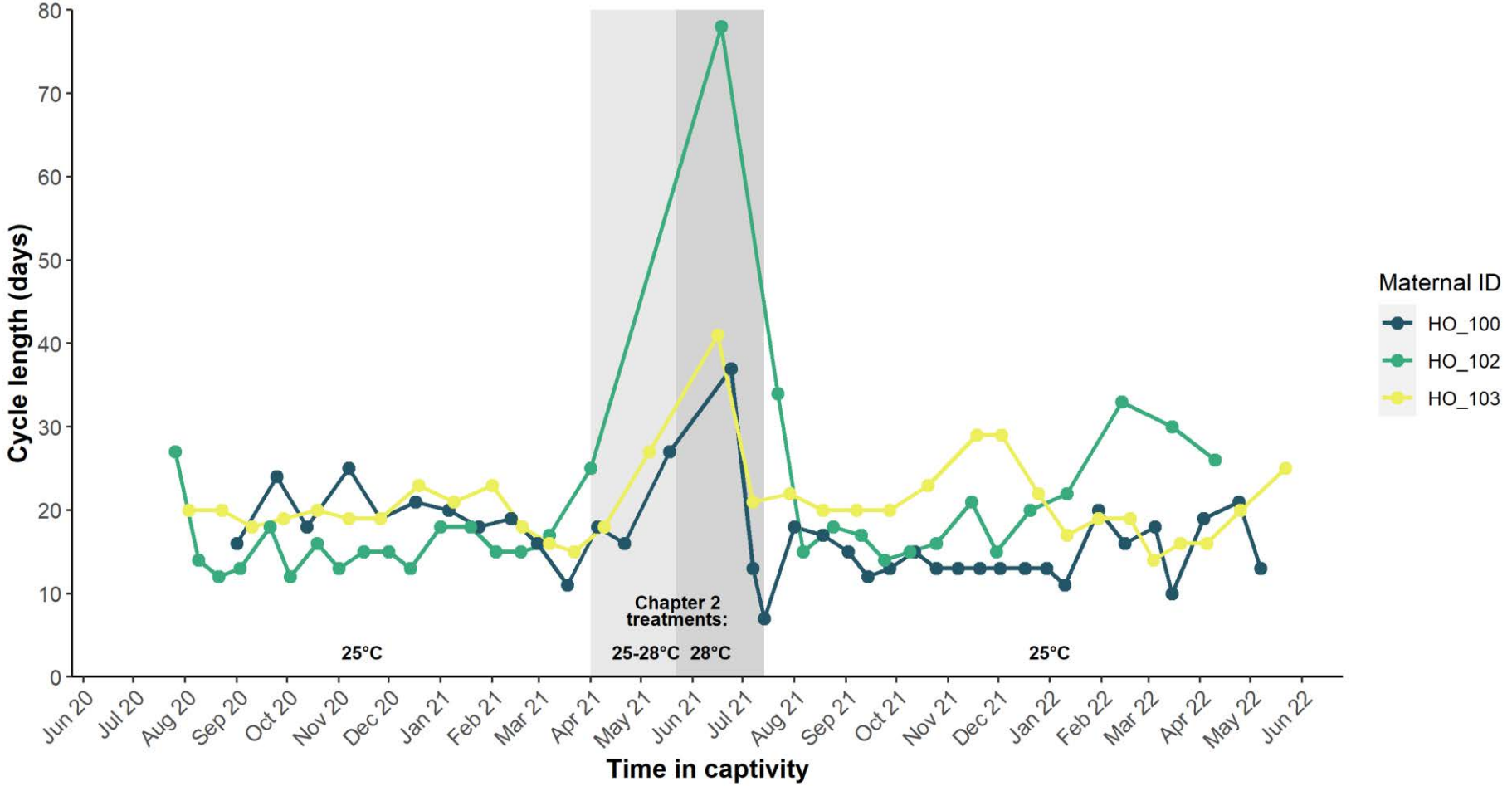

Figure 7.4 *The cycle time in days from one clutch of egg cases to the next across time in captivity for three female epaulette sharks. Vertical grey bars represent the Chapter 2 experiments when water temperature was on a 25-28°C or 28°C diel cycle (see Table 2.1 and Figure 2.2).*

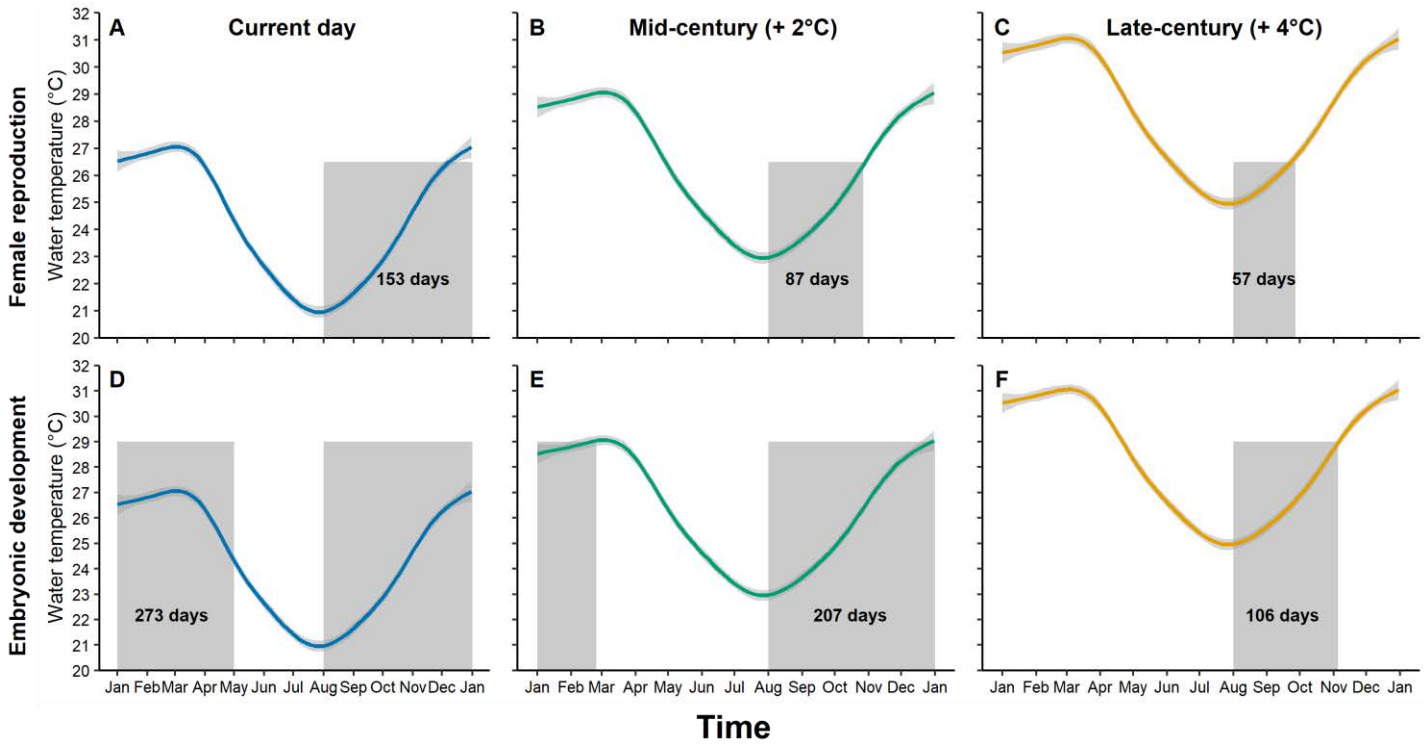

Figure 7.5 *The shortening of the annual female reproductive thermal window (panels A, B, & C) and in ovo embryonic development time (panels D, E, & F) based off of the temperature profile of the Heron Island reef flat from January 2021- 2022 (data sourced from AIMS, 2022) and predicted warming scenarios SSP5-8.5 for mid and late century ocean warming (Fox-Kemper et al., 2021). Coloured fits represent the generalized additive model smoother of the daily average temperatures, and grey boxes represent the suitable reproductive and development times based on findings from Heupel et al. (1999) and this thesis. These predictions assume epaulette sharks shorten but do not shift their reproductive season in response to ocean warming and that ocean warming will ensue equally across seasons.*

7.4 Conclusions and future directions

In this thesis, I provide evidence that reproductively active female epaulette sharks and their offspring are vulnerable and sensitive to increasing water temperatures not unlike those predicted with climate change. Using the knowledge that female reproduction likely begins to shut down around 26.5°C (the average water at Heron Island in January; Figure 7.3), on the southern GBR, the window of time for successful female reproduction under a +2°C warming scenario narrows by 42% and by 62% under a +4°C warming scenario (Figure 7.5ABC). Next, incorporating these thermal limits and windows of time for female egg production with the time needed for *in ovo* development and the upper thermal threshold of development (T_{pejus} =29°C; Chapter 6), conditions for optimal offspring development are reduced by 24% and 61% under +2 and +4°C warming scenarios respectively (Figure 7.5DEF).

These predictions illustrated in Figure 7.5 are based off daily average southern GBR water temperatures and assume the following:

1. That the lowest winter temperatures under warming scenarios are cool enough to initiate reproduction,
2. warming will occur evenly across seasons,
3. daily fluctuations in water temperatures from tides do not have a large effect,
4. sharks would not move off reef flats and relocate to cooler, deeper reefs,
5. the epaulette shark's generation time is too slow for intergenerational adaptation,
6. and that epaulette sharks would only shorten but not shift their reproduction season.

More comprehensive modelling may help better include these factors; however, for all these assumptions, more research is first needed to better inform a more complex model. Beyond addressing these assumptions, I also recommend the following future research questions:

1. **What is the generation time of epaulette sharks in the wild?** This could be addressed with a mark and re-capture florescent vertebrae tag

(*i.e.,* oxytetracycline) study on a location like Heron Island where recapture rates from year to year are high. Answering this question may help elucidate the capacity for intergenerational plasticity of epaulette sharks (*i.e.,* will this species be able to adapt fast enough to keep pace with ocean warming?), where short generation times would allow more adaptability, as more generations would occur over shorter periods of time. Given that epaulette sharks are a "least concern" listed species, a small lethal study in the wild could be conducted to obtain these age at maturity data. Anecdotally, in the public aquaria sector, epaulette sharks can take anywhere from 2-8 years to mature in captivity (Personal communication S. Tempesta, New England Aquarium). However, many species mature more quickly in captivity, partially due to ideal temperatures and feeding conditions, and it is important to also assess wild individuals.

2. **How do daily fluctuations in abiotic factors effect growth, development, and reproduction?** In this thesis, I used constant temperature treatments in most of my studies; however, in many environments inhabited by epaulette sharks, temperature, salinity, acidity, and pCO_2/pO_2 can change rapidly and often. Perhaps these environments provide epaulette sharks temporal thermal refuge, for example, that was not provided in my laboratory studies (*e.g.,* Chapter 6 herein with constant elevated temperature treatments). Research on the early growth and development of bamboo shark embryos, where individuals experienced short periods of warming each day, did cause detrimental effects (Walton 2020), indicating there is more research needed with better replication of the natural environmental rhythms that these benthic, coastal sharks experience in the wild.
3. **Where are key life stages of epaulette sharks located in relation to reef flats?** From my research and all other previous research on Heron Island (*e.g.,* Gervais *et al.,* 2018; Heupel *et al.,* 1999; Heupel and Bennett 2007; Nay *et al.,* 2020; Peach 2002; Renshaw and Dodd 2010; Wise *et al.,* 1998), there have been no reports of adults over 75 cm TL nor any egg cases found on the reef flat, indicating larger adults and embryos may be

located off the reef slope in more stable environmental conditions. Furthermore, from my field work at Balgal Beach on the mid-GBR, all captured sharks ranged from 57-73 cm TL (n=12), indicating that this shallow inter-tidal area is also dominated by sub-adult to small adult sized sharks. Therefore, by just studying this species on the shallow reef flats, we may be inadvertently missing important life history stage cohorts of the population that experience different thermal profiles on environments beyond the reef flats.

4. **Do different epaulette shark populations exhibit different physiological tolerances?** Epaulette sharks are found on reef flats, and therefore the majority of studies on the species are from these conspecifics, given their easy accessibility. However, epaulette sharks from deeper, intermediate reefs that are not directly associated with intertidal zones have not been fully studied for the same traits. In the current study, four sharks were from shallow reef-flat type environments, and six sharks were from intermediate reefs. Yet, no differences in MO_2 or reproductive traits were found, but it is important to note that my sample sizes were small. Studying two discrete populations, where one population experiences larger fluctuations (*i.e.,* reef flats) than the other (*i.e.,* standard reefs), may help us elucidate whether the well-known epaulette shark's physiological toughness is a product of certain environments or ubiquitous across the species regardless of location.
5. **What is the current connectivity of epaulette shark populations, and can these data inform their ability to relocate in the future?** If multiple epaulette shark populations living in close proximity, for example Heron Island and the other reefs comprising the Capricorn Bunker group, demonstrate different population genetic structure, this would indicate epaulette sharks do not typically move away from their associated reef. This concept has been seen in the California horn shark (*Heterodontus francisci*), a species with similar benthic habitat requirements to epaulette sharks, where there was genetic distinction between island and coastal populations, and migrations between

locations appeared to be rare (Canfield *et al.,* 2022). Similarly, another benthic elasmobranch, the thorny skate (*Amblyraja radiata*), does not undertake large movement patterns (Kneebone *et al.,* 2020). Research in this area may help us better understand if habitat-dependent chondrichthyans that we assume to not undertake large movement patterns are at risk from climate change if their current day geographical and thermal ranges become non-ideal or uninhabitable.

Answering these questions and addressing the assumptions made to conduct the preliminary thermal modelling of reproduction and development will not only improve our understanding of this species but provide a better understanding of ocean warming effects on tropical, coastal, benthic elasmobranchs that already live near their thermal optima. The epaulette shark studied in my thesis is only one of nine species in the *Hemiscyllium* genus, where eight other species are endemic to Northwest Australia and Indonesia. *H. ocellatum* is likely the best protected species of these nine, as to our current knowledge, it is only found within the Great Barrier Reef Marine Park, meaning they are afforded large-scale protection. Indeed, even within the areas open to recreational fishing, the bag limit is one per person and two per boat (Queensland Fisheries, 2022), but to our knowledge this species is not targeted by recreational anglers. The current, larger threat is collection for the aquarium trade, but given this species amenability to captive breeding, this pressure is likely not a large issue. For the other eight *Hemiscyllium* species, five are listed as vulnerable, two are near threatened, and the population trends of all eight species are either decreasing or unknown (IUCN, 2022). Furthermore, seven of these species are found in smaller geographic ranges than *H. ocellatum*, where artisanal fisheries may target this species for consumption or aquarium trade (Jutan *et al.,* 2018; Vanderwright *et al.,* 2021). Furthermore, the biology of these other species is not well studied compared to *H. ocellatum*, where we assume, given their similar morphologies, that they are all biologically similar (Allen *et al.,* 2016, Vanderwright *et al.,* 2021). Although more research on these individual species would be prudent and necessary, I also encourage that the research over the past three decades and in this thesis on *H. ocellatum* should be applied to other *Hemiscyllium* sharks to conserve and manage this unique group of carpet sharks, species that are not found outside the Indo-Pacific region.

In conclusion, my thesis has added valuable knowledge to the field on comparative energetic measurements in large fishes, improved our understanding of how current day thermal physiology of sharks relates to their environment, and assessed how different life stages may be impacted by ocean warming scenarios in the future. From previous research and this thesis, it stands that ocean warming will be the largest issue for this coastal shark species (Table 7.1), and that more research is needed to determine how this indicator species will fare under combinations of ocean acidification, warming, and deoxygenation. I believe it is important that we establish biological and physiological understandings of these fishes now, under current day conditions, so that we can track shifting baselines of their physiological ecology into the future. Indeed, starting to answer these questions in 10 to 20 years may be too late, as we may miss the changes that have already occurred under climate change. Ultimately, stronger conservation, management, and general attention to ensuing climate change is needed to protect this already vulnerable taxon that provides immense ecological, economic, and cultural resources and benefits to society.

Table 7.1 *A summary table of the effects of ocean acidification (OA) and ocean warming (OW) effects on epaulette sharks (Hemiscyllium ocellatum).*

Life stage	Ocean Acidification	Ocean Warming	Publications
Embryos	o No impacts on growth, development, or hatching success	o Decreased hatching success at 32°C o Development time ~30 days shorter at 31°C o Reduced metabolic rate at 31°C	OA: Johnson *et al.,* 2016 OW: Gervais *et al.*, 2016; Wheeler *et al.,* 2021
Neonates	o No impacts on survivorship	o Fed exogenously more quickly o Increased recovery time from exercise o Reduced survivorship and disruption in coloration/pattern at 32°C	OA: Johnson *et al.,* 2016 OW: Gervais *et al.,* 2016; Wheeler *et al.,* 2021
Juveniles	o Not studied	o 62.5% mortality, reduced growth and feeding rates at 32°C	Gervais *et al.,* 2018
Adults	o No change in metabolic rate o Evidence of physiological buffering (changes in plasma acid-base regulatory ions) o No change in foraging or sheltering behaviour	o Metabolic rate maintained between 25 and 28°C o Female reproduction disrupted at 28°C	OA: Heinrich *et al.,* 2014; 2015 OW: Wheeler *et al.,* 2022; Current thesis

References

Abujanra, F., Agostinho, A. A., & Hahn, N. S. (2009). Effects of the flood regime on the body condition of fish of different trophic guilds in the Upper Paraná River floodplain, Brazil. *Brazilian Journal of Biology*, *69*, 469–479. doi: 10.1590/s1519-69842009000300003

Adams, K. R., Fetterplace, L. C., Davis, A. R., Taylor, M. D., & Knott, N. A. (2018). Sharks, rays and abortion: The prevalence of capture-induced parturition in elasmobranchs. *Biological Conservation*, 217(September 2017), 11–27. doi: 10.1016/j.biocon.2017.10.010

Ahnelt, H., Sauberer, M., Ramler, D., Koch, L., & Pogoreutz, C. (2020). Negative allometric growth during ontogeny in the large pelagic filter-feeding basking shark. *Zoomorphology*, *139*, 71–83. doi:

Alhajji, A. H., Hsu, H. H., Alkhamis, Y. A., Alsaqufi, A. S., Ajmal Khan, S., & Nazeer, Z. (2022). Maturity and reproduction in the Arabian carpet shark, *Chiloscyllium arabicum* from the Saudi Arabian waters of the Arabian Gulf. *Marine Biology Research*, 1–11. doi: 10.1080/17451000.2022.2131824

Anderson, W. G. (2012). The endocrinology of 1α-hydroxycorticosterone in elasmobranch fish: A review. *Comparative Biochemistry and Physiology - A Molecular and Integrative Physiology, 162(2),* 73–80. doi:10.1016/j.cbpa.2011.08.015

Andreassen, A.H., Hall, P., Khatibzadeh, P., Jutfelt, F., Kermen, F. (2022). Brain dysfunction during warming is linked to oxygen limitation in larval zebrafish. *Proceedings of the National Academy of Science USA,* 119, e2207052119. doi:10.1073/pnas.2207052119

Angilletta Jr, M.J. (2009). Thermal Adaptations. Oxford University Press, New York, pp 1-18.

Angilletta, M. J., & Sears, M. W. (2000). The metabolic cost of reproduction in an oviparous lizard. *Functional Ecology*, 14(1), 39–45. doi: 10.1046/j.1365-2435.2000.00387.x

Arnold, P. A., Delean, S., Cassey, P., & White, C. R. (2021). Meta-analysis reveals that resting metabolic rate is not consistently related to fitness and performance in animals. *Journal of Comparative Physiology B*, 191(6), 1097–1110. doi: 10.1007/s00360-021-01358-w

Auer, S.K., Agreda, E., Chen, A.H., Irshad, M., Solowey, J. (2021). Late-stage pregnancy reduces upper thermal tolerance in a live-bearing fish. *Journal of Thermal Biology* 99, 103022. doi: 10.1016/j.jtherbio.2021.103022

Australian Institute of Marine Science (AIMS). (2022). Sea Water Temperature Logger Data at Heron Island, Great Barrier Reef From 24 Nov 1995 to 26 Jun 2022, https://apps.aims.gov.au/metadata/view/446a0e73-7c30-4712-9ddb-ba1fc29b8b9a, accessed 21-Sep-2022.

Awruch, C. (2015). Reproduction strategies. In R. Shadwick, A. Farrell, & C. Brauner (Eds.), *Physiology of elasmobranch fishes: structure and interaction with environment*, *vol 34A* (pp. 255-297). London: Academic Press.

Awruch, C. A., Pankhurst, N. W., Frusher, S. D., & Stevens, J. D. (2009). Reproductive seasonality and embryo development in the draughtboard shark *Cephaloscyllium laticeps*. *Marine and Freshwater Research*, *60*(12), 1265–1272. doi:10.1071/MF09030

Awruch, C. A., Pankhurst, N. W., Frusher, S. D., & Stevens, J. D. (2008). Endocrine and morphological correlates of reproduction in the draughtboard shark *Cephaloscyllium laticeps* (Elasmobranchii: Scyliorhinidae). *Journal of Experimental Zoology Part A: Ecological Genetics and Physiology*, *309(4),* 184–197. doi: 10.1002/jez.445

Awruch, C.A., Frusher, S.D., Stevens, J.D., Barnett, A. (2012). Movement patterns of the draughtboard shark *Cephaloscyllium laticeps* (Scyliorhinidae) determined by passive tracking and conventional tagging. *Journal of Fish Biology* 80: 1417–1435.

Bass, N. C., Day, J., Guttridge, T. L., Knott, N. A., & Culum, B. (2021). Intraspecific variation in diel patterns of rocky reef use suggests temporal partitioning in Port Jackson sharks. *Marine and Freshwater Research, 72,* 1445-1456.

Bates, D., Mächler, M., Bolker, B., & Walker, S. (2015). Fitting linear mixed-effects models using lme4. *Journal of Statistical Software, 67*, 1–48. doi: 10.18637/jss.v067.i01

Baum, J. K., & Worm, B. (2009). Cascading top-down effects of changing oceanic predator abundances. *Journal of Animal Ecology*, *78*(4), 699–714. doi:10.1111/j.1365-2656.2009.01531.x

Bell, G. (1980). The Costs of Reproduction and Their Consequences. *The American Naturalist,* 116(1), 45–76.

Billard, R., & Lecointre, G. (2001). Biology and conservation of sturgeon and paddlefish. *Reviews in Fish Biology and Fisheries*, *10*, 355–392. doi: 10.1023/A:1012231526151

Bouyoucos, I. A., Morrison, P. R., Weideli, O. C., Jacquesson, E., Planes, S., Simpfendorfer, C. A., Brauner, C. J., & Rummer, J. L. (2020). Thermal tolerance and hypoxia tolerance are associated in blacktip reef shark (Carcharhinus melanopterus) neonates. *Journal of Experimental Biology,* 223, jeb221937. doi:10.1242/jeb.221937

Bouyoucos, I. A., Watson, S.-A., Planes, S., Simpfendorfer, C. A., Schwieterman, G. D., Whitney, N. M., & Rummer, J. L. (2020). The power struggle: Assessing interacting global change stressors via experimental studies on sharks. *Scientific Reports, 10*(1), 19887. doi:10.1038/s41598-020-76966-7

Bouyoucos, I., Simpfendorfer, C., Planes, S., Schwieterman, G., Weideli, O., & Rummer, J. (2022). Thermally insensitive physiological performance allows neonatal sharks to use coastal habitats as nursery areas. *Marine Ecology Progress Series*, 682, 137–152. doi:10.3354/meps13941

Brosset, P., Fromentin, J.-M., Beveren, E. V., Lloret, J., Marques, V., Basilone, G., Bonanno, A., Carpi, P., Donato, F., Keč, V. Č., Felice, A. D., Ferreri, R., Gašparević, D., Giráldez, A., Gücü, A., Iglesias, M., Leonori, I., Palomera, I., Somarakis, S., … Saraux, C. (2017). Spatio-temporal patterns and environmental controls of small pelagic fish body condition from contrasted Mediterranean areas. *Progress in Oceanography*, 151, 149–162. doi:10.1016/j.pocean.2016.12.002

Brown, F. A. (1972). The "Clocks" Timing Biological Rhythms: Recent discoveries suggest that the mysterious biological clock phenomenon results from a continuous interaction between organisms and the subtle geophysical environment. *American Scientist,* 60(6), 756–766.

Buddle, A. L., Otway, N. M., Dyke, J. U. V., Thompson, M. B., Murphy, C. R., Dowland, S. N., Simpfendorfer, C. A., Ellis, M. T., & Whittington, C. M. (2020). Structural

changes to the uterus of the dwarf ornate wobbegong shark (*Orectolobus ornatus*) during pregnancy. *Journal of Morphology,* 281, 428-437. doi: 10.1002/jmor.21109

Butler, P.J., & Metcalfe, J.D. (1988). Cardiovascular and respiratory systems. In: Shuttleworth T.J. (Ed.), *Physiology of elasmobranch fishes*. Berlin (Germany): Springer. pp. 1-47.

Byrnes, E. E., Daly, R., Leos-Barajas, V., Langrock, R., & Gleiss, A. C. (2021). Evaluating the constraints governing activity patterns of a coastal marine top predator. Marine Biology, 168(1), 1–15. doi:10.1007/s00227-020-03803-w

Cailliet, G.M., J.A. Musick, C.A. Simpfendorfer, and J.D. Stevens. (2005). Ecology and life history characteristics of chondrichthyan fish. Chapter 3, pages 12-18, In: Fowler, S.L., R.D. Cavanagh, M. Camhi, G.H. Burgess, G. Cailliet, S.V. Fordham, C.A. Simpfendorfer, & J.A. Musick (Eds.), *Sharks, Rays and Chimaeras: The Status of the Chondrichthyan Fishes, Status Survey*. (pp. 12-18). IUCN/Shark Specialist Group. IUCN, Gland, Switzerland and Cambridge, UK.

Callard, I. P., S, G. J., & Koob, T. J. (2005). Endocrine control of the female reproductive tract. In: Hamlett, W.C., ed. Reproductive Biology and Phylogeny of Chondrichthyes. CRC Press, pp 283–300.

Canfield, S. J., Galván-Magaña, F., & Bowen, B. W. (2022). Little Sharks in a Big World: Mitochondrial DNA Reveals Small-scale Population Structure in the California Horn Shark (*Heterodontus francisci*). *Journal of Heredity, April,* 1–13. doi:10.1093/jhered/esac008

Capapé, C., Mnasri-Sioudi, N., El Kamel-Moutalibi, O., Boumaïza, M., Ben Amor, M. M., & Reynaud, C. (2014). Food and feeding habits of the small-spotted catshark, *Scyliorhinus canicula* (Chondrichthyes : Scyliorhinidae) from the northern coast of Tunisia (central Mediterranean). *Journal of Ichthyology*, *54*(1), 111–126. doi:10.1134/S0032945214010020

Chabot, D., Steffensen, J. F., & Farrell, A. P. (2016). The determination of standard metabolic rate in fishes. Journal of Fish Biology, 88(1), 81–121. doi:10.1111/jfb.12845

Chapman, C. A., & Renshaw, G. M. C. (2009). Hematological responses of the grey carpet shark (Chiloscyllium punctatum) and the epaulette shark (*Hemiscyllium ocellatum*) to anoxia and re-oxygenation. *Journal of Experimental Zoology Part A: Ecological Genetics and Physiology*, *311*(6), 422–438. doi: 10.1002/jez.539

Chapman, C. A., Harahush, B. K., & Renshaw, G. M. C. (2011). The physiological tolerance of the grey carpet shark (*Chiloscyllium punctatum*) and the epaulette shark (*Hemiscyllium ocellatum*) to anoxic exposure at three seasonal temperatures. *Fish Physiology and Biochemistry*, *37*(3), 387–399. doi:10.1007/s10695-010-9439-y

Chen, W. K., & Liu, K. M. (2006). Reproductive biology of whitespotted bamboo shark *Chiloscyllium plagiosum* in northern waters off Taiwan. *Fisheries Science*, *72*(6), 1215–1224. doi:10.1111/j.1444-2906.2006.01279.x

Clark, E., Von Schmidt, K. (1965). Sharks of the central gulf coast of Florida. *Bulletin of Marine Science*, *15*,13–83.

Clark, T. D., Sandblom, E., & Jutfelt, F. (2013). Aerobic scope measurements of fishes in an era of climate change: Respirometry , relevance and recommendations. The Journal of Experimental Biology, 216(15), 2771–2782. doi:10.1242/jeb.084251

Clark, T.D., Roche, D.G., Binning, S.A., Speers-Roesch, B., Sundin, J. (2017). Maximum thermal limits of coral reef damselfishes are size dependent and resilient to near-future ocean acidification. *J Exp Biol* 220: 3519-3526. doi:10.1242/jeb.162529

Compagno, L.J.V., Dando, M., Fowler, S. (2005). A field guide to the sharks of the world. Harper Collins Publishers Ltd, London.

Cone, R. S. (1989). The need to reconsider the use of condition indices in fishery science. *Transactions of the American Fisheries Society (1900)*, *118*(5), 510–514. doi: 10.1577/1548-8659(1989)118<0511:TNTRTU>2.3.CO;2

Conrath, C.L., Musick, J.A. (2004). Reproductive Biology of Elasmobranchs. In: Carrier, J., Musick, J., eds. Biology of Sharks and Their Relatives, Second Edition. CRC Press, Boca Raton, pp 291-311.

Corsso, J. T., Gadig, O. B. F., Barreto, R. R. P., & Motta, F. S. (2018). Condition analysis of the Brazilian sharpnose shark *Rhizoprionodon lalandii*: evidence of maternal investment for initial post-natal life. *Journal of Fish Biology*, *93*(6), 1038–1045. doi:10.1111/jfb.13780

Cortés, E. (2000). Life History Patterns and Correlations in Sharks. Reviews in Fisheries Science, 8(4), 299–344. doi:10.1080/10408340308951115

Craig, J. M., Papoulias, D. M., Thomas, M. V., Annis, M. L., & Boase, J. (2009). Sex assignment of lake sturgeon (*Acipenser fluvescens*) based on plasma sex hormone and vitellogenin levels. *Journal of Applied Ichthyology*, *25*, 60–67. doi:10.1111/j.1439-0426.2009.01289.x

Craik, J. C. A. (1978). An annual cycle of vitellogenesis in the elasmobranch *Scyliorhinus canicula*. *Journal of the Marine Biological Association of the United Kingdom*, *58*, 719–726. doi:10.1017/S0025315400041369

Dabruzzi, T.F., Bennett, W.A., Rummer, J.L., Fangue, N.A. (2013). Juvenile Ribbontail Stingray, *Taeniura lymma* (Forsska 1775) (Chondrichthyes, Dasyatidae), demonstrate a unique suite of physiological adaptations to survive hyperthermic nursery conditions. *Hydrobiologia* 701: 37-49.

Dahlke, F.T., Wohlrab, S., Butzin, M., Pörtner, H.-O. (2020). Thermal bottlenecks in the life cycle define climate vulnerability of fish. *Science* 369: 65–70.

DeMarco, V. (1993). Metabolic rates of female viviparous lizards (*Sceloporus jarrovi*) throughout the reproductive cycle: do pregnant lizards adhere to standard allometry? *Physiological Zoology*, 66(1), 166–180.

Di Santo, V. (2015). Ocean acidification exacerbates the impacts of global warming on embryonic little skate, *Leucoraja erinacea* (Mitchill). *Journal of Experimental Marine Biology and Ecology, 463,* 72–78. doi:10.1016/j.jembe.2014.11.006

Dudgeon, C. L., Corrigan, S., Yang, L., Allen, G. R., Erdmann, M. V., Fahmi, Sugeha, H. Y., White, W. T., & Naylor, G. J. P. (2019). Walking, swimming or hitching a ride? Phylogenetics and biogeography of the walking shark genus Hemiscyllium. *Marine and Freshwater Research, 71,* 1107-1117. doi: 10.1071/MF19163

Dulvy, N. K., & Reynolds, J. D. (1997). Evolutionary transitions among egg-laying, live-bearing and maternal inputs in sharks and rays. *Proceedings of the Royal Society B: Biological Sciences*, *264*(1386), 1309–1315. doi:10.1098/rspb.1997.0181

Dulvy, N. K., Fowler, S. L., Musick, J. A., Cavanagh, R. D., Kyne, P. M., Harrison, L. R., Carlson, J. K., Davidson, L. N. k, Fordham, S. V., Francis, M. P., Pollock, C. M.,

Simpfendorfer, C. A., Burgess, G. H., Carpenter, K. E., Compagno, L. J. v, Ebert, D. A., Gibson, C., Heupel, M. R., Livingstone, S. R., … White, W. T. (2014). Extinction risk and conservation of the world's sharks and rays. *ELife,* 3, e00590. doi:10.7554/eLife.00590

Dulvy, N. K., Pacoureau, N., Rigby, C. L., Pollom, R. A., Jabado, R. W., Ebert, D. A., Finucci, B., Pollock, C. M., Cheok, J., Derrick, D. H., Herman, K. B., Sherman, C. S., VanderWright, W. J., Lawson, J. M., Walls, R. H. L., Carlson, J. K., Charvet, P., Bineesh, K. K., Fernando, D., … Simpfendorfer, C. A. (2021). Overfishing drives over one-third of all sharks and rays toward a global extinction crisis. *Current Biology*, *31*(21), 4773-4787.e8. doi:10.1016/j.cub.2021.08.062

Dunlap, J. C., & Loros, J. J. (2016). Yes, circadian rhythms actually do affect almost everything. Cell Research, 26(7), 759–760. doi:10.1038/cr.2016.65

Ebert, D. A., Dando, M., Fowler, S., & Jabado, R. (2021). *Sharks of the world: A Complete Guide*. Princeton University Press.

Ebert, D.A., Compagno, L. J. V., & Cowley, P. D. (2007). Aspects of the reproductive biology of skates (Chondrichtyes: Rajiformes: Rajoidei) from southern Africa. *ICES Journal of Marine Science*, *65*, 81–102. doi:10.1093/icesjms/fsm169

Elisio, M., Awruch, C. A., Massa, A. M., Macchi, G. J., & Somoza, G. M. (2019). Effects of temperature on the reproductive physiology of female elasmobranchs: The case of the narrownose smooth-hound shark (*Mustelus schmitti*). *General and Comparative Endocrinology*, *284*(August), 113242. doi:10.1016/j.ygcen.2019.113242

Ellis, J. R., Cruz-Martínez, A., Rackham, B. D., & Rogers, S. I. (2005). The distribution of chondrichthyan fishes around the British Isles and implications for conservation. *Journal of Northwest Atlantic Fishery Science*, *35*(November 2004), 195–213. doi:10.2960/J.v35.m485

Estalles, M., Perez Comesaña, J. E., Tamini, L. L., & Chiaramonte, G. E. (2009). Reproductive biology of the skate, *Rioraja agassizii* (Müller and Henle, 1841), off Puerto Quequén, Argentina. *Journal of Applied Ichthyology*, *25*: 60–65. doi:10.1111/j.1439-0426.2008.01103.x

Falahiehzadeh, N., & Salamat, N. (2020). Histomorphological and endocrine assessment of female Arabian carpetshark, *Chiloscyllium arabicum* (Elasmobranchii: Hemiscylliidae) from the Persian Gulf during annual reproductive cycle. *Journal of Fish Biology,* 97(4), 938–952. doi: 10.1111/jfb.14419

Fangue, N.A., Bennett, W.A. (2003). Thermal tolerance responses of laboratory-acclimated and seasonally acclimatized Atlantic stingray, *Dasyatis sabina*. *Copeia* 2: 315–325.

Farrell, A. P. (2016). Pragmatic perspective on aerobic scope: Peaking, plummeting, pejus and apportioning. Journal of Fish Biology, 88(1), 322–343. doi:10.1111/jfb.12789

Ferretti, F., Worm, B., Britten, G. L., Heithaus, M. R., & Lotze, H. K. (2010). Patterns and ecosystem consequences of shark declines in the ocean. *Ecology Letters*, *13*(8), 1055–1071. doi:10.1111/j.1461-0248.2010.01489.x

Ferry-Graham, A. L. A., & Gibb, A. C. (2001). Comparison of Fasting and Post-feeding Metabolic Rates in a Sedentary Shark, *Cephaloscyllium ventriosum. Copeia*, 2001(4), 1108–1113.

Field, I.C., Meekan, M.G., Buckworth, R.C., & Bradshaw, C.J. (2009). Chapter 4: Susceptibility of sharks, rays and chimaeras to global extinction. In: Sims, D.W. (Ed.), *Advances in Marine Biology* 56:275–363. doi:10.1016/S0065-2881(09)56004-X

Finstad, W.O., & Nelson, D.R. (1975). Circadian activity rhythm in the horn shark, *Heterodontus francisci*: effect of light intensity. *Bulletin of Southern California Academy of Sciences, 7*, 20-26.

Firth, B.L., Drake, D.A.R., Power, M. (2021). Seasonal and environmental effects on upper thermal limits of eastern sand darter *(Ammocrypta pellucida)*. *Conservation Physiology* 9, coab057. doi:10.1093/conphys/coab057

Foucart, T., Lourdais, O., Denardo, D. F., & Heulin, B. (2014). Influence of reproductive mode on metabolic costs of reproduction: Insight from the bimodal lizard *Zootoca vivipara*. *Journal of Experimental Biology*, 217(22), 4049–4056. doi: 10.1242/jeb.104315

Foulkes, N.S., Whitmore, D., Vallone, D., & Bertolucci, C. (2016). Studying the evolution of the vertebrate circadian clock: the power of fish as comparative models. In: Foulkes, N.S., (Ed.), *Advances in genetics: genetics, genomics and fish phenomics* (Vol.95). Cambridge (MA): Harvard University Press. pp. 1-30.

Fox-Kemper, B., Hewitt, H.T., Xiao, C., Adalgeirsdottir, G., Drijfhout, S.S., Edwards, T.L., Golledge, N.R., Hemer, M., Kopp, R.E., Krinner, G. *et al.* (2021). Ocean, Cryosphere and Sea Level Change. In: Masson-Delmotte V, Zhai P, Pirani A, Connors SL, Pean C, Berger S, Caud N, Chen Y, Goldfarb L, Gomis MI *et al*., eds. Climate Change 2021: The Physical Science Basis. Contribution of Working Group I to the Sixth Assessment Report of the Intergovernmental Panel on Climate Change. Cambridge University Press, Cambridge, United Kingdom and New York, NY, USA, pp. 1211–1362, doi:10.1017/9781009157896.011.

Freitas, V., Cardoso, J.F.M.F., Lika, K., Peck, M.A., Campos, J., Kooijman, S.A.L.M., van der Veer, H.W. (2010). Temperature tolerance and energetics: a dynamic energy budget-based comparison of North Atlantic marine species. *Philosophical Transactions of the Royal Society B* 365: 3553-3565.

Froese, R. (2006). Cube law, condition factor and weight-length relationships: History, meta-analysis and recommendations. *Journal of Applied Ichthyology*, *22*(4), 241–253. doi:10.1111/j.1439-0426.2006.00805.x

Fu, A. L., Hammerschlag, N., Lauder, G. V., Wilga, C. D., Kuo, C. Y., & Irschick, D. J. (2016). Ontogeny of head and caudal fin shape of an apex marine predator: The tiger shark (*Galeocerdo cuvier*). *Journal of Morphology*, *277*(5), 556–564. doi:10.1002/jmor.20515

Fulton, T. W., 1904: The rate of growth of fishes. Twenty-second Annual Report, Part III. Fisheries Board of Scotland, Edinburgh, pp. 141–241.

Gallagher, A. J., & Hammerschlag, N. (2011). Global shark currency: The distribution frequency and economic value of shark ecotourism. *Current Issues in Tourism*, *14*(8), 797–812. doi:10.1080/13683500.2011.585227

Gallagher, A. J., Wagner, D. N., Irschick, D. J., & Hammerschlag, N. (2014). Body condition predicts energy stores in apex predatory sharks. *Conservation Physiology*, *2*(1), 1–8. doi:10.1093/conphys/cou022

Gallucci, V. F., Taylor, I. G., & Erzini, K. (2006). Conservation and management of exploited shark populations based on reproductive value. *Canadian Journal of Fisheries and Aquatic Sciences*, *63*(4), 931–942. doi:10.1139/f05-267

Gendron, S.M., Menzies, S. (2004). Elasmobranch Acclimation and Introduction, In: Smith M, Warmolts D, Thoney D, Hueter R eds. Elasmobranch Husbandry Manual: Captive Care of Sharks, Rays, and their Relatives. Ohio Biological Survey, Inc, Columbus, pp 151-162.

Gervais, C. R., Nay, T. J., Renshaw, G., Johansen, J. L., Steffensen, J. F., & Rummer, J. L. (2018). Too hot to handle? Using movement to alleviate effects of elevated temperatures in a benthic elasmobranch, *Hemiscyllium ocellatum*. *Marine Biology, 165(11),* 162. doi:10.1007/s00227-018-3427-7

Gervais, C., Mourier, J., & Rummer, J. L. (2016). Developing in warm water: Irregular colouration and patterns of a neonate elasmobranch. *Marine Biodiversity, 46(4),* 743–744. doi:10.1007/s12526-015-0429-2

Gillooly, J. F., & Baylis, J. R. (1999). Reproductive success and the energetic cost of parental care in male smallmouth bass. *Journal of Fish Biology,* 54(3), 573–584. doi:10.1111/j.1095-8649.1999.tb00636.x

Gillooly, J. F., & Dodson, S. I. (2000). The relationship of neonate mass and incubation temperature to embryonic development time in a range of animal taxa. *Journal of Zoology*, 251(3), 369–375. doi:10.1017/S095283690000710X

Gunderson, A.R., Stillman, J.H. (2015). Plasticity in thermal tolerance has limited potential to buffer ectotherms from global warming. *Philosophical Transactions of the Royal Society B* 282, 20150401. doi: 10.1098/rspb.2015.0401

Hammerschlag, N., & Sulikowski, J. (2011). Killing for conservation: The need for alternatives to lethal sampling of apex predatory sharks. *Endangered Species Research*, *14*(2), 135–140. doi:10.3354/esr00354

Hammerschlag, N., Schmitz, O. J., Flecker, A. S., Lafferty, K. D., Sih, A., Atwood, T. B., Gallagher, A. J., Irschick, D. J., Skubel, R., & Cooke, S. J. (2019). Ecosystem function and services of aquatic predators in the anthropocene. *Trends in Ecology and Evolution*, *34*(4), 369–383. doi:10.1016/j.tree.2019.01.005

Hammerschlag, N., Skubel, R. A., Sulikowski, J., Irschick, D. J., & Gallagher, A. J. (2018). A comparison of reproductive and energetic states in a marine apex predator (the tiger shark, *Galeocerdo cuvier*). *Physiological and Biochemical Zoology*, 91(4), 933–942. doi: 10.1086/698496

Harahush, B. K., Fischer, A. B. P., & Collin, S. P. (2007). Captive breeding and embryonic development of *Chiloscyllium punctatum* Muller & Henle, 1838 (Elasmobranchii: Hemiscyllidae). *Journal of Fish Biology,* 71(4), 1007–1022. doi:10.1111/j.1095-8649.2007.01569.x

Hare, J. A., Morrison, W. E., Nelson, M. W., Stachura, M. M., Teeters, E. J., Griffis, R. B., Alexander, M. A., Scott, J. D., Alade, L., Bell, R. J., Chute, A. S., Curti, K. L., Curtis, T. H., Kircheis, D., Kocik, J. F., Lucey, S. M., McCandless, C. T., Milke, L. M., Richardson, D. E., … Griswold, C. A. (2016). A vulnerability assessment of fish and invertebrates to climate change on the northeast U.S. continental shelf. *PLoS ONE*, *11*(2), 1–30. doi:10.1371/journal.pone.0146756

Hastings, J. W., & Sweeney, B. M. (1957). On the mechanism of temperature independence in a biological clock*. *Proceedings of the National Academy of Sciences,* 43(9), 804–811. doi:10.1073/pnas.43.9.804

Hayes, J. P. and Shonkwiler, J. S. (2001). Morphometric indicators of body condition: worthwhile or wishful thinking? In: Spearman J. R., ed. Body composition analysis of animals: a handbook of non-destructive methods. Cambridge Univ. Press, pp 8–38.

Hayward, A., Gillooly, J.F. (2011). The cost of sex: quantifying energetic investment in gamete production by males and females. *PLoS One 6*, e16557. doi: 10.1371/journal.pone.0016557

Heinrich, D. D. U., Rummer, J. L., Morash, A. J., Watson, S., Simpfendorfer, C. A., Heupel, M. R., & Munday, P. L. (2014). A product of its environment: The epaulette shark (*Hemiscyllium ocellatum*) exhibits physiological tolerance to elevated environmental CO_2. *Conservation Physiology, 2,* 1–12. doi:10.1093/conphys/cou047.

Heinrich, D. D. U., Watson, S., Rummer, J. L., Brandl, S. J., Simpfendorfer, C. A., Heupel, M. R., & Munday, P. L. (2015). Foraging behaviour of the epaulette shark *Hemiscyllium ocellatum* is not affected by elevated CO_2. *ICES Journal of Marine Science*. doi:10.1093/icesjms/fst176

Heupel, M. R., & Bennett, M. B. (1996). A myxosporean parasite (Myxosporea: Multivalvulida) in the skeletal muscle of epaulette sharks, *Hemiscyllium ocellatum* (Bonnaterre), from the Great Barrier Reef. *Journal of Fish Diseases*, *19*(2), 189–191. doi:10.1111/j.1365-2761.1996.tb00700.x

Heupel, M. R., Whittier, J. M., & Bennett, M. B. (1999). Plasma steroid hormone profiles and reproductive biology of the epaulette shark, *Hemiscyllium ocellatum*. *Journal of Experimental Zoology, 284,* 586–594. doi:10.1002/(SICI)1097-010X(19991001)284:5<586::AID-JEZ14>3.0.CO;2-B

Heupel, M., & Bennett, M. (1998). Observations on the diet and feeding habits of the epaulette shark, *Hemiscyllium ocellatum* (Bonnaterre), on Heron Island Reef, Great Barrier Reef, Australia. *Marine and Freshwater Research*, *49*, 753–756.

Heupel, M., & Bennett, M. (2007). Estimating abundance of reef-dwelling sharks: A case study of the epaulette shark, *Hemiscyllium ocellatum* (Elasmobranchii: Hemiscyllidae). *Pacific Science*, *61*(3), 383–394. doi:10.2984/1534-6188(2007)61[383:EAORSA]2.0.CO;2

Heupel, M.R., Whittier, J.M., Bennett, M.B. (1999). Plasma steroid hormone profiles and reproductive biology of the epaulette shark, *Hemiscyllium ocellatum*. *Journal of Experimental Zoology, 284,* 586–594. doi: 10.1002/(SICI)1097-010X(19991001)284:5<586::AID-JEZ14>3.0.CO2-B

Hight, B.V., Lowe, C.G. (2007). Elevated body temperatures of adult female leopard sharks, *Triakis semifasciata*, while aggregating in shallow nearshore embayments: evidence for behavioral thermoregulation? *Journal of Experimental Marine Biology and Ecology* 352:114–128. doi:10.1016/j.jembe.2007.07.021

Hoff, G. R. (2008). A nursery site of the Alaska skate (*Bathyraja parmifera*) in the eastern Bering Sea. *Fishery Bulletin*, *106*(3), 233–244.

Hoffmayer, E. R., Parsons, G. R., & Horton, J. (2006). Seasonal and interannual variation in the energetic condition of adult male Atlantic sharpnose shark *Rhizoprionodon terraenovae* in the northern Gulf of Mexico. *Journal of Fish Biology*, *68*(2), 645–653. doi:10.1111/j.0022-1112.2006.00942.x

Hove, J. R., & Moss, S. A. (1997). Effect of MS-222 on response to light and rate of metabolism of the little skate *Raja erinacea*. Marine Biology, 128(4), 579–583. doi:10.1007/s002270050124

Huey, R. B., Kearney, M. R., Krockenberger, A., Holtum, J. A. M., Jess, M., & Williams, S. E. (2012). Predicting organismal vulnerability to climate warming: Roles of behaviour, physiology and adaptation. Philosophical Transactions of the

Royal Society B: Biological Sciences, 367(1596), 1665–1679. doi:10.1098/rstb.2012.0005

Hughes, T. P., Kerry, J. T., Álvarez-Noriega, M., Álvarez-Romero, J. G., Anderson, K. D., Baird, A. H., Babcock, R. C., Beger, M., Bellwood, D. R., Berkelmans, R., Bridge, T. C., Butler, I. R., Byrne, M., Cantin, N. E., Comeau, S., Connolly, S. R., Cumming, G. S., Dalton, S. J., Diaz-Pulido, G., … Wilson, S. K. (2017). Global warming and recurrent mass bleaching of corals. Nature, 543(7645), 373–377. doi:10.1038/nature21707

Hussey, N. E., Cocks, D. T., Dudley, S. F. J., McCarthy, I. D., & Wintner, S. P. (2009). The condition conundrum: application of multiple condition indices to the dusky shark *Carcharhinus obscurus*. *Marine Ecology Progress Series*, *380*, 199–212. doi:10.3354/meps07918

Illing, B., Downie, A.T., Beghin, M., Rummer, J.L. (2020). Critical thermal maxima of early life stages of three tropical fishes: Effects of rearing temperature and experimental heating rate. *Journal of Thermal Biology* 90, 102582. doi: 10.1016/j.jtherbio.2020.102582

Inoue, T., Shimoyama, K., Saito, M., Wong, M. K.-S., Ikeba, K., Nozu, R., Matsumoto, R., Murakumo, K., Sato, K., Tokunaga, K., Kofuji, K., Takagi, W., & Hyodo, S. (2022). Long-term monitoring of egg-laying cycle using ultrasonography reveals the reproductive dynamics of circulating sex steroids in an oviparous catshark, *Scyliorhinus torazame*. *General and Comparative Endocrinology*, 327, 114076. doi: 10.1016/j.ygcen.2022.114076

Irschick, D. J., & Hammerschlag, N. (2014). A new metric for measuring condition in large predatory sharks. *Journal of Fish Biology*, *85*(3), 917–926. doi:10.1111/jfb.12484

Irschick, D. J., & Hammerschlag, N. (2015). Morphological scaling of body form in four shark species differing in ecology and life history. *Biological Journal of the Linnean Society*, *114*(1), 126–135. doi:10.1111/bij.12404

Irschick, D. J., Fu, A., Lauder, G., Wilga, C., Kuo, C. Y., & Hammerschlag, N. (2017). A comparative morphological analysis of body and fin shape for eight shark species. *Biological Journal of the Linnean Society*, *122*(3), 589–604. doi: 10.1093/biolinnean/blx088

IUCN (2022). The IUCN Red List of Threatened Species. Version 2022-1. https://www.iucnredlist.org

Janse M, Firchau B, Mohan PJ (2004) Elasmobranch nutrition, food handling, and feeding techniques. In: Elasmobranch Husbandry Manual (eds), Smith M, Warmolts D, Thoney D, Hueter R. Ohio Biological Survey, Inc. pp 183-200.

Jerde, C. L., Kraskura, K., Eliason, E. J., Csik, S. R., Stier, A. C., & Taper, M. L. (2019). Strong Evidence for an Intraspecific Metabolic Scaling Coefficient Near 0.89 in Fish. Frontiers in Physiology, 10(September), 1–17. doi:10.3389/fphys.2019.01166

Johansen, J. L., Nadler, L. E., Habary, A., Bowden, A. J., & Rummer, J. (2021). Thermal acclimation of tropical coral reef fishes to global heat waves. *ELife*, 10, 1–29.

Johnson, C.R. (1976). Diel variation in the thermal tolerance of *Gambusia affinis affinis* (Pisces: Poeciliidae). *Comp Biochem Physiol A* 55: 337–340. doi: 10.1016/0300-9629(76)90056-6

Johnson, M. S., Kraver, D. W., Renshaw, G. M. C., & Rummer, J. L. (2016). Will ocean acidification affect the early ontogeny of a tropical oviparous elasmobranch

(*Hemiscyllium ocellatum*)? *Conservation Physiology, 4(1),* 1–11. doi:10.1093/conphys/cow003

Jutan, Y., Retraubun, A., Khouw, A., Nikijuluw, V., & Pattikawa, J. (2018). Study on the population of Halmahera walking shark (*Hemiscyllium halmahera*) in Kao Bay, North Maluku, Indonesia. *International Journal of Fisheries and Aquatic Studies, 6(5),* 36–41.

Kadar, J., Ladds, M., Mourier, J., Day, J., & Brown, C. (2019). Acoustic accelerometry reveals diel activity patterns in premigratory Port Jackson sharks. Ecology and Evolution, 9(16), 8933–8944. doi:10.1002/ece3.5323

Karsten, A. H., & Turner, J. W. (2003). Fecal Corticosterone Assessment in the Epaulette Shark, *Hemiscyllium ocellatum*. *Journal of Experimental Zoology*, *299A*(2), 188–196. doi:10.1002/jez.a.10300

Kellermann, V., Chown, S. L., Schou, M. F., Aitkenhead, I., Janion-Scheepers, C., Clemson, A., Scott, M. T., & Sgrò, C. M. (2019). Comparing thermal performance curves across traits: How consistent are they? Journal of Experimental Biology, 222(11). doi:10.1242/jeb.193433

Kelly, M. L., Collin, S. P., Hemmi, J. M., & Lesku, J. A. (2020). Evidence for Sleep in Sharks and Rays: Behavioural, Physiological, and Evolutionary Considerations. Brain, Behavior and Evolution, 94(1–4), 37–50. doi:10.1159/000504123

Kelly, M. L., Collins, S. P., Lesku, J. A., Hemmi, J. M., Collin, S. P., Radford, C. A., Collin, S. P., & Radford, C. A. (2022). Energy conservation characterizes sleep in sharks. Biology Letters, 18, 20210259.

Kelly, M. L., Murray, E. R. P., Kerr, C. C., Radford, C. A., Collin, S. P., Lesku, J. A., & Hemmi, J. M. (2020). Diverse Activity Rhythms in Sharks (Elasmobranchii). Journal of Biological Rhythms, 476–488. doi:10.1177/0748730420932066

Kelly, M. L., Spreitzenbarth, S., Kerr, C. C., Hemmi, J. M., Lesku, J. A., Radford, C. A., & Collin, S. P. (2021). Behavioural sleep in two species of buccal pumping sharks (*Heterodontus portusjacksoni* and *Cephaloscyllium isabellum*). Journal of Sleep Research, June, 1–10. doi:10.1111/jsr.13139

Kempster, R. M., Hart, N. S., & Collin, S. P. (2013). Survival of the Stillest: Predator Avoidance in Shark Embryos. PLoS ONE, 8(1), 4–9. doi:10.1371/journal.pone.0052551

Kim, W. S., Kim, J. M., Yi, S. K., & Huh, H. T. (1997). Endogenous circadian rhythm in the river puffer fish Takifugu obscurus. Marine Ecology Progress Series, 153(1–3), 293–298. doi:10.3354/meps153293

Kingsolver, J.G., Umbanhowar, J. (2018). The analysis and interpretation of critical temperatures. *Journal of Experimental Biology* 221, jeb167858. doi:10.1242/jeb.167858

Kinsey, D.W., & Kinsey, B.E. (1967). Diurnal changes in oxygen content of the water over the coral reef platform at heron island. Australian Journal of Marine and Freshwater Research, 18:23–34.

Kishore Kumar, M., Jayakumar, N., Karuppasamy, K., Manikandavelu, D., Uma, A., & Kavipriya, M. (2021). Length-weight relationships of eight elasmobranch species captured along the Coromandel coast of Tamil Nadu, Eastern Indian Ocean. *Journal of Applied Ichthyology*, *37*(3), 487–491. doi:10.1111/jai.14179

Kneebone, J., Sulikowski, J., Knotek, R., McElroy, W.D., Gervelis, B., Curtis, T., Jurek, J., Mandelman, J. (2020). Using conventional and pop-up satellite transmitting

tags to assess the horizontal movements and habitat use of thorny skate (*Amblyraja radiata*) in the Gulf of Maine. *ICES J Mar Sci* 77: 2790–2803.

Kneebone, J., Winton, M., Danylchuk, A., Chisholm, J., & Skomal, G. B. (2018). An assessment of juvenile sand tiger (*Carcharias taurus*) activity patterns in a seasonal nursery using accelerometer transmitters. *Environmental Biology of Fishes*, 101(12), 1739–1756. doi:10.1007/s10641-018-0821-4

Komoroske, L.M., Connon, R.E., Lindberg, J., Cheng, B.S., Castillo, G., Hasenbein, M., Fangue, N.A. (2014). Ontogeny influences sensitivity to climate change stressors in an endangered fish. *Conservation Physiology* 2, cou008. doi:10.1093/conphys/cou008

Komsta, L. (2022). Outliers: tests for outliers. R package version 0.15. https://CRAN.R-project.org/package=outliers

Koob, T. J., & Callard, I. A. N. P. (1999). Reproductive endocrinology of female elasmobranchs: lessons from the little skate (*Raja erinacea*) and spiny dogfish (*Squalus acanthias*). *Journal of Experimental Zoology*, *284*, 557–574. doi: 10.1002/(sici)1097-010x(19991001)284:5<557::aid-jez12>3.3.co;2-g

Koob, T. J., & Callard, I. P. (1985). Progesterone treatment causes early oviposition in *Raja erinacea*. *Bulletin of the Mount Desert Island Biological Laboratory*, 25, 138–139.

Koob, T. J., Tsang, P., & Callard, I. P. (1986). Plasma estradiol, testosterone, and progesterone levels during the ovulatory cycle of the skate (*Raja Erinacea*). *Biology of Reproduction*, 35(2), 267–275. doi: 10.1095/biolreprod35.2.267

Kousteni, V., & Megalofonou, P. (2020). Reproductive strategy of *Scyliorhinus canicula (*L., 1758): A holistic approach based on macroscopic measurements and microscopic observations of the reproductive organs. *Marine and Freshwater Research, 71(6),* 596–616. doi:10.1071/MF18474

Krebs, C. J. and Singleton, G. R. 1993. Indices of condition for small mammals. *Australian Journal of Zoology, 41,* 317–323.

Labocha, M. K., Schutz, H., & Hayes, J. P. (2014). Which body condition index is best? *Oikos,* 123(1), 111–119. doi:10.1111/j.1600-0706.2013.00755.x

Lambert, Y., & Dutil, J.-D. (1997). Can simple condition indices be used to monitor and quantify seasonal changes in the energy reserves of Atlantic cod (*Gadus morhua*)? *Canadian Journal of Fisheries and Aquatic Sciences*, *54*, 104–112.

Last, P.R., White, W.T., de Carvalho, M.R., Séret, B., Stehmann, M.F., & Naylor, G.J.P. (2016). Rays of the world. CSIRO Publishing, Clayton.

Lauder, G.V., & Di Santo, V. (2015). Swimming mechanics and energetics of elasmobranch fishes. In: Shadwick, R.E., Farrell, A.P., & Brauner, C.J., (Eds.), *Physiology of elasmobranch fishes: structure and interaction with environment* (Vol. 34A). London (England): Academic Press. pp. 219-254.

Lawson, C. L., Dudgeon, C. L., Richardson, A. J., Broadhurst, M. K., & Bennett, M. B. (2022). Flexibility for fuelling reproduction in a pelagic ray (*Mobula eregoodoo*) suggested by bioenergetic modelling. *Journal of Fish Biology*, 100(3), 783–792. doi: 10.1111/jfb.14995

Lawson, C. L., Halsey, L. G., Hays, G. C., Dudgeon, C. L., Payne, N. L., Bennett, M. B., White, C. R., & Richardson, A. J. (2019). Powering Ocean Giants: The Energetics of Shark and Ray Megafauna. *Trends in Ecology and Evolution*, 34(11), 1009–1021. doi: 10.1016/j.tree.2019.07.001

Le Cren, E. D. (1951) The length–weight relationship and seasonal cycle in gonad weight and condition in the perch (*Perca fluviatilis*). *Journal of Animal Ecology. 20(2)*, 201–219.

Lear, K. O., Morgan, D. L., Whitty, J. M., Beatty, S. J., & Gleiss, A. C. (2021). Wet season flood magnitude drives resilience to dry season drought of a euryhaline elasmobranch in a dry-land river. *Science of the Total Environment*, *750*, 142234. doi:10.1016/j.scitotenv.2020.142234

Lear, K. O., Morgan, D. L., Whitty, J. M., Whitney, N. M., Byrnes, E. E., Beatty, S. J., & Gleiss, A. C. (2020). Divergent field metabolic rates highlight the challenges of increasing temperatures and energy limitation in aquatic ectotherms. *Oecologia,* 193(2), 311–323. doi:10.1007/s00442-020-04669-x

Lear, K. O., Whitney, N. M., Brewster, L. R., Morris, J. J., Hueter, R. E., & Gleiss, A. C. (2017). Correlations of metabolic rate and body acceleration in three species of coastal sharks under contrasting temperature regimes. *Journal of Experimental Biology,* November, jeb.146993. doi:10.1242/jeb.146993

Lechenault, H., Wrisez, F., & Mellinger, J. (1993). Yolk utilization in *Scyliorhinus canicula*, an oviparous dogfish. *Environmental Biology of Fishes*, 38(1–3), 241–252. doi:10.1007/BF00842920

Leiva, F.P., Calosi, P., Verberk, W.C.E.P. (2019). Scaling of thermal tolerance with body mass and genome size in ectotherms: a comparison between water- and air-breathers. *Philosophical Transactions of the Royal Society B* 374, 20190035. doi:10.1098/rstb.2019.0035

Lenth, R.V. (2022). *emmeans:* Estimated Marginal Means, aka Least-Squares Means. R package version 1.7.2. https://CRAN.R-project.org/package=emmeans

Leurs, G., O'Connell, C. P., Andreotti, S., Rutzen, M., & Vonk Noordegraaf, H. (2015). Risks and advantages of using surface laser photogrammetry on free-ranging marine organisms: A case study on white sharks *Carcharodon carcharias*. *Journal of Fish Biology*, *86*(6), 1713–1728. doi:10.1111/jfb.12678

Lindenmayer, D. B., & Likens, G. E. (2011). Direct Measurement Versus Surrogate Indicator Species for Evaluating Environmental Change and Biodiversity Loss. Ecosystems, 14(1), 47–59. doi:10.1007/s10021-010-9394-6

Luongo, S. M., & Lowe, C. G. (2018). Seasonally acclimated metabolic Q10of the California horn shark*, Heterodontus francisci.* Journal of Experimental Marine Biology and Ecology, 503(February), 129–135. doi:10.1016/j.jembe.2018.02.006

Lutterschmidt, W.I., Hutchison, V.H. (1997). The critical thermal maximum: history and critique. *Canadian Journal of Zoology* 75: 1561-1574.

Lyons, K., Carlisle, A. B., & Lowe, C. G. (2017). Influence of ontogeny and environmental exposure on mercury accumulation in muscle and liver of male Round Stingrays. *Marine Environmental Research,* 130, 30–37. doi:10.1016/j.marenvres.2017.07.004

Lyons, K., Galloway, A. S., Adams, D. H., Reyier, E. A., Barker, A. M., Portnoy, D. S., & Frazier, B. S. (2020). Maternal provisioning gives young-of-the-year Hammerheads a head start in early life. *Marine Biology*, *167*(11), 1–13. doi:10.1007/s00227-020-03766-y

Martin, B. T., Heintz, R., Danner, E. M., Nisbet, R. M., & Dussutour, A. (2017). Integrating lipid storage into general representations of fish energetics. *The Journal of Animal Ecology*, *86*(4), 812–825. doi:10.1111/1365-2656.12667

McBride, R. S., Somarakis, S., Fitzhugh, G. R., Albert, A., Yaragina, N. A., Wuenschel, M. J., Alonso-Fernández, A., & Basilone, G. (2015). Energy acquisition and allocation to egg production in relation to fish reproductive strategies. *Fish and Fisheries* (Oxford, England), 16(1), 23–57. doi: 10.1111/faf.12043

Merciere, A., & Norin, T. (2021). Package *RespiroRS*. R package. https://github.com/Alexmerciere/RespiroRS/.

Merly, L., Lange, L., Meÿer, M., Hewitt, A. M., Koen, P., Fischer, C., … Hammerschlag, N. (2019). Blood plasma levels of heavy metals and trace elements in white sharks (*Carcharodon carcharias*) and potential health consequences. *Marine Pollution Bulletin*, *142*(March), 85–92. doi:10.1016/J.MARPOLBUL.2019.03.018

Messmer, V., Pratchett, M.S., Hoey, A.S., Tobin, A.J., Coker, D.J., Cooke, S.J., Clark, T.D. (2017). Global warming may disproportionately affect larger adults in a predatory coral reef fish. *Global Change Biology* 23: 2230–2240.

Metcalfe, J.D., & Butler, P.J. (1984). Changes in activity and ventilation in response to hypoxia in unrestrained, unoperated dogfish (*Scyliorhinus canicula L*.). *Journal of Experimental Biology, 108*, 411-418.

Miklos, P., Katzman, S. M., & Cech, J. J. (2003). Effect of temperature on oxygen consumption of the leopard shark, *Triakis semifasciata.* Environmental Biology of Fishes, 66(1), 15–18. doi:10.1023/A:1023287123495

Moorhead, S. G., Gallagher, A. J., Merly, L., & Hammerschlag, N. (2020). Variation of body condition and plasma energy substrates with life stage, sex, and season in wild-sampled nurse sharks *Ginglymostoma cirratum*. *Journal of Fish Biology*, (November). doi:10.1111/jfb.14612

Morgan, R., Finnøen, M.H., Jutfelt, F. (2018). CT_{max} is repeatable and doesn't reduce growth in zebrafish. *Scientific Reports* 8,7009. doi: 10.1038/s41598-018-25593-4

Morgan, R., Sundin, J., Finnøen, M. H., Dresler, G., Vendrell, M. M., Dey, A., Sarkar, K., & Jutfelt, F. (2019). Are model organisms representative for climate change research? Testing thermal tolerance in wild and laboratory zebrafish populations. *Conserv Physiol* 6, coz036. doi: 10.1093/conphys/coz036

Motta, F. S., Caltabellotta, F. P., Namora, R. C., & Gadig, O. B. F. (2014). Length-weight relationships of sharks caught by artisanal fisheries from southeastern Brazil. *Journal of Applied Ichthyology*, *30*(1), 239–240. doi:10.1111/jai.12234

Moura, C. de A., Lima, J. P. da S., Silveira, V. A. M., Miguel, M. A. L., & Luchiari, A. C. (2017). Time place learning and activity profile under constant light and constant dark in zebrafish (*Danio rerio*). Behavioural Processes, 138, 49–57. doi:10.1016/j.beproc.2017.02.015

Mulvey, J. M., & Renshaw, G. M. C. (2009). GABA is not elevated during neuroprotective neuronal depression in the hypoxic epaulette shark (*Hemiscyllium ocellatum*). *Comparative Biochemistry and Physiology - A Molecular and Integrative Physiology*, *152*(2), 273–277. doi:10.1016/j.cbpa.2008.10.017

Munns, S. L. (2013). Gestation increases the energetic cost of breathing in the lizard *Tiliqua rugosa*. *The Journal of Experimental Biology*, 216(2), 171–180. doi: 10.1242/jeb.067827

Murphy, B. R., Willis, D. W., & Springer, T. A. (1991). The relative weight index in fisheries management: status and needs. *Fisheries*, *16*(2), 30–38. doi: 10.1577/1548-8446(1991)016<0030:TRWIIF>2.0.CO;2

Musa, S. M., Czachur, M. V., & Shiels, H. A. (2018). Oviparous elasmobranch development inside the egg case in 7 key stages. PLoS ONE, 13(11), 1–29. doi:10.1371/journal.pone.0206984

Nakaya, K., White, W. T., & Ho, H. C. (2020). Discovery of a new mode of oviparous reproduction in sharks and its evolutionary implications. *Scientific Reports*, 1–12. doi: 10.1038/s41598-020-68923-1

Nay, T. J., Longbottom, R. J., Gervais, C. R., Johansen, J. L., Steffensen, J. F., Rummer, J. L., & Hoey, A. S. (2021). Regulate or tolerate: Thermal strategy of a coral reef flat resident, the epaulette shark, *Hemiscyllium ocellatum*. *Journal of Fish Biology ,98(3), 723-732*. doi:10.1111/jfb.14616

Nelson, D. R., & Johnson, R. H. (1970). Diel Activity Rhythms in the Nocturnal, Bottom-Dwelling Sharks, *Heterodontus francisci* and *Cephaloscyllium ventriosum*. Copeia, 1970(4), 732–739. doi:10.2307/1442315

Nilsson, J.-Å., & Råberg, L. (2001). The Resting Metabolic Cost of Egg Laying and Nestling Feeding in Great Tits. *Oecologia*, 128(2), 187–192. doi: 10.1007/s004420100653

Nixon, A. J., & Gruber, S. H. (1988). Diel metabolic and activity patterns of the lemon shark (Negaprion brevirostris). Journal of Experimental Zoology, 248(1), 1–6. doi:10.1002/jez.1402480102

Olmeda, J. F. L., Madrid, J. A., Vázquez, F. J. S., López, J. F., Madrid, J. A., & Vázquez, F. J. S. (2006). Light and Temperature Cycles as Zeitgebers of Zebrafish (*Danio rerio*) Circadian Activity Rhythms. Chronobiology International, 23(3), 537–550. doi:10.1080/07420520600651065

Olsson, M., Shine, R., & Bak-Olsson, E. (2000). Locomotor impairment of gravid lizards: Is the burden physical or physiological? *Journal of Evolutionary Biology*, 13(2), 263–268. doi: 10.1046/j.1420-9101.2000.00162.x

Ospina AF, Mora C (2004) Effect of body size on reef fish tolerance to extreme low and high. *Environ Biol Fish* 70: 339–343.

Papastamatiou, Y. P., Watanabe, Y. Y., Demšar, U., Leos-Barajas, V., Bradley, D., Langrock, R., Weng, K., Lowe, C. G., Friedlander, A. M., & Caselle, J. E. (2018). Activity seascapes highlight central place foraging strategies in marine predators that never stop swimming. Movement Ecology, 6(1), 1–15. doi:10.1186/s40462-018-0127-3

Pattarapongpan, S., Arnupapboon, S., Ali, A., & Takashi Fritz, M. (2021). Yield per recruit and spawning per recruit of brownbanded bamboo shark, *Chiloscyllium punctatum* in Southeast Asia. *Journal of Fisheries and Environment, 45(3),* 14–27.

Payne, E. J., & Rufo, K. S. (2012). Husbandry and growth rates of neonate epaulette sharks, *Hemiscyllium ocellatum* in captivity. *Zoo Biology*, *31*(6), 718–724. doi:10.1002/zoo.20426

Payne, N. L., Smith, J. A., van der Meulen, D. E., Taylor, M. D., Watanabe, Y. Y., Takahashi, A., Marzullo, T. A., Gray, C. A., Cadiou, G., & Suthers, I. M. (2016). Temperature dependence of fish performance in the wild: Links with species biogeography and physiological thermal tolerance. Functional Ecology, 30(6), 903–912. doi:10.1111/1365-2435.12618

Peach, M. B. (2002). Rheotaxis by epaulette sharks, *Hemiscyllium ocellatum* (Chondrichthyes:Hemiscylliidae), on a coral reef flat. *Australian Journal of Zoology*, 50(4), 407–414. https://doi.org/10.1071/ZO01081

Peig, J., & Green, A. J. (2009). New perspectives for estimating body condition from mass/length data: The scaled mass index as an alternative method. *Oikos,* 118(12), 1883–1891. doi:10.1111/j.1600-0706.2009.17643.x

Penney, C.M., Burness, G., Tabh, J.K.R., Wilson, C.C. (2021). Limited transgenerational effects of environmental temperatures on thermal performance of a cold-adapted salmonid. *Conservation Physiology* 9, coab021. doi: 10.1093/conphys/coab021.

Pereira Santos, C., Sampaio, E., Pereira, B.P., Pegado, M.R., Borges, F.O., Wheeler, C.R., Bouyoucos, I.A., Rummer, J.L., Santos, C.F., Rosa, R. (2021). Elasmobranch Responses to Experimental Warming, Acidification, and Oxygen Loss—A Meta-Analysis. *Frontiers in Marine Science* 8,735377. doi: 10.3389/fmars.2021.735377

Pinheiro J, Bates D, DebRoy S, Sarkar D, R Core Team (2021) nlme: linear and nonlinear mixed effects models. R package version 3.1-153. https://CRAN.R-project.org/package=nlme>.

Pistevos, J. C. A., Nagelkerken, I., Rossi, T., Olmos, M., & Connell, S. D. (2015). Ocean acidification and global warming impair shark hunting behaviour and growth. *Scientific Reports, 5(1),* 16293. doi:10.1038/srep16293

Pörtner, H. O., & Farrell, A. P. (2008). Ecology: Physiology and climate change. Science, 322(5902), 690–692. doi:10.1126/science.1163156

Pörtner, H. O., & Peck, M. A. (2010). Climate change effects on fishes and fisheries: Towards a cause-and-effect understanding. *Journal of Fish Biology*, 77(8), 1745–1779. doi:10.1111/j.1095-8649.2010.02783.x

Pörtner, H.O., Farrell, A.P. (2008). Physiology and climate change. *Science* 322: 690-692.

Pottier, P., Burke, S., Drobniak, S.M. (2022). Methodological inconsistencies define thermal bottlenecks in fish life cycle: a comment on Dahlke *et al.* 2020. *Evolutionary Ecology*. doi: 10.1007/s10682-022-10157-w

Pouca, C. V., Gervais, C., Reed, J., Michard, J., & Culum, B. (2019). Quantity discrimination in Port Jackson sharks incubated under elevated temperatures. *Behavioral Ecology and Sociobiology*, *73*(7), 1-9.

Pretorius, C., & Griffiths, C. L. (2013). Patterns of egg deposition and egg development in the catsharks *Poroderma pantherinum* and *Haploblepharus pictus*. *African Zoology, 48(1),* 115–124. doi:10.1080/15627020.2013.11407574

Przeslawski R, Byrne M, Mellin C (2015) A review and meta-analysis of the effects of multiple abiotic stressors on marine embryos and larvae. *Glob Chang Biol* 21: 2122–2140.

Queensland Government (2022). Recreational fishing rules: general possession limits. https://www.qld.gov.au/recreation/activities/boating-fishing/rec-fishing/rules/limits-tidal#sharks

R Core Team. (2021). R: A language and environment for statistical computing. R Foundation for Statistical Computing, Vienna, Austria. https://www.R-project.org/.

Rangel, B. D. S., Hammerschlag, N., Sulikowski, J. A., & Moreira, R. G. (2021). Physiological markers suggest energetic and nutritional adjustments in male sharks linked to reproduction. *Oecologia*, 196(4), 989–1004. doi: 10.1007/s00442-021-04999-4

Rangel, B. de S., Moreira, R. G., Niella, Y. V., Sulikowski, J. A., & Hammerschlag, N. (2021). Metabolic and nutritional condition of juvenile tiger sharks exposed to regional differences in coastal urbanization. *Science of the Total Environment*, 780, 146548. doi: 10.1016/j.scitotenv.2021.146548

Rangel, B. S., Moreira, R. G., Rider, M. J., Sulikowski, J. A., Gallagher, A. J., Heithaus, M. R., Cooke, S. J., Kaufman, L., & Hammerschlag, N. (2022). Physiological state predicts space use of sharks at a tourism provisioning site. *Animal Behaviour, 191*, 149–163. doi: 10.1016/j.anbehav.2022.07.004

Raoult, V., Tosetto, L., & Williamson, J. E. (2018). Drone-based high-resolution tracking of aquatic vertebrates. *Drones*, *2*, drones2040037. doi:10.3390/drones2040037

Rasmussen, L. E. L., Hess, D. L., & Luer, C. A. (1999). Alterations in serum steroid concentrations in the clearnose skate, *Raja eglanteria*: Correlations with season and reproductive status. *Journal of Experimental Zoology*, 284(5), 575–585. doi: 10.1002/(SICI)1097-010X(19991001)284:5<575::AID-JEZ13>3.0.CO;2-I

Reardon, E. E., & Chapman, L. J. (2010). Hypoxia and energetics of mouth brooding: Is parental care a costly affair? *Comparative Biochemistry and Physiology Part A: Molecular & Integrative Physiology, 156(4),* 400–406. doi:10.1016/j.cbpa.2010.03.007

Recsetar, M.S., Zeigler, M.P., Ward, D.L., Bonar, S.A., Caldwell, C.A. (2012). Relationship between fish size and upper thermal tolerance. *Transactions of the American Fisheries Society* 141:1433–1438.

Reebs, S. G. (2002). Plasticity of diel and circadian activity rhythms in fishes. *Reviews in Fish Biology and Fisheries,* 12(4), 349–371. doi:10.1023/A:1025371804611

Renshaw, G. M. C., Wise, G., & Dodd, P. R. (2010). Ecophysiology of neuronal metabolism in transiently oxygen-depleted environments: Evidence that GABA is accumulated pre-synaptically in the cerebellum. *Comparative Biochemistry and Physiology - A Molecular and Integrative Physiology*, *155*(4), 486–492. doi:10.1016/j.cbpa.2009.10.039

Reznick, D. (1985). Costs of Reproduction: An Evaluation of the Empirical Evidence. *Oikos*, 44(2), 257–267.

Ritcher, H., Lückstädt, C., Focken, U., & Becker, K. (2000). An improved procedure to assess fish condition on the basis of length-weight relationships. *Archive of Fishery and Marine Research*, *48*(3), 255–264.

Rizzo, E., & Bazzoli, N. (2019). Reproduction and embryogenesis. In B. Baldisserotto, E. Urbinati, & J. Cyrino (Eds.), *Biology and physiology of freshwater neotropical fish* (pp. 287- 313). San Diego: Elsevier Science & Technology.

Rodda, K.R. (2000). Chapter 5: Embryonic respiration and ventilation. In *Development in the Port Jackson Shark Embryo*. Thesis: University of Adelaide, 147.

Rohner, C. A., Richardson, A. J., Prebble, C. E. M., Marshall, A. D., Bennett, M. B., Weeks, S. J., … Pierce, S. J. (2015). Laser photogrammetry improves size and demographic estimates for whale sharks. *PeerJ*, *2015*(4), 1–20. doi:10.7717/peerj.886

Rosa, R., Baptista, M., Lopes, V. M., Pegado, M. R., Ricardo Paula, J., Trubenbach, K., Leal, M. C., Calado, R., & Repolho, T. (2014). Early-life exposure to climate

change impairs tropical shark survival. *Proceedings of the Royal Society B: Biological Sciences, 281(1793),* 20141738. doi:10.1098/rspb.2014.1738

Rossouw, G. J. (1987). Function of the liver and hepatic lipids of the lesser sand shark, *Rhinobatos annulatus* (Müller & Henle). *Comparative Biochemistry and Physiology B: Biochemistry & Molecular Biology*, *86(4),* 785–790. doi:10.1016/0305-0491(87)90225-2

Routley, M. H., Nilsson, G. E., & Renshaw, G. M. C. (2002). Exposure to hypoxia primes the respiratory and metabolic responses of the epaulette shark to progressive hypoxia. *Comparative Biochemistry and Physiology Part A: Molecular & Integrative Physiology, 131(2),* 313–321. doi:10.1016/S1095-6433(01)00484-6

Rummer, J. L., Binning, S. A., Roche, D. G., & Johansen, J. L. (2016). Methods matter: Considering locomotory mode and respirometry technique when estimating metabolic rates of fishes. Conservation Physiology, 4(1), 1–13. doi:10.1093/conphys/cow008

Salinas-De-León, P., Phillips, B., Ebert, D., Shivji, M., Cerutti-Pereyra, F., Ruck, C., Fisher, C.R., Marsh, L. (2018). Deep-sea hydrothermal vents as natural egg-case incubators at the Galapagos Rift. *Scientific Reports 8*:1–7. doi:10.1038/s41598-018-20046-4

Sánchez-Vázquez, F. J., López-Olmeda, J. F., Vera, L. M., Migaud, H., López-Patiño, M. A., & Míguez, J. M. (2019). Environmental cycles, melatonin, and circadian control of stress response in fish. Frontiers in Endocrinology, 10(JUN), 1–18. doi:10.3389/fendo.2019.00279

Schielzeth, H., Dingemanse, N. J., Nakagawa, S., Westneat, D. F., Allegue, H., Teplitsky, C., Réale, D., Dochtermann, N. A., Garamszegi, L. Z., & Araya-Ajoy, Y. G. (2020). Robustness of linear mixed-effects models to violations of distributional assumptions. *Methods in Ecology and Evolution*, *11*(9), 1141–1152. doi:10.1111/2041-210X.13434

Schneider, C. A., Rasband, W. S., & Eliceiri, K. W. (2012). NIH Image to ImageJ: 25 years of image analysis. Nature Methods, 9(7), 671–675. doi:10.1038/nmeth.2089

Schwieterman, G. D., Bouyoucos, I. A., Potgieter, K., Simpfendorfer, C. A., Brill, R. W., & Rummer, J. L. (2019). Analysing tropical elasmobranch blood samples in the field: Blood stability during storage and validation of the HemoCueR haemoglobin analyser. *Conservation Physiology,* 7(1), 1–10. doi: 10.1093/conphys/coz081

Schwieterman, G. D., Crear, D. P., Anderson, B. N., Lavoie, D. R., Sulikowski, J. A., Bushnell, P. G., & Brill, R. W. (2019). Combined effects of acute temperature change and elevated pCO2 on the metabolic rates and hypoxia tolerances of clearnose skate (Rostaraja eglanteria), summer flounder (*Paralichthys dentatus*), and thorny skate (Amblyraja radiata). Biology, 8(3). doi:10.3390/biology8030056

Schwieterman, G. D., Rummer, J. L., Bouyoucos, I. A., Bushnell, P. G., & Brill, R. W. (2021). A lack of red blood cell swelling in five elasmobranch fishes following air exposure and exhaustive exercise. *Comparative Biochemistry and Physiology Part A: Molecular & Integrative Physiology*, *258*, 110978. doi:10.1016/j.cbpa.2021.110978

Seebacher, F., White, C.R., Franklin, C.E. (2015). Physiological plasticity increases resilience of ectothermic animals to climate change. *Nature Climate Change* 5: 61-66.

Sen, S., Chakraborty, S. K., Elayaperumal, V., Zacharia, P. U., Jaiswar, A. K., Dash, G., Kizhakudan, S. J., Bharadiya, S. A., & Gohel, J. K. (2018). Reproductive strategy of milk shark, *Rhizoprionodon acutus* (Ruppell 1837), along north-eastern Arabian Sea. *Ichthyological Research*, *65*(3), 324–333. doi:10.1007/s10228-018-0627-6

Shipley, O. N., Brownscombe, J. W., Danylchuk, A. J., Cooke, S. J., O'Shea, O. R., & Brooks, E. J. (2018). Fine-scale movement and activity patterns of Caribbean reef sharks (*Carcharhinus perezi*) in the Bahamas. *Environmental Biology of Fishes,* 101(7), 1097–1104. doi:10.1007/s10641-017-0656-4

Siddig, A. A. H., Ellison, A. M., Ochs, A., Villar-Leeman, C., & Lau, M. K. (2016). How do ecologists select and use indicator species to monitor ecological change? Insights from 14 years of publication in Ecological Indicators. *Ecological Indicators*, 60, 223–230. doi:10.1016/j.ecolind.2015.06.036

Silva-Garay, L., & Lowe, C. G. (2021). Effects of temperature and body-mass on the standard metabolic rates of the round stingray, *Urobatis halleri* (Cooper, 1863). Journal of Experimental Marine Biology and Ecology, 540(January), 151564. doi:10.1016/j.jembe.2021.151564

Simpfendorfer, C. A., Heupel, M. R., White, W. T., & Dulvy, N. K. (2011). The importance of research and public opinion to conservation management of sharks and rays: A synthesis. *Marine and Freshwater Research*, *62*(6), 518–527. doi:10.1071/MF11086

Sims, D., & Davies, S. (1994). Does specific dynamic action (SDA) regulate retinr of appetite in the lesser spotted dogfish, *Scyliorhinus canicula*? Journal of Fish Biology, 45, 341–348.

Sinclair, B. J., Marshall, K. E., Sewell, M. A., Levesque, D. L., Willett, C. S., Slotsbo, S., Dong, Y., Harley, C. D. G., Marshall, D. J., Helmuth, B. S., & Huey, R. B. (2016). Can we predict ectotherm responses to climate change using thermal performance curves and body temperatures? Ecology Letters, 19(11), 1372–1385. doi:10.1111/ele.12686

Skirving, W. (2020). Status of Bleaching Heat Stress on the Great Barrier Reef, Australia. https://coralreefwatch.noaa.gov/satellite/analyses_guidance/gbr_heat_stress_event2020_status_asof2 0200416.pdf .

Smith, C., & Wootton, R. J. (1995). The costs of parental care in teleost fishes. *Reviews in Fish Biology and Fisheries,* 5(1), 7–22. doi:10.1007/BF01103363

Spargo, E., Pratt, O. E., & Daniel, P. M. (1979). Metabolic functions of skeletal muscles of man, mammals, birds and fishes: A Review. *Journal of the Royal Society of Medicine*, 72(12), 921–925. doi:10.1177/014107687907201211

Speed, C. W., Meekan, M. G., Field, I. C., McMahon, C. R., & Bradshaw, C. J. A. (2012). Heat-seeking sharks: Support for behavioural thermoregulation in reef sharks. *Marine Ecology Progress Series*, *463*, 231–244. doi:10.3354/meps09864

Speers-Roesch, B., & Treberg, J. R. (2010). The unusual energy metabolism of elasmobranch fishes. *Comparative Biochemistry and Physiology Part A*, 155(4), 417–434. doi:10.1016/j.cbpa.2009.09.031

Speers-Roesch, B., Norin, T., & Driedzic, W. R. (2018). The benefit of being still: Energy savings during winter dormancy in fish come from inactivity and the cold, not from metabolic rate depression. Proceedings of the Royal Society B: Biological Sciences, 285(1886). doi:10.1098/rspb.2018.1593

Stallings, C. D., Coleman, F. C., Koenig, C. C., & Markiewicz, D. A. (2010). Energy allocation in juveniles of a warm-temperate reef fish. *Environmental Biology of Fishes*, 88(4), 389–398. doi:10.1007/s10641-010-9655-4

Stetter, M.D. (2004). Diagnostic imaging of elasmobrnachs. In: In: Smith, M., Warmolts, D., Thoney, D., & Hueter, R., (Eds.), *The elasmobranch husbandry manual: captive care of sharks, rays and their relatives.* Columbus (OH): Ohio Biological Survey. pp. 297-306.

Stevens, E.D., Fry, F.E.J. (1974). Heat transfer and body temperatures in non-thermoregulatory teleosts. *Canadian Journal of Zoology* 52: 1137–1145.

Stevens, G.C. (1989). The latitudinal gradient in geographical range: how many species coexist in the tropics. *American Naturalist 133*:240–256

Stevenson, R. D., & Woods, W. A. (2006). Condition indices for conservation: new uses for evolving tools. *Integrative and Comparative Biology*, *46*(6), 1169–1190. doi:10.1093/icb/icl052

Sulikowski, J., Wheeler, C.R., Gallagher, A., Prohaska, B., Langan, J., & Hammerschlag, N. (2016). Seasonal and life-stage variation in the reproductive ecology of a marine apex predator, the tiger shark Galeocerdo cuvier, at a protected female-dominated site. *Aquatic Biology*, *24*(3), 175–184. doi:10.3354/ab00648

Svendsen, M. B. S., Bushnell, P. G., & Steffensen, J. F. (2016). Design and setup of intermittent-flow respirometry system for aquatic organisms. Journal of Fish Biology, 88(1), 26–50. doi:10.1111/jfb.12797

Tovar-Ávila, J., Walker, T. I., & Day, R. W. (2007). Reproduction of *Heterodontus portusjacksoni* in Victoria, Australia: Evidence of two populations and reproductive parameters for the eastern population. *Marine and Freshwater Research*, *58*(10), 956–965. doi:10.1071/MF06230

Tullis, A., & Baillie, M. (2005). The metabolic and biochemical responses of tropical whitespotted bamboo shark *Chiloscyllium plagiosum* to alterations in environmental temperature. Journal of Fish Biology, 67(4), 950–968. doi:10.1111/j.0022-1112.2005.00795.x

Tunnah, L., MacKellar, S. R. C., Barnett, D. A., MacCormack, T. J., Stehfest, K. M., Morash, A. J., Semmens, J. M., & Currie, S. (2016). Physiological responses to hypersalinity correspond to nursery ground usage in two inshore shark species (*Mustelus antarcticus* and *Galeorhinus galeus*). The Journal of Experimental Biology, 219(13), 2028–2038. doi:10.1242/jeb.139964

Van Dyke, J. U., & Beaupre, S. J. (2011). Bioenergetic components of reproductive effort in viviparous snakes: Costs of vitellogenesis exceed costs of pregnancy. *Comparative Biochemistry and Physiology Part A: Molecular and Integrative Physiology*, 160(4), 504–515. doi: 10.1016/j.cbpa.2011.08.011

VanderWright WJ, Dudgeon CL, Erdmann MV, Sianipar A, Dulvy NK (2021) Extinction risk and the small population paradigm in the micro-endemic radiation of epaulette sharks. In: DellaSala DA, Goldstein, MI, eds. Imperiled: the Encyclopedia of Conservation. Elsevier Inc, pp 752-762. doi:10.1016/b978-0-12-821139-7.00130-6

Vaudo, J. J., & Heithaus, M. R. (2013). Microhabitat Selection by Marine Mesoconsumers in a Thermally Heterogeneous Habitat: Behavioral Thermoregulation or Avoiding Predation Risk? PLoS ONE, 8(4). doi:10.1371/journal.pone.0061907

Vézina, F., & Williams, T. D. (2002). Metabolic Costs of Egg Production in the European Starling (Sturnus vulgaris). *Physiological and Biochemical Zoology*, 75(4), 377–385. doi: 10.1086/343137

Vézina, F., Salvante, K. G., & Williams, T. D. (2003). The metabolic cost of avian egg formation: Possible impact of yolk precursor production? *Journal of Experimental Biology*, 206(24), 4443–4451. doi: 10.1242/jeb.00702

Vézina, F., Speakman, J. R., & Williams, Tony D. (2006). Individually Variable Energy Management Strategies in Relation to Energetic Costs of Egg Production. *Ecology,* 87(10), 2447–2458.

Viblanc, V. A., Bize, P., Criscuolo, F., Le Vaillant, M., Saraux, C., Pardonnet, S., Gineste, B., Kauffmann, M., Prud'homme, O., Handrich, Y., Massemin, S., Groscolas, R., & Robin, J.-P. (2012). Body Girth as an Alternative to Body Mass for Establishing Condition Indexes in Field Studies: A Validation in the King Penguin. *Physiological and Biochemical Zoology, 85(5),* 533–542. doi:10.1086/667540

Vilmar, M., Di Santo, V. (2022). Swimming performance of sharks and rays under climate change. *Rev Fish Biol Fisheries;* doi: 10.1007/s11160-022-09706-x

von Herbing, I.H. (2002). Effects of temperature on larval fish swimming performance: the importance of physics to physiology. *Journal of Fish Biology, 61*, 865-876.

Wallman, H.L., Bennett, W.A. (2006). Effects of parturition and feeding on thermal preference of Atlantic stingray, *Dasyatis sabina* (Lesueur). *Environmental Biology of Fishes 75*:259–267. doi:10.1007/s10641-006-0025-1

Ward-Paige, C. A., Keith, D. M., Worm, B., & Lotze, H. K. (2012). Recovery potential and conservation options for elasmobranchs. *Journal of Fish Biology*, *80*(5), 1844–1869. doi:10.1111/j.1095-8649.2012.03246.x

Weideli, O. C., Bouyoucos, I. A., Papastamatiou, Y. P., Mescam, G., Rummer, J. L., & Planes, S. (2019). Same species, different prerequisites: investigating body condition and foraging success in young reef sharks between an atoll and an island system. *Scientific Reports*, *9*(1), 1–11. doi:10.1038/s41598-019-49761-2

Wells, Z.R.R., McDonnell, L.H., Chapman, L.J., Fraser, D.J. (2016). Limited variability in upper thermal tolerance among pure and hybrid populations of a cold-water fish. *Conservation Physiology* 4, cow063; doi:10.1093/conphys/cow063

Wheeler, C. R., Gervais, C. R., Johnson, M. S., Vance, S., Rosa, R., Mandelman, J. W., & Rummer, J. L. (2020). Anthropogenic stressors influence reproduction and development in elasmobranch fishes. *Reviews in Fish Biology and Fisheries,* 0. doi:10.1007/s11160-020-09604-0

Wheeler, C. R., Lang, B. J., Mandelman, J. W., & Rummer, J. L. (2022b). The upper thermal limit of epaulette sharks (*Hemiscyllium ocellatum*) is conserved across three life history stages, sex and body size. *Conservation Physiology*, 10(1), coac074. doi:10.1093/conphys/coac074

Wheeler, C.R., Kneebone, J., Heinrich, D., Strugnell, J.M., Mandelman, J.W., Rummer, J.L. (2022a). Diel rhythm and thermal independence of metabolic rate in a

benthic shark. *Journal of Biological Rhythms* 37: 484–497. doi: 10.1177/07487304221107843

Wheeler, C.R., Rummer, J.L., Bailey, B., Lockwood, J., Vance, S., Mandelman, J.W. (2021). Future thermal regimes for epaulette sharks (*Hemiscyllium ocellatum*): growth and metabolic performance cease to be optimal. *Scientific Reports* 11, 454. doi: 10.1038/s41598-020-79953-0

White, W. T., Blaber, S. J. M., & Craig, J. F. (2012). The current status of elasmobranchs: Biology, fisheries and conservation. *Journal of Fish Biology*, *80*(5), 897–900. doi:10.1111/j.1095-8649.2012.03268.x

Whitney, N. M., Lear, K. O., Gaskins, L. C., & Gleiss, A. C. (2016). The effects of temperature and swimming speed on the metabolic rate of the nurse shark (*Ginglymostoma cirratum,* Bonaterre). Journal of Experimental Marine Biology and Ecology, 477, 40–46. doi:10.1016/j.jembe.2015.12.009

Wilder, S. M., Raubenheimer, D., & Simpson, S. J. (2016). Moving beyond body condition indices as an estimate of fitness in ecological and evolutionary studies*. Functional Ecology, 30(1),* 108–115. doi: 10.1111/1365-2435.12460

Wise, G., Mulvey, J. M., & Renshaw, G. M. C. (1998). Hypoxia tolerance in the epaulette shark (*Hemiscyllium ocellatum*). *Journal of Experimental Zoology, 281(June 1997),* 1–5. doi:10.1002/(SICI)1097-010X(19980501)281:1<1::AID-JEZ1>3.0.CO;2-S

Wood, S. (2021). Package *mgcv.* R package, version 1.8- 36. https://cran.rproject.org/web/packages/mgcv/index.html

Wood, S.N. (2011). Fast stable restricted maximum likelihood and marginal likelihood estimation of semiparametric generalized linear models. J R Stat Soc B 73:3-36.

Wosnick, N., Awruch, C. A., Adams, K. R., Gutierre, S. M. M., Bornatowski, H., Prado, A. C., & Freire, C. A. (2018). Impacts of fisheries on elasmobranch reproduction: High rates of abortion and subsequent maternal mortality in the shortnose guitarfish. *Animal Conservation*, 1–9. doi: 10.1111/acv.12458

Zhang, Y., Kieffer, J.D. (2014). Critical thermal maximum (CT_{max}) and hematology of shortnose sturgeons *(Acipenser brevirostrum)* acclimated to three temperatures. *Canadian Journal of Zoology* 92: 215-221.

Ziegeweid, J.R., Jennings, C.A., Peterson, D.L. (2008). Thermal maxima for juvenile shortnose sturgeon acclimated to different temperatures. *Environmental Biology of Fishes* 82:299-307.

Zuo, W., Moses, M. E., West, G. B., Hou, C., & Brown, J. H. (2012). A general model for effects of temperature on ectotherm ontogenetic growth and development. Proceedings of the Royal Society B: Biological Sciences, 279(1734), 1840–1846. doi:10.1098/rspb.2011.2000

APPENDIX

APPENDIX A: SUPPORTING INFORMATION FOR CHAPTER 1

Table S1.1. The rearing temperature (°C) and associated incubation days (± standard deviation if reported) for 28 species of elasmobranchs. The * symbol notes data sourced from Hoff 2008, and ** denotes a personal communication reported in Hoff 2008.

Common Name	**Temperature (°C)**	**Incubation days (± s.d.)**	**Source**
Alaska skate (*Bathyraja parmifera*)	4.4	1290	Hoff 2008
Barndoor skate (*Dipturus laevis*)	9.8	421 ± 34	Parent *et al.,* 2008
Big skate (*Raja binoculata*)	11.5	277	Hitz and Reid 1968**
Bignose fanskate (*Sympterygia acuta*)	18.0	125	Mabragaña *et al.,* 2015
Blonde skate (*Raja brachyura)*	14.1	217	Clark 1922*
Brown banded bamboo shark (*Chiloscyllium punctatum)*	23.0	153 ± 13	Harahush *et al.,* 2007
	26.0	98 ± 9	Rosa *et al.,* 2014
	30.0	79 ± 11	Rosa *et al.,* 2014
Chain catshark (*Scyliorhinus rotifer)*	12.3	256	Castro *et al.,* 1988*
Clearnose skate (*Raja eglanteria)*	9.1	368	Perkins 1965*
	20.0	85 ± 6	Luer *et al.,* 2007
	21.0	82	Luer and Gilbert 1985*
	24.0	63	Libby and Gilbert, 1960*
Cuckoo skate (*Leucoraja naevus)*	13.2	248	Clark 1922*
Dark shy shark (*Haploblepharus pictus)*	14.0	242	Pretorius and Griffiths 2013
	17.0	190	Pretorius and Griffiths 2013
Draughtboard shark (*Cephaloscyllium laticeps)*	16.5	365	Awruch *et al.,* 2009
Epaulette shark (*Hemiscyllium ocellatum)*	25.0	140.3 ± 4.6	Payne and Rufo 2012
	27.0	126 ± 4.4	Wheeler *et al.,* 2021
	29.0	110 ± 7.4	Wheeler *et al.,* 2021

Common Name	Temperature (°C)	Incubation days (± s.d.)	Source
	31.0	102.4 ± 7	Wheeler *et al.*, 2021
Leopard catshark (*Poroderma pantherinum)*	14.0	266	Pretorius and Griffiths 2013
	17.0	125	Pretorius and Griffiths 2013
Little skate (Leucoraja erinacea)	10.0	279	Steele *et al.*, 2004*
Mottled skate (Beringraja pulchra)	8.0	233	Kang *et al.*, 2013
	13.0	199	Kang *et al.*, 2013
	18.0	157	Kang *et al.*, 2013
Port Jackson shark (*Heterodontus portusjacksoni)*	20.0	315	Rodda and Seymour 2008
Small spotted catshark (*Scyliorhinus canicula)*	10.0	334	Thomason *et al.*, 1996
	13.3	165	Ellis and Shackley 1995*
	14.7	177.7	Griffiths *et al.*, 2012
	16.0	160	Ballard *et al.*, 1993*
	16.0	205	Thomason *et al.*, 1996
Small-eyed ray (*Raja microcellata)*	12.5	214.2 ± 4.4	Hume 2019
	14.5	187.3 ± 2.3	Hume 2019
	14.7	217	Clark 1922*
	16.5	166.5 ± 3.9	Hume 2019
Smallnose fanskate (*Sympterygia bonapartii)*	16.5	135 ± 10	Jañez and Sueiro 2007
Spiny rasp skate (*Okamejei kenojei)*	14.6	137	Ishihara *et al.*, 2002*
Spotted ratfish (*Hydrolagus colliei)*	12.8	300	Dean 1906*
Spotted skate (*Raja montagui)*	15.9	155	Clark 1922*
Thornback skate (*Raja clavata)*	14.3	170	Clark 1922*
	14.9	139	Ellis and Shackley 1995*
	15.4	137	Clark 1922*
Thorny skate (*Amblyraja radiata)*	4.6	912	Berestovskii 1994
	9.8	446.7 ± 46.7	Parent *et al.*, 2008

Common Name	Temperature (°C)	Incubation days (± s.d.)	Source
Undulate ray (*Raja undulata)*	15.0	171	Serra-Pereira *et al.,* 2015
White spotted bamboo shark (*Chiloscyllium plagiosum)*	25.0	126 ± 9.2	Tullis and Peterson 2000
	26.0	107 ± 9.3	Chen and Liu 2006
Winter skate (*Leucoraja ocellata)*	9.8	371.2 ± 41.9	Parent *et al.,* 2008
Yellow-nosed skate (*Dipturus chilensis)*	13.6	247 ± 13	Concha *et al.,* 2018

Table S1.2. A comparison from the current study and Hoff (2008) of the nonlinear least squares (nls) regression coefficients (± standard deviation (not reported in Hoff 2008)) between temperature and incubation days from a simple exponential identity function.

Nonlinear least squares formula: incubation days ~ a * temperature^b		
Parameters	*a (± s.d.)*	*b (± s.d.)*
Current study	9343.57 ± 1189.52	-1.44 ± 0.06
Hoff 2008	13101.45	-1.62

APPENDIX B: SUPPORTING INFORMATION FOR CHAPTER 2

Table S2.1. The mean (± standard error) water quality parameters measured throughout the study.

Salinity (ppt)	**pH**	**NH_3 (ppm)**	**Nitrites (ppm)**	**Nitrates (ppm)**
35.2 ± 0.40	8.1 ± 0.15	< 0.25	< 0.25	< 0.25

Table S2.2. Comparison of $\dot{M}O_2$ mean between experimental treatments using a linear mixed effects model (lme4) with shark ID, trial number, and sex as random effects.

A. Model selection

Model number	Model structure	Log (likelihood)	AIC	ΔAIC	df
1 (full model)	Mean $\dot{M}O_2$ ~ treatment Random= (ID, trial number, sex)	-333.70	689.40	-----	11
2	Mean $\dot{M}O_2$ ~ treatment Random= (ID, sex)	-334.18	688.36	1.03	10
3	Mean $\dot{M}O_2$ ~ treatment Random= (trial number, sex)	-342.37	704.73	-15.34	10
4	Mean $\dot{M}O_2$ ~ treatment Random= (ID, trial number)	-333.72	687.44	1.95	10
5	Mean $\dot{M}O_2$ ~ treatment Random= (ID)	-334.26	686.52	2.88	9
6	Mean $\dot{M}O_2$ ~ treatment Random= (trial number)	-344.87	707.74	-18.34	9
7	Mean $\dot{M}O_2$ ~ treatment Random= (sex)	-342.37	702.73	-13.34	9

B. Model output from the selected model 5.

df	Sum of squares	Mean squared error	F-value
6	440.18	73.36	0.41

Table S2.3. Comparison of $\dot{M}O_{2RestMin}$ between experimental treatments using a linear mixed effects model (lme4) with shark ID, trial number, and sex as random effects.

A. Model selection

Model number	Model structure	Log (likelihood)	AIC	ΔAIC	df
1 (full model)	$\dot{M}O_{2RestMin}$ ~ treatment Random= (ID, trial number, sex)	-298.35	618.70	-----	11
2	$\dot{M}O_{2RestMin}$ ~ treatment Random= (ID, sex)	-298.35	616.70	-2.00	10
3	$\dot{M}O_{2RestMin}$ ~ treatment Random= (trial number, sex)	-301.48	622.95	4.25	10
4	$\dot{M}O_{2RestMin}$ ~ treatment Random= (ID, trial number)	-298.35	616.70	-2.00	10
5	$\dot{M}O_{2RestMin}$ ~ treatment Random= (ID)	-298.35	614.70	-4.00	9
6	$\dot{M}O_{2RestMin}$ ~ treatment Random= (trial number)	-301.48	620.95	2.25	9
7	$\dot{M}O_{2RestMin}$ ~ treatment Random= (sex)	-301.48	620.95	2.25	9

B. Model output from the selected model 5.

df	Sum of squares	Mean squared error	F-value
6	480.14	80.02	0.97

Table S2.4. Comparison of $\dot{M}O_{2RestMax}$ between experimental treatments using a linear mixed effects model (lme4) with shark ID, trial number, and sex as random effects.

A. Model selection

Model number	Model structure	Log (likelihood)	AIC	ΔAIC	df
1 (full model)	$\dot{M}O_{2RestMax}$ ~ treatment Random= (ID, trial number, sex)	-385.01	792.02	-----	11
2	$\dot{M}O_{2RestMax}$ ~ treatment Random= (ID, sex)	-385.01	790.02	-2.00	10
3	$\dot{M}O_{2RestMax}$ ~ treatment Random= (trial number, sex)	-389.24	798.48	6.46	10
4	$\dot{M}O_{2RestMax}$ ~ treatment Random= (ID, trial number)	-387.32	794.63	2.62	10
5	$\dot{M}O_{2RestMax}$ ~ treatment Random= (ID)	-387.38	792.77	0.75	9
6	$\dot{M}O_{2RestMax}$ ~ treatment Random= (trial number)	-404.67	827.33	35.32	9
7	$\dot{M}O_{2RestMax}$ ~ treatment Random= (sex)	-389.24	796.48	4.46	9

B. Model output from the selected model 2.

df	Sum of squares	Mean squared error	F-value
6	4177.33	696.22	1.12

Table S2.5. Comparison of the diel scope of $\dot{M}O_2$ between experimental treatments using a linear mixed effects model (lme4) with shark ID, trial number, and sex as random effects.

A. Model selection

Model number	Model structure	Log (likelihood)	AIC	ΔAIC	df
1 (full model)	Diel scope ~ treatment Random= (ID, trial number, sex)	-378.86	779.71	-----	11
2	$\dot{M}O_{2RestMax}$ ~ treatment Random= (ID, sex)	-378.89	777.78	-1.93	10
3	Diel scope ~ treatment Random= (trial number, sex)	-383.69	787.38	7.66	10
4	Diel scope ~ treatment Random= (ID, trial number)	-381.84	783.68	3.97	10
5	Diel scope ~ treatment Random= (ID)	-381.97	781.93	2.22	9
6	Diel scope ~ treatment Random= (trial number)	-403.50	824.99	45.28	9
7	Diel scope ~ treatment Random= (sex)	-383.69	785.38	5.66	9

B. Model output from the selected model 2.

df	Sum of squares	Mean squared error	F-value
6	3793.48	632.25	1.19

Table S2.6. Routine or standard metabolic rate estimates for elasmobranchs while buccal pumping during confined respirometry trials across various temperature treatments and life stages available from the literature. For studies where values were not directly reported in the text, values were extrapolated from figures using ImageJ (Schneider *et al.,* 2012). For studies where $\dot{M}O_2$ was not reported in per kg units, values were corrected using the mean animal mass reported. When life stage was not reported it was inferred from the mean reported total length or weight. (Table from associated publication Wheeler *et al.,* 2022a).

Order	Family	Genus and Species (Common Name)	Life Stage	Temperature (°C)	Mean $\dot{M}O_2$ ± S.E.M. (mg O_2 kg^{-1} hr^{-1})	Study
Carcharhiniformes	Carcharhinidae	***Carcharhinus melanopterus*** (blacktip reef shark)	Neonate	28	147.7 ± 8.4	Bouyoucos et al. (2020b)
				31	132.9 ± 7.1	
				25	100.3 ± 8.1	Bouyoucos et al. (2022)
				28	125.5 ± 4.8	
				33	149.4 ± 8.0	
		Negaprion acutidens (sicklefin lemon shark)		25	183.2 ± 14.3	
				28	227.2 ± 8.3	
				33	260.7 ± 11.1	
		Triaenodon obesus (whitetip reef shark)	Neonate	26.2-27.9	76.4 ± 24.0	Whitney et al. (2007)
	Scyliorhinidae	***Cephaloscyllium laticeps*** (Draughtboard shark)	Adult	17.5	~ 88	Kelly et al. (2022)
		Cephaloscyllium ventriosum (Swell shark)		16	44.7 ± 4.8	Ferry-Graham and Gibb (2001)
		Scyliorhinus canicula	Juvenile	15	63.0 ± 1.5	Sims and Davies (1994)
		(Small spotted-catshark)	Adult	15	55.0 ± 1.5	
	Triakidae	***Triakis semifasciata***	Adult	12	52.4 ± 5.9	Miklos et al. (2003)
		(leopard shark)		14	61.7 ± 4.2	
				20	107.6 ± 4.2	
				24	153 ± 10.0	
		Mustelus antarcticus (gummy shark)	Juvenile	17	282.4 ± 14.5	Tunnah et al. (2016)
		Galeorhinus galeus (school shark)		17	206.3 ± 9.3	
Heterodontiformes	Heterodontidae	***Heterodontus francisci*** (horn shark)	Adult	14	30.6 ± 3.4	Luongo and Lowe (2018)
				16	33.9 ± 2.3	
				20	44.9 ± 2.4	
				22	57.9 ± 2.7	
Myliobatiformes	Urotrygonidae	***Urobatis halleri*** (round stingray)	Juvenile	15	79.8 ± 6.5	Silva-Garay and Lowe (2021)
				23	203.6 ± 16.7	
				27	378.0 ± 34.8	
		Adult		15	78.2 ± 8.2	
				23	172.3 ± 12.7	
				27	239.3 ± 32.3	

(continued)

Order	Family	Genus and Species (Common Name)	Life Stage	Temperature (°C)	Mean $\dot{M}O_2$ ± S.E.M. (mg O_2 kg^{-1} hr^{-1})	Study
	Dasyatidae	***Taeniura lymma*** (bluespotted fantail ray)	Juvenile	24.5	99.5 ± 16.6	Dabruzzi et al. (2013)
				27.5	165.0 ± 16.0	
				30.5	211.7 ± 16.7	
Orectolobiformes	Ginglymostomatidae	***Ginglymostoma cirratum*** (nurse shark)	Juvenile	23	36.0 ± 2.8	Whitney et al. (2016)
				30	60.0 ± 6.0	
	Hemiscylliidae	***Chiloscyllium plagiosum*** (whitespotted bamboo shark)	Juvenile	15	33.7 ± 3.9	Tullis and Baillie (2005)
				20	81.5 ± 7.8	
				24.5	91.2 ± 10.8	
				30	149.6 ± 19.5	
		Hemiscyllium ocellatum (epaulette shark)	Adult	25	56.0 ± 8.6	Current study
				28	61.8 ± 10.2	
				25	63.7 ± 5.2	Routley et al. (2002)
			Juveniles and subadults	28.6	65.2 ± 2.1	Heinrich et al. (2014)
			Neonate	27	47.2 ± 4.4	Wheeler et al. (2021)
				29	50.9 ± 5.5	
				31	36.8 ± 3.0	
Rajiformes	Rajidae	***Amblyraja radiata*** (thorny skate)	Adult	5	15.9 ± 3	Schwieterman et al. (2019)
				9	27.7 ± 4.8	
				13	33.6 ± 3.7	
		Leucoraja erinacea (little skate)	Adult	10	20.1 ± 2.0	Hove and Moss (1997)
		Raja eglanteria (clearnose skate)	Adult	20	38.2 ± 4.5	Schwieterman et al. (2019)
				24	46.4 ± 5.5	
				28	56.8 ± 4.5	

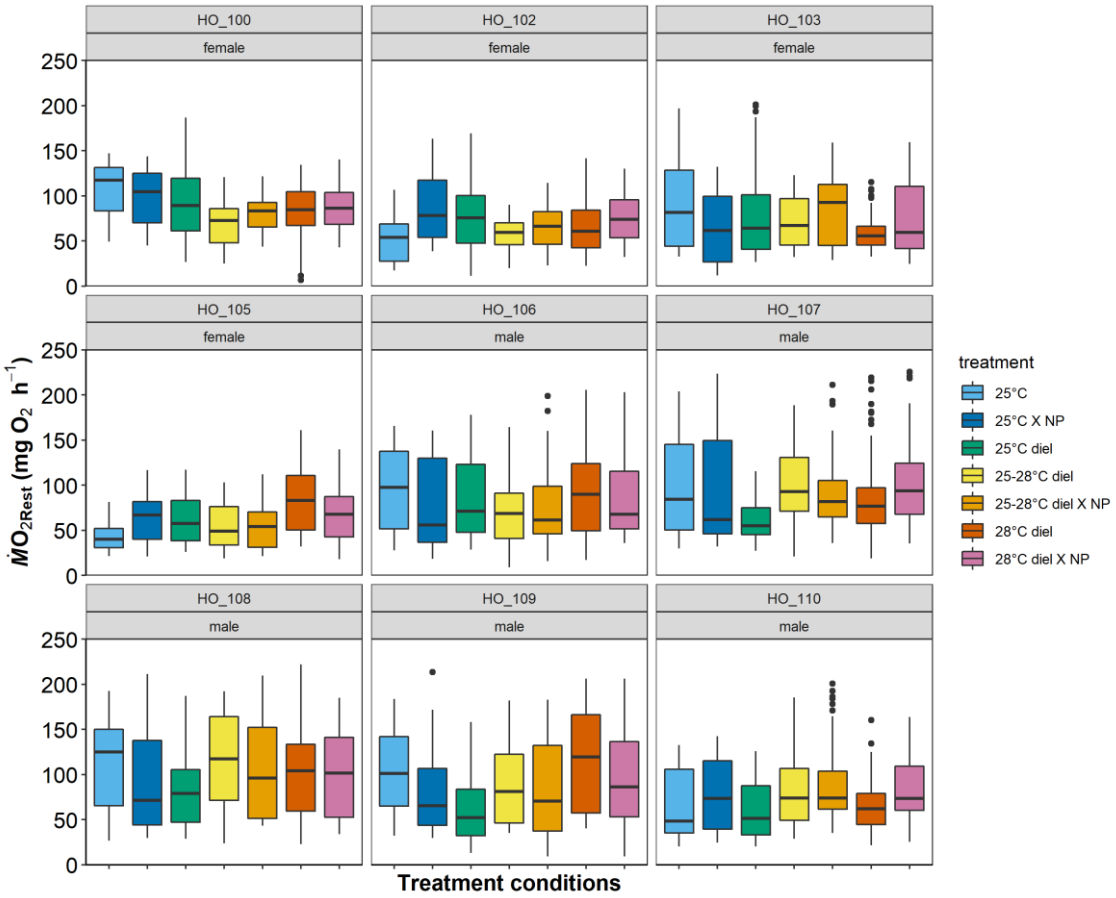

Figure S2.1. Boxplots of mean $\dot{M}O_{2Rest}$ across treatments for each shark in the study. NP represents no photoperiod. Boxplot fill colors correspond to the treatment groups in Figures 2 and 3.

APPENDIX C: SUPPORTING INFORMATION FOR CHAPTER 3

Table S3.0 The mean (± SD) water quality parameters monitored hourly (*) and weekly (**) throughout the study.

Temperature (°C)*	**Salinity (ppt)***	**pH****	**NH_3 (ppm)****	**Nitrites (ppm)****	**Nitrates (ppm) ****
24.9 ± 0.28	35.2 ± 0.40	8.1 ±0.15	< 0.25	< 0.25	< 0.25

Table S3.1. Figure 3.1 linear mixed effect modelling:

A. The log-log length-weight linear mixed effects models (lmer from lme4).

Model number	Model structure	Log(likelihood)	AIC	df
1	Log(mass) ~ log(length) + sex + location + (1|ID)	353.3113	-694.623	6
2	Log(mass) ~ log(length) + sex + (1|ID)	348.3358	-686.672	5
3	Log(mass) ~ log(length) + location + (1|ID)	352.8984	-695.797	5
4	Log(mass) ~ log(length) + (1|ID)	347.1954	-686.391	4

B. Predicted versus fitted residual plot and qqplot for model 4.

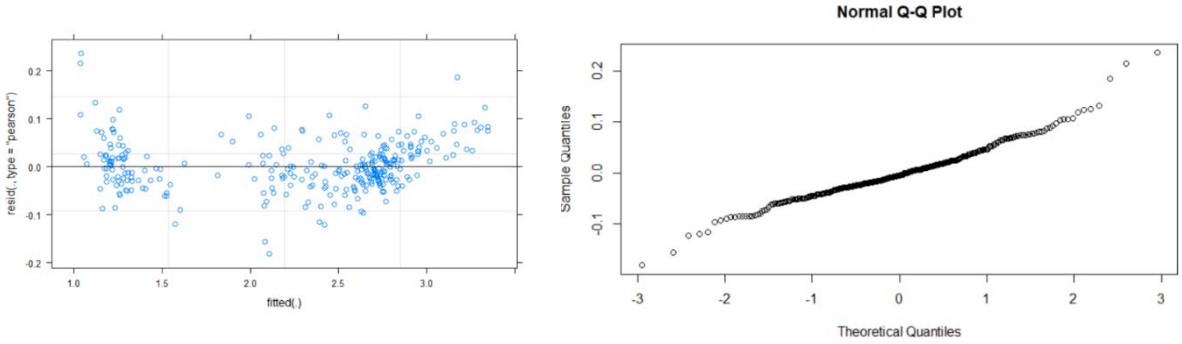

C. Model output from the selected model 4.

Random effect	Variance	Std.Dev.
ID	0.002916	0.05400
Residual	0.004169	0.06456

Fixed effects	Estimate	Std. Error	df	t value	Pr(>|t|)
Intercept	-2.21629	0.04025	192.52984	-55.07	0.0000
log10(length)	2.78156	0.02393	202.64897	116.22	0.0000

Table S3.2. Figure 3.2 linear models of body proportions via log-ratio regression:

A. Body proportion model: lm(cbind(log(head/tail), log(trunk/tail)) ~ life history stage)

i. Predicted versus fitted residual plot and qqplot for tail proportion over life history stages model.

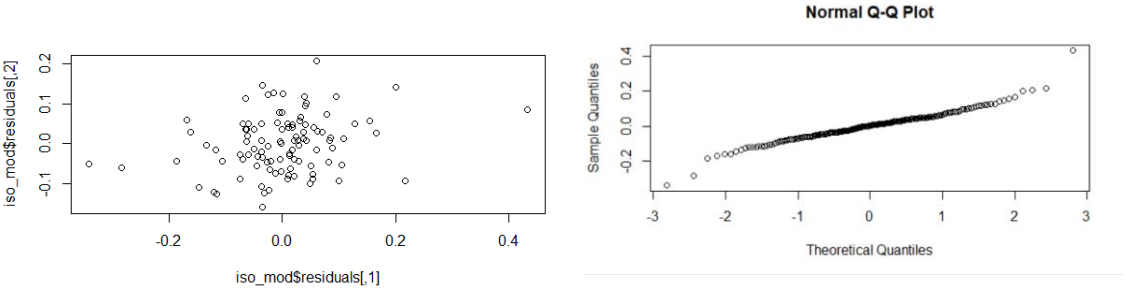

ii. Coefficients of the body proportion model:

Term	estimate	std.error	statistic	p.value
(Intercept)	-1.44269	0.01420	-101.588	< 2e-16
Juvenile	-0.13371	0.02125	-6.293	9.26e-09
Subadult	-0.13656	0.02073	-6.588	2.38e-09
Mature female	-0.07530	0.02400	-3.137	0.00227
Mature male	-0.10655	0.02259	-4.718	8.10e-06

iii. Post-hoc pairwise comparison from *emmeans* package:

Contrast	estimate	std.error	df	t.ratio	adj.p.value
Neonate - Subadult	0.1645	0.0194	96	8.4835	0.0000
Neonate - Juvenile	0.1591	0.0199	96	8.0070	0.0000
Neonate - Mature male	0.1299	0.0211	96	6.1484	0.0000
Neonate - Mature female	0.1091	0.0225	96	4.8580	0.0000
Subadult - Mature female	-0.0554	0.0230	96	-2.4131	0.1206
Juvenile - Mature female	-0.0500	0.0234	96	-2.1413	0.2114
Subadult - Mature male	-0.0346	0.0217	96	-1.5966	0.5032
Juvenile - Mature male	-0.0292	0.0221	96	-1.3226	0.6779
Mature female - Mature male	0.0208	0.0244	96	0.8515	0.9136
Juvenile - Subadult	0.0054	0.0204	96	0.2624	0.9989

Table S3.3. Figure 3.3 linear mixed effects models of girths across life history and female reproductive stages:

A. **Pectoral girth model:** lmer ((pectoral girth/TL) ~ reproductive status + (1|ID))

   i. Predicted versus fitted residual plot and qqplot for pectoral girth over life history stages model.

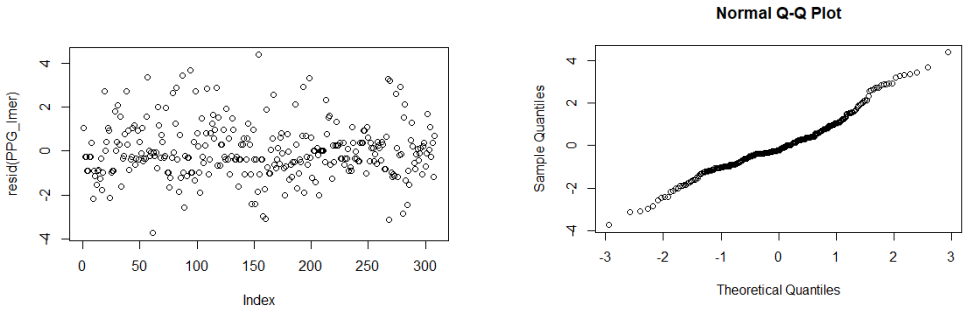

   ii. Random and fixed effects from the pectoral girth model:

Random effects	Variance	Std. Dev.
ID (Intercept)	5.351	2.313
Residual	1.741	1.319

Fixed Effects	Estimate	Std. Error	df	t value	Pr(>|t|)
Intercept	29.834	0.522	40.783	57.127	0.000
Juvenile	-7.205	1.196	29.039	-6.025	0.000
Resting	-3.938	1.095	27.606	-3.595	0.001
Follicular	-0.738	1.095	27.551	-0.674	0.506
Encapsulating	0.642	1.097	27.772	0.585	0.563
Post-oviposition	-1.390	1.121	30.276	-1.241	0.224
Mature male	-4.059	1.208	30.254	-3.361	0.002

   iii. Post-hoc pairwise comparison from emmeans package:

Contrast	estimate	std.error	df	statistic	adj.p.value
Resting - Encapsulating	-4.5806	0.2851	272.4909	-16.0693	0.0000
Resting - Follicular	-3.2000	0.2772	272.8941	-11.5451	0.0000
Resting - Post-oviposition	-2.5477	0.3652	270.1959	-6.9756	0.0000

Follicular - Encapsulating	-1.3805	0.2086	266.5260	-6.6179	0.0000
Encapsulating - Post-oviposition	2.0328	0.3163	266.4810	6.4266	0.0000
Neonate - Juvenile	7.2050	1.1958	32.3061	6.0254	0.0000
Juvenile - Encapsulating	-7.8475	1.4452	29.0972	-5.4299	0.0001
Juvenile - Follicular	-6.4670	1.4436	28.9648	-4.4797	0.0019
Juvenile - Post-oviposition	-5.8147	1.4631	30.5835	-3.9742	0.0066
Neonate - Resting	3.9381	1.0955	30.7299	3.5948	0.0173
Neonate - Mature male	4.0595	1.2078	33.6415	3.3609	0.0290
Encapsulating - Mature male	4.7020	1.4552	29.9228	3.2311	0.0422
Follicular - Mature male	3.3214	1.4536	29.7886	2.2849	0.2841
Juvenile - Resting	-3.2670	1.4438	28.9971	-2.2628	0.2953
Follicular - Post-oviposition	0.6523	0.3077	266.4630	2.1200	0.3439
Juvenile - Mature male	-3.1456	1.5308	30.8205	-2.0549	0.4030
Post-oviposition - Mature male	2.6691	1.4730	31.4279	1.8120	0.5502
Neonate - Post-oviposition	1.3904	1.1208	33.6656	1.2405	0.8731
Neonate - Follicular	0.7381	1.0953	30.6699	0.6739	0.9931
Neonate - Encapsulating	-0.6425	1.0974	30.9131	-0.5854	0.9968
Resting - Mature male	0.1214	1.4538	29.8215	0.0835	1.0000

B. **Pelvic girth model**: lmer ((pelvic girth/TL) ~ reproductive status + (1|ID))

i. Predicted versus fitted residual plot and qqplot for pelvic girth over life history stages model.

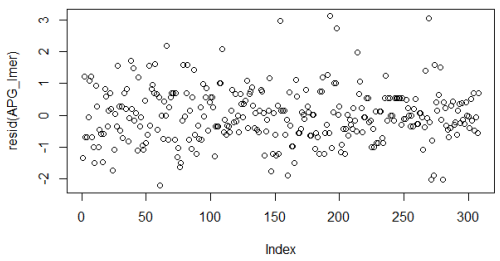

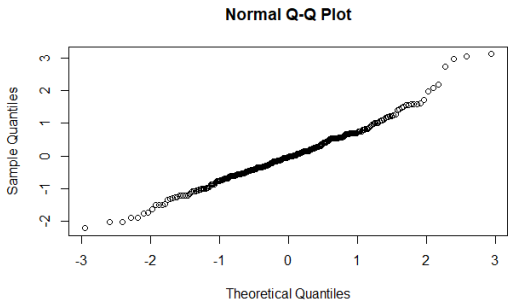

ii. Random and fixed effects from pelvic girth model:

Random effects	Variance	Std. Dev.
ID (Intercept)	5.0733	2.2524
Residual	0.8253	0.9085

Fixed Effects	Estimate	Std. Error	df	t value	Pr(>|t|)
Intercept	25.2013	0.4763	38.9966	52.9096	0.0000
Juvenile	-3.8809	1.1326	32.3834	-3.4265	0.0017
Resting	-0.5892	1.0437	31.5444	-0.5645	0.5764
Follicular	1.6300	1.0436	31.5275	1.5618	0.1283
Encapsulating	2.3685	1.0447	31.6582	2.2672	0.0303
Post-oviposition	1.4532	1.0564	33.1246	1.3756	0.1782
Mature male	-0.2431	1.1387	33.0912	-0.2135	0.8322

iii. Post-hoc pairwise comparison from *emmeans* package:

Contrast	estimate	std.error	df	statistic	adj.p.value
Resting - Encapsulating	-2.2192	0.1913	269.2226	-11.6031	0.0000
Resting - Follicular	-2.9577	0.1967	269.0269	-15.0395	0.0000
Resting - Post-oviposition	-2.0424	0.2518	267.9175	-8.1116	0.0000
Follicular - Encapsulating	-0.7386	0.1436	266.1612	-5.1416	0.0000
Encapsulating - Post-oviposition	0.9153	0.2178	266.1405	4.2024	0.0007
Juvenile - Encapsulating	-6.2494	1.3858	32.6921	-4.5096	0.0014
Juvenile - Follicular	-5.5109	1.3850	32.6158	-3.9789	0.0060
Juvenile - Post-oviposition	-5.3341	1.3947	33.5437	-3.8246	0.0088
Neonate - Juvenile	3.8809	1.1326	34.5072	3.4265	0.0242
Juvenile - Mature male	-3.6378	1.4579	33.6670	-2.4951	0.1933
Juvenile - Resting	-3.2917	1.3851	32.6256	-2.3766	0.2406
Neonate - Encapsulating	-2.3685	1.0447	33.7403	-2.2672	0.2889
Encapsulating - Mature male	2.6117	1.3908	33.1663	1.8779	0.5082
Neonate - Follicular	-1.6300	1.0437	33.6021	-1.5618	0.7064

Follicular - Mature male	-1.4532	1.0564	35.2906	-1.3756	0.8107
Post-oviposition - Mature male	1.8731	1.3900	33.0895	1.3476	0.8245
Neonate - Post-oviposition	1.6964	1.3996	34.0233	1.2120	0.8846
Follicular - Post-oviposition	0.1767	0.2119	266.1322	0.8343	0.9812
Neonate - Resting	0.5892	1.0437	33.6200	0.5645	0.9974
Neonate - Mature male	-0.3461	1.3900	33.0994	-0.2490	1.0000
Resting - Mature male	0.2431	1.1387	35.2553	0.2135	1.0000

C. **First dorsal fin girth model**: lmer((first dorsal fin girth/TL) ~ reproductive status + (1|ID))

i. Predicted versus fitted residual plot and qqplot for first dorsal fin girth over life history stages model.

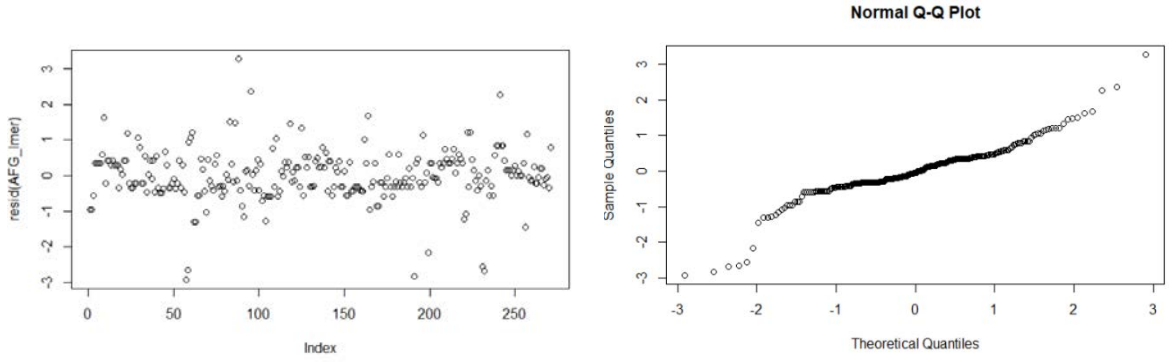

ii. Random and fixed effects from first dorsal fin girth model:

Random effects	**Variance**	**Std. Dev.**
ID (Intercept)	2.7337	1.6534
Residual	0.6647	0.8153

Fixed Effects	**Estimate**	**Std. Error**	**df**	**t value**	**Pr(>|t|)**
Intercept	21.4511	0.3615	40.6441	59.3339	0.0000
Juvenile	-2.3900	0.8430	31.1923	-2.8351	0.0080
Resting	-1.7821	0.7745	30.0159	-2.3008	0.0285
Follicular	-0.5796	0.7744	29.9750	-0.7485	0.4600
Encapsulating	-0.4591	0.7756	30.1639	-0.5920	0.5583

Post-oviposition	-0.7091	0.7883	32.2198	-0.8996	0.3750
Mature male	-0.6709	0.8496	32.1872	-0.7898	0.4354

iii. Post-hoc pairwise comparison from emmeans package:

Contrast	estimate	std.error	df	statistic	adj.p.value
Resting - Encapsulating	-1.3230	0.1763	271.7170	-7.5034	0.0000
Resting - Follicular	-1.2025	0.1713	272.0277	-7.0207	0.0000
Resting - Post-oviposition	-1.0730	0.2258	270.0201	-4.7513	0.0000
Neonate - Juvenile	2.3900	0.8430	33.2943	2.8351	0.0077
Neonate - Resting	1.7821	0.7746	32.0479	2.3008	0.0281
Juvenile - Encapsulating	-1.9309	1.0251	30.7505	-1.8836	0.0691
Juvenile - Follicular	-1.8104	1.0242	30.6407	-1.7676	0.0871
Juvenile - Post-oviposition	-1.6809	1.0347	31.9363	-1.6245	0.1141
Juvenile - Mature male	-1.7191	1.0821	32.1167	-1.5886	0.1219
Encapsulating - Post-oviposition	0.2500	0.1955	267.2890	1.2790	0.2020
Resting - Mature male	-1.1112	1.0297	31.3230	-1.0791	0.2888
Follicular - Encapsulating	-0.1205	0.1287	267.3251	-0.9363	0.3500
Neonate - Post-oviposition	0.7091	0.7883	34.3824	0.8996	0.3746
Neonate - Mature male	0.6709	0.8496	34.3479	0.7898	0.4351
Neonate - Follicular	0.5796	0.7744	32.0046	0.7485	0.4596
Follicular - Post-oviposition	0.1295	0.1899	267.2762	0.6819	0.4959
Neonate - Encapsulating	-0.6079	1.0243	30.6642	-0.5935	0.5572
Juvenile - Resting	0.4591	0.7756	32.2048	0.5920	0.5580
Encapsulating - Mature male	0.2118	1.0305	31.4100	0.2055	0.8385
Follicular - Mature male	0.0913	1.0296	31.2992	0.0887	0.9299
Post-oviposition - Mature male	-0.0382	1.0401	32.6072	-0.0367	0.9709

D. **Second dorsal fin girth model:** lmer(second dorsal fin girth/TL ~ reproductive status + (1|ID))

i. Predicted versus fitted residual plot and qqplot for second dorsal fin girth over life history stages model.

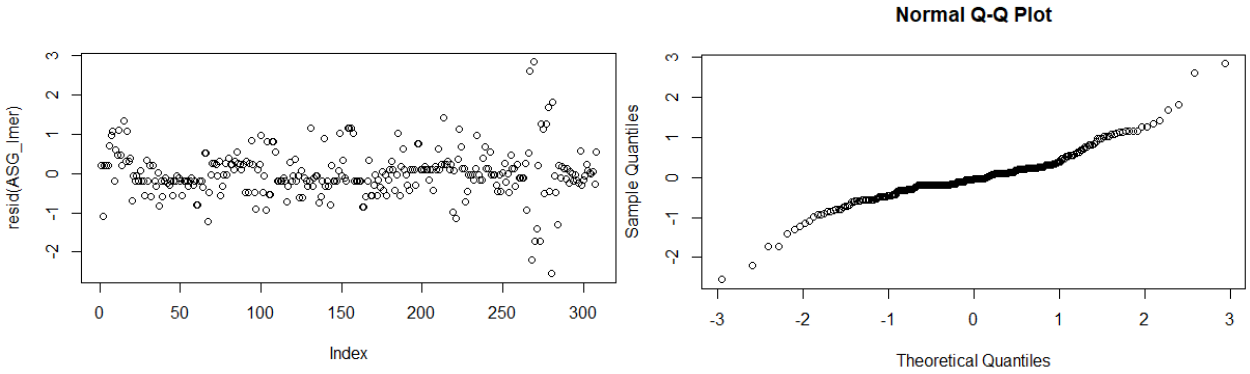

ii. Random and fixed effects for ASG model:

Random effects	Variance	Std. Dev.
ID (Intercept)	4.0455	2.0113
Residual	0.4013	0.6335

Fixed Effects	Estimate	Std. Error	df	t value	Pr(>|t|)
Intercept	18.9571	0.4136	38.3890	45.8389	0.0000
Resting	-3.4698	0.9239	33.5809	-3.7558	0.0007
Follicular	-2.8638	1.0034	34.5914	-2.8540	0.0072
Encapsulating	-2.5202	0.9309	34.6198	-2.7073	0.0105
Post-oviposition	-2.4556	0.9238	33.5707	-2.6581	0.0119
Mature male	-2.4423	0.9244	33.6597	-2.6420	0.0124

iii. Post-hoc pairwise comparison from emmeans package:

Contrast	estimate	std.error	df	statistic	adj.p.value
Resting - Follicular	-1.0142	0.1333	267.9014	-7.6060	0.0000

Resting - Encapsulating	-1.0275	0.1373	267.7796	-7.4865	0.0000
Resting - Post-oviposition	-0.9496	0.1757	267.1162	-5.4057	0.0000
Neonate - Resting	3.4698	0.9239	35.1084	3.7558	0.0006
Neonate - Mature male	2.8638	1.0034	36.1587	2.8540	0.0071
Neonate - Post-oviposition	2.5202	0.9309	36.1882	2.7073	0.0103
Neonate - Follicular	2.4556	0.9238	35.0978	2.6581	0.0118
Neonate - Encapsulating	2.4423	0.9244	35.1903	2.6420	0.0122
Neonate - Juvenile	2.4446	1.0001	35.6781	2.4444	0.0196
Juvenile - Resting	1.0252	1.2295	34.4628	0.8339	0.4101
Encapsulating - Post-oviposition	0.0779	0.1519	266.0568	0.5131	0.6083
Resting - Mature male	-0.6060	1.2322	34.7703	-0.4918	0.6259
Follicular - Post-oviposition	0.0646	0.1476	266.0520	0.4379	0.6618
Encapsulating - Mature male	0.4215	1.2326	34.8159	0.3420	0.7344
Follicular - Mature male	0.4082	1.2322	34.7644	0.3313	0.7424
Juvenile - Mature male	0.4192	1.2904	35.1362	0.3249	0.7472
Post-oviposition - Mature male	0.3436	1.2375	35.3701	0.2776	0.7829
Follicular - Encapsulating	-0.0133	0.1000	266.0704	-0.1331	0.8942
Juvenile - Post-oviposition	0.0756	1.2348	35.0602	0.0612	0.9515
Juvenile - Follicular	0.0110	1.2295	34.4569	0.0089	0.9929
Juvenile - Encapsulating	-0.0023	1.2299	34.5082	-0.0019	0.9985

E. **Girth condition analysis (GCA/A_{gc}) model:** lmer (A_{gc} ~ reproductive status + (1|ID))

i. Predicted versus fitted residual plot and qqplot for A_{gc} over life history stages model.

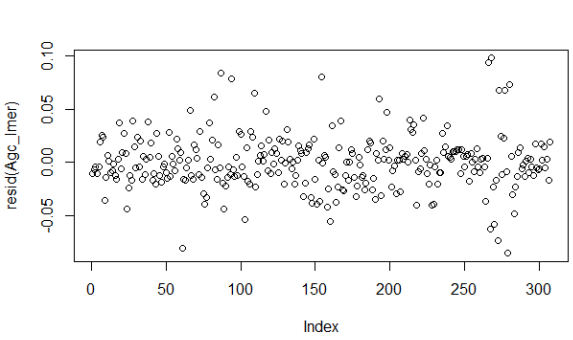

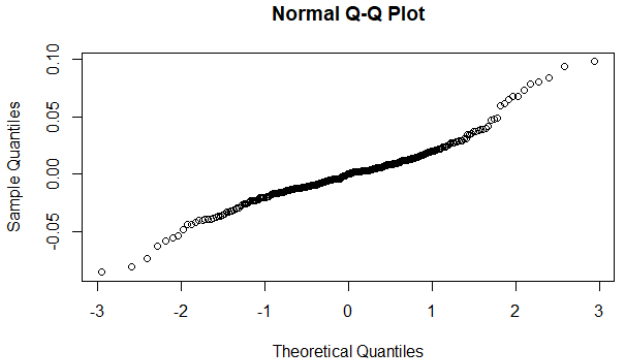

ii. Random and fixed effects for A_{gc} model:

Random effects	**Variance**	**Std. Dev.**
ID (Intercept)	0.005538	0.07442
Residual	0.000743	0.02726

Fixed Effects	**Estimate**	**Std. Error**	**df**	**t value**	**Pr(>|t|)**
Intercept	0.9544	0.0155	38.9702	61.4063	0.0000
Juvenile	-0.1592	0.0372	33.3514	-4.2758	0.0002
Resting	-0.0977	0.0343	32.6350	-2.8445	0.0076
Follicular	-0.0213	0.0343	32.6227	-0.6204	0.5393
Encapsulating	0.0012	0.0344	32.7348	0.0362	0.9713
Post-oviposition	-0.0315	0.0347	33.9900	-0.9073	0.3706
Mature male	-0.0784	0.0374	33.9566	-2.0956	0.0437

iii. Post-hoc pairwise comparison from *emmeans* package:

Contrast	**estimate**	**std.error**	**df**	**statistic**	**adj.p.value**
Resting - Encapsulating	-0.0989	0.0059	267.4488	-16.7617	0.0000
Resting - Post-oviposition	-0.0764	0.0057	267.6084	-13.3064	0.0000
Resting - Follicular	-0.0662	0.0076	266.5447	-8.7630	0.0000
Follicular - Encapsulating	-0.0226	0.0043	265.1156	-5.2330	0.0000

Encapsulating - Post-oviposition	0.0327	0.0065	265.0988	5.0076	0.0000
Neonate - Juvenile	0.1592	0.0372	35.0066	4.2758	0.0024
Juvenile - Encapsulating	-0.1605	0.0457	33.4732	-3.5139	0.0198
Juvenile - Follicular	-0.1379	0.0456	33.4086	-3.0214	0.0649
Neonate - Resting	0.0977	0.0343	34.2592	2.8445	0.0951
Juvenile - Post-oviposition	-0.1277	0.0459	34.1948	-2.7824	0.1087
Neonate - Mature male	0.0784	0.0374	35.6378	2.0956	0.3770
Encapsulating - Mature male	0.0796	0.0458	33.8752	1.7385	0.5962
Juvenile - Mature male	-0.0808	0.0480	34.2963	-1.6848	0.6303
Follicular - Post-oviposition	0.0102	0.0064	265.0921	1.6001	0.6824
Juvenile - Resting	-0.0615	0.0456	33.4156	-1.3475	0.8246
Follicular - Mature male	0.0571	0.0458	33.8102	1.2466	0.8706
Post-oviposition - Mature male	0.0469	0.0460	34.6005	1.0185	0.9462
Neonate - Post-oviposition	0.0315	0.0347	35.6727	0.9073	0.9690
Neonate - Follicular	0.0213	0.0343	34.2464	0.6204	0.9957
Resting - Mature male	-0.0193	0.0458	33.8173	-0.4223	0.9995
Neonate - Encapsulating	-0.0012	0.0344	34.3633	-0.0362	1.0000

Table S3.4. Figure 5 generalized linear mixed effects model of condition metrics across life history stages: lmer(A_{gc} ~K_n*life history stage + (1|ID))

i. Predicted versus fitted residual plot and qqplot for K_n vs A_{gc} model

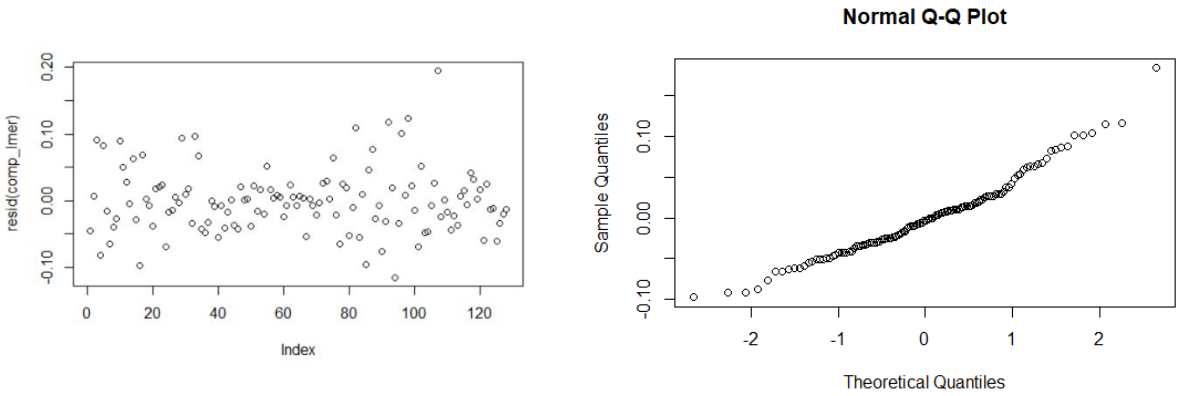

ii. Random and fixed effects for condition metric comparison model:

Random effects	Variance	Std. Dev.
ID (Intercept)	0.0003376	0.01837
Residual	0.0025870	0.05086

Fixed Effects	Estimate	Std. Error	df	t value	Pr(>|t|)
Intercept	0.7104	0.0490	127.2405	14.5099	0.0000
K_n	0.3539	0.0693	127.2405	5.1065	0.0000
Juvenile	0.0159	0.0647	127.3745	0.2455	0.8064
Subadult	-0.0616	0.0957	127.2444	-0.6440	0.5208
Mature female	-0.2012	0.1222	127.2488	-1.6472	0.1020
Mature male	-0.2637	0.0923	127.2405	-2.8567	0.0050
K_n:Juvenile	-0.2379	0.0980	127.9146	-2.4279	0.0166
K_n:Subadult	-0.1098	0.1469	127.2548	-0.7475	0.4561
K_n:Mature female	0.0897	0.1859	127.2642	0.4827	0.6301
K_n:Mature male	0.2038	0.1393	127.2405	1.4626	0.1461

iii. ANOVA:

Fixed Effects	Sum Sq	Mean Sq	NumDF	DenDF	F value	Pr(>F)
K_n	0.1076	0.1076	1	127.4473	41.5914	0.0000
Life history stage	0.0329	0.0082	4	127.2910	3.1783	0.0158
K_n: Life history stage	0.0336	0.0084	4	127.3831	3.2441	0.0143

iv. Slopes at each life history stage from *emmeans* package (*emtrends*):

Life history stage	Slope	SE	df	lower.CL	upper.CL
Neonate	0.3539	0.0722	136.5624	0.2111	0.4967
Juvenile	0.1160	0.0744	133.1432	-0.0312	0.2633
Subadult	0.2441	0.1350	136.6148	-0.0228	0.5111
Mature female	0.4436	0.1798	136.6403	0.0881	0.7992
Mature male	0.5576	0.1260	136.5624	0.3086	0.8067

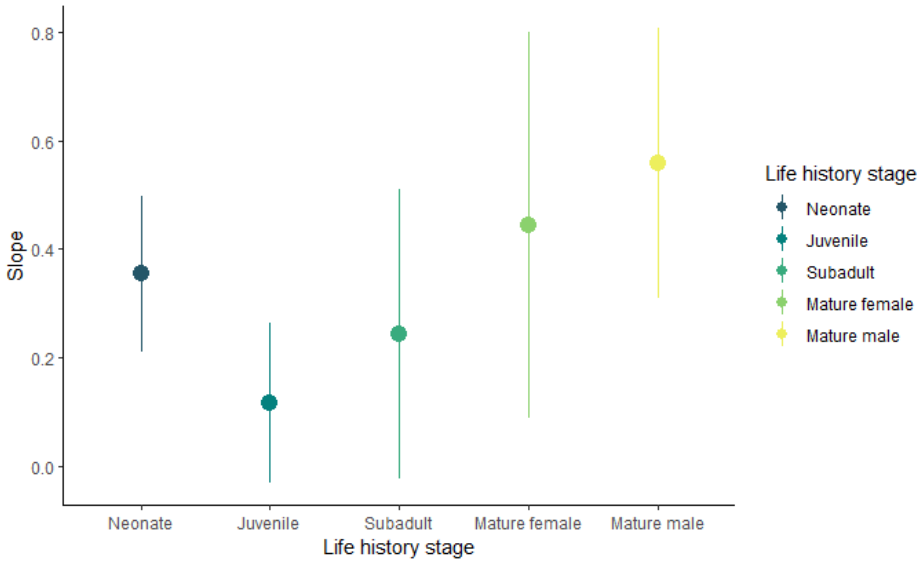

Figure S3.1. The estimated slope (± 95% CL) for each life history stage. Only juveniles and adult males have differing slopes.

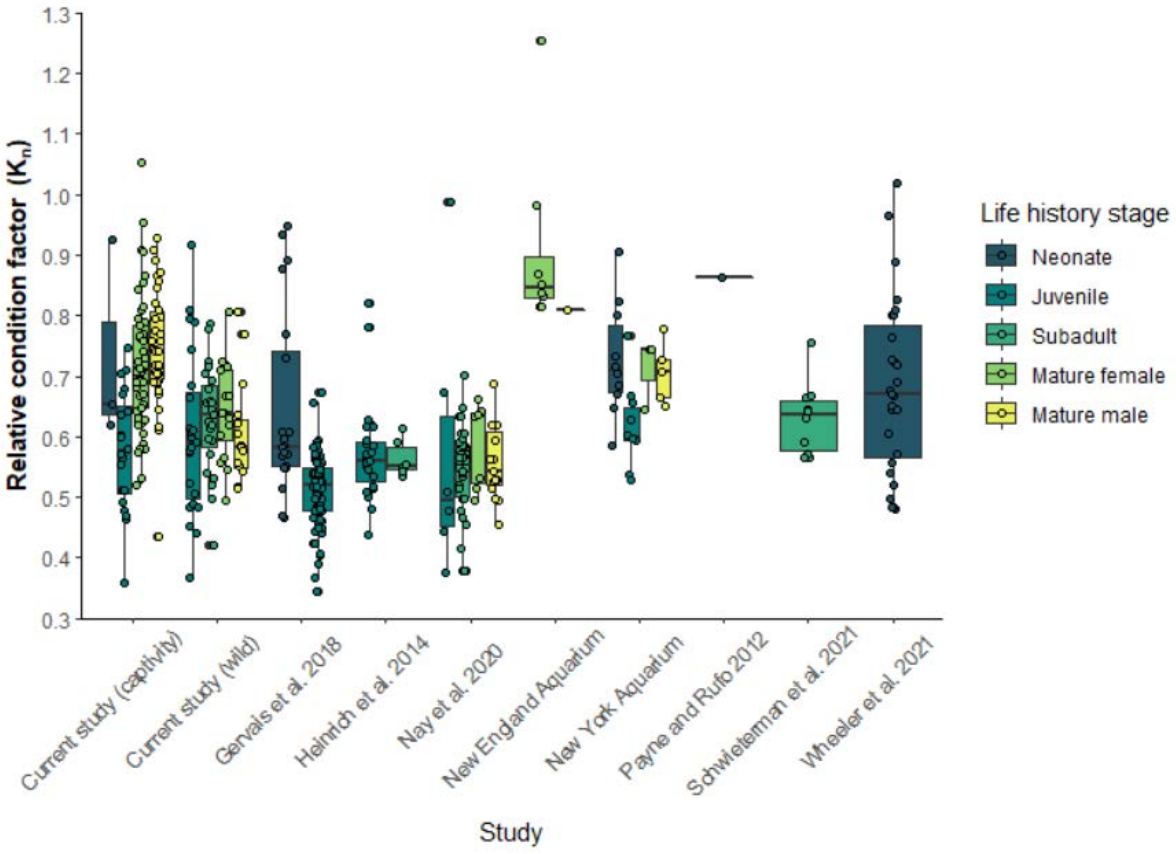

Figure S3.2. Relative body condition (K_n) across life history stages and data sources.

Table S4.1. The mean (± s.d.) water quality parameters monitored hourly (*) and weekly (**) throughout the study.

Temperature (°C)*	**Salinity (ppt)***	**pH****	**NH_3 (ppm)****	**Nitrites (ppm)****	**Nitrates (ppm) ****
24.9 ± 0.28	35.2 ± 0.40	8.1 ±0.15	< 0.25	< 0.25	< 0.25

Table S4.2. $\dot{M}O_2$ across mass:

A. aov(log($\dot{M}O_2$) ~ log(mass) + reproductive status + ID)

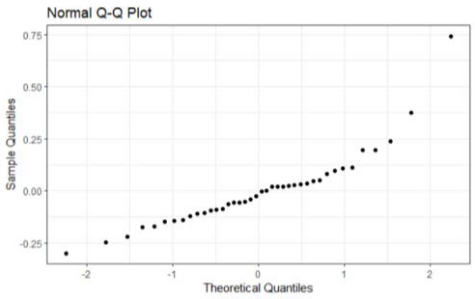

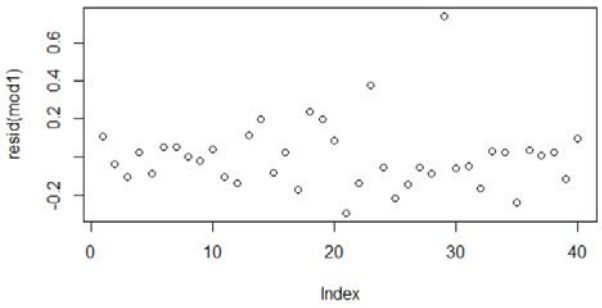

B. ANCOVA Table

Variable	Sum Sq	df	F value	Pr(>F)
Mass	0.247294	1	6.142568	0.018659
Status	0.040133	2	0.498433	0.61212
ID	1.860861	4	11.55553	6.43E-06
Residuals	1.288291	32	NA	NA

C. Estimated marginal means

Status	emmean	SE	df	lower.CL	upper.CL
Pre-encapsulating	3.985396	0.05827	32	3.866704	4.104087
Encapsulating	3.91946	0.053167	32	3.811161	4.027758
Post-oviposition	3.990731	0.073084	32	3.841865	4.139598

Table S4.3. Testosterone (T) across the female reproductive cycle

A. aov(log(T) ~ reproductive status + ID)

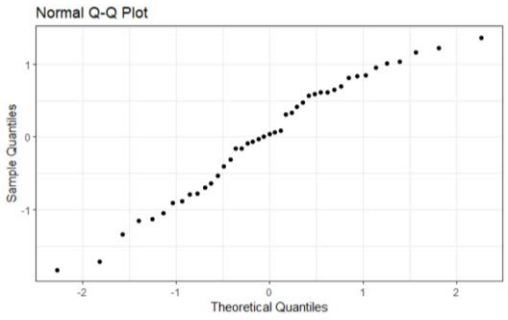

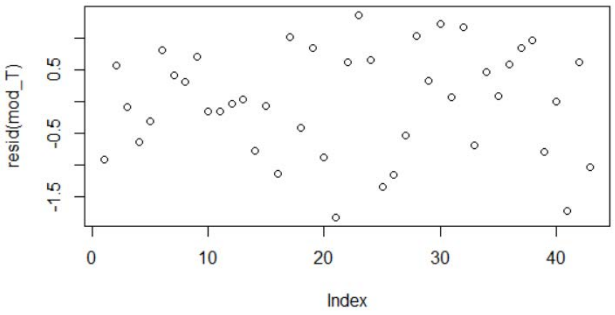

B. ANCOVA Table

Variable	Sum Sq	df	F value	Pr(>F)
Status	11.31359	2	7.080759	0.002551
ID	6.171025	4	1.931108	0.12635
Residuals	28.76028	36	NA	NA

C. Estimated marginal means

Status	emmean	SE	df	lower.CL	upper.CL
Pre-encapsulating	6.987453	0.242342	36	6.495959	7.478946
Encapsulating	5.800671	0.223294	36	5.347811	6.253532
Post-oviposition	6.675869	0.31054	36	6.046065	7.305674

D. Post-hoc comparison

Contrast	Estimate	SE	df	t.ratio	p.value
(Pre-encapsulating) - Encapsulating	1.186782	0.323382	36	3.669908	0.0022
(Pre-encapsulating) - (Post-oviposition)	0.311583	0.385809	36	0.807612	0.700785
Encapsulating - (Post-oviposition)	-0.8752	0.383766	36	-2.28055	0.071542

Table S4.4. Estradiol (E_2) across the female reproductive cycle

A. aov(log(E_2) ~ reproductive status + ID)

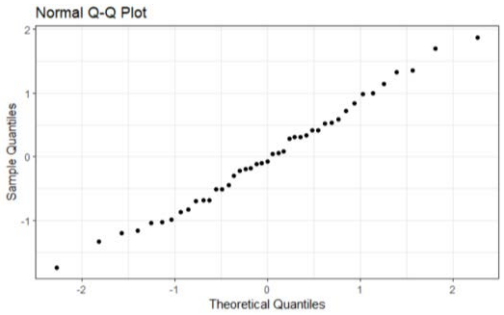

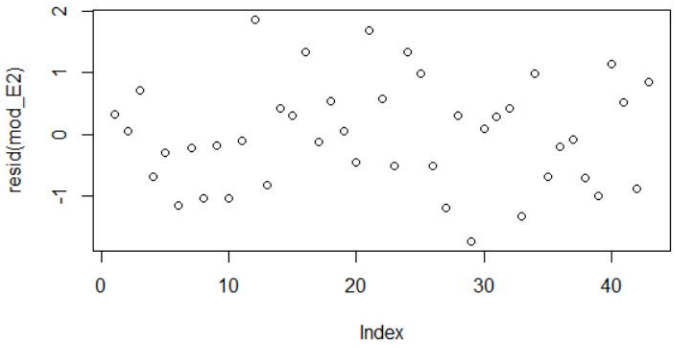

B. ANCOVA Table

Variable	Sum Sq	df	F value	Pr(>F)
Status	0.904292	2	0.532992	0.591406
ID	0.493193	4	0.145345	0.963892
Residuals	30.5394	36	NA	NA

C. Estimated marginal means

Status	emmean	SE	df	lower.CL	upper.CL
Pre-encapsulating	6.527483	0.249726	36	6.021016	7.03395
Encapsulating	6.185949	0.230097	36	5.719291	6.652606
Post-oviposition	6.399012	0.320001	36	5.750019	7.048004

Table S4.5. Progesterone (P_4) across the female reproductive cycle

A. aov(log(P_4) ~ reproductive status + ID)

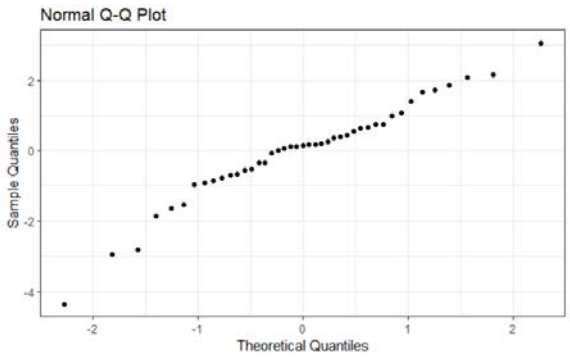

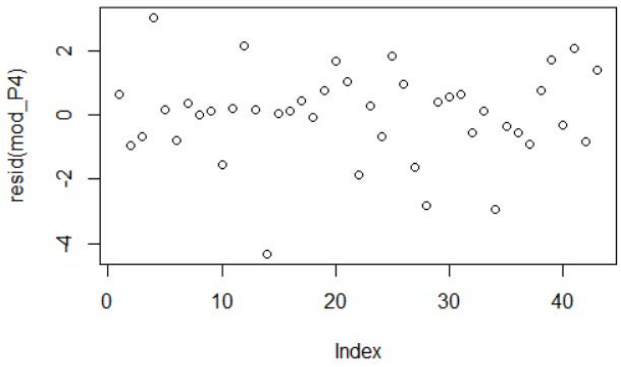

B. ANCOVA Table

Variable	Sum Sq	df	F value	Pr(>F)
Status	13.13154	2	2.850299	0.070939
ID	8.310589	4	0.901937	0.47308
Residuals	82.92738	36	NA	NA

C. Estimated marginal means

Status	emmean	SE	df	lower.CL	upper.CL
Pre-encapsulating	5.85005	0.411511	36	5.015467	6.684634
Encapsulating	6.058091	0.379165	36	5.289108	6.827074
Post-oviposition	7.353287	0.527315	36	6.283842	8.422731

Table S4.6. Hct across the female reproductive cycle

A. aov(log(hct) ~ reproductive status + ID)

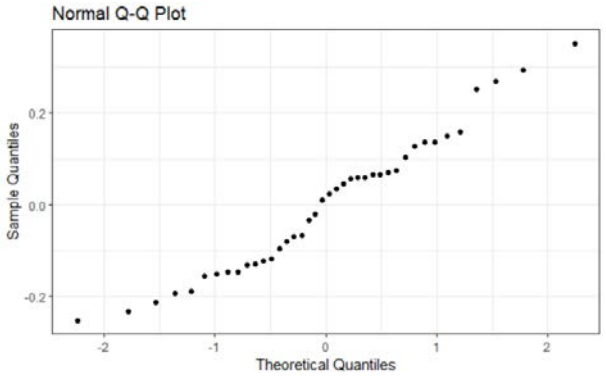

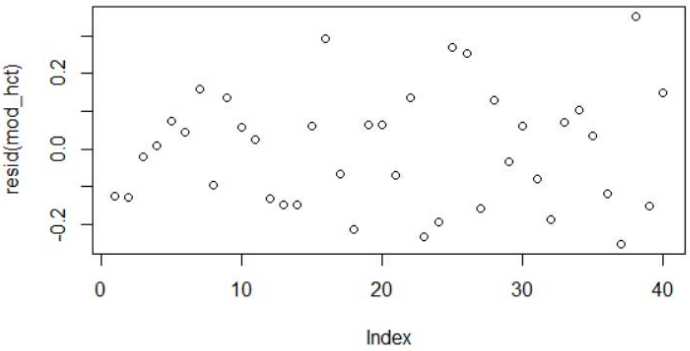

B. ANCOVA Table

Variable	Sum Sq	df	F value	Pr(>F)
Status	0.028451	2	0.516587	0.601297
ID	0.795315	4	7.220301	2.72E-04
Residuals	0.908736	33	NA	NA

C. Estimated marginal means

Status	emmean	SE	df	lower.CL	upper.CL
Pre-encapsulating	2.666355	0.04327	33	2.578321	2.75439
Encapsulating	2.670282	0.059668	33	2.548885	2.791678
Post-oviposition	2.611347	0.045029	33	2.519736	2.702958

Table S4.7. Hb across the female reproductive cycle

A. aov(log(hb) ~ reproductive status + ID)

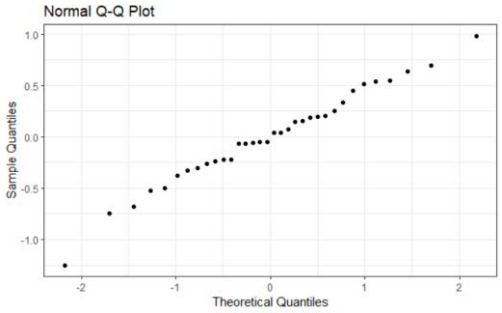

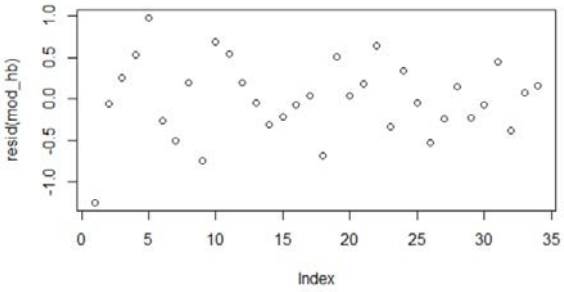

D. ANCOVA Table

Variable	Sum Sq	df	F value	Pr(>F)
Status	0.276393	2	0.537493	0.590333
ID	0.131469	4	0.127832	0.971028
Residuals	6.942062	27	NA	NA

E. Estimated marginal means

Status	emmean	SE	df	lower.CL	upper.CL
Pre-encapsulating	3.580669	0.140706	27	3.291964	3.869373
Encapsulating	3.471021	0.216311	27	3.027187	3.914855
Post-oviposition	3.719474	0.141931	27	3.428255	4.010693

Table S4.8. MCHC across the female reproductive cycle

B. aov(log(MCHC) ~ reproductive status + ID)

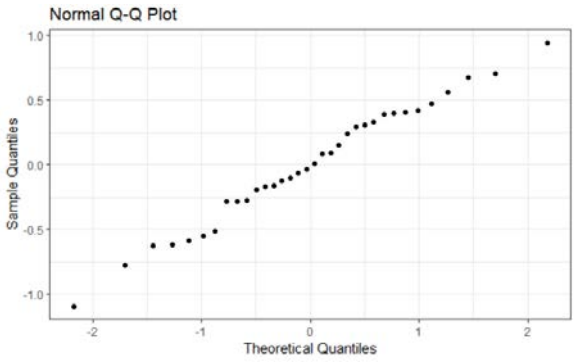

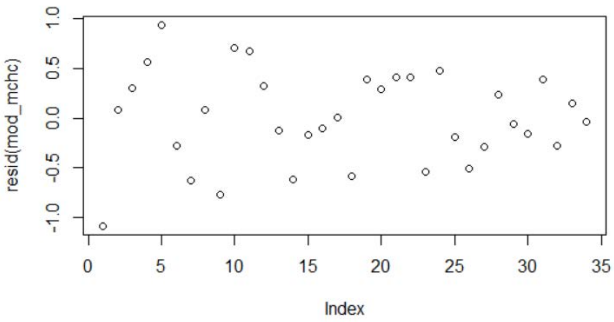

F. ANCOVA Table

Variable	Sum Sq	df	F value	Pr(>F)
Status	0.364101	2	0.679151	0.515499
ID	0.642732	4	0.599438	0.666216
Residuals	7.237512	27	NA	NA

G. Estimated marginal means

Status	emmean	SE	df	lower.CL	upper.CL
Pre-encapsulating	5.500174	0.143669	27	5.205389	5.794958
Encapsulating	5.445094	0.220866	27	4.991914	5.898275
Post-oviposition	5.696262	0.14492	27	5.398911	5.993614

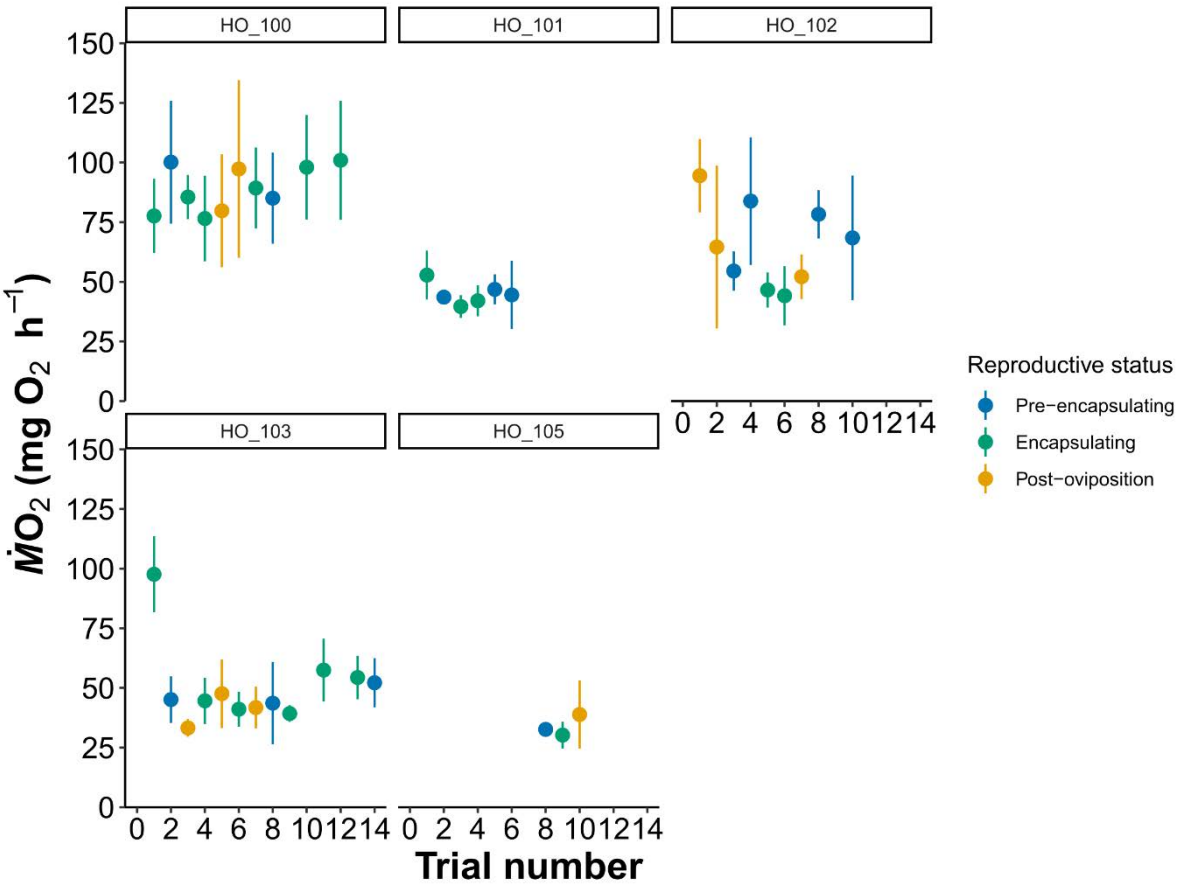

Figure S4.1. Mean $\dot{M}O_2$ (± s.d.) of each trial for each shark (individual panels) in the study by reproductive status represented by colour.

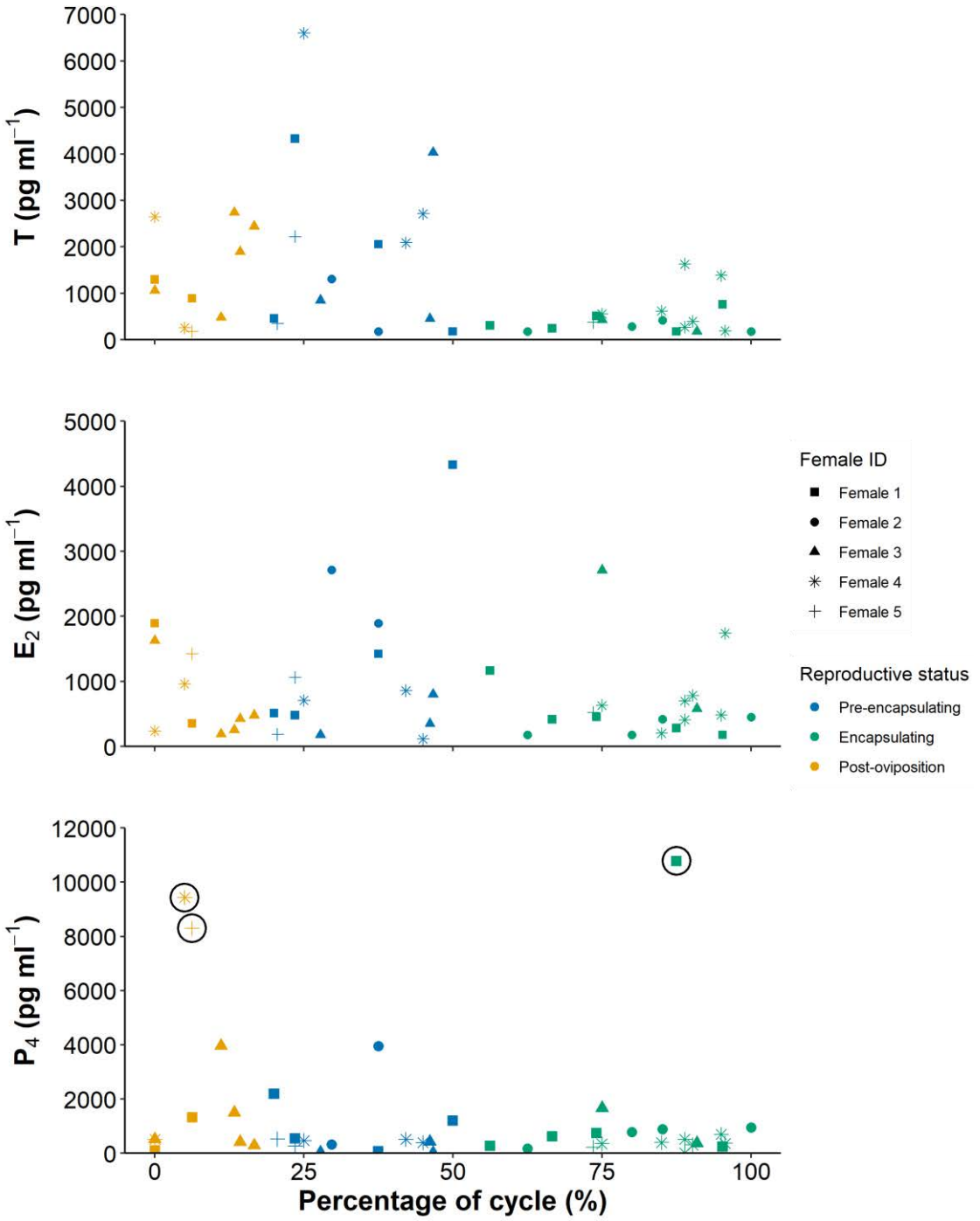

Figure S4.2 The circulating concentrations of sex steroid hormones (A) testosterone (T (pg ml^{-1})), (B) estradiol (E_2 (pg ml^{-1})), and (C) progesterone (P_4 (pg ml^{-1})) across an average egg production cycle, where 0 and 100% represent egg deposition of one clutch to the next. Colours represent the three reproductive statuses described in Figure 4.1, and point shapes represent the five female sharks in the study.

S5.0 Test for outliers

A. Outlier in CT_{max}:

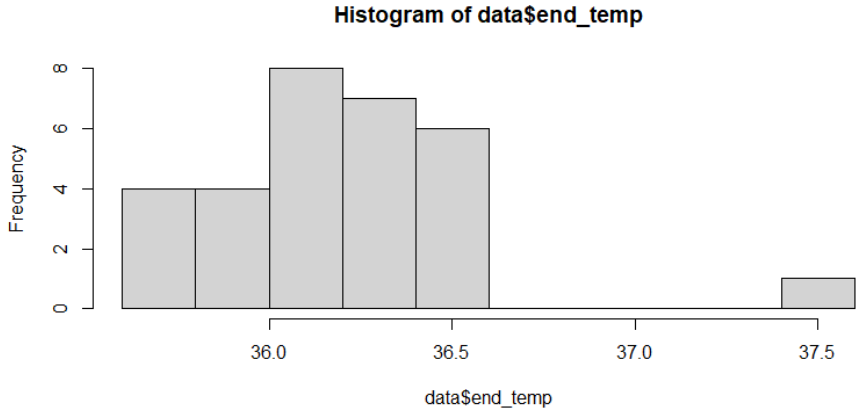

B. Dixon's Q test:

Q = 0.50595, p-value = 0.001172

Accept the alternative hypothesis: highest value 37.45 is an outlier.

C. Outlier removed:

- Individual HO-325, a mature female was removed.

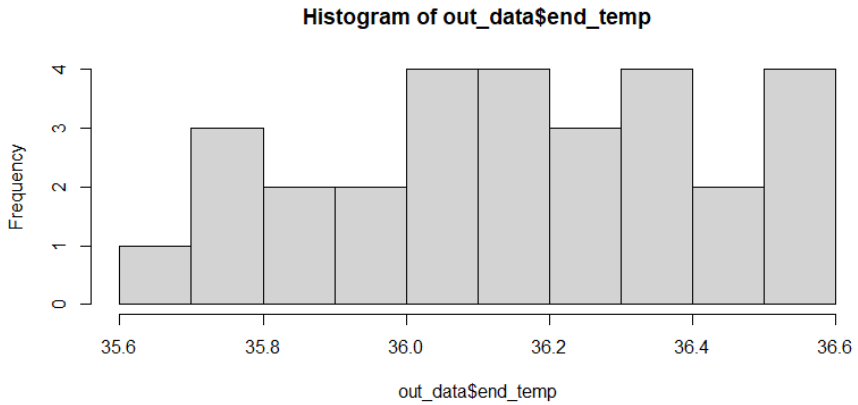

S5.1. Experimental parameter effects on CT_{max}

lm(CT_{max} ~ number of holding days + trial starting temperature*time of day of trial)

Term	Sum of squares	df	F statistic	p-value
Holding days	0.02635	1	0.328933	0.571624
Trial starting temp	0.040435	1	0.504751	0.484267
Time of day of trial	0.014232	1	0.177664	0.67714
Start temp*time of day	0.113742	1	1.419858	0.245077
Residuals	1.922588	24	NA	NA

S5.2. Life history stage, sex, and body size effects on CT_{max}

lm(centered CT_{max} ~ status + sex + mass + life history stage*sex*mass)

Term	Sum of squares	df	F statistic	p-value
Life history stage	0.081812	2	0.601321	0.558732
Mass	0.090298	1	1.327384	0.264344
Sex	0.190384	1	2.798658	0.111634
Life history stage*mass	0.6207	2	4.562174	0.024959
Life history stage*sex	0.425097	2	3.124483	0.068425
Mass*sex	0.410419	1	6.033195	0.024426
Life history stage*mass*sex	0.033445	1	0.491641	0.492162
Residuals	1.224482	18	NA	NA

S5.3. CT_{max} trial activity proportions

glmer(activity type ~ status + sex + (1|ID), family= binomial(link= "logit"))

Random effect	**Variance**	**Std. Dev.**		
ID	0.6632	0.8143		
Fixed effects	**Estimate**	**Std. Error**	**Z value**	**Pr(>|z|)**
Intercept	-2.7838	0.6405	-4.346	1.39e-05
Status:Mature	0.6646	0.5937	1.120	0.2629
Status:Subadult	1.1167	0.6307	1.771	0.0766
Sex:Male	0.3642	0.4773	0.763	0.4454

Type II Wald Chi squared tests

Term	**Chisq.**	**df**	**Pr(>Chisq)**
Status	3.1385	2	0.2082
Sex	0.5823	1	0.4454

S5.4. Resting ventilation rate generalized additive model

gam(ventilation rate ~ status + sex + status:sex + s(exp_time, k= -1, by= status:sex), correlation= corAR1())

Term	Estimate	Std. Error	t value	Pr(>|t|)
Intercept	38.861	1.713	22.680	<2e-16
Status:subadult	8.120	2.070	3.922	0.000107
Status:mature	3.622	1.833	1.976	0.049045
Sex:male	3.641	1.852	1.966	0.050154
Status:subadult *Sex:male	-8.424	2.377	-3.544	0.000453
Status:mature*Sex:male	-8.093	2.143	-3.777	0.000189

Type II Wald Chi squared tests

Term	F	df	Pr(>Chisq)
Status	9.091	2	0.000145
Sex	3.866	1	0.050154
Status:Sex	8.049	2	0.000389

Estimated marginal means comparisons: ~Status + (1|Sex)

Sex	contrast	estimate	std.error	df	statistic	adj.p.value
Female	Juvenile - Subadult	-14.697	4.266606	318.8413	-3.44465	0.001871
	Juvenile - Mature	-4.83555	2.057458	318.8413	-2.35025	0.050559
	Subadult - Mature	9.8614	4.070024	318.8413	2.422934	0.042075
Male	Juvenile - Subadult	0.232448	1.687651	318.8413	0.137735	0.989596
	Juvenile - Mature	5.054203	1.326929	318.8413	3.808946	4.90E-04
	Subadult - Mature	4.821754	1.601639	318.8413	3.010512	0.007908

Table S6.1 *In ovo* growth rates, yolk consumption, and embryonic metabolic rates

A. Embryonic Growth Rates: lmer(embryo length ~ development day + temperature + (1|round))

Mixed linear effects model		**Effects size: 0.85**		
Contrast (°C)	**Estimate ± SE**	**df**	**t-ratio**	**p-value**
27- 29	-1.245 ± 0.182	570	-6.856	<0.0001
27- 31	-1.582 ± 0.211	570	-7.502	<0.0001
29- 31	-0.337 ± 0.238	570	-1.416	0.3333

B. Yolk-sac Consumption Rates: gamm(yolk sac area ~ s(development day) + temperature + (1|round))

Generalized additive model (GAM)		**Effects size: 0.73**		
Contrast (°C)	**Estimate ± SE**	**df**	**t-ratio**	**p-value**
27- 29	1.61 ± 0.157	598	10.245	<0.0001
27- 31	1.181 ± 0.182	598	6.495	<0.0001
29- 31	-0.432 ± 0.205	598	-2.108	0.0890

C. Embryonic Metabolic Rates: gamm($MO_{2Embryonic}$ ~ s(development day) + temperature + (1|round))

Generalized additive model (GAM)		**Effects size: 0.77**		
Contrast (°C)	**Estimate ± SE**	**df**	**t-ratio**	**p-value**
27- 29	-0.601 ± 0.0735	184	-8.19	<0.0001
27- 31	-0.363 ± 0.0751	184	-4.83	<0.0001
29- 31	0.600 ± 0.356	184	2.76	0.0176

Table S6.2 Linear mixed effects models of *in ovo* incubation time and time of first feeding post-hatch

A. Incubation Time: lmer(incubation days ~ temperature + (1|round))

Contrast (°C)	Estimate ±SE	df	t-ratio	p-value
27- 29	15.21 ± 2.80	24	5.431	<0.0001
27- 31	24.19 ± 2.95	24	8.192	<0.0001
29- 31	8.98 ± 3.37	24	2.666	0.0348

B. Time of First Feeding: lmer(time of first feeding ~ temperature + (1|round))

Contrast (°C)	Estimate ± SE	df	t-ratio	p-value
27- 29	0.571 ± 0.584	24	0.978	0.598
27- 31	6.31 ± 0.616	24	10.2	<0.0001
29- 31	5.74 ± 0.702	24	8.17	<0.0001

Table S6.3 Linear mixed effects models of neonate mass, length, and Fulton's condition factor at hatching

A. Mass: lmer(mass ~ temperature + (1|round))

Contrast (°C)	Estimate ± SE	df	t-ratio	p-value
27- 29	0.893 ± 0.746	24	1.197	0.4463
27- 31	2.619 ± 0.786	24	3.331	0.0076
29- 31	1.726 ± 0.896	24	1.926	0.1532

B. Length: lmer(length ~ temperature + (1|round))

Contrast (°C)	Estimate ± SE	df	t-ratio	p-value
27- 29	-0.836 ± 0.637	24	-1.312	0.4022
27- 31	0.683 ± 0.671	24	1.018	0.5729
29- 31	1.519 ± 0.765	24	1.985	0.1377

C. Body Condition (Fulton's Index): lmer(K ~ temperature + (1|round))

Contrast (°C)	Estimate ± SE	df	t-ratio	p-value
27- 29	0.0664 ± 0.0424	24	1.565	0.2797
27- 31	0.00762 ± 0.0447	24	0.170	0.9841
29- 31	-0.05881 ± 0.0510	24	-1.153	0.4919

Table S6.4 Neonate resting metabolic rate (RMR), maximum metabolic rate (MMR), aerobic scope, and recovery time from MMR to RMR

D. $\dot{M}O_{2Rest}$: lmer(MO_{2Rest} ~ temperature + (1|round))

Contrast (°C)	Estimate ± SE	df	t-ratio	p-value
27- 29	-16.89 ± 4.84	24	-3.488	0.0052
27- 31	-2.82 ± 5.11	24	-0.552	0.8464
29- 31	-14.07 ± 5.82	24	2.418	0.0590

A. $\dot{M}O_{2Max}$: lmer(MO_{2Max} ~ temperature + (1|round))

Contrast (°C)	Estimate ± SE	df	t-ratio	p-value
27- 29	-19.8 ± 5.92	24	-3.350	0.0072
27- 31	15.9 ± 6.24	24	2.541	0.0455
29- 31	35.7 ± 7.11	24	5.017	0.0001

B. Aerobic Scope: lmer(AS ~ temperature + (1|round))

Contrast (°C)	Estimate ± SE	df	t-ratio	p-value
27- 29	-2.93 ± 6.60	24	-0.445	0.8972
27- 31	18.67 ± 6.96	24	2.684	0.0335
29- 31	21.60 ± 7.93	24	2.724	0.0307

C. $\dot{M}O_{2max}$ Recovery Time: lmer(Recovery time ~ temperature + (1|round))

Contrast (°C)	Estimate ± SE	df	t-ratio	p-value
27- 29	-35.7 ± 11.4	24	-3.150	0.0116
27- 31	-66.9 ± 12.0	24	-5.598	<0.0001
29- 31	-31.2 ± 13.5	24	-2.289	0.0768